

心御高覽

電氣試驗所研究報告

第二百三十七號

RESEARCHES
OF THE
ELECTROTECHNICAL LABORATORY

KIYOSHI TAKATSU, DIRECTOR.

NO. 237

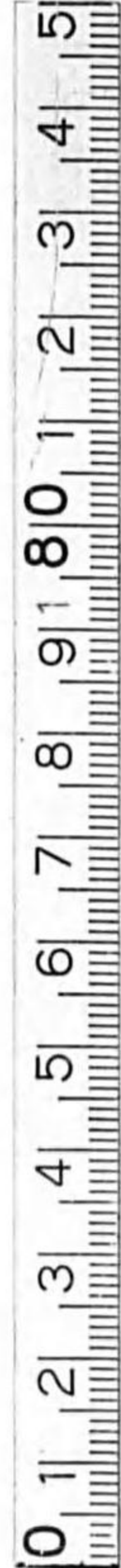
CALCULATIONS ON VACUUM TUBES AND
THE DESIGN OF TRIODES

By

Yuziro KUSUNOSE

Sept., 1928.

ELECTROTECHNICAL LABORATORY,
MINISTRY OF COMMUNICATIONS,
TOKYO, JAPAN.



始



14.5-9

RESEARCHES
 OF THE
 ELECTROTECHNICAL LABORATORY
 KIYOSHI TAKATSU, DIRECTOR.

NO. 237

CALCULATIONS ON VACUUM TUBES AND
 THE DESIGN OF TRIODES

By

Yuziuro KUSUNOSE

SYNOPSIS

The primary object of the paper is to present in simple form a method of designing triode vacuum tubes.

The working conditions of a triode can be predicted from its static characteristics which are determinable from the electrode configurations. The first two chapters of the paper are devoted to these investigations.

As formulas now available for calculations of the characteristics and the amplification constant have been derived from tubes with electrodes of the simplest structures, special considerations have to be taken for applying them to the present tubes of more complicated structures. Such measures being taken, approximation of calculation to experiment, which may be regarded sufficient for the purpose of designing, has been reached.

For the derivation of various working conditions of a triode from its static characteristics, the writer has worked out a graphical representation of the alter-



編
 所
 寄贈本

nating and direct components of the anode working currents for various anode and grid voltages, approximating the static characteristics as a linear relation. The resulting dynamic characteristic diagram where currents are expressed in the unit of saturation current, and voltages in that of saturating voltage, is applicable to any triode in evaluating the working voltages, currents and powers for a given circuit arrangement as well as given anode and grid voltages, whether the tube be used as an amplifier, an oscillator, or a modulator.

In the last chapter, an essential case of the designing process is shown, in which the use of the triode is indicated and its power output given. The working points are first determined on the dynamic characteristic diagram so as to conform to the use of the triode. All the quantities in the working condition are thus known, being expressed in the units as given above. The power output is known as a quantity $\frac{\text{Power Output}}{\text{Saturation Current} \times \text{Saturating Voltage}}$ where the product in the denominator may accordingly be determined, and this product is next to be split into its component parts. An alternative problem arises here which type of a tube is to be selected, high anode voltage and low emission, or low anode voltage and high emission, and the solution will need both the economical and technical considerations. The amplification constant is then determined so as to comply with the saturating voltage, grid loss being considered.

After this, generally speaking, configurations of the anode and grid are determined from the power and the saturating voltage, grid mesh construction from the amplification constant, and dimensions of the cathode from the saturation current and the estimated life.

All the descriptions throughout the paper are illustrated by numerical examples on various types of tubes tested at the Laboratory.

CONTENTS

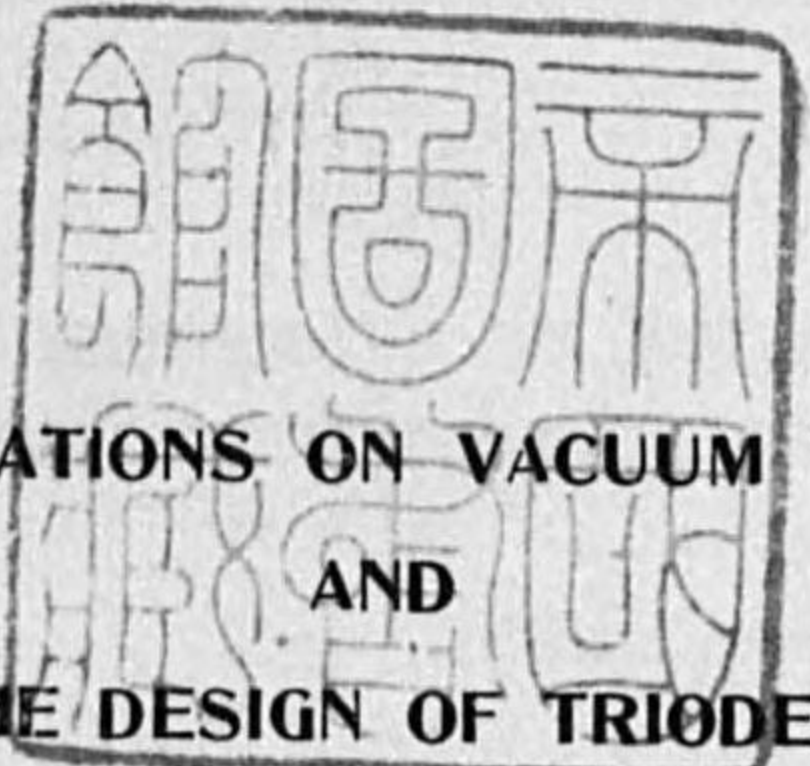
	PAGE
INTRODUCTION.	1
CHAPTER I. COMPUTATION OF CHARACTERISTIC FROM THE ELECTRODE CONFIGURATIONS.	2
(1) Diode Characteristics.	2
(2) Triode Characteristics.	15
(3) Parameters of a Triode.	28
i) Amplification Constant.	28
ii) Mutual Conductance and Anode Impedance.	39
(4) Saturating Part of the Characteristic.	41
(5) Examples for the Computation of Characteristics.	47
CHAPTER II. DETERMINATION OF OPERATIONS OF A TRIODE FROM ITS STATIC CHARACTERISTICS.	90
(1) Preliminary Work.	90
(2) The Dynamic Characteristic Diagram.	109
CHAPTER III. THE DESIGN OF TRIODES.	126
(1) Working Points on the Dynamic Characteristic Diagram.	126
(2) Saturating Voltage and Saturation Current.	127
(3) Amplification Constant.	128
(4) Dimensions of the Electrodes.	131
(5) Design of the Cathode.	135
(6) Examples on the Triode Design.	140
SUMMARY.	159

LIST OF TUBES GIVEN IN EXAMPLES

Type	Page	Type	Page
102-D	26	PAY	68
205-B	48	PBN	153
205-D	49	R	29, 69
211-A	50	RS 15	28
216-A	51	RE-11	70
228-A	17	RE-84	36, 71
ABT	30, 52	RG-46	12
BE	31, 53	RS-15	72, 106
BN	44	S-53	17
DER	54	T-100	40
DEV	55	T-450A	73
H	56	TA 04/5	74
KL-1	46	TA 08/10	38
KN-155	6	TA 10/600	19
KN-156	7	TA 10/3000	75
LS-5	57	TR-V	76
MR-1	8	TR-VII	28
MR-4	9	UN-154	77
MR-6	10	UN-155	78
MR-7A	11	UN-159	79
MS III	58	UV-199	26, 80, 81
MT-1	59	UV-201A	27, 34, 82, 83
MT-2	60	UV-202	84
MT-4	26, 38, 61	UV-203	33
MT-6	62	UV-203A	85
MT-7A	26, 63	UV-204	17, 27, 86, 106
MT-7B	64	UV-204A	22, 27
MT-9	26, 65	UV-206	17, 87
MU-20	66	UV-212	13
PAK	147	UX-201A	88
PAM	144	UX-210	113
PAV	30	UX-213	14, 15
PAX	67	VM-100	116
		WD-11	89

LIST OF SYMBOLS

A	anode effective area (cm ² .)	L_g	ratio of total length of effective grid wires to axial length of grid.
a	ratio of grid conductor area to grid surface area	m	number of points of support of filament
c	conversion factor of k for plane-electrode tubes	n	number of grid wires parallel to filament
d_f	filament diameter (cm.)	p	pitch of adjacent grid wires (cm.)
d_g	grid wire diameter (cm.)	P	power output of a tube (watt)
e_a	anode voltage (volt)	q	portion of filament power radiated through anode
e_f	filament terminal voltage (volt)	r	anode impedance or internal resistance (ohm)
e_f'	effective filament voltage (volt)	\bar{r}	mean anode impedance (ohm)
e_g	grid voltage (volt)	R	alternating current resistance of a closed resonance circuit (ohm)
e_g'	equivalent grid voltage (volt)	\bar{R}	anode circuit impedance (resistive) (ohm)
e_s	saturating voltage (volt)	r_f	filament radius (cm.)
E_a	steady anode voltage (volt)	r_g	grid wire radius (cm.)
E_g	steady grid voltage or grid bias voltage (volt)	s	number of supports of grid wires which lie in the stream of electrons
\mathcal{E}_a	alternating anode voltage, max. value (volt)	t	thickness of grid support (cm.)
\mathcal{E}_g	alternating grid voltage, max. value (volt)	w	permissible anode loss per unit area (watt/cm ²)
g	mutual conductance (mho)	W_a	anode loss (watt)
G	perveance	W_f	filament heating power (watt)
i	electron current (amp.)	W_g	grid loss (watt)
i_a	anode current, instantaneous value (amp.)	W_l	grid leak loss (watt)
i_g	grid current (amp.)	x_a	distance of anode to cathode axis (cm.)
i_f	filament current (amp.)	x_g	distance of grid to cathode axis (cm.)
I_a	anode mean or direct current (amp.)	z_a	mean shortest distance of anode to filament (cm.)
I_g	grid mean or direct current (amp.)	z_g	mean shortest distance of grid to filament (cm.)
I_s	saturation current (amp.)	α	specific power output
\mathcal{I}_a	anode alternating current, fundamental component max. value (amp.)	η	anode power conversion efficiency
k	amplification constant		
l	total length of filament (cm.)		
L	life of cathode (hour)		



CALCULATIONS ON VACUUM TUBES
AND
THE DESIGN OF TRIODES

By

Yuziro KUSUNOSE

INTRODUCTION

The rapid growth of radio communication has its origin in the introduction of vacuum tubes, which at the present time form indispensable parts of radio apparatuses, and accordingly a large variety of tubes has come out on the market throughout the world.

In the course of this progress, the designing of vacuum tubes has been developed through the experiences of the leading manufacturers, but it does not seem to have been carried to a point where it had been well standardized as in other electrical apparatuses.

The writer has devoted himself to the study on the design problems for several years, and arrived at a definite procedure as is described in this paper, which he believes to be of some use to valve manufacturers, although it is not at all considered to be perfect as is desirable.

The writer's thanks are due to E. Yokoyama, Chief of Radio Section, under whose direction the present work has been carried out and also to N. Kato, I. Miura, S. Maeda and others of the Section for their assistances to the investigations.

CHAPTER I,
COMPUTATION OF CHARACTERISTICS FROM
THE ELECTRODE CONFIGURATIONS

(1) Diode Characteristics.

If a diode has a cathode of uniform potential all over the surface, such as an indirectly-heated cathode, or if the anode voltage is very high compared with the filament terminal voltage, the well-known space-charge equation applies to the determination of anode current i_a at a given anode voltage e_a :⁽¹⁾

$$i_a = Ge_a^{\frac{3}{2}} \dots \dots \dots (1)$$

When the cathode consists of a filament heated by a direct current at a terminal voltage e_f , the above equation must be corrected for the non-uniformity of anode-to-cathode potential difference along the length of the filament, and the modification may be expressed by the following equations, anode voltage being measured from the negative leg of the filament:⁽²⁾

$$\text{for } e_a < e_f: i_a = \frac{2}{5} G \frac{1}{e_f} e_a^{\frac{5}{2}} = \frac{2}{5} G e_f^{\frac{3}{2}} \left(\frac{e_a}{e_f} \right)^{\frac{5}{2}} \dots \dots \dots (2)$$

$$\text{for } e_a > e_f: i_a = \frac{2}{5} G \frac{1}{e_f} \left[e_a^{\frac{5}{2}} - (e_a - e_f)^{\frac{5}{2}} \right]$$

$$= \frac{2}{5} G e^{\frac{3}{2}} \left[\left(\frac{e_a}{e_f} \right)^{\frac{5}{2}} - \left(\frac{e_a}{e_f} - 1 \right)^{\frac{5}{2}} \right] \dots \dots \dots (3)$$

The two equations may be reduced to a single one, as

$$i_a = \frac{2}{5} G e_f^{\frac{3}{2}} f \left(\frac{e_a}{e_f} \right) \dots \dots \dots (4)$$

(1) I. Langmuir: Phys. Rev. 21, p. 419, 1923 and 22, p. 347, 1923.
(2) Van der Bijl: "Thermionic Vacuum Tube," p. 64.

The values of $f \left(\frac{e_a}{e_f} \right)$ computed for a series of values of $\frac{e_a}{e_f}$ are shown in TABLE I on page 160.

If the filament voltage is not known, it may be calculated from dimensions of the filament by means of CHART II, working temperature or saturation current being assumed. For the use of the chart, the description on page 136 is to be referred.

The constant G which is called "perveance" may be determined from the electrode configurations, and in ordinary cases (Fig. 1),

$$G = 2.33 \times 10^{-6} \frac{A}{x_a^2} \dots \dots \dots (5)$$

in which A = effective anode area.

x_a = distance of the anode surface from the axis of the filament.

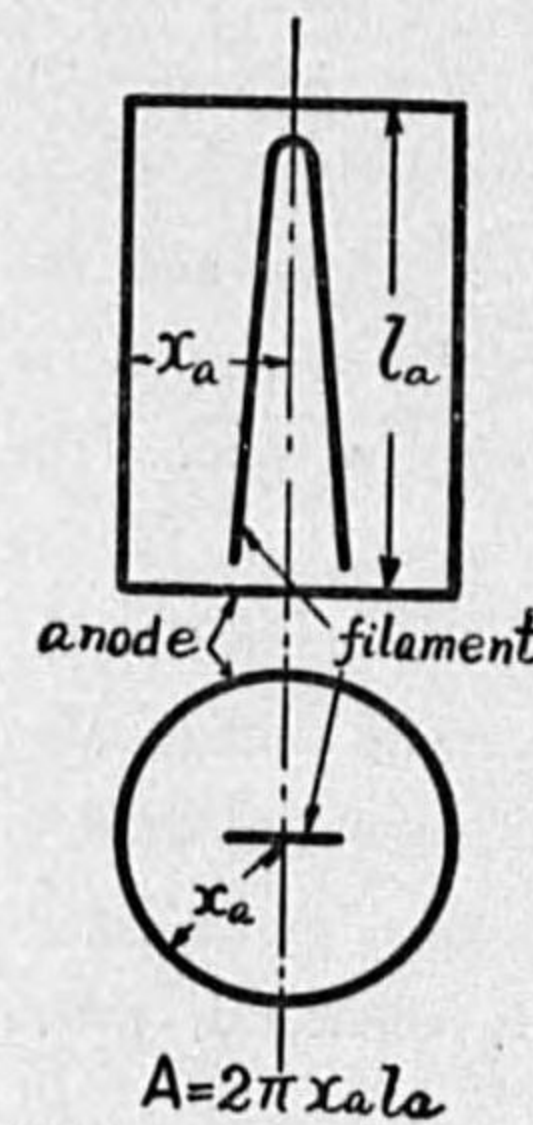


FIG. 1.

All quantities relating to dimensions are expressed in centimeter units, and those relating to electricity in volts, amperes, ohms, watts, etc., unless otherwise specified.

The original equation given by Langmuir⁽¹⁾ for a diode with parallel plane anode and cathode, distance between them being x_a , is

$$i_a = 2.33 \times 10^{-6} \frac{A}{x_a^2} e_a^{\frac{3}{2}}$$

and for a diode with cylindrical anode of radius x_a , and coaxial cathode of radius r_c , length of the system being l_a , it is

$$i_a = 14.65 \times 10^{-6} \frac{l_a}{\beta^2 x_a} e_a^{\frac{3}{2}} = 2.33 \times 10^{-6} \frac{A}{\beta^2 x_a^2} e_a^{\frac{3}{2}}$$

The value of β^2 depends on $\frac{x_a}{r_c}$, but for most practical cases at which this ratio is greater than 10 or so, β^2 tends to unity, and moreover in the complicated structures of filament usually met in practice the meaning of this ratio becomes vague, so we intend to consider β^2 as unity. This being done, the two equations become identical either for plane or cylindrical forms of electrodes,

The above relation for G is equally applicable to anodes of either plane or cylindrical forms. For plane anode tubes the effective anode area is however not the actual whole area of the anode metal, but that area on which electrons are

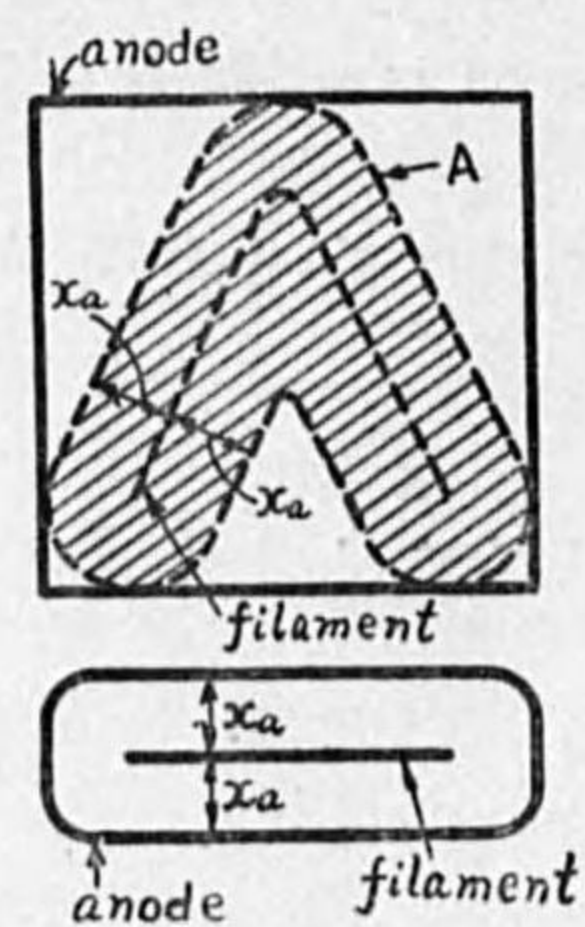


FIG. 2.

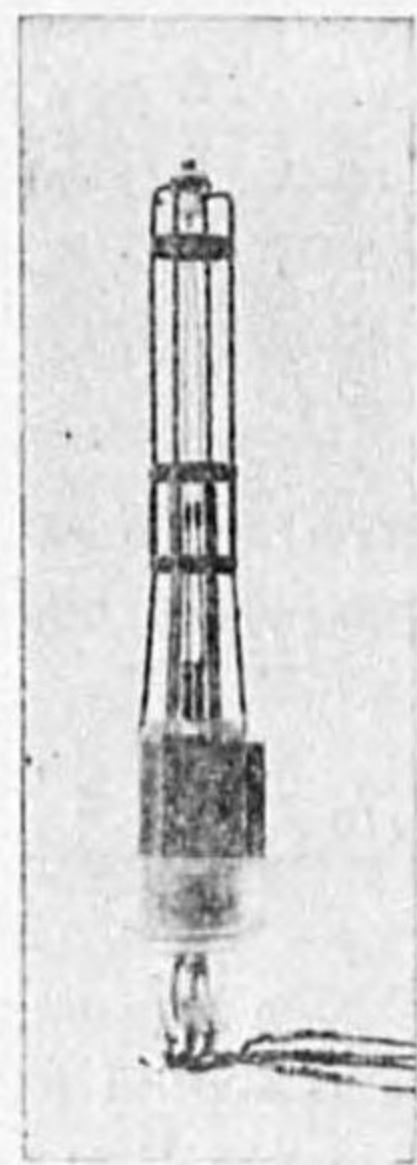


FIG. 3.

considered to bombard, and the writer has empirically found that this area may be taken as that comprised in the breadth $2x_a$ along the filament length projected on the anode, as illustrated in Fig. 2.

The above diode equations are sufficiently accurate for designing, although there are neglected the various minor effects, such as those due to initial velocities of electrons, contact potential difference, magnetic field around the cathode, nonuniformity of cathode temperature causing partial saturation, superposition of anode current on the filament current, and so forth.

When the filament is supported by such a structure as shown in Fig. 3, which is often the case with high-power rectifier tubes, the supporting structure must be considered as grid of a triode and the characteristic must be computed by the equation for the triode assuming the grid voltage as zero. (See example 5, page 10)

When the anode return is not connected to the negative end of the filament, the anode voltage must be corrected to the value measured from the negative end by adding a voltage which is equal to the potential of the point, where return is connected, above the negative end.

When the filament is lighted by alternating current, and the anode return is at one end of the filament, anode voltage measured above the negative end fluctuates per complete cycle between e_a and $e_a + \sqrt{2}e_f$, e_f being the effective value, and the anode

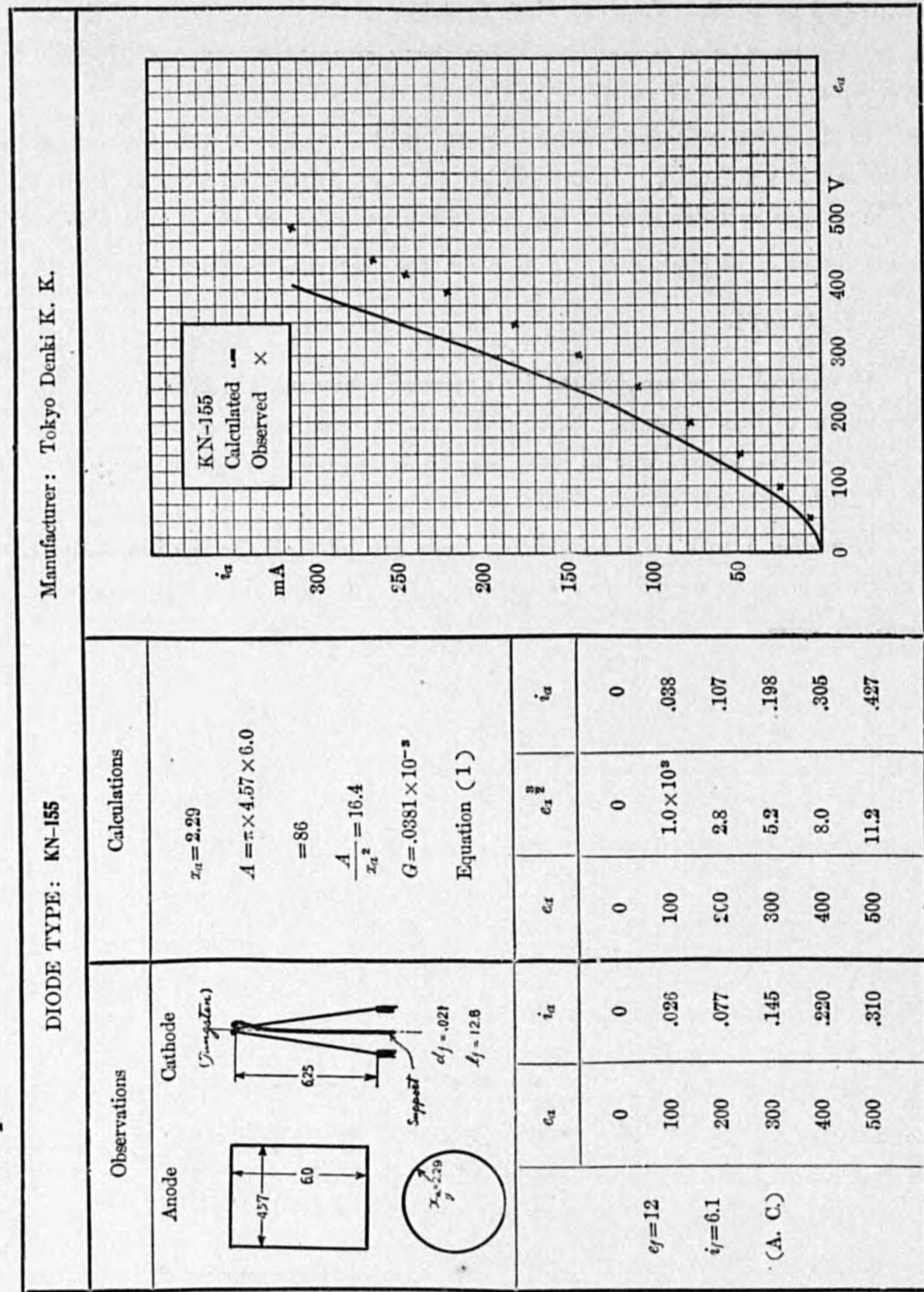
current at an anode voltage e_a shall be taken as the average value of the currents computed for e_a and $e_a + \sqrt{2}e_f$. For rough estimations, equation (1) may however be applied to this case.

If the anode voltage is referred to the neutral point of the filament voltage, filament being lighted by d. c., equation (1) may be applied even at such a low anode voltage as twice that of the filament within an error of 1%. When the anode return is at one leg of the filament, the error will be 10% at $\frac{e_a}{e_f} = 7.5$, and 1% at $\frac{e_a}{e_f} = 71$.

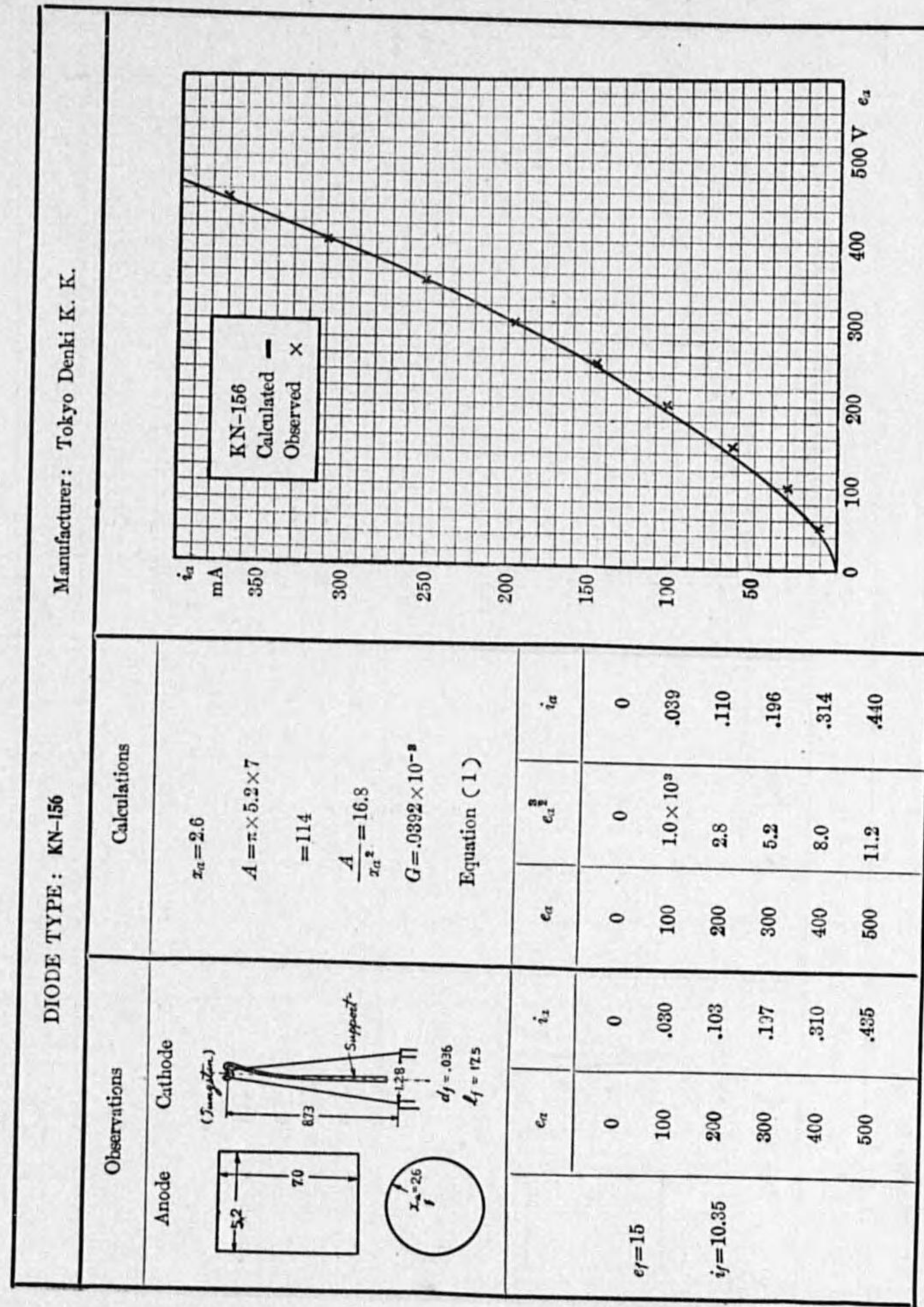
If residual gases are existent by appreciable amount, the characteristic may be affected in various manners. The anode current usually increases steeper than the $\frac{3}{2}$ power of the voltage due to ionization, in a vacuum lower than, say, 10^{-4} mm. Hg. Such tubes are of no practical value.

Examples 1 to 9 on the following pages are intended for the illustration of the computing methods as well as for showing their validity in comparison with the observed data.

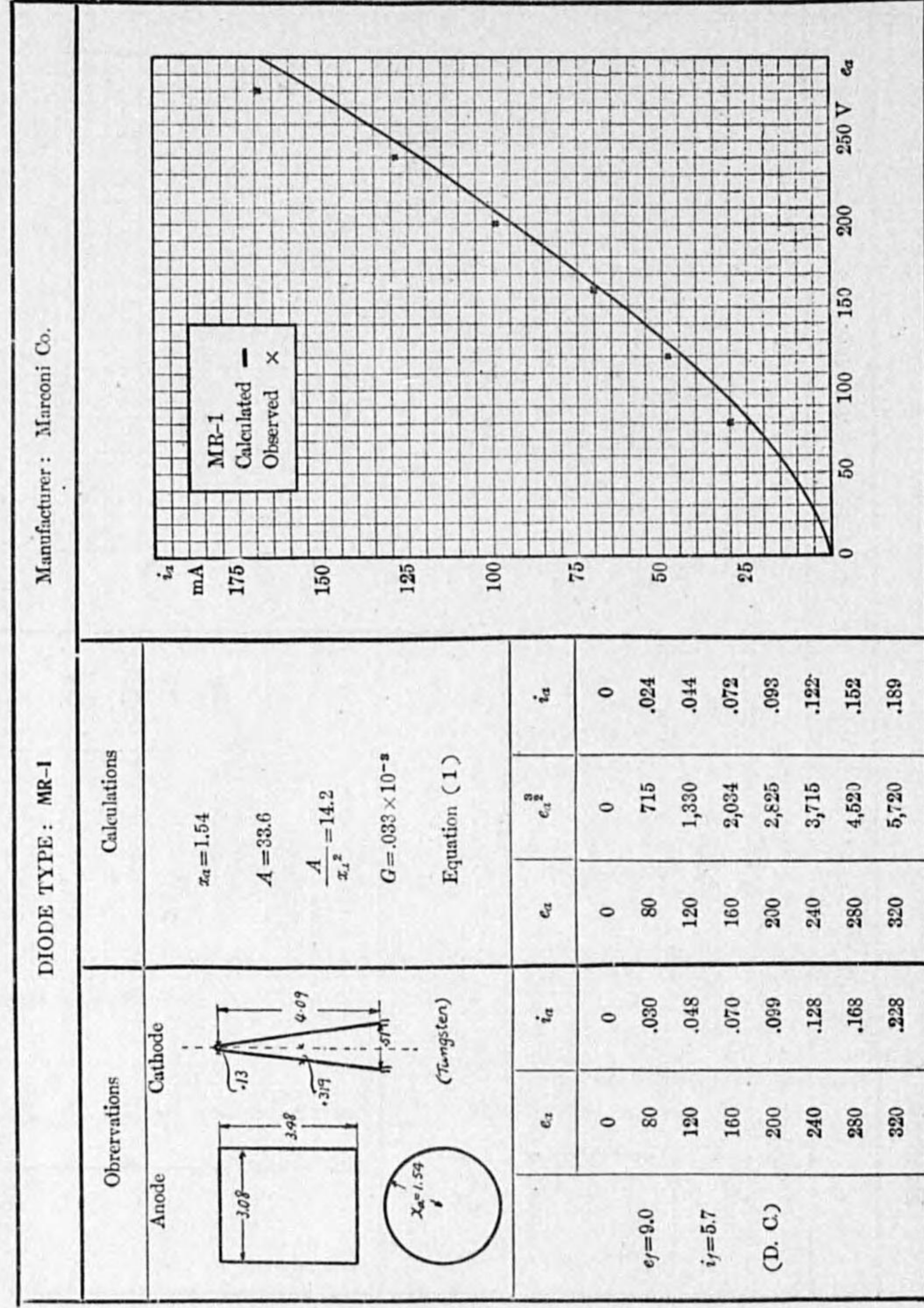
Example 1.



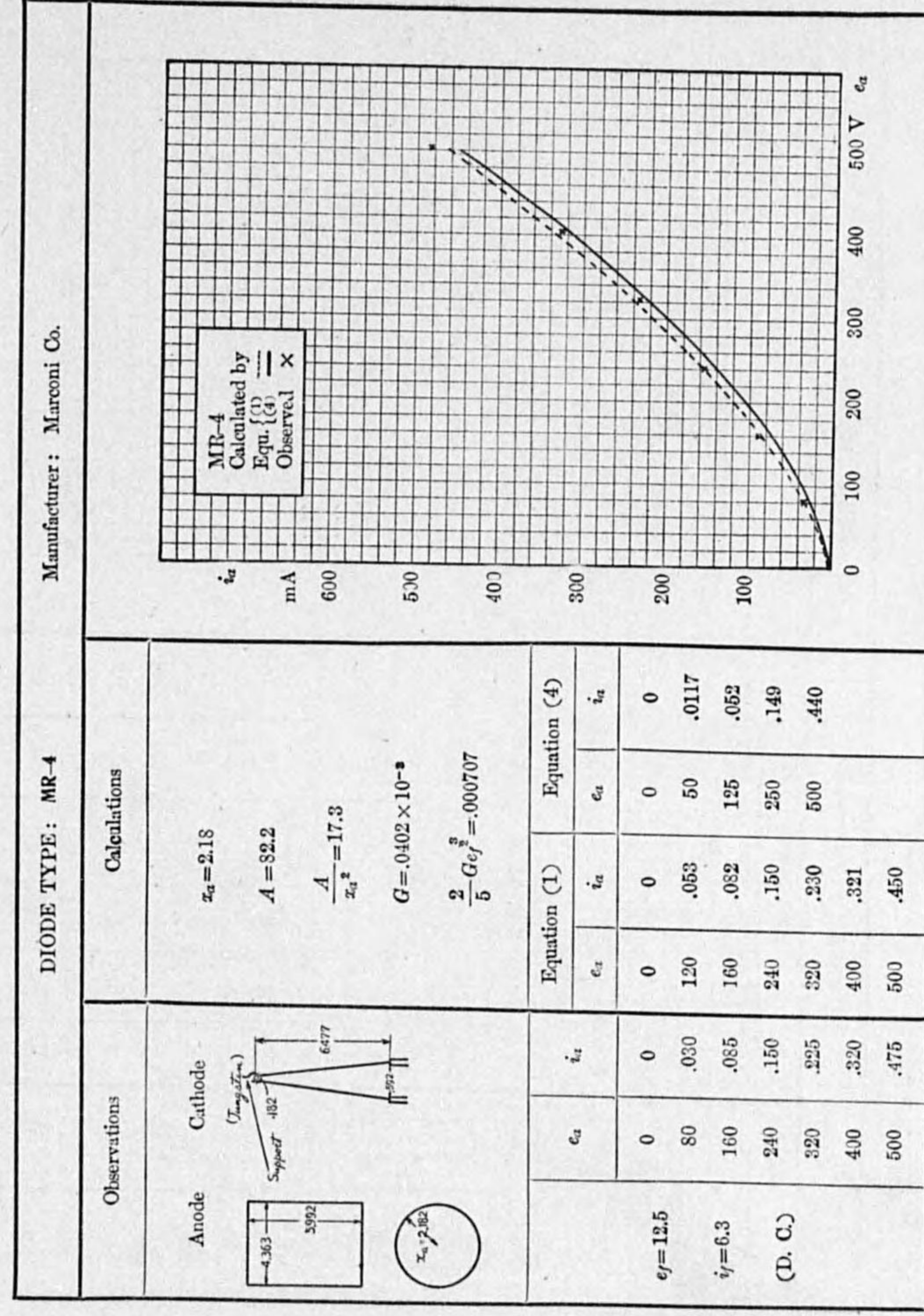
Example 2.



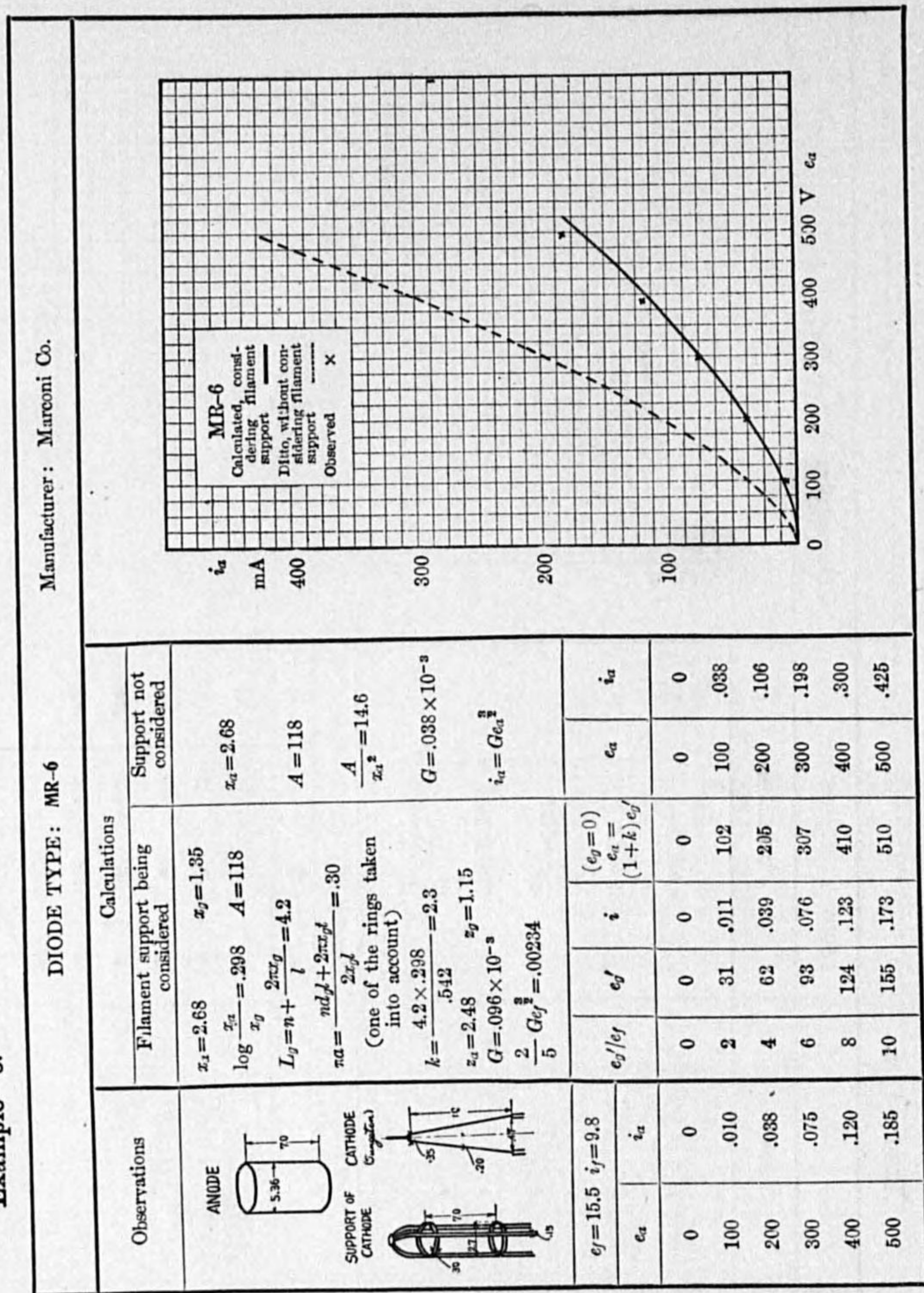
Example 3.



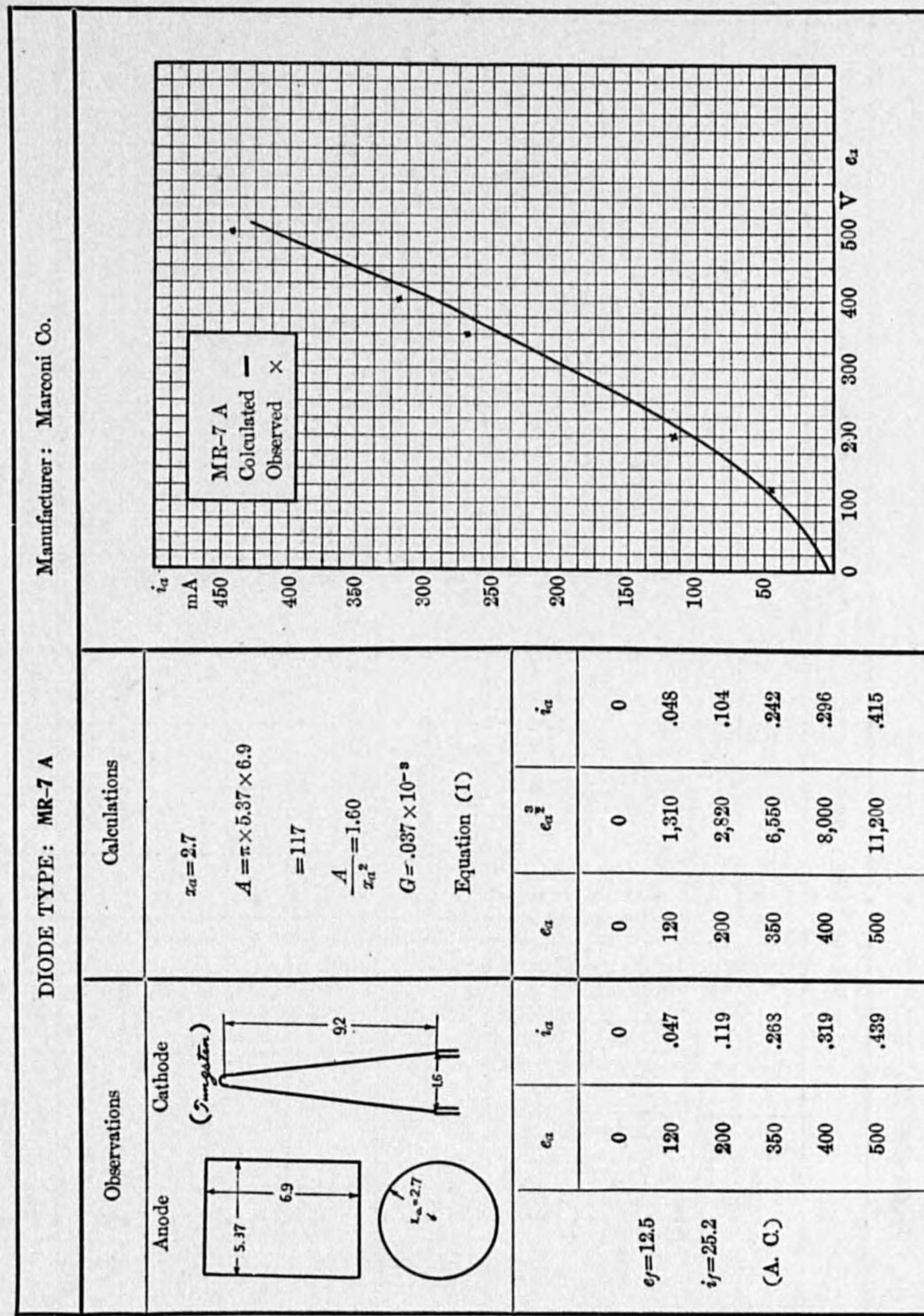
Example 4.



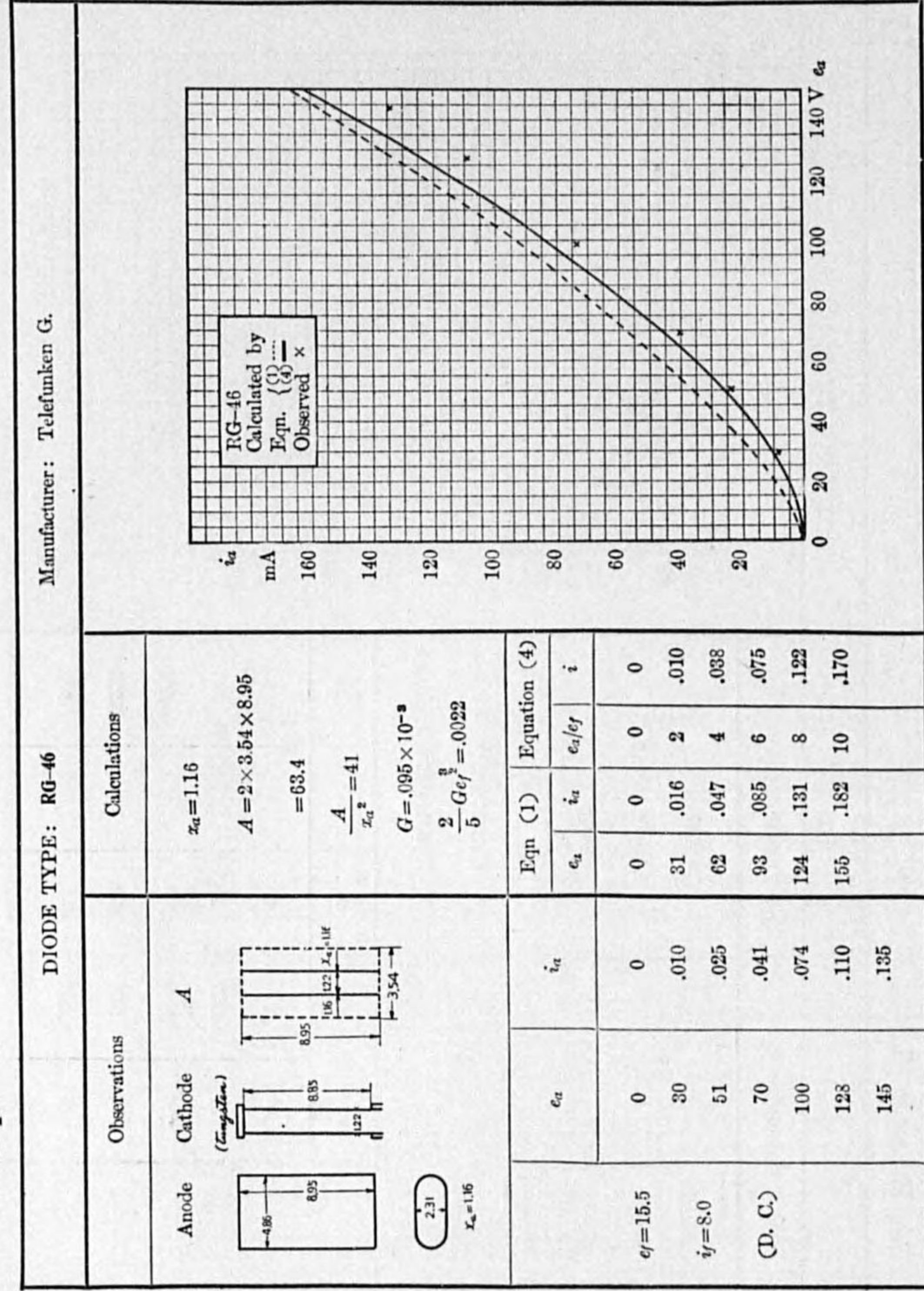
Example 5.



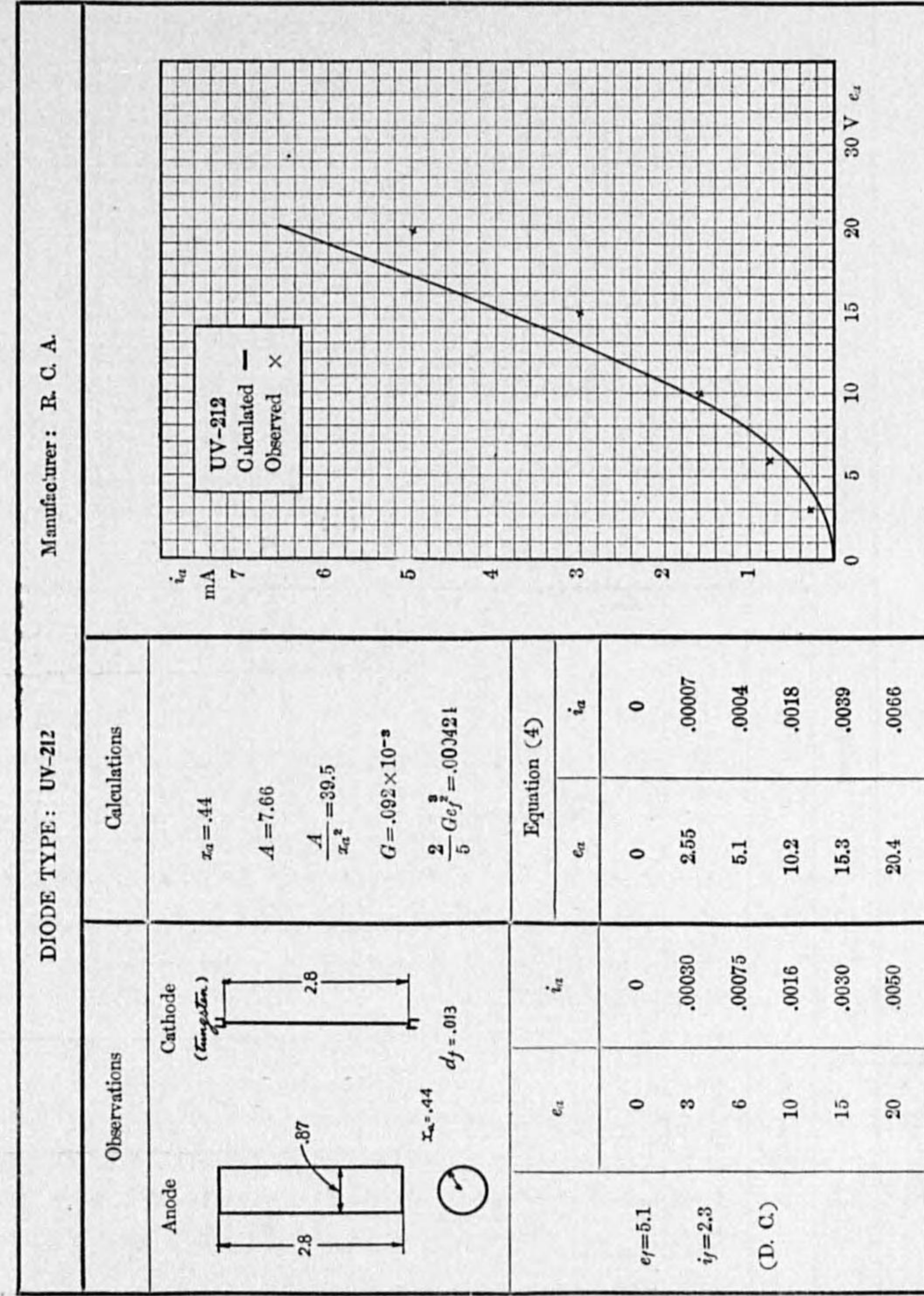
Example 6.



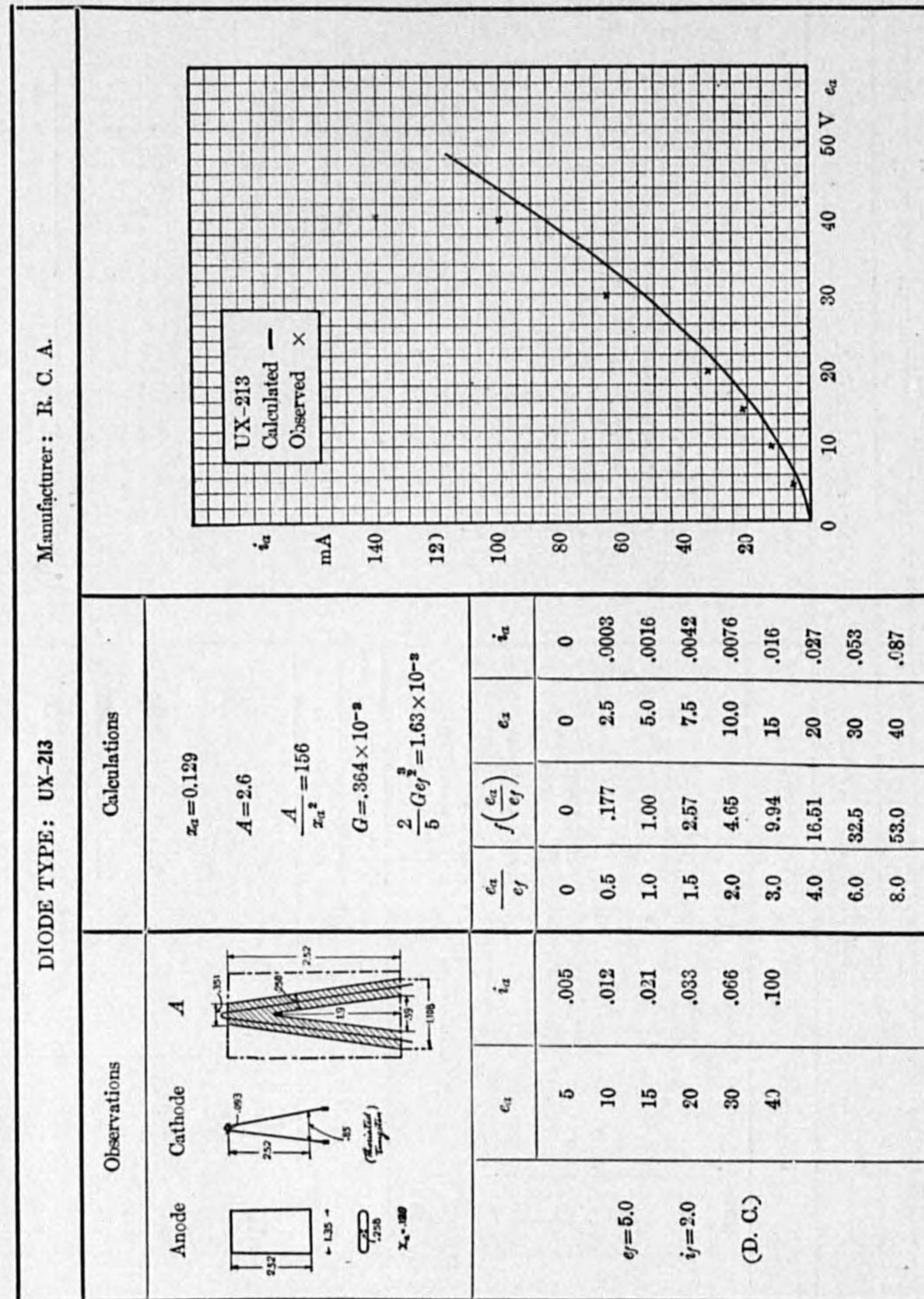
Example 7.



Example 8.



Example 9.



(2) Triode Characteristics.

In a triode, an anode voltage e_a and a grid voltage e_g produce as their combined effect a certain strength of electric field around the cathode, and the same electric field can be produced if the grid exists as an only anode and is at the voltage⁽³⁾

$$e_g' = \frac{e_a + k e_g}{1 + k} \dots \dots \dots (6)$$

where k is the amplification constant.

The space current is mainly governed by the electrostatic action of the system of electrodes, and if it be assumed that the two conditions above cited give equal space current, the characteristic of the triode will be expressed by the following equations which are obtained by replacing e_a in the equations (1) and (4) by e_g' :

$$i = G e_g'^{\frac{3}{2}} \dots \dots \dots (7)$$

$$i = \frac{2}{5} G e_f^{\frac{3}{2}} f\left(\frac{e_g'}{e_f}\right) \dots \dots \dots (8)$$

in which $f\left(\frac{e_g'}{e_f}\right)$ may be obtained from TABLE I on page 160,

and $G = 2.33 \times 10^{-6} \frac{\text{gride area}}{x_g^2}$.

For cylindrical electrodes, effective grid area = $2\pi x_g l$
and effective anode area = $2\pi x_a l = A$

hence $G = 2.33 \times 10^{-6} \frac{A}{x_a x_g}$,

in which x_a , x_g are the distances of the anode and grid surfaces respectively from the cathode axis. But the writer found by experiments that in the case of triodes having cylindrical anode and grid, and a cathode of other than a single axially-spanned filament, such as V-shaped, the values of x_a and x_g in the expression of

(3) W. H. Eccles: "Continuous Wave Wireless Telegraphy," p. 338.

G should be replaced by the mean shortest distances from the respective electrodes to the filament z_a and z_g , which should be taken in such a way as illustrated in Fig. 4.

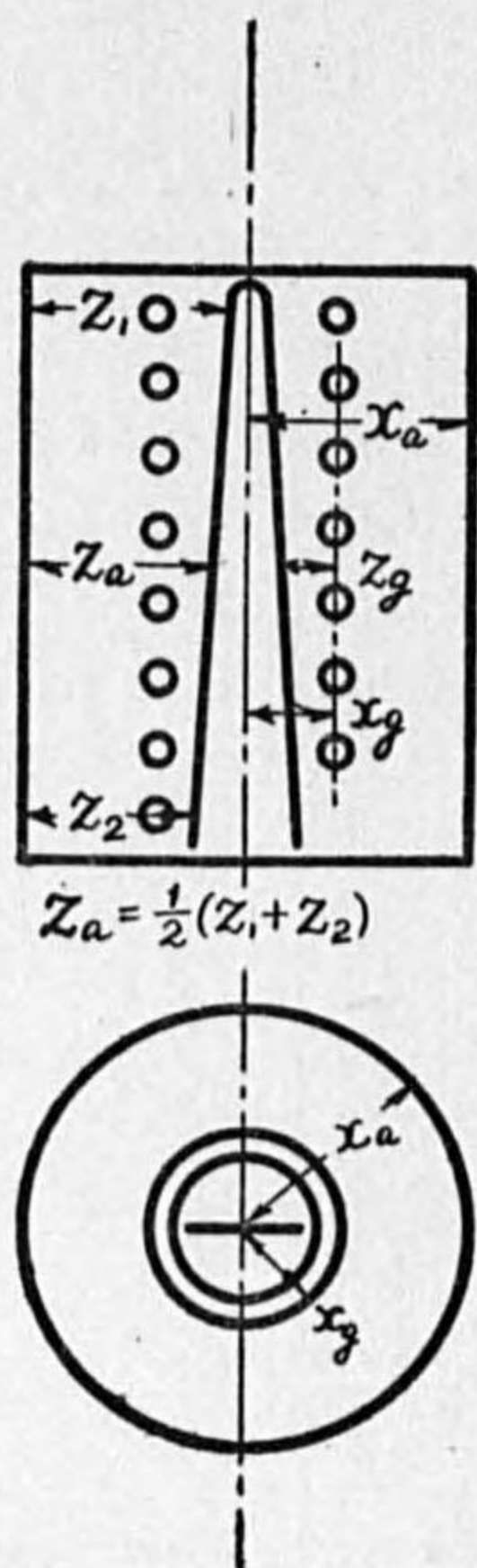


FIG. 4.

Then generally

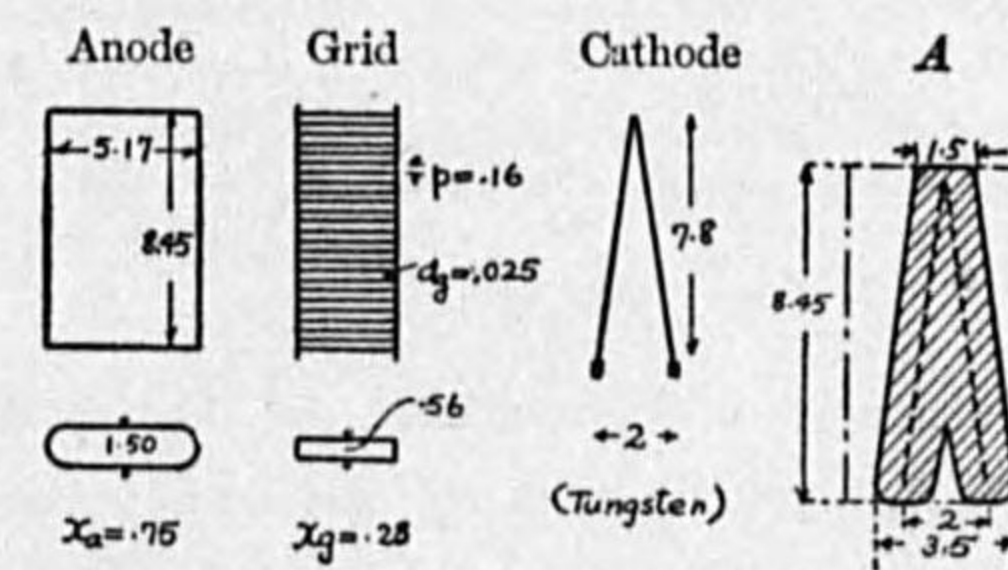
$$G = 2.33 \times 10^{-6} \frac{A}{z_a z_g} \dots \dots \dots (9)$$

This expression may also be applied to tubes with plane electrodes and in this case evaluation of the anode effective area A should be in accordance with that described for the diode. (Fig. 2)

Example 10. Characteristics of triodes with cylindrical anode and grid, and V-shaped filament.

Tube	UV-206 (R.C.A.)	228-A (Western E.L. Water-cooled)	S-53 (Nihon Musen K.)
Dimensions	$x_a = 2.0$ $z_a = 1.71$ $A = 103$ $x_g = 0.98$ $z_g = 0.69$ $e_g = 11$	$x_a = 1.73$ $z_a = 1.20$ $A = 148$ $x_g = 1.05$ $z_g = 0.50$ $e_g = 21.5$	$x_a = 2.77$ $z_a = 2.46$ $A = 146$ $x_g = 0.98$ $z_g = 0.67$ $e_g = 15$
Characteristics			

Example 11. Evaluation of the effective area of a plane anode.
Triode type Cymotron UV-204 (Tokyo Denki K. K.).
Dimensions are shown in Fig. 5.



(UV-204. T. E. C.)
FIG. 5.

The effective anode area

$$A = 2 \times 2.5 \times 8.45 = 42.3$$

and $G = 0.446 \times 10^{-6}$

If the actual area is taken

$$A' = 2 \times 5.17 \times 8.45 = 87.3$$

and $G' = 0.965 \times 10^{-3}$

The calculated curves are shown in Fig. 6, which shows the validity of taking $A = 42.3$.

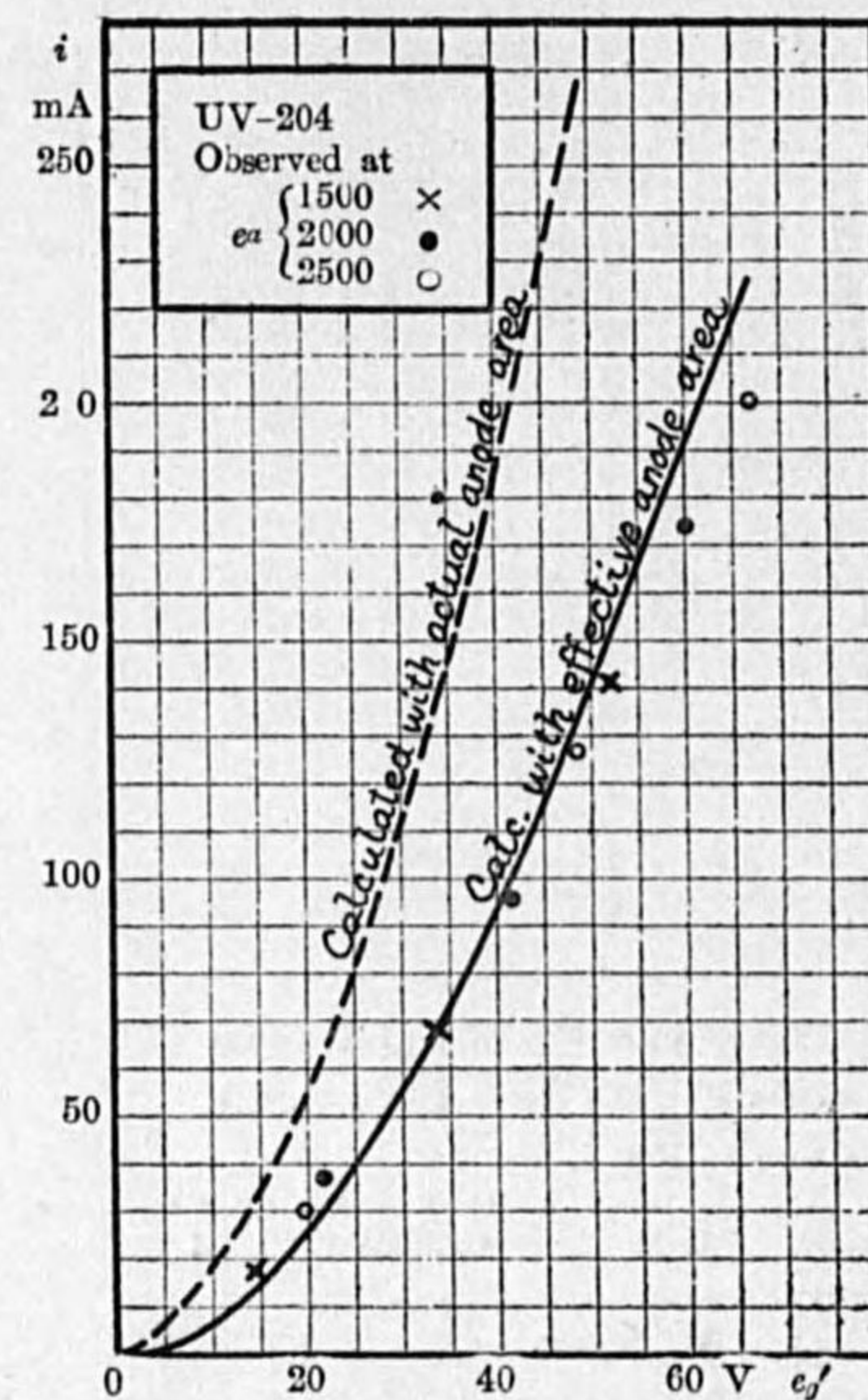


FIG. 6.

If e_a and e_g are given and k is computed by the method described in the following section, the equivalent grid voltage e_g' can be calculated by equation (6), and space current i at the given anode and grid voltages is obtained by equation (7) or (8).

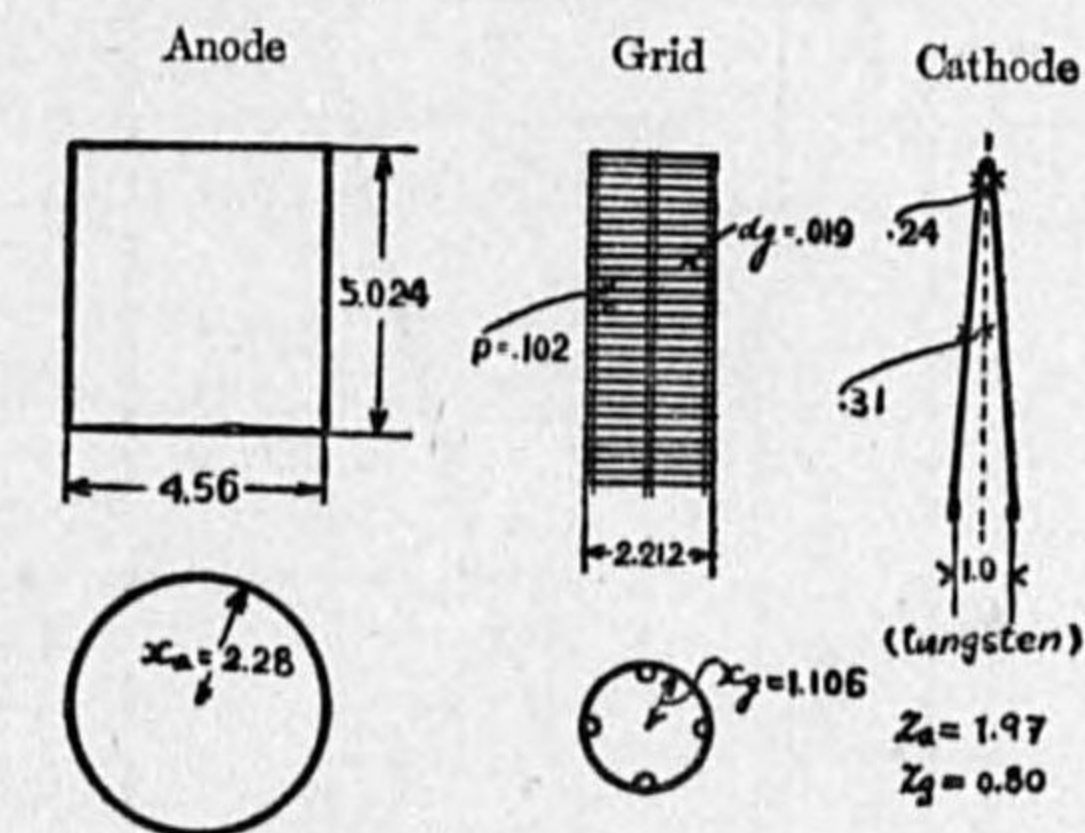
The depiction of the anode current-grid voltage characteristic curves may be simplified in the following manner.

First obtain the numerical relation between i and $\frac{e_g'}{e_f}$ and from it the relation

of i to e_g' for a given value of e_f . Then assume that $e_a = 0$, or $e_g' = \frac{k}{1+k} e_p$, and i versus e_g curve can be drawn and this corresponds to the characteristic for the anode voltage zero. In order to obtain a characteristic for any anode voltage e_a , this curve for $e_a = 0$ should be shifted horizontally to the negative grid voltage direction by an amount of $\frac{e_a}{k}$ in the grid voltage scale, because i is solely determined by $e_a + ke_g$ and an increase of anode voltage by e_a' can be compensated by the reduction of grid voltage by $\frac{e_a'}{k}$ to keep $e_a + ke_g$ unvaried and hence to give equal space current.

It should be remembered that a slightest error in the calculated value of k causes a considerable amount of error on the resulting values of i especially at high anode voltages.

Example 12. Computation of static characteristics.
Triode type TA10/600 (Philips' Lamp Works)
Dimensions are shown in Fig. 7.



(TA 10/600)

FIG. 7.

Calculation:

$$A = 2\pi \times 2.28 \times 5.02 = 72.0$$

$$z_a = 1.97 \quad z_g = 0.80$$

From equation (9)

$$G = 0.110 \times 10^{-3} \quad e_f = 12.5 \text{ (rating)}$$

$$\frac{2}{5} G e_f^{\frac{3}{2}} = 0.00208$$

i calculated by equation (8) is as follows and is plotted in Fig. 8, together with the observed data.

$\frac{e_g'}{e_f}$	e_g'	i
0	0	0
1	12.5	.0021
3	37.5	.0206
5	62.5	.050
8	100	.110

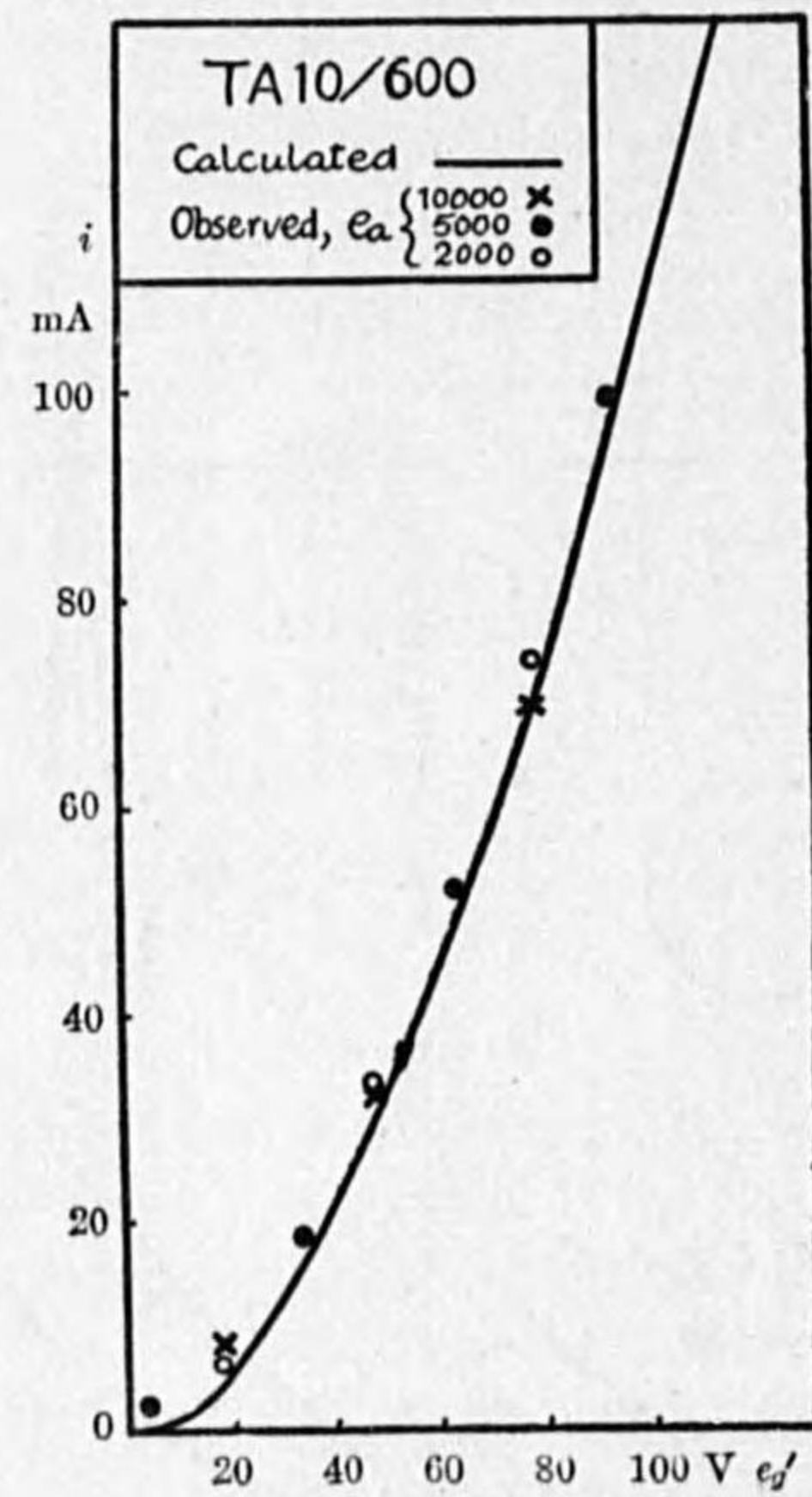


FIG. 8.

Amplification constant calculated by equation (12) given later is $k=112$, while the observed value is 114.

To draw i versus e_g characteristics, assume $e_a=0$, then

$$e_g' = \frac{k}{1+k} e_g$$

or $e_g = 1.01e_g'$

i to e_g relations are then obtained as in the following table.

Draw i versus e_g curve for $e_a=0$ as shown in Fig. 9. To obtain characteristic curve for an anode voltage e_a , shift this curve to the left by $\frac{e_a}{k}$ in grid voltage scale. The resulting curves are shown in Fig. 9, in which the observed data are also plotted.

i	e_g'	e_g
0	0	0
.0021	12.5	12.6
.0206	37.5	37.9
.050	62.5	63.2
.110	100	101

e_a	e_a/k
2,000	17.8
6,000	53.7
10,000	89.4

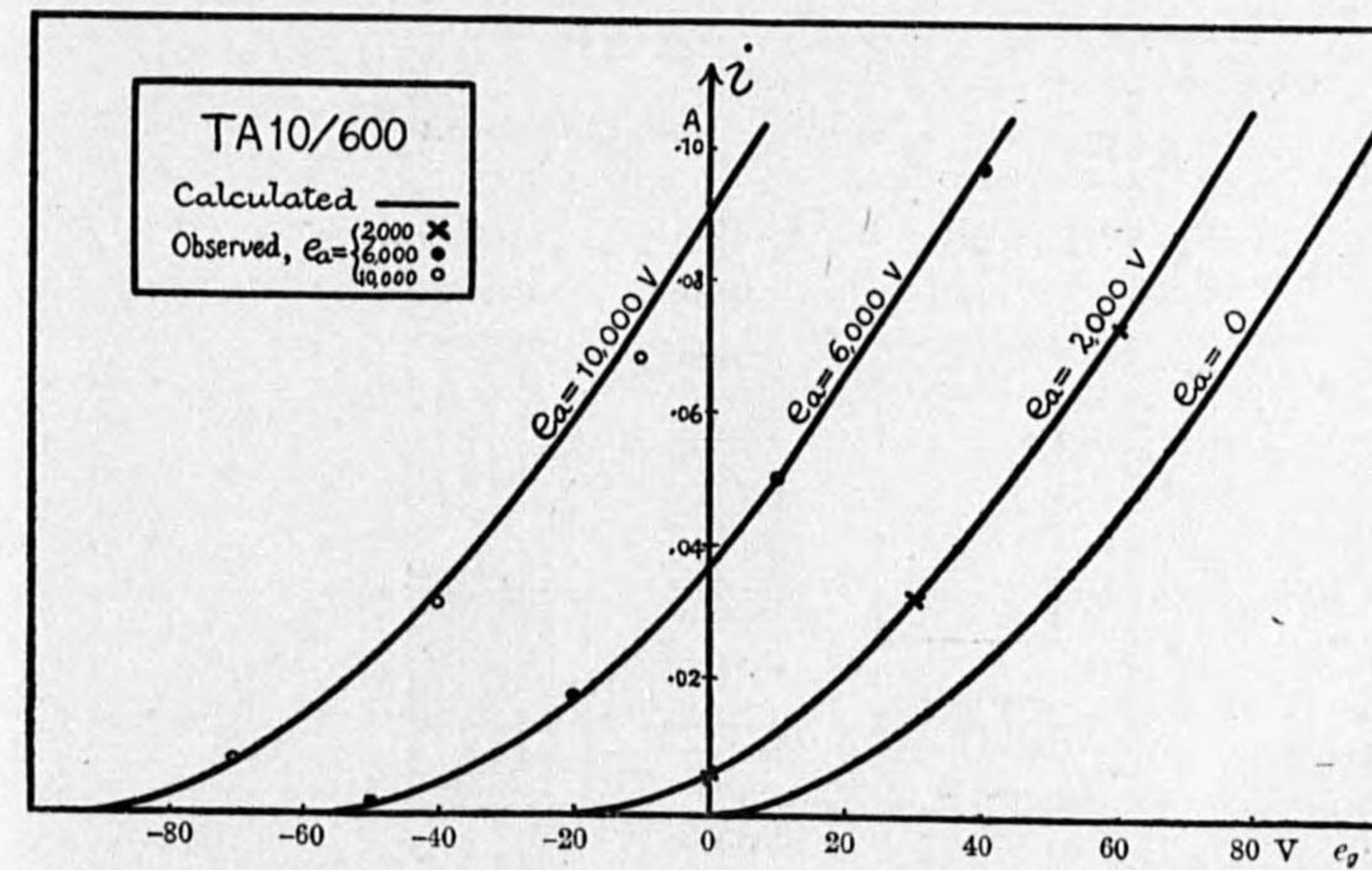


FIG. 9.

Observed data of the tube:

$$e_f = 12.5 \quad i_f = 6.58 \quad k = 114$$

e_a	e_g	$e_g' = \frac{e_a + ke_g}{1+k}$	i_a	i_g	$i = i_a + i_g$
10,000	-70	17.56	.008	0	.008
	-40	47.2	.032	0	.032
	-10	77.0	.069	0	.069
6,000	-50	2.63	.002	0	.002
	-20	32.7	.018	0	.018
	10	62.0	.050	.0010	.051
	40	91.8	.094	.0035	.098
2,000	0	17.4	.006	0	.006
	30	47.1	.030	.0025	.033
	60	76.8	.070	.0035	.074

Example 13. Computation of static characteristics.

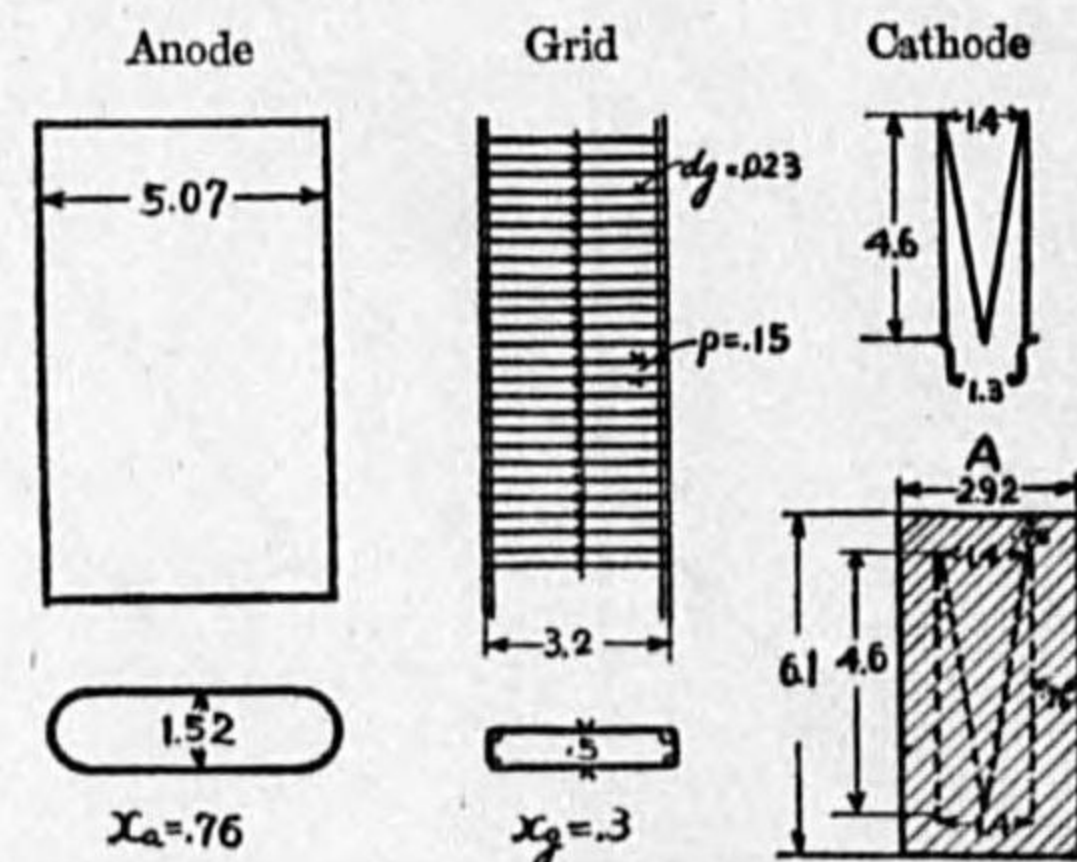
Triode type UV-204A (R. C. A.)

Calculations; refer to Fig. 10 for the dimensions,

$$x_a = x_a = 0.76 \quad x_g = x_g = 0.30 \quad A = 2 \times 6.1 \times 2.92 = 35.4$$

$$G = 0.361 \times 10^{-3}$$

$$e_f = 11 \text{ (rating)} \quad \frac{2}{3} Ge_f^{\frac{3}{2}} = 0.0052$$



(UV-204A)
FIG. 10.

$\frac{e_g'}{e_f}$	e_g'	$f\left(\frac{e_g'}{e_f}\right)$	i
0	0	0	0
2	22	4.65	.024
4	44	16.51	.086
6	66	32.5	.169
8	88	53.0	.276
10	110	74.0	.385

i versus e_g' curve is drawn as shown in Fig. 11, in which observed values are also plotted to show the validity of the calculation.

By the calculation explained later,

$$L_g = 12.6 \quad c = 1.6 \quad \mu_a = 0.50 \quad k = \frac{1.7 \times 12.6 \times .404}{.335} = 25.8 \quad (k \text{ observed} = 23)$$

To draw i versus e_g characteristics, first assume $e_a = 0$,

$$\text{then } e_g' = \frac{k}{1+k} e_g \text{ or } e_g = 1.04 e_g'$$

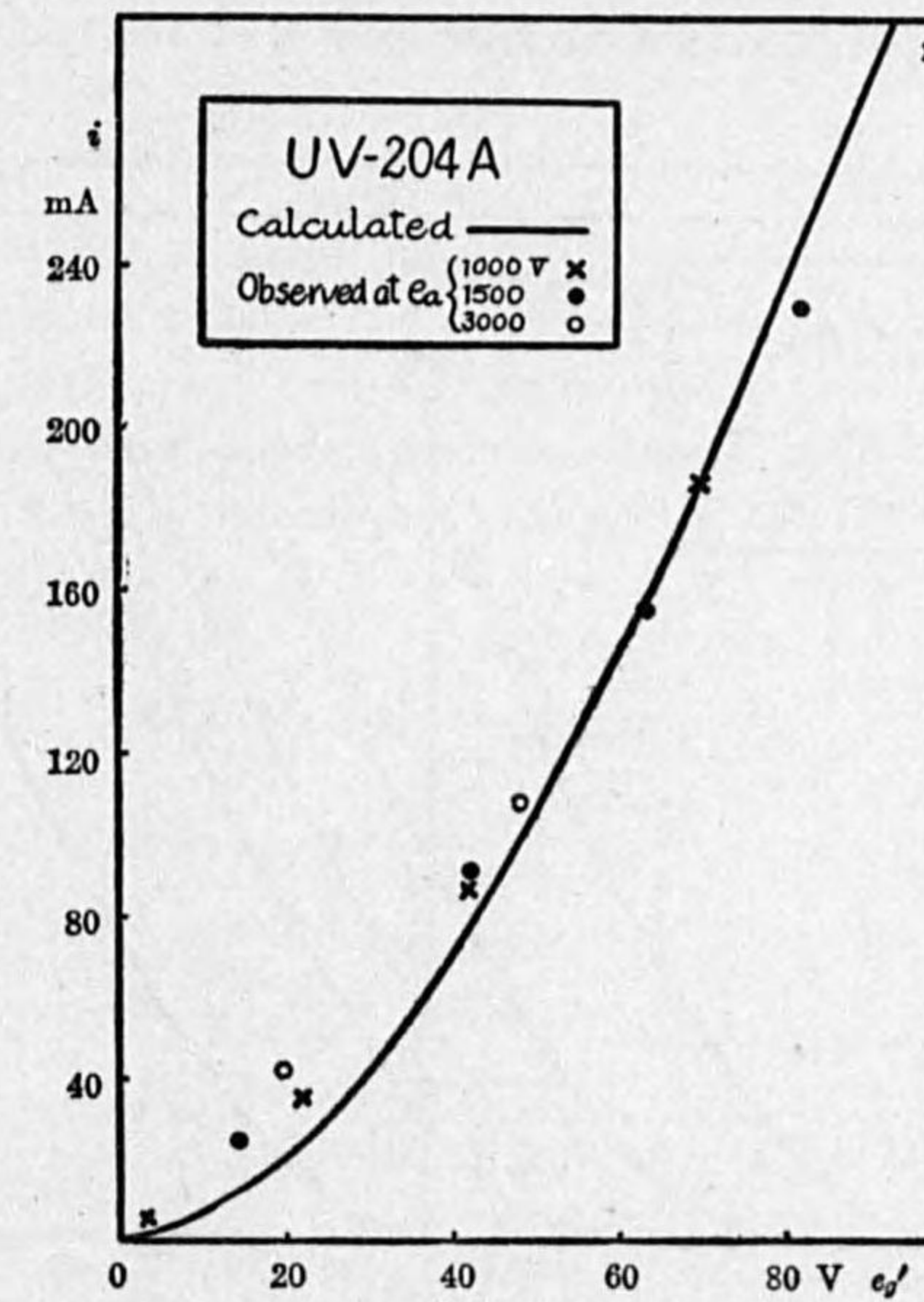


FIG. 11.

i	e_g'	e_g	e_a	$\frac{e_a}{k}$
0	0	0	1,000	39
.024	22	23	1,500	58
.086	44	46	2,000	77
.169	66	69	3,000	116
.276	88	92		
.385	110	114		

Draw i versus e_g curve for $e_a=0$ as shown in Fig. 12.

For any anode voltage e_a this curve should be shifted by $\frac{e_a}{k}$ given in the table.

The resulting characteristic curves are shown in Fig. 12. There is a considerable error in the curve for $e_a=3,000$ V. This is caused by the discrepancy of the calculated value of k from the actual one. If the observed value of k is taken in the above calculations the resulting curves are of course consistent with the calculated ones.

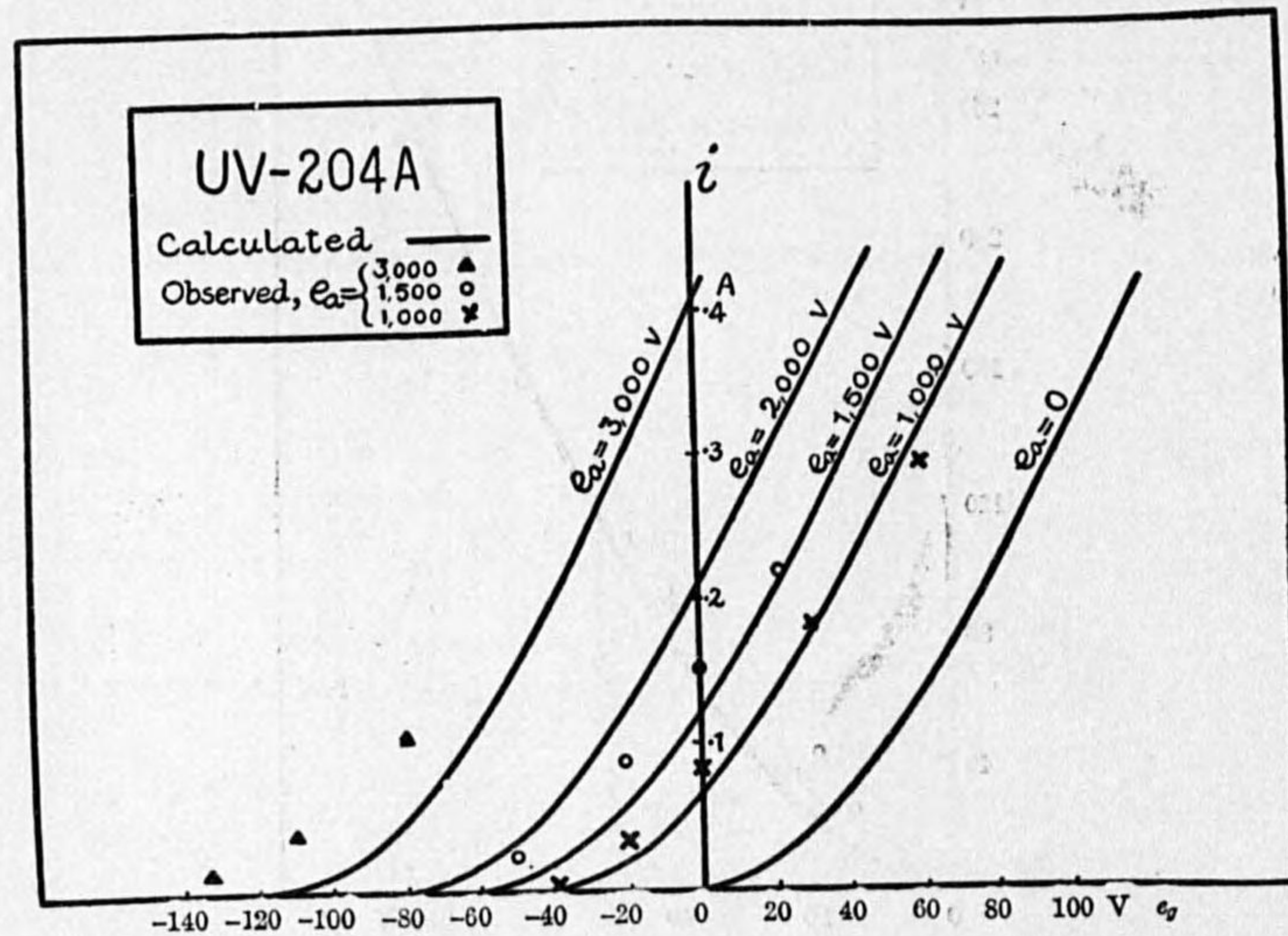


FIG. 12.

Observed data of the tubes:

$$e_g=11 \quad i_g=3.9 \quad k=23$$

e_a	e_g	$e_g' = \frac{e_a + ke_g}{1+k}$	i_a	i_g	$i = i_a + i_g$
1,000	-40	3.3	.005	0	.005
	-21	22	.035	0	.035
	0	42	.086	0	.086
	30	70	.172	.011	.183
	60	98	.274	.019	.293
1,500	-51	14	.024	0	.024
	-21	42	.090	0	.090
	0	63	.154	.001	.155
	21	82	.220	.009	.229
3,000	-131	0	.013	0	.013
	-110	19.6	.041	0	.041
	-80	43	.107	0	.107

The space current i is the sum of anode and grid currents,

$$i = i_a + i_g \quad \dots \dots \dots (10)$$

As long as the grid is negative, $i_g=0$ and $i_a=i$, but when grid becomes positive, grid current begins to flow. In the ordinary tubes, the grid is so constructed that it does not greatly absorb the space current, and as long as the positive grid voltage is low, grid current is not appreciable compared with anode current, and in this region the following formulas are applicable for the rough estimation of the grid current:⁽⁴⁾

$$i_g = \gamma a \sqrt{\frac{e_g}{e_a}} \cdot i_a = \frac{\gamma a \sqrt{\frac{e_g}{e_a}}}{1 + \gamma a \sqrt{\frac{e_g}{e_a}}} i.$$

and hence

$$i_a = \frac{i}{1 + \gamma a \sqrt{\frac{e_g}{e_a}}} \quad \dots \dots \dots (11)$$

in which $\gamma = \sqrt{\frac{\log \frac{x_a}{r_c}}{\log \frac{x_g}{r_c}}}$ are usually of the order: $\gamma = 1 - 2 \div 1.5$.

(4) H. Lange: Z f. hochfrequ. Techn., p. 105, April 1923.

The writer's empirical formula $i_g = 0.2 \sqrt{\frac{ke_g}{e_a + ke_g}} \cdot i$ is also applicable in some cases. Error in i_g does not much affect the value of i_a at low grid voltages.

When the grid voltage becomes so high as to approach the anode voltage, the characteristics are severely affected by secondary emissions from the electrodes, and grid current usually increases very rapidly while anode current falls off in equal rate.

At $e_g = 0$, the electron current is totally absorbed in the grid if the grid voltage is positive.

Example 14. Calculation of grid current.

Tube	Observed data					Calculated grid current	
	e_a	e_g	i_a	i_g	i	$i_g = 1.5 a \sqrt{e_g/e_a} i_a$	$i_g = 0.2 \sqrt{\frac{ke_g}{e_a + ke_g}} \cdot i$
102-D ($a=.156$) ($k=30$)	100	5.2	.0046	.0003	.0049	.00025	.00030
	100	8.3	.0074	.0004	.0078	.00050	.00051
	148	5.2	.0065	.0003	.0068	.00029	.00039
	148	8.3	.0100	.0004	.0104	.00055	.00065
UV-199 ($a=.108$) ($k=6.6$)	20	6	.0023	.0002	.0025	.00020	.00014
	20	16	.0040	.0005	.0045	.00058	.00027
	60	10	.0038	.0003	.0041	.00025	.00020
	100	16	.0042	.0003	.0045	.00027	.00022
MT-4 ($a=.274$) ($k=140$)	1000	100	.072	.011	.083	.0093	.0084
	1000	140	.120	.012	.132	.018	.0135
	2000	80	.057	.009	.066	.0047	.0064
	2000	120	.112	.010	.122	.0112	.0120
	3000	20	.014	.002	.016	.0015	.0012
	3000	140	.153	.008	.161	.043	.0160
MT-7 A ($a=.153$) ($k=80$)	1000	80	.100	.016	.116	.0064	.0085
	1000	139	.230	.028	.258	.0195	.019
	5000	20	.106	.005	.111	.0016	.0042
	5000	70	.208	.015	.223	.0037	.0127
MT-9 ($a=.245$) ($k=90$)	1000	80	.305	.027	.332	.031	.031
	3000	40	.223	.012	.235	.0094	.017
	5000	20	.230	.003	.233	.0033	.012

Tube	Observed data					Calculated grid current	
	e_a	e_g	i_a	i_g	i	$i_g = 1.5 a \sqrt{e_g/e_a} i_a$	$i_g = 0.2 \sqrt{\frac{ke_g}{e_a + ke_g}} \cdot i$
UV-204 A ($a=.16$) ($k=25$)	1000	30	.172	.011	.183	.006	.010
	1000	60	.274	.019	.293	.009	.018
	5000	21	.220	.009	.229	.006	.009
UV-201 A ($a=.105$) ($k=7$)	20	5	.0025	.0001	.0026	.0002	.00013
	20	15	.0095	.0013	.0108	.0013	.00064
	60	5	.0065	.0001	.0066	.0003	.00026
	60	10	.0113	.0004	.0117	.0007	.00056

Example 15. Characteristics at highly positive grid voltage (Fig. 13). A tube, with a grid of remarkable secondary emission (Fig. 14), and another with less appreciable secondary emission (Fig. 15).

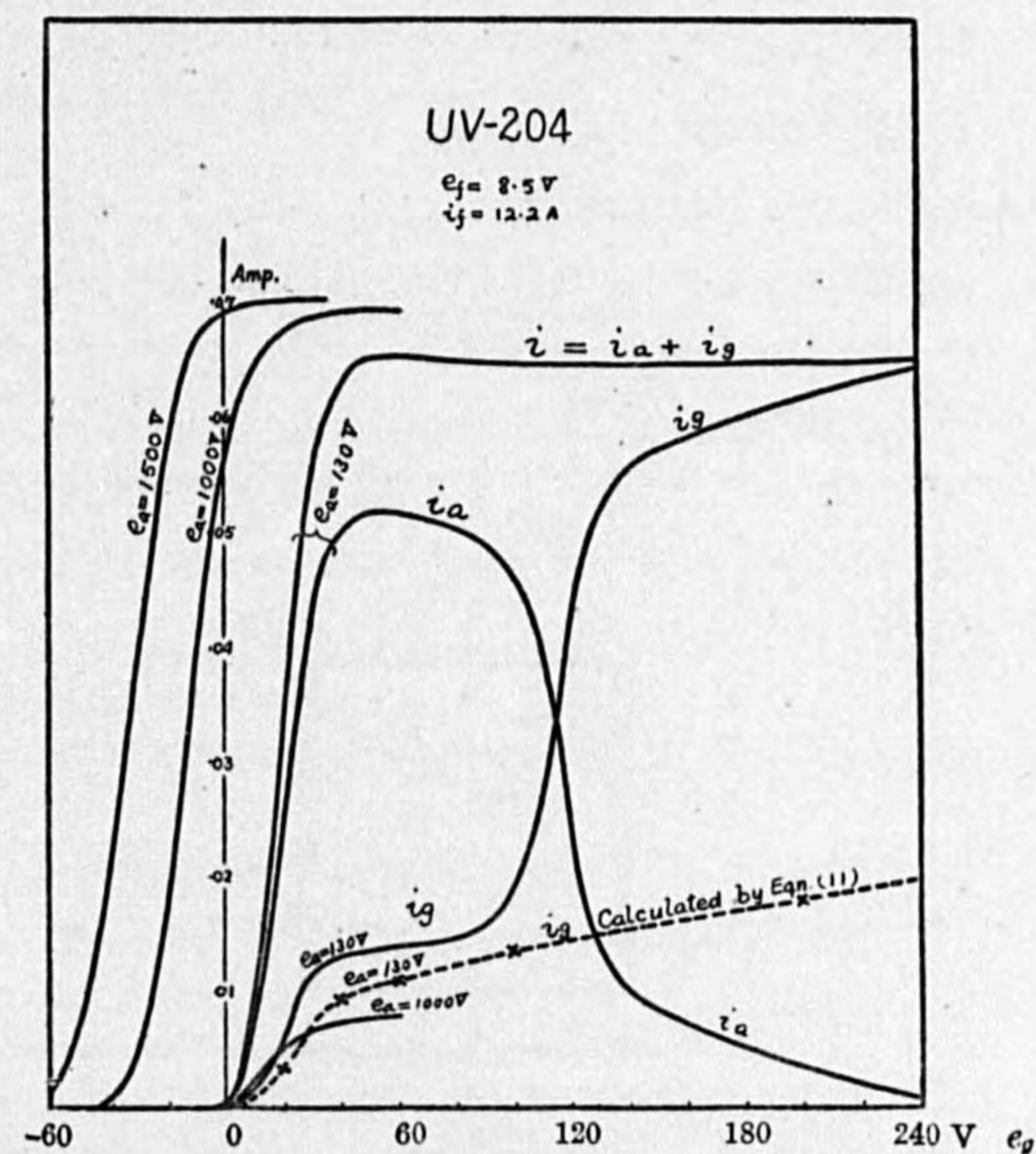


FIG. 13.

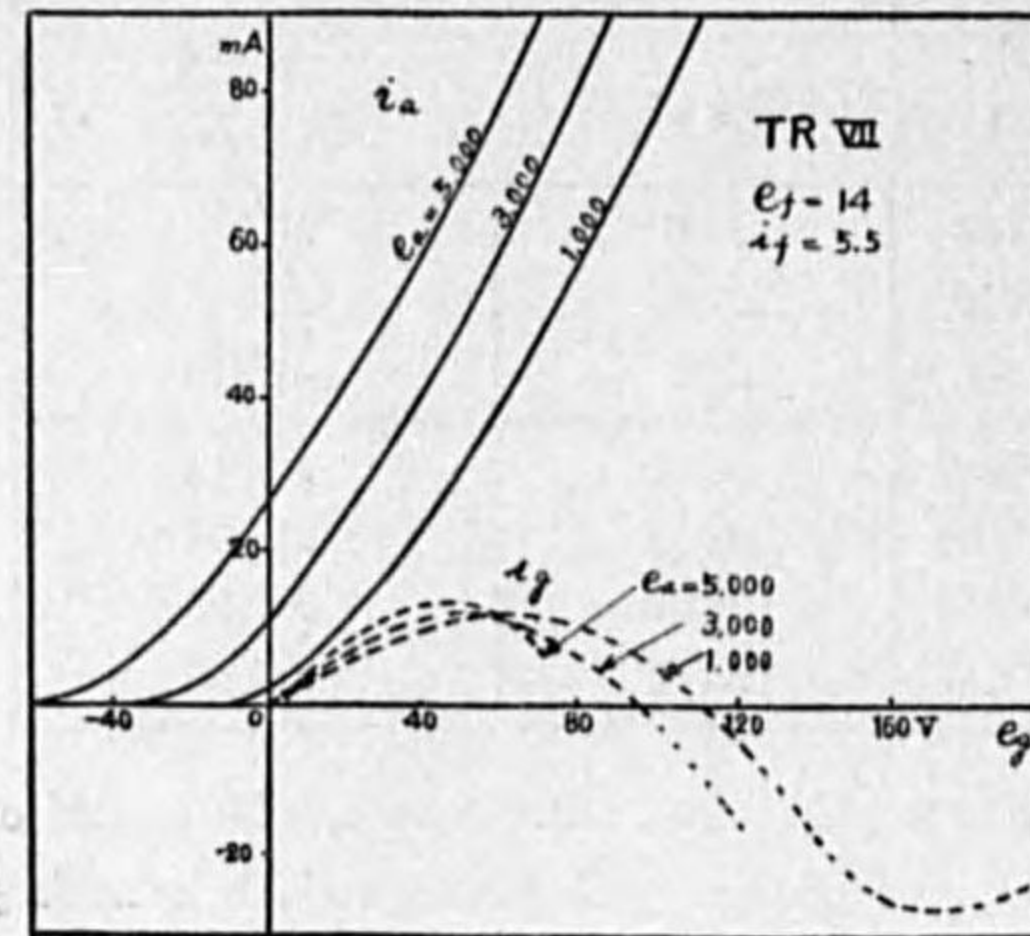


FIG. 14.

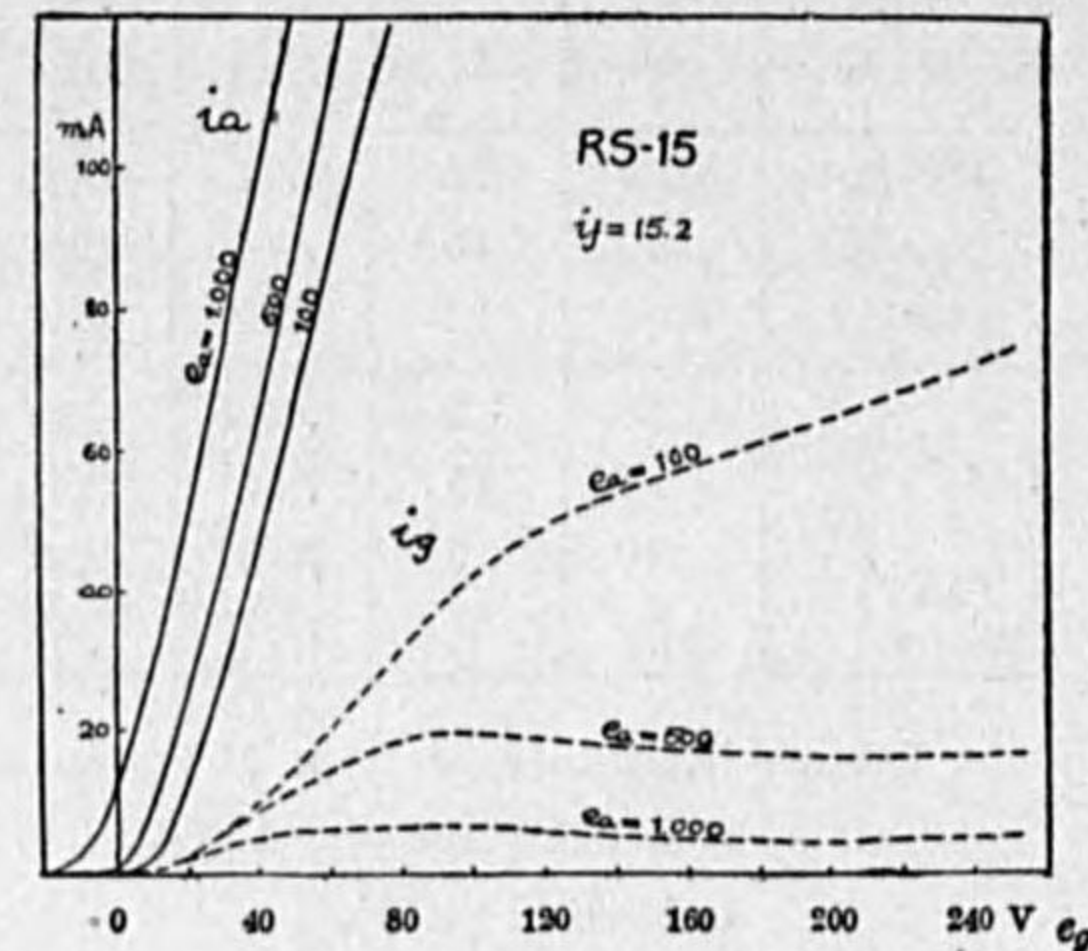


FIG. 15.

(3) Parameters of a Triode.

(i) Amplification Constant.

By the amplification constant k is meant that the electrostatic influence of the grid upon the cathode is k times that of the anode, and theoretical formulas are available for its computation.

Notations regarding the electrode dimensions are illustrated in Fig. 16,

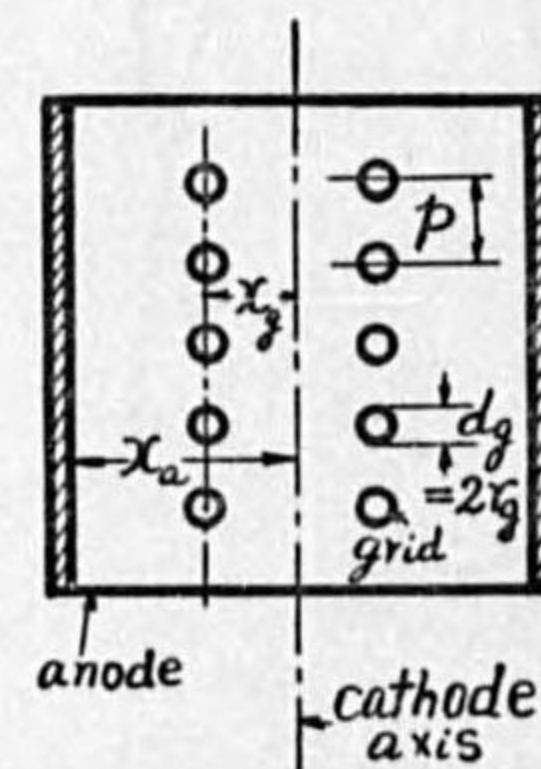


FIG. 16.

For $r_g \ll p \ll x_g$,

and for plane-electrode tubes⁽⁵⁾,

$$k = \frac{2\pi x_g}{p} \cdot \frac{\frac{x_a}{x_g} - 1}{\log_e \frac{p}{2\pi r_g}} \dots \dots \dots (k1)$$

and for cylindrical-electrode tubes⁽⁶⁾,

$$k = \frac{2\pi x_g}{p} \cdot \frac{\log \frac{x_a}{x_g}}{\log \frac{p}{2\pi r_g}} \dots \dots \dots (k2)$$

if the condition $r_g \ll p \ll x_g$ is not fulfilled, the more general formula for cylindrical-electrode tubes is to be applied,⁽⁷⁾

$$k = \frac{\frac{2\pi x_g}{p} \cdot \log \frac{x_a}{x_g} - \log \cosh \frac{2\pi r_g}{p}}{\log \cosh \frac{2\pi r_g}{p} - \log \sinh \frac{2\pi r_g}{p}} \dots \dots \dots (k3)$$

The formulas for cylindrical electrodes were originally derived for grid wires parallel to the filament, but they are equally applicable to grids of a spiral or a system of parallel wires spanned crossways to the length of the filament.

Example 16. Amplification constant of tubes with simple structure.

(a) Triode type R (S. F. R.)

A receiving tube with cylindrical anode and spiral grid. Dimensions are shown in Ex. 46 on page 69.

$$x_a = 0.44 \quad x_g = 0.18 \quad p = 0.16 \quad d_g = 0.028 \quad r_g = 0.014$$

$$\frac{2\pi x_g}{p} = 7.1 \quad \frac{2\pi r_g}{p} = 0.55 \quad \log \frac{x_a}{x_g} = 0.39$$

(5) W. Schottkey: Archiv f. Elektrotechnik, 8, p. 21, 1919.

(6) M. Abraham: Archiv f. Elektrotechnik, 8, p. 42, 1919.

R. W. King: Phys. Rev., 15, p. 256, 1920.

(7) F. B. Vogdes: Phys. Rev., 24, p. 683, 1924 and 25, p. 255, 1925.

$$(k3) \quad k = \frac{7.1 \times 0.39 - 0.06}{0.064 + 0.237} = 9.2$$

$$(k2) \quad k = 7.1 \times \frac{0.39}{0.26} = 10.6$$

Observed value of $k=9.8$

By equation (12)

$$k=9.2$$

(b) Triode type A B T (made at the Laboratory)

Electrode configurations are similar to the above.

$$x_a=0.20 \quad x_g=0.14 \quad p=0.12 \quad r_g=0.0085$$

$$\frac{2\pi x_g}{p} = 7.3 \quad \frac{2\pi r_g}{p} = 0.44 \quad \log \frac{x_a}{x_g} = 0.155$$

$$(k3) \quad k = \frac{7.3 \times 0.155 - 0.04}{0.04 + 0.345} = 2.8$$

$$(k2) \quad k = 7.3 \times \frac{0.155}{0.357} = 3.2$$

Observed value of $k=2.9$

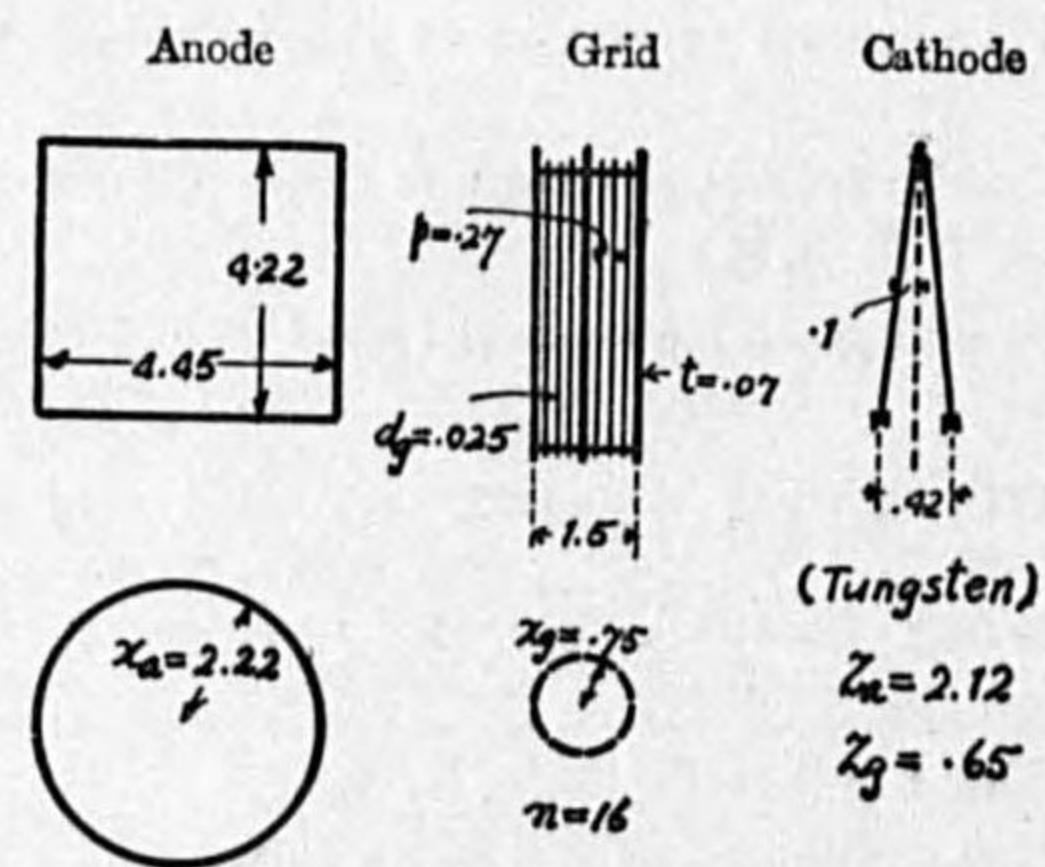
By equation (12),

$$L_g=7.3 \quad c=1 \quad \pi a=0.44, \quad k = \frac{7.3 \times 0.155}{0.385} = 2.9$$

Example 17. Triodes with grid wires arranged in parallel to the filament.

(a) Type P A V (the Laboratory)

Dimensions are shown in Fig. 17.



(PAV)
FIG. 17.

Of 16 grid wires, 4 wires forming the support have the radius $r_g' = 0.035$ and the other 12 wires $r_g'' = 0.0125$ average radius being $r_g = 0.018$

$$x_a = 2.22 \quad x_g = 0.75 \quad n = 16$$

$$p = \frac{2\pi x_g}{n} = 0.27 \quad \log \frac{x_a}{x_g} = 0.472$$

$$(k3) \quad k = \frac{16 \times 0.472 - 0.029}{0.029 + 0.433} = 16.3$$

k observed = 16.7 (at $e_a = 1500$, $e_g = -30$)

By equation (12),

$$L_g = 16 \quad c = 1 \quad \pi a = 0.38$$

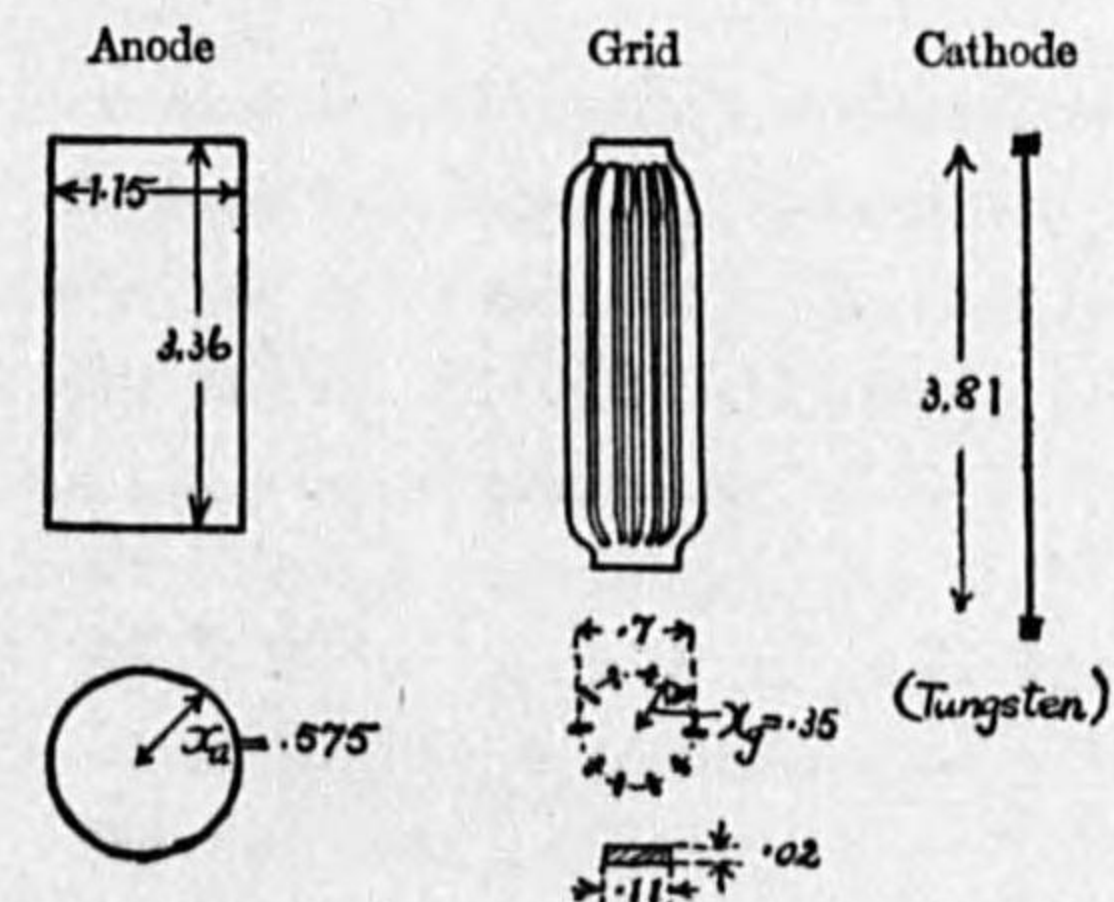
$$k = \frac{16 \times 0.472}{0.444} = 17.0$$

(b) Type B N (Siemens Halske A. G.)

The grid is formed of wires of rectangular cross-section (Fig. 18). Consider an equivalent circular wire of equal perimeter, as the electrostatic capacity is mainly governed by the surface area.

Thus

$$r_g = \frac{2 \times (0.11 + 0.02)}{2\pi} = 0.041$$



(BN)
FIG. 18.

$$n=10 \quad x_a=0.58 \quad x_g=0.35$$

$$p = \frac{2\pi r_g}{n} = 0.22 \quad \log \frac{x_a}{x_g} = 0.219 \quad \frac{2\pi r_g}{p} = 1.17$$

$$(k3) \quad k = \frac{10 \times 0.219 - 0.248}{0.248 - 0.164} = 23.1$$

$$k \text{ observed} = 26$$

In an actual triode in which anode and grid are plane, the cathode is not actually plane but is a filament arranged on a plane surface and, accordingly, does not strictly conform to the condition from which the formula has been derived. But by trying the formulas on these cases, the writer has found that the formula for plane ($k1$) is applicable for a tube with W-shaped filament, while it gives a somewhat larger value for a tube with V-shaped filament. The formula for cylinder ($k2$), if applied to these tubes, gives lower values than observed ones. Comparing the two formulas, we find that they are different only in terms of $\frac{x_a}{x_g}$ and

$$\frac{k \text{ plane}}{k \text{ cylinder}} = \frac{\frac{x_a}{x_g} - 1}{\log_e \frac{x_a}{x_g}}$$

This ratio is shown in a curve in Fig. 19.

The writer applied the formula for cylindrical electrodes to various types of plane electrode tubes and the ratio of the observed to the calculated values for each tube was computed and plotted into Fig. 19. From this we know that for approximate calculations of k for plane-electrode tubes, the formula for cylindrical electrodes may be applied if some factor is multiplied. The two straight lines in Fig. 19 give these factors for either W-shaped or V-shaped filament, and these factors, being designated by c , are tabulated in TABLE II on page 160. For plane-electrode tubes in which the grid consists of a mesh, the value of k computed by the formula for cylinder agrees well with the observed one, and c is to be taken as unity.

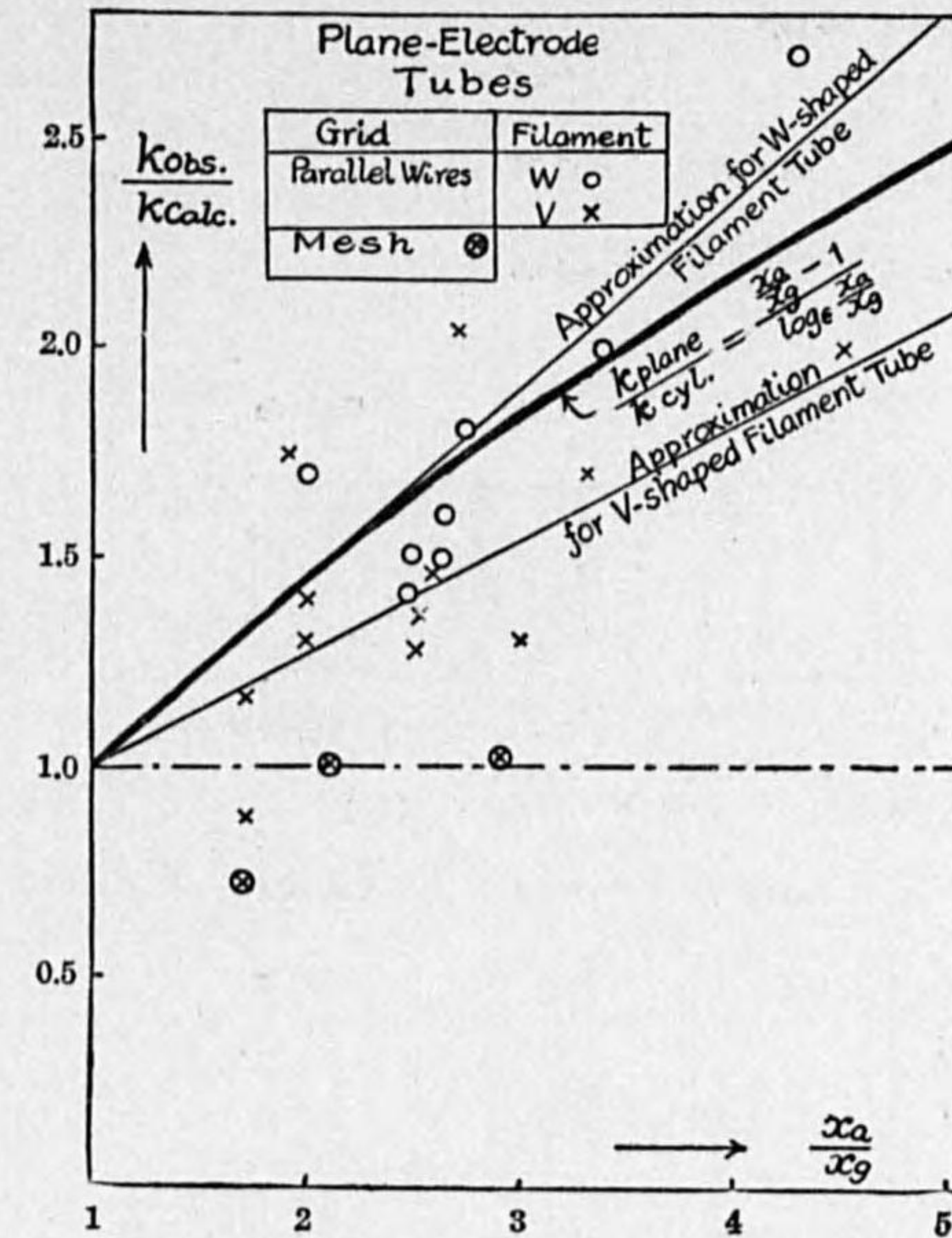


FIG. 19.

Example 18. A plane-electrode tube with a cathode of W-shaped filament.

Type UV-203 (Tokyo Denki K. K.)

Dimensions, (Fig. 20)

$$x_a=0.49 \quad x_g=0.19 \quad p=0.12 \quad r_g=0.0085$$

$$\frac{2\pi r_g}{p} = 9.95 \quad \frac{2\pi r_g}{p} = 0.445 \quad \frac{p}{2\pi r_g} = 2.25 \quad \frac{x_a}{x_g} = 2.60 \quad \log \frac{x_a}{x_g} = 0.412$$

By the equation for plane,

$$(k1) \quad k = 9.95 \times \frac{1.60}{2.34 \times 0.353} = 19.6$$

by the equation for cylinder,

$$(k2) \quad k = 9.95 \times \frac{0.412}{0.353} = 11.6$$

The observed value of $k=15.9$

By equation (12),

$$L_g = 9.95 \quad \pi a = 0.445 \quad c = 1.74$$

$$k = \frac{9.95 \times 0.412 \times 1.74}{0.467} = 15.3$$

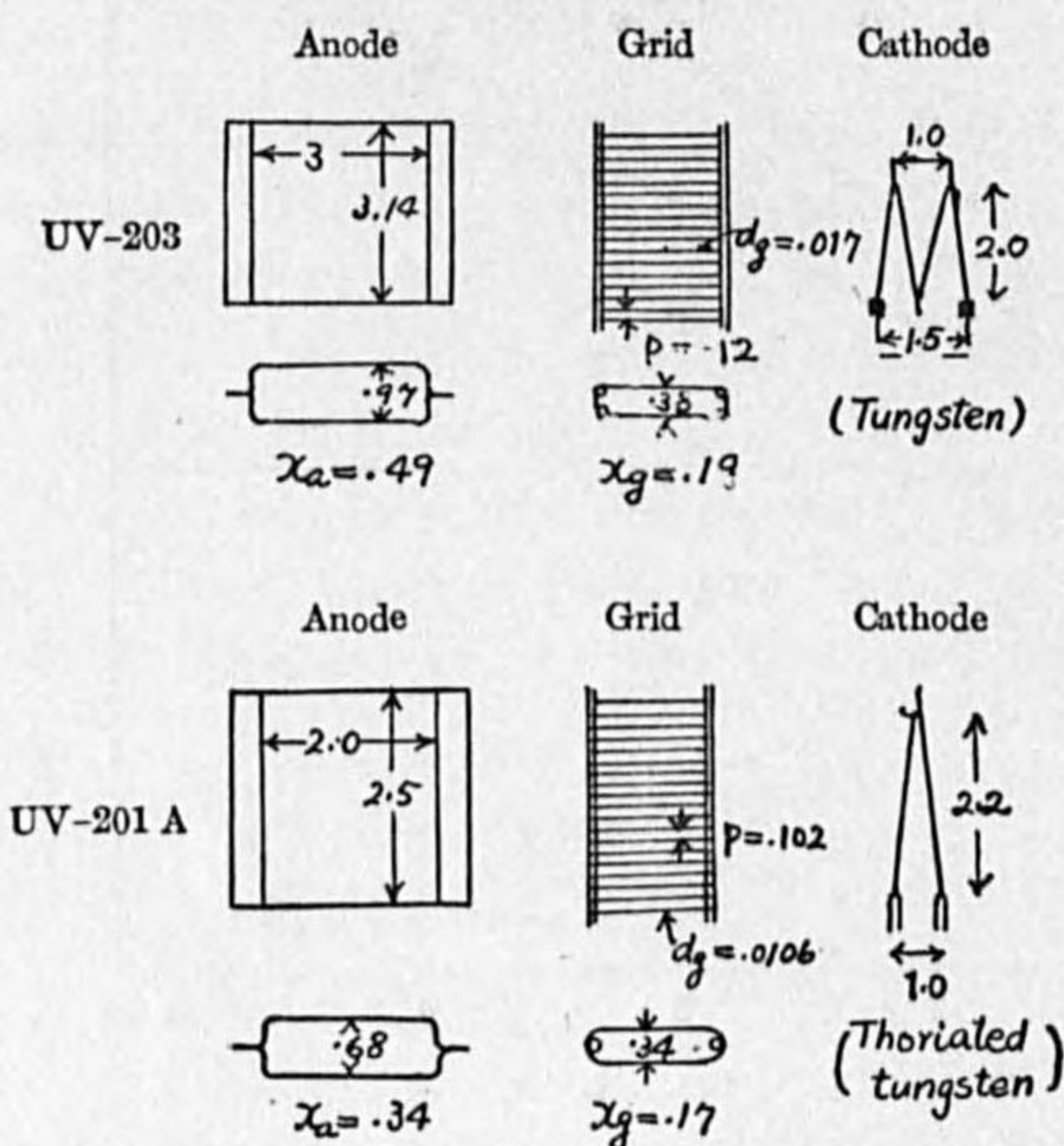


FIG. 20.

Example 19. A plane electrode tube with a cathode of V-shaped filament.

Type UV-201A (R. C. A)

Dimensions (Fig. 20.):

$$x_a = 0.34 \quad x_g = 0.17 \quad p = 0.102 \quad r_f = 0.0053$$

$$\frac{2\pi r_g}{p} = 10.5 \quad \frac{2\pi r_g}{p} = 0.33 \quad \frac{p}{2\pi r_g} = 3.03 \quad \frac{x_a}{x_g} = 2.0 \quad \log \frac{x_a}{x_g} = 0.301$$

By the equation for plane,

$$k = 10.5 \times \frac{1.0}{2.30 \times 0.482} = 9.4$$

By the equation for cylinder,

$$k = 10.5 \times \frac{0.301}{1.022} = 3.1$$

k observed = 8.2

By equation (12),

$$L_g = 10.5 \quad \pi a = 0.33 \quad c = 1.30$$

$$k = \frac{10.5 \times 0.301 \times 1.30}{0.505} = 8.1$$

The formula (13) is a more general form of (12), and this is to be taken as a standard formula. In this formula $\log \cosh \frac{2\pi r_g}{p}$ is of the order of 0.1 and is small compared with $\frac{2\pi x_g}{p} \log \frac{x_a}{x_g}$ which is usually of the order of 10 to 100, and so the formula may be reduced to a simpler form:

$$k = \frac{c \frac{2\pi x_g}{p} \log \frac{x_a}{x_g}}{\log \coth \frac{2\pi r_g}{p}}$$

In the above formula grid is considered to be formed of parallel wires only. But in actual cases supports are usually added and in some cases grid is constructed of wires weaved into a mesh.

The writer has brought out the following deductions in order to make the formula equally applicable to these cases.

The quantity $\frac{2\pi x_g}{p}$ means the "total active length of grid wires per unit axial length of the grid," because $2\pi x_g$ is the length of one turn of grid wire in circular form and $\frac{1}{p}$ is the number of turns per unit length. This quantity is denoted by L_g thus

$$L_g = \frac{2\pi x_g}{p}$$

Example 20. A cylindrical electrode tube, with a spiral wire of wide pitch of winding.
Type RE-84 (Telefunken G.)

Dimensions are shown in Ex. 43 on page 71.

$$x_a = 0.253 \quad x_g = 0.125 \quad p = 0.25 \quad r_g = 0.025$$

$$\frac{2\pi r_g}{p} = 3.14 \quad \frac{2\pi r_g}{p} = 0.628 \quad \log \frac{x_a}{x_g} = 0.323$$

$$k = \frac{3.14 \times 0.323}{0.25} = 3.96$$

$$k \text{ observed} = 4.5$$

If actual length of the spiral grid wire per unit axial length of the grid is taken instead of $\frac{2\pi r_g}{p}$

$$L_g = \sqrt{1 + \left(\frac{2\pi r_g}{p}\right)^2} = 3.30$$

and

$$k = \frac{3.30 \times 0.323}{0.25} = 4.4$$

which is more coincident with the observed value.

For a grid consisting of a square mesh of very thin wires

$$L_g = \frac{4\pi x_g}{p},$$

but when grid wire is not of small diameter, effect of overlapping of the wires should be considered. At each crossing point of two wires, active length of one wire is reduced by an amount equal to the diameter of the wire, and as the number of the crossing per unit axial length of grid is $\frac{2\pi x_g}{p^2}$ (Fig. 21),

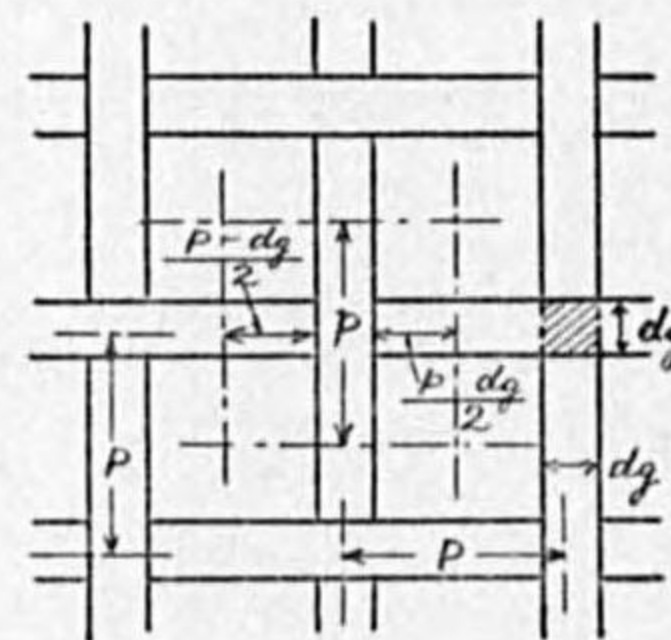


FIG. 21.

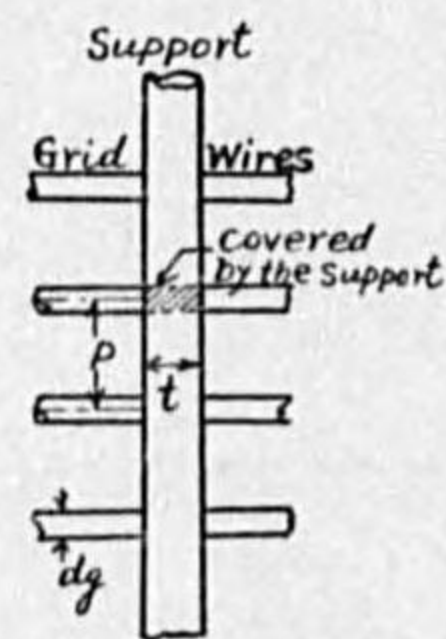


FIG. 22.

$$L_g = \frac{4\pi x_g}{p} - \frac{2\pi x_g}{p^2} d_g = \frac{4\pi x_g}{p} \left(1 - \frac{r_g}{p}\right)$$

Effect of grid support should be considered in the same way and for a grid of parallel wires,

$$L_g = \frac{2\pi x_g}{p} + s - \frac{st}{p},$$

in which s is the number of grid supporting wires which is active in influencing on the space charge or is in the path of the electron current. $\frac{st}{p}$ is the amount of reduction of effective length of the grid wires due to the grid support covering a portion of each grid wire. (Fig. 22)

For a grid made of a mesh, the effect of supports may not be considered, as the total length of the wires is very large, and moreover the increase of L_g due to supports is usually canceled by the reduction of it due to the support covering a portion of the mesh.

The quantity $\frac{2\pi r_g}{p}$ in the formula of k on page 35 signifies π -times $\frac{d_g}{p}$ or " π -times the ratio of the grid conductor projected area to the grid surface area," and this ratio of areas being denoted by a ,

$$\pi a = \pi \frac{(\text{grid wire projected area per unit length of the grid})}{2\pi x_g}$$

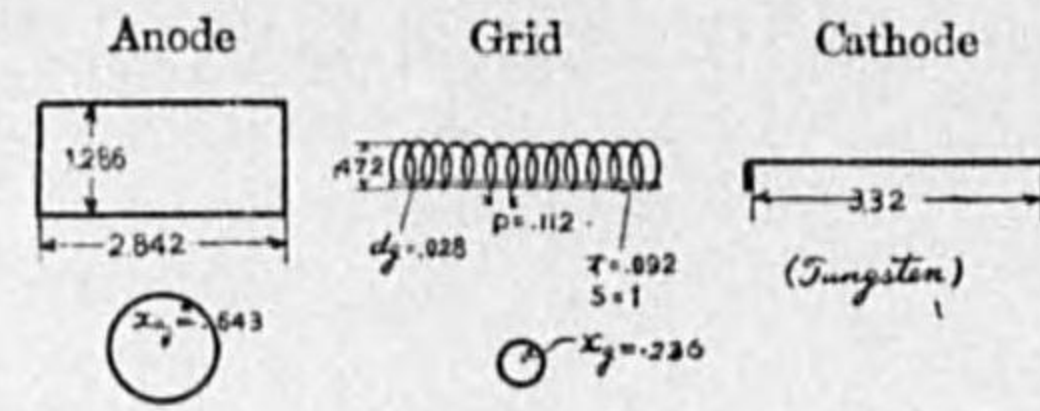
For a grid of a mesh or of a system of parallel wires,

$$\pi a = \frac{L_g d_g}{2x_g} = \frac{L_g r_g}{x_g}.$$

If the parallel wire grid has supports,

$$\pi a = \frac{(L_g - s) d_g + st}{2x_g}$$

Example 21. A triode with grid supported by a thick wire.
Type TA 08/10 (Philips' Lamp Works)



(TA 08/10)
FIG. 23.

$$x_a = 0.643 \quad x_g = 0.236 \quad p = 0.112 \quad r_g = 0.014$$

$$\log \frac{x_a}{x_g} = 0.436$$

Without considering the support;

$$\frac{2\pi x_g}{p} = 13.2 \quad \frac{2\pi r_g}{p} = 0.79 \quad k = 31.6$$

Considering the support, $s=1$ $t=0.092$

$$L_g = \frac{2\pi x_g}{p} + s \left(1 - \frac{t}{p}\right) = 13.4 \quad \pi a = \frac{(L_g - s)d_g + st}{2x_g} = 0.93$$

$$k = 43$$

Observed value of $k=46$

Example 22. A triode with grid formed of a mesh.

Type MT-4 (Marconi Co.)

Dimensions (See example 38, page 61)

$$x_a = 2.17 \quad x_g = 0.93 \quad p = 0.13 \quad r_g = 0.011 \quad \log \frac{x_a}{x_g} = 0.368$$

Without consideration of the overlapping of grid wires,

$$L_g = \frac{4\pi x_g}{p} = 90 \quad \pi a = \frac{L_g r_g}{x_g} = 1.06$$

$$k = \frac{90 \times 0.368}{0.105} = 315$$

Considering the overlapping;

$$L_g = \frac{4\pi x_g}{p} \left(1 - \frac{r_g}{p}\right) = 90 \times 0.91 = 81 \quad \pi a = \frac{L_g r_g}{x_g} = 0.96$$

$$k = \frac{81 \times 0.368}{0.129} = 230$$

Observed value of $k=210$.

The formula for the amplification constant finally attains the form:

$$k = \frac{c L_g \log \frac{x_a}{x_g}}{\log \coth \pi a} \dots \dots \dots (12)$$

The TABLES II, III and IV on pages 160 and 161 will facilitate calculations.

The amplification constant is mainly governed by grid construction and depends little on anode area and filament configuration. Main factors determining k are $\frac{x_a}{x_g}$, $\frac{p}{x_g}$, and $\frac{r_g}{p}$, and similar tubes of equal relative dimensions give equal values of k whatever the size may be.

(ii) Mutual Conductance and Anode Impedance.

The mutual conductance for given anode and grid voltages (e_a, e_g) can be obtained by differentiation of the characteristic equation, thus

$$g = \frac{\partial i_a}{\partial e_g} = \frac{2}{5} G \frac{1}{e_f} \cdot \frac{\partial}{\partial e_g} \left[e_g'^{\frac{5}{2}} - (e_g' - e_f)^{\frac{5}{2}} \right]$$

$$\approx 1.5 G \frac{k}{1+k} \left(\sqrt{e_g'} - \frac{1}{4} \frac{e_f}{\sqrt{e_g'}} \right) \dots \dots \dots (13)$$

in which
$$e_g' = \frac{e_a + k e_g}{1+k}$$

This is strictly applicable when grid current is not appreciable.

The mutual conductance is principally governed by the perveance G which is proportional to the anode effective area and is inversely proportional to the electrode distances.

The anode impedance r may also be obtained as

$$r = \frac{\partial e_a}{\partial i_a} \dots \dots \dots (14)$$

but it is more convenient to calculate it from the known values of k and g by the relation

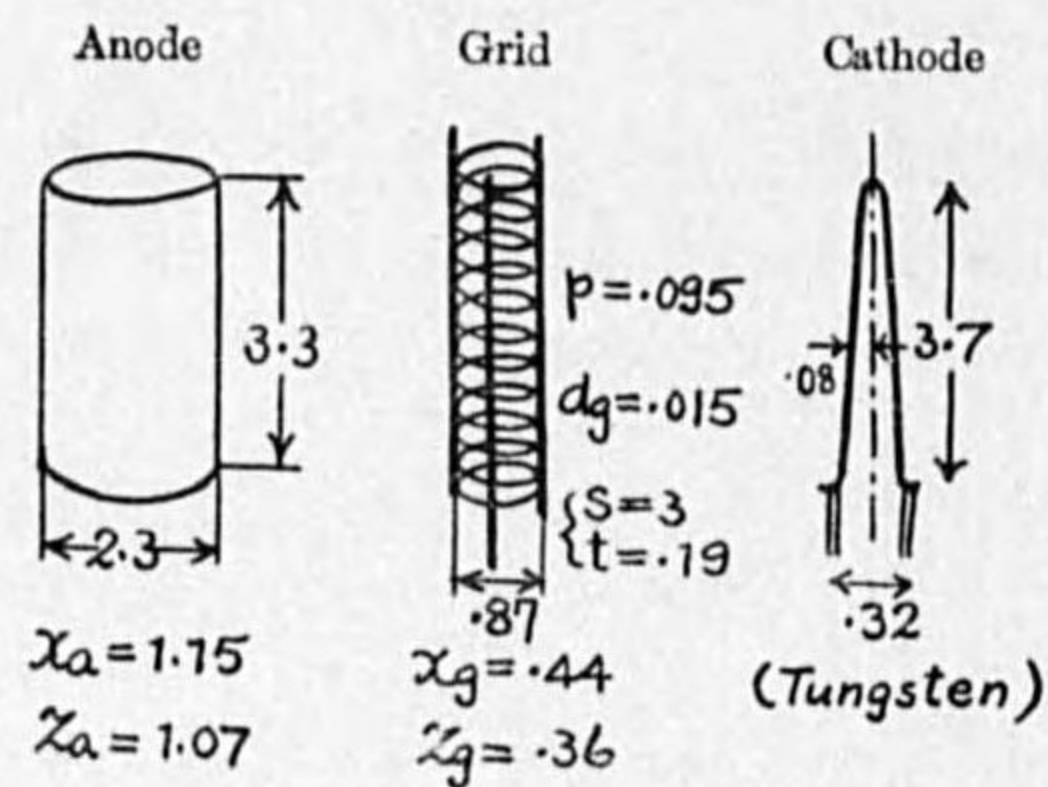
$$r = \frac{k}{g} \dots \dots \dots (15)$$

Example 23. Calculation of mutual conductance and anode impedance.

Triode type T-100 (Marconi Co.)

Dimensions (Fig. 24),

$$\begin{aligned} x_a &= 1.15 & x_g &= 0.44 & p &= 0.095 & r_g &= 0.0075 & A &= 23.9 \\ k \text{ calc.} &= 52.7 & z_a &= 1.15 - 0.08 = 1.07 & z_g &= 0.44 - 0.08 = 0.36 \\ e_f &= 10 \text{ V (rating)} \\ G &= 0.127 \times 10^{-3} & 1.5 G \frac{k}{1+k} &= 0.187 \times 10^{-3}. \end{aligned}$$



(T-100)
FIG. 24.

1) To obtain g and r for $e_a=1,500$ and $e_g=0$.

$$\begin{aligned} e_f' &= \frac{1,500}{52.7+1} = 27.9 & \sqrt{e_f'} &= 5.28 \\ g &= 0.187 \times 10^{-3} \times 4.81 = 0.00090 & r &= \frac{52.7}{0.00090} = 585,000 \end{aligned}$$

Observed values:

$$k=48 \quad g=0.00089 \quad r=540,000$$

2) For $e_a=2,000$, and $e_g=-20$.

$$e_f' = \frac{2000 - 20 \times 52.7}{52.7 + 1} = 17.7 \quad \sqrt{e_f'} = 4.20$$

$$g=0.000675 \quad r=78,100$$

Observed values:

$$k=48 \quad g=0.000675 \quad r=71,000$$

(4) Saturating Part of the Characteristic.

The saturation current I_s depends upon the material of which the cathode is made, and for a given material it depends upon the dimensions and working temperature of the cathode. General features of three kinds of materials widely used for cathodes are described in the following.

(i) Tungsten.

Its working temperature is generally 2300° to 2500°K, and is widely used for high-power tubes.

The emission can be calculated by means of CHART II annexed to this paper and explained on page 136.

Examples of the application of the chart: dimensions of filament and its heating current being given, to find the terminal voltage and emission.

$$a) \quad r_f=0.006 \quad l=9.9$$

i_f	e_f		I_s	
	Calculated	Observed	Calculated	Observed
1.7	10.8	9.4	0.0083	0.009
1.9	12.8	11.5	0.033	0.026
2.1	14.8	14.0	0.21	0.22
2.3	16.8	17.0	0.60	0.46

b) $r_f=0.0125$ $l=9.6$

i_f	e_f		I_s	
	Calculated	Observed	Calculated	Observed
5.4	7.9	7.4	0.0465	0.044
5.8	8.7	8.4	0.15	0.14
6.2	9.7	9.4	0.32	0.38
6.8	11.1	10.5	0.82	0.90

The saturation current is quite a variable quantity, and they are much affected by the existence of residual gas and thorium.

(ii) Thoriated Tungsten.

A small quantity of thoria is contained in tungsten and is reduced to thorium in the process of activation and forms an atomic layer on the tungsten surface and thus facilitates the electron emission, the working temperature being of the order of 1900°K. This kind of filament requires less heating power than pure tungsten for equal emission and is widely used for receiving and medium power tubes. The emission depends among other things on the degree of activation, that is the area on the cathode covered by thorium, and moreover thorium is very sensitive to residual gases.

The relation between the working temperature and the heating current or voltage can be calculated by the same chart as that for tungsten, but the emission is quite variable. The curves in Fig. 72 on page 139 may be applied for a rough estimation of emission obtainable on the most favourable conditions.

(iii) Oxide-coated Cathode.

This type of cathode works at still lower temperature of the order of 1100°K, and is used for receiving and low power amplifying or transmitting tubes.

The material on which the oxides of barium, strontium, calcium or other similar metals are coated is different according to the process of manufacture, and platinum, nickel, tungsten, or alloys of these metals are generally used. Thus the calculation of cathode characteristics are different for materials used.

The following table shows general characteristics for the three types of filament.

Filament	Working temperature	Emission per unit heating power	Commonly used heating power
Tungsten	2300-2500°K	2-5 mA/watt	75-80 watt/cm. ²
Thoriated tungsten	1900-2100°K	20-100 "	30 "
Oxide-coated	900-1100°K	50-150 "	5 "

The point at which the anode current commences to saturate occurs at an anode voltage such as

$$e_s = \left(\frac{I_s}{G} \right)^{\frac{2}{3}}$$

If the cathode consists of a uniformly emissive surface of equal potential all over it, the characteristic would sharply bend to saturate as soon as the anode voltage reached saturating voltage e_s . But in actual cases slow bending of the characteristic curve is invariably observed, which is caused by the non-uniformity of filament temperature as well as the voltage drop along the filament. The expression of anode current considering the latter cause only is as follows⁽⁸⁾; in a range of the anode voltage for saturation: $e_s < e_a < e_s + e_f$

$$i = \frac{1}{5} G \frac{1}{e_f} \left\{ e_s^{\frac{3}{2}} (5e_a - 3e_s) - 2(e_a - e_f)^{\frac{3}{2}} \right\}$$

in which e_a should be replaced by e_f' in case of a triode. This equation represents a curve which is continuous to that shown by equation (3) at anode voltage $e_a = e_s$.

This expression does however, not sufficiently conform with the observed values as shown in Ex. 24, and this fact shows that the non-uniformity of emissive power on the cathode is the more important factor.

Accurate calculation of this part of characteristic is very complicated, as the

(8) Van der Bijl, loc. cit. on p. 2.

temperature distribution along the filament must be known, but the writer finds no need of it for the designing purpose as this part of characteristic is of little practical importance.

In dull-emitter tubes such as thoriated tungsten or oxide-coated filament tubes, the saturation does not appear so sharply as in bright-emitter tubes with tungsten filament. This is because that the temperature difference along the filament is more marked in the former, as the working temperature is low and, besides radiation considerable portion of heat is lost at the ends of the filament due to conduction of leads. In oxide-coated filament tubes rough surface of the filament augments the above phenomenon of partial saturation.

Example 24. Calculation of the saturating part of characteristics.

(a) Triode type BN (Siemens Halske A. G.)

Dimensions are given in Ex. 17b on page 31.

$$I_s = 0.022 \text{ (observed value is taken)} \quad e_f = 4.7 \text{ (tungsten filament.)}$$

$$z_a = 0.58 \quad z_g = 0.35 \quad A = 12.1 \quad \frac{A}{z_a z_g} = 60$$

$$G = 0.14 \times 10^{-3} \quad \frac{2}{5} G e_f^{\frac{3}{2}} = .00057 \quad \frac{1}{5} G \frac{1}{e_f} = 0.00595 \times 10^{-3}$$

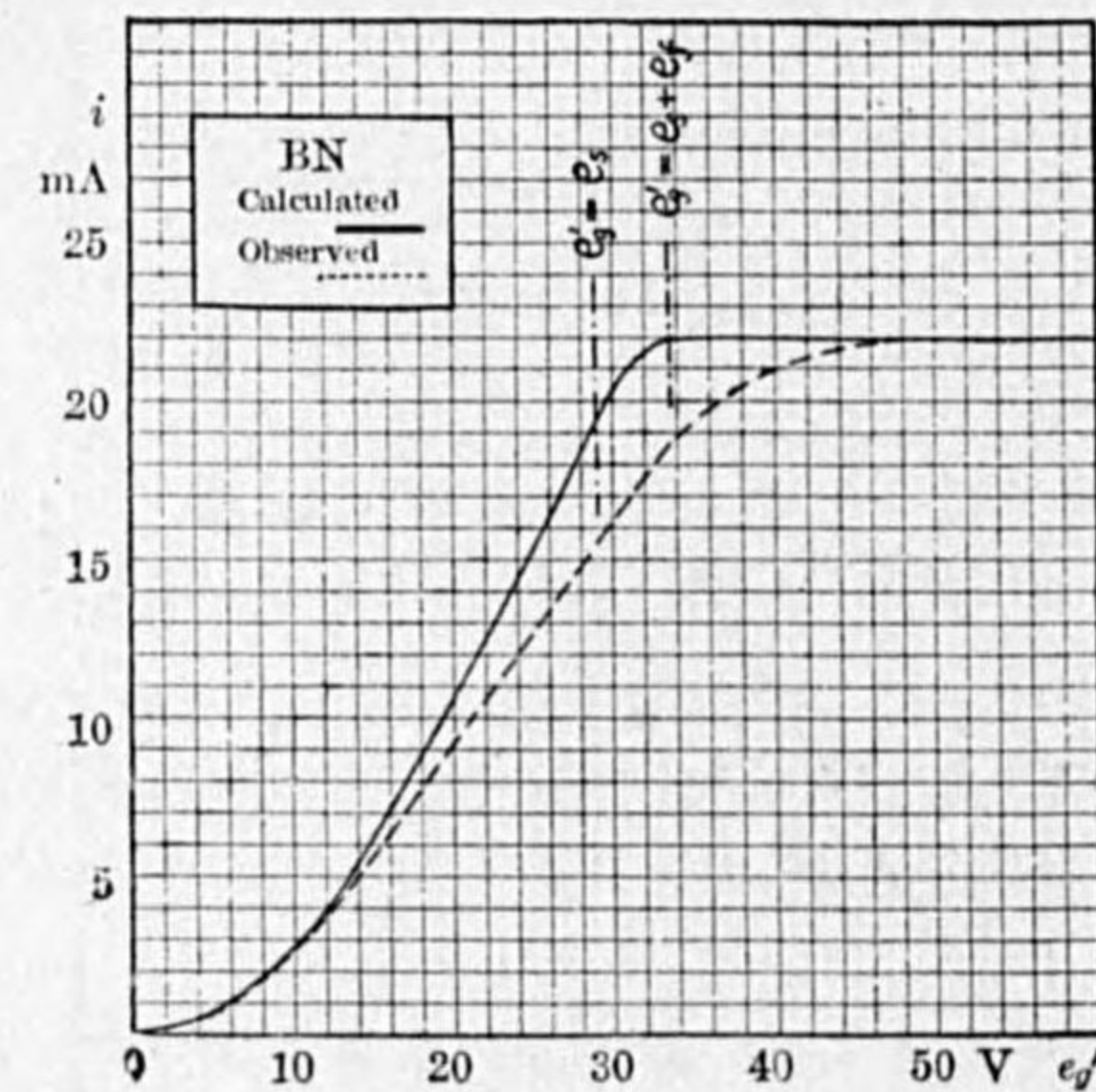


FIG. 25.

$$e_s = \left(\frac{0.022}{0.14 \times 10^{-3}} \right)^{\frac{2}{3}} = 29.1$$

Below saturation $e_g' < e_s$			Saturating part $e_s < e_g' < e_s + e_f$			
$\frac{e_g'}{e_f}$	e_g'	i	e_g'	$(5e_g' - 3e_s)e_s^{\frac{3}{2}}$	$2(e_g' - e_f)^{\frac{3}{2}}$	i
0	0	0	30	9,870	6,480	0.0196
2	9.4	0.0026	31	10,620	7,100	0.0209
4	19	0.0097	32	11,330	7,780	0.0211
6	28	0.0185	33	12,190	8,520	0.0218

(b) Diode type UX-213 (R. C. A.)

Dimensions and characteristics are given in Ex. 9 on page 14.

Thoriated-tungsten filament, $e_f = 3.4$ $i_f = 1.5$

$$z_a = 1.29 \quad A = 2.6 \quad G = 0.364 \times 10^{-3}$$

$$I_s = 0.058 \text{ (observed value being taken),} \quad e_s = 29.3$$

The results of calculation are shown in Fig. 26.

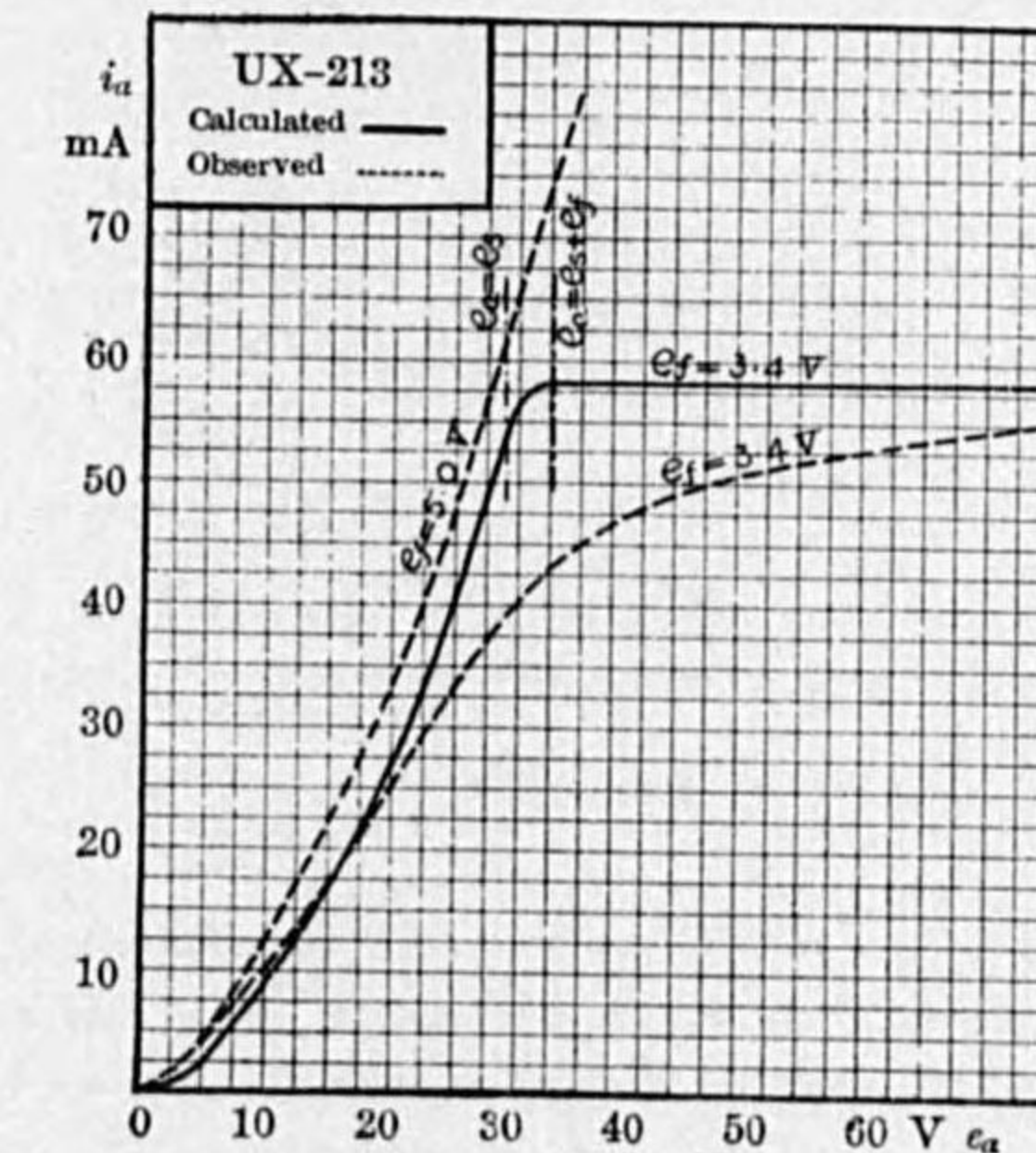


FIG. 26.

(c) Triode type KL-1 (Marconi Co.)

This tube, being of indirectly-heated type, has no potential difference on the cathode surface.

$$z_a = 0.223 \quad z_g = 0.111 \quad A = 5.97 \quad \frac{A}{z_a z_g} = 241$$

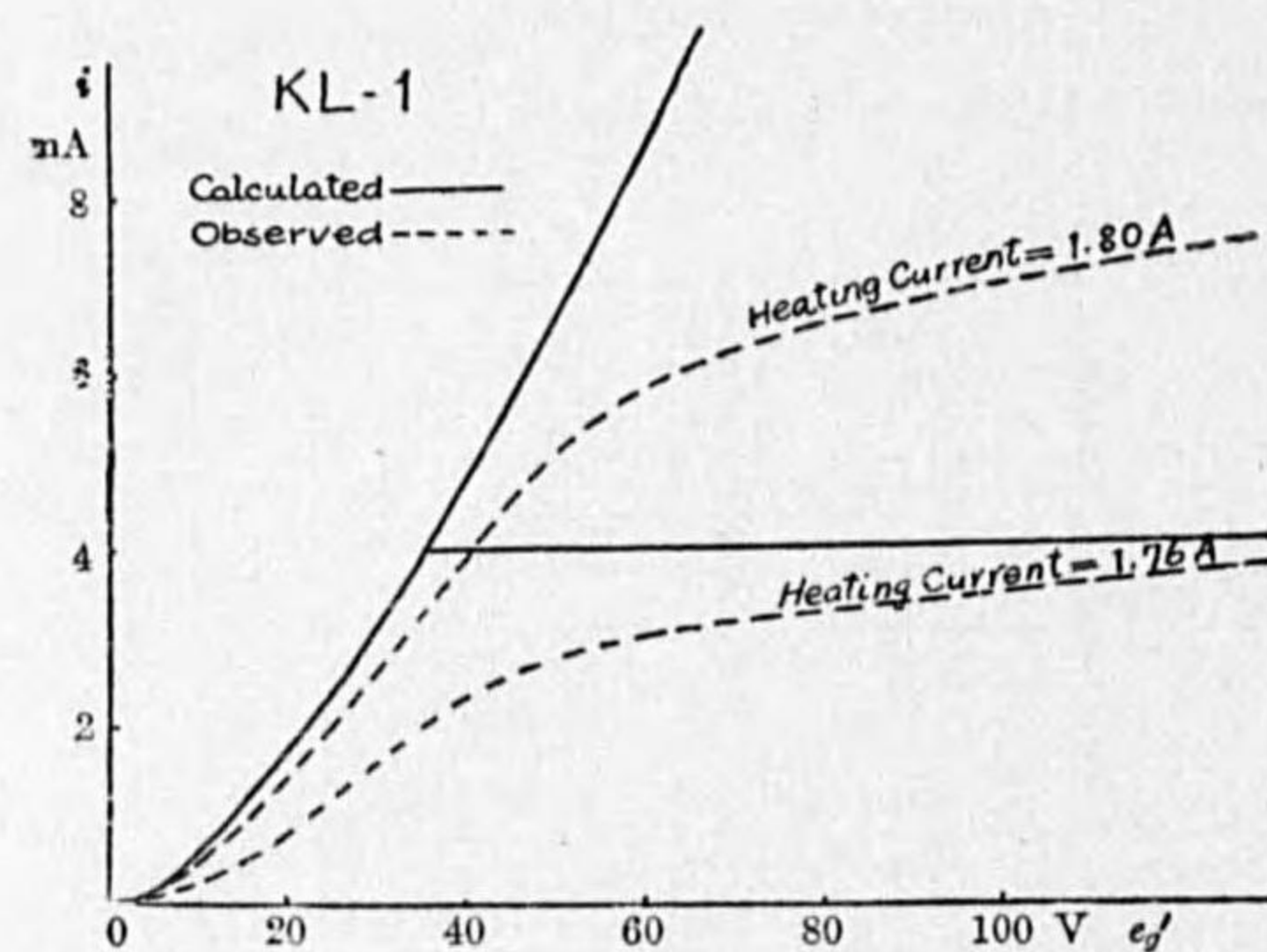
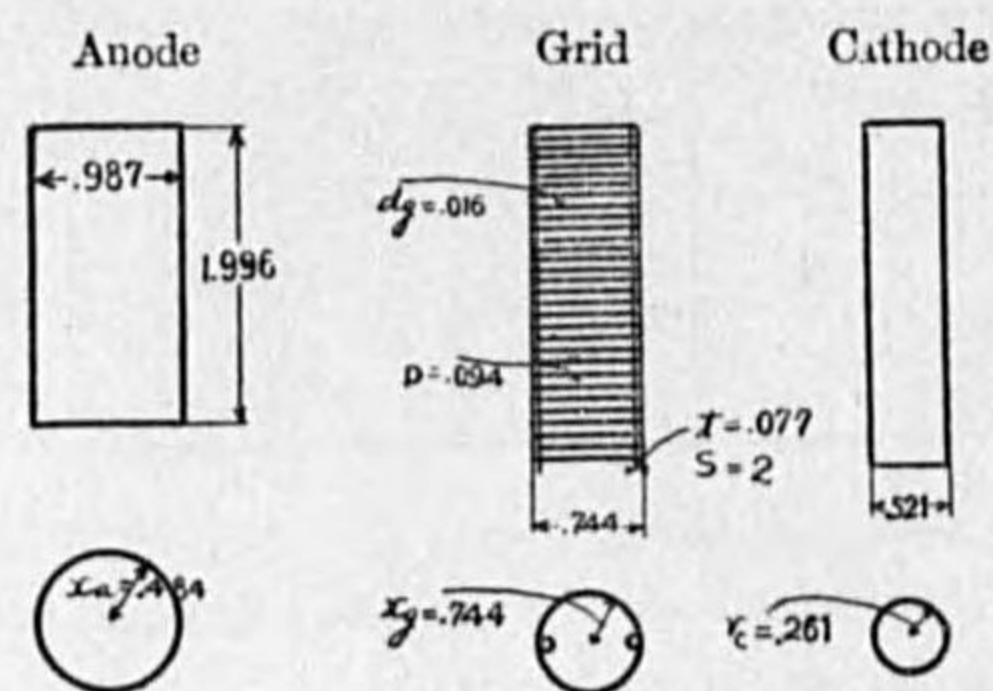


FIG. 27.

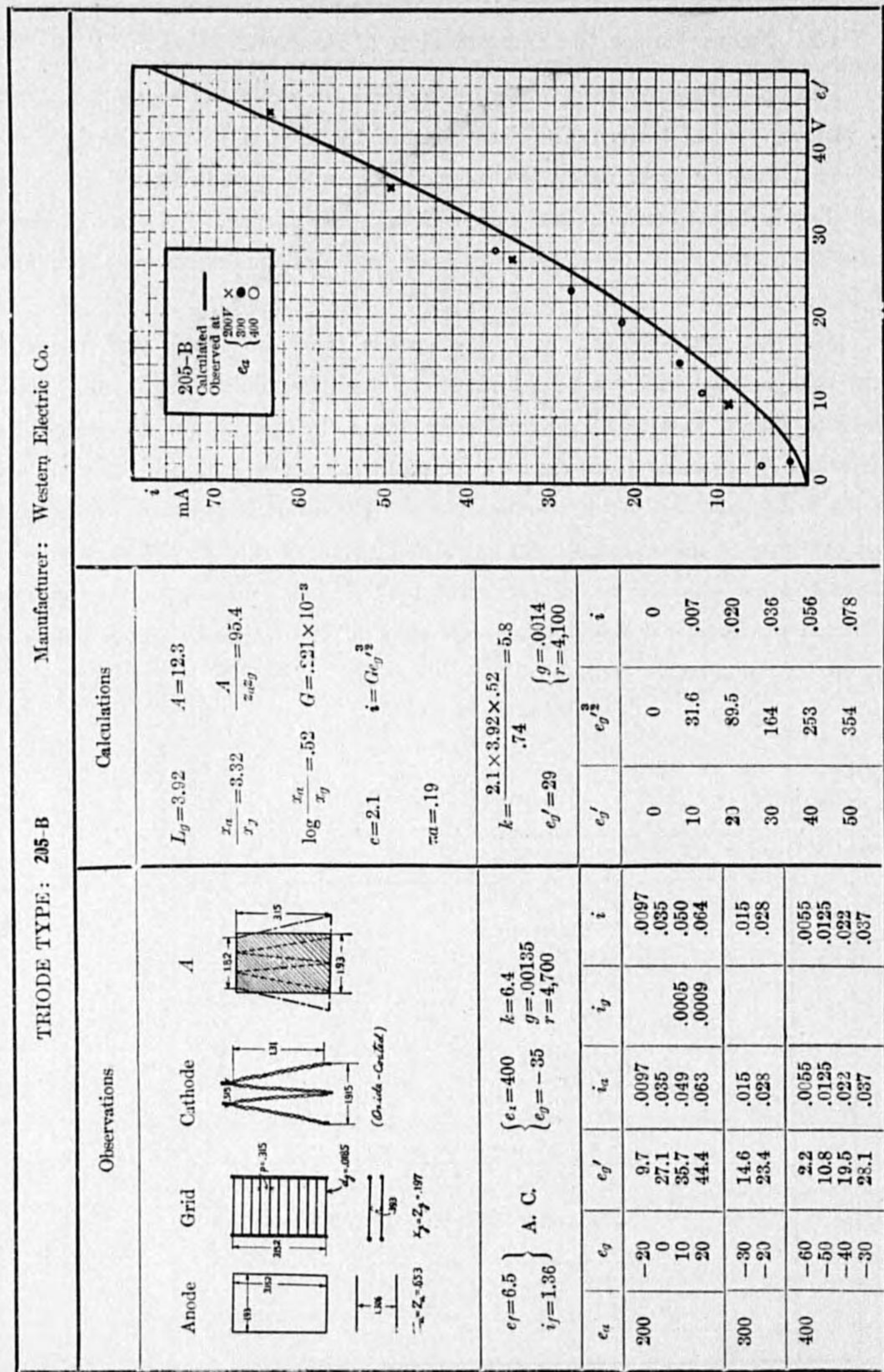
If the cathode has uniform emissive power all over the surface and if the electron current is to saturate at 4.0 mA for instance, the characteristic should have a sharp bending at this current as shown in Fig. 27. But the observed curves show very slow bending for saturation, which is attributed to the non-uniformity of temperature or emissive power on the cathode surface.

(5) Examples for the Computation of Characteristics.

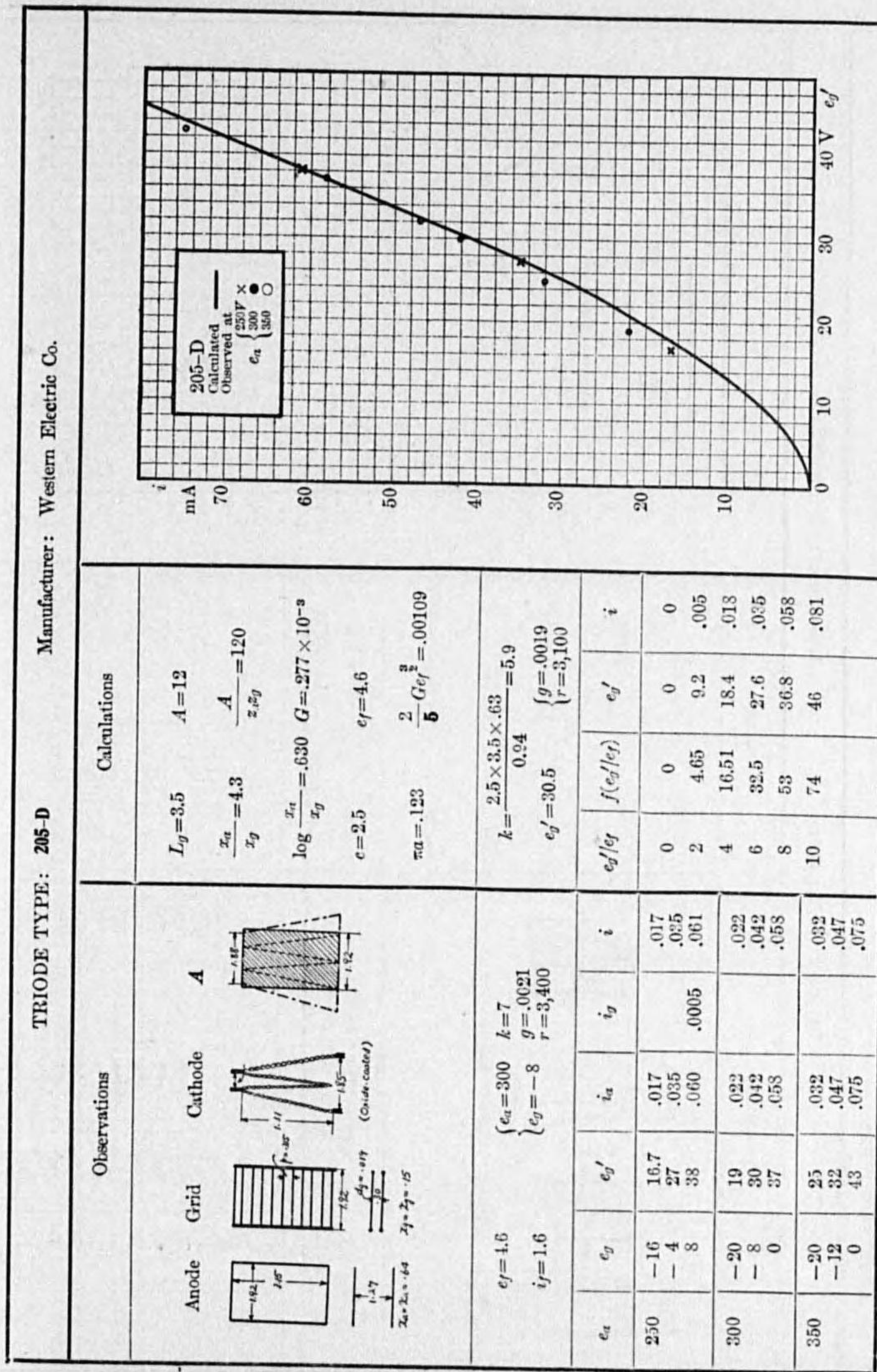
Examples given on the following pages show the method of computation applied to various types of tubes. The dimensions of the electrodes were directly obtained in some cases by breaking up the tubes, but in most cases this could not be done and the microscopic cathetometer was used for this purpose, and error of observations were, therefore, unavoidable in measuring small dimensions such as diameter of wire.

Filaments were lighted with d. c. unless otherwise noted, and anode and grid voltages were referred to the negative leg of the filament. Rated values of filament voltage were taken in most cases for both observations and calculations. The three parameters were observed at particular anode and grid voltages given in the tables, and the mutual conductance and the anode impedance were calculated for the same condition, with the calculated value of the amplification constant. Characteristics were shown as the relation of electron current to the equivalent grid voltage, as this is the simplest expression of characteristics and is determined by the least number of factors.

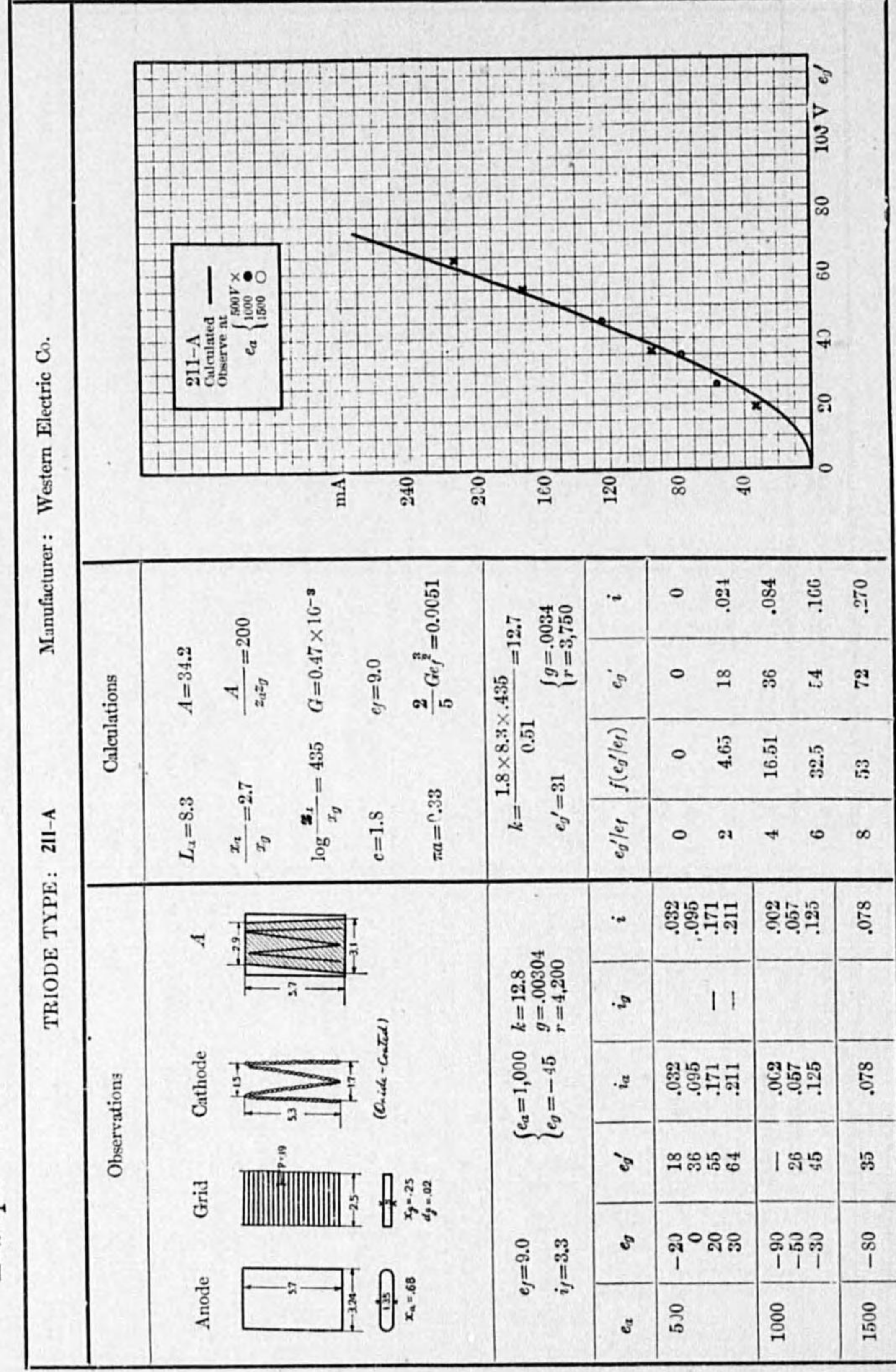
Example 25.



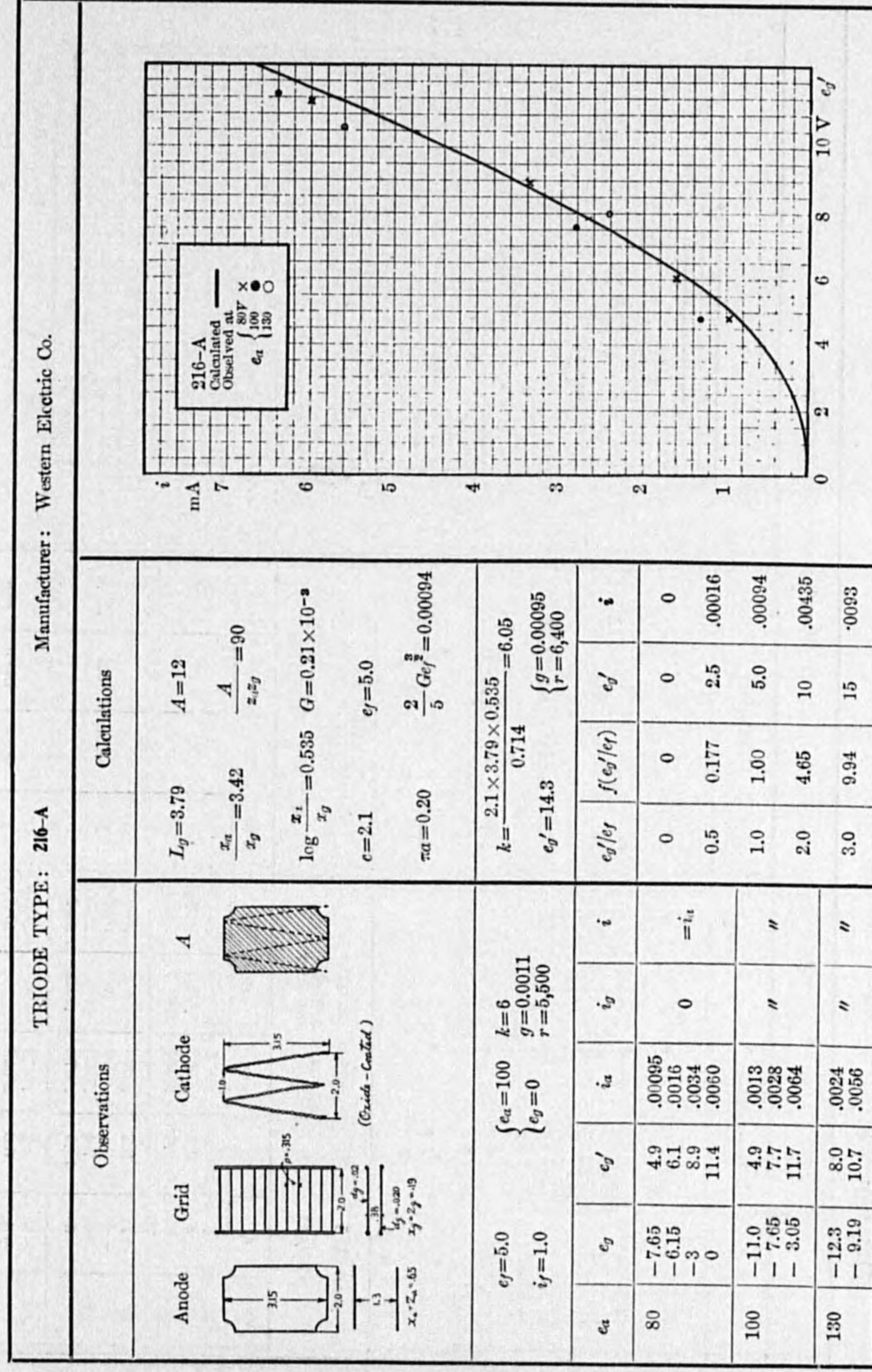
Example 26.



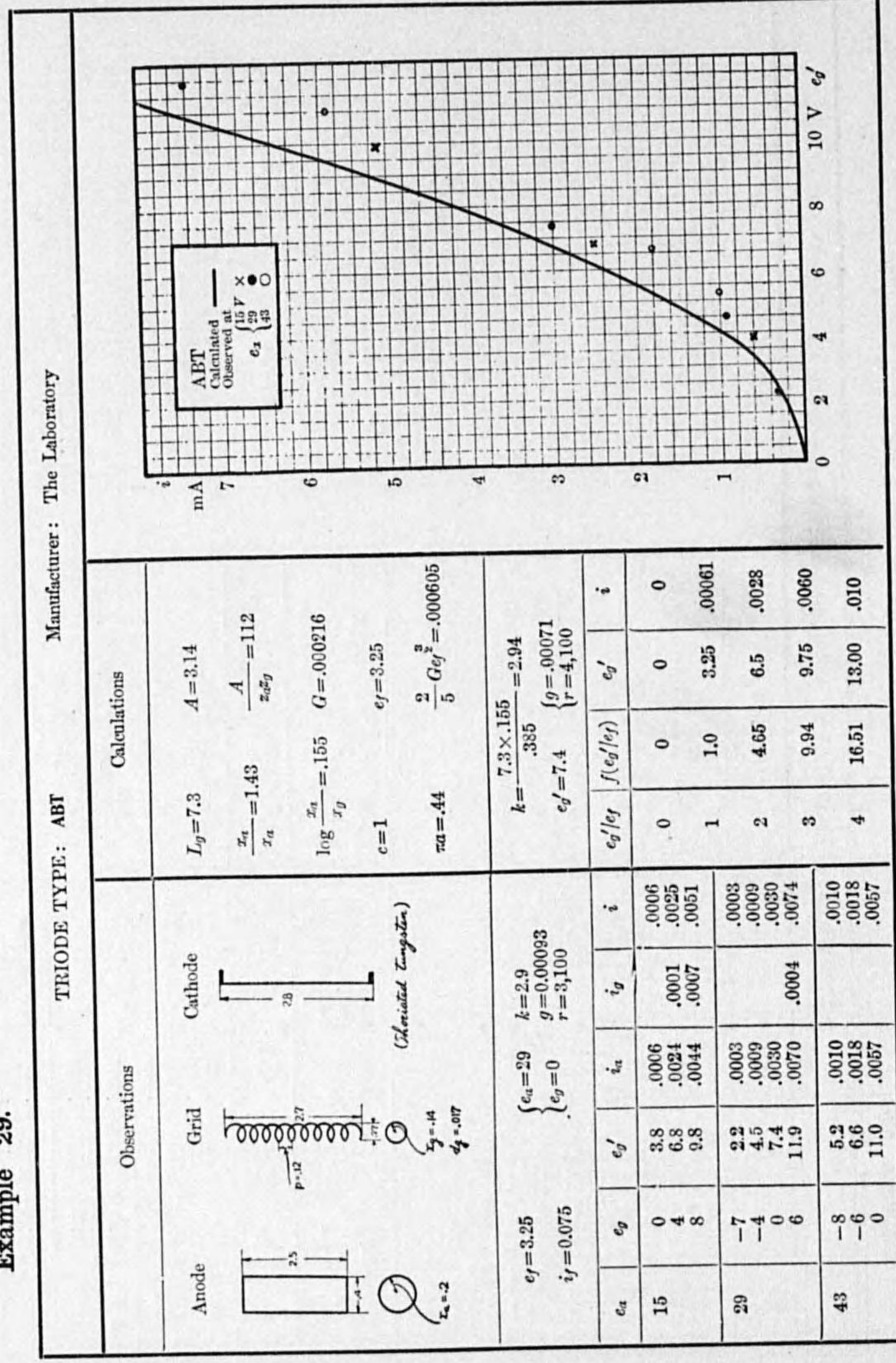
Example 27.



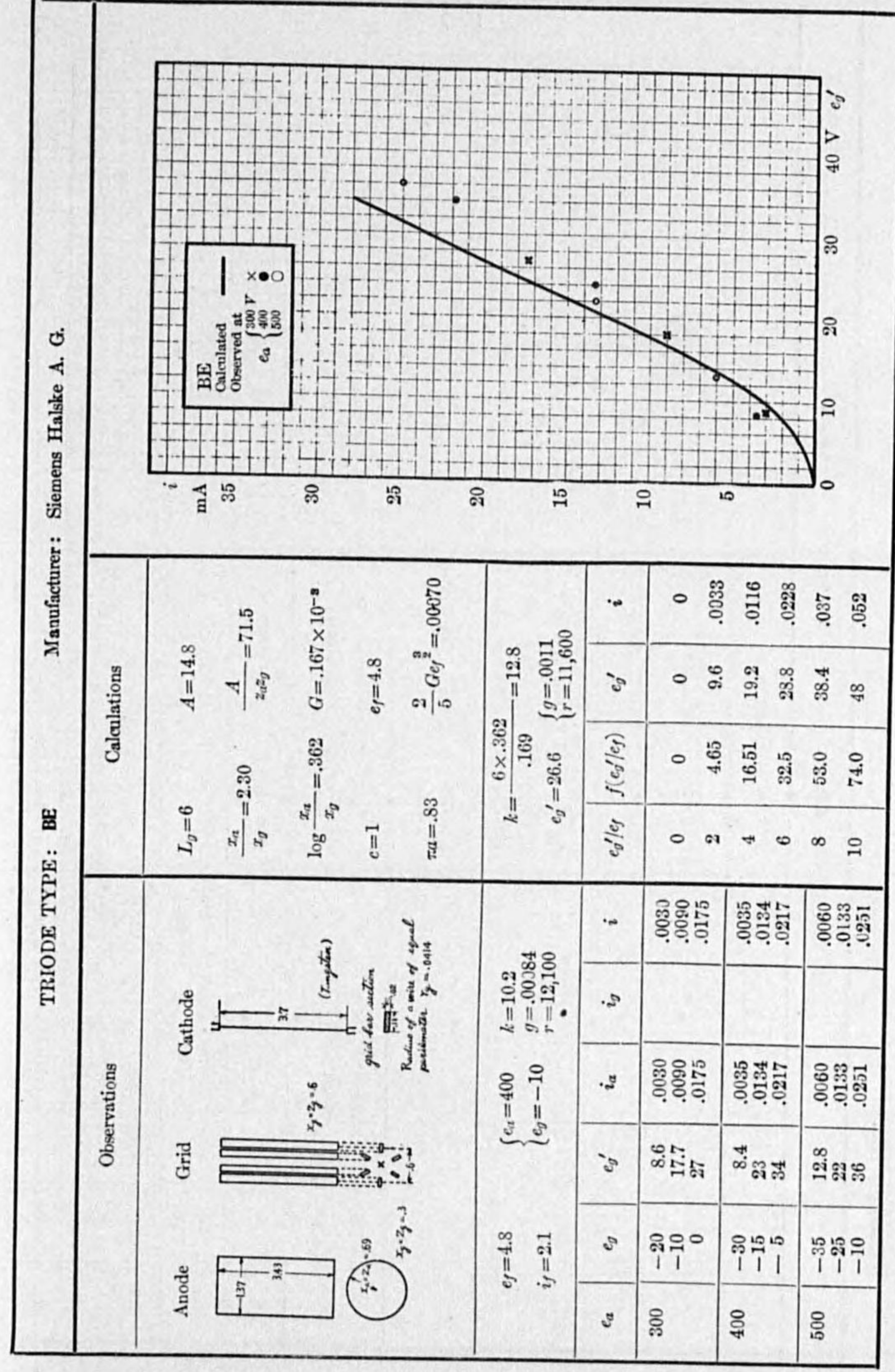
Example 28.



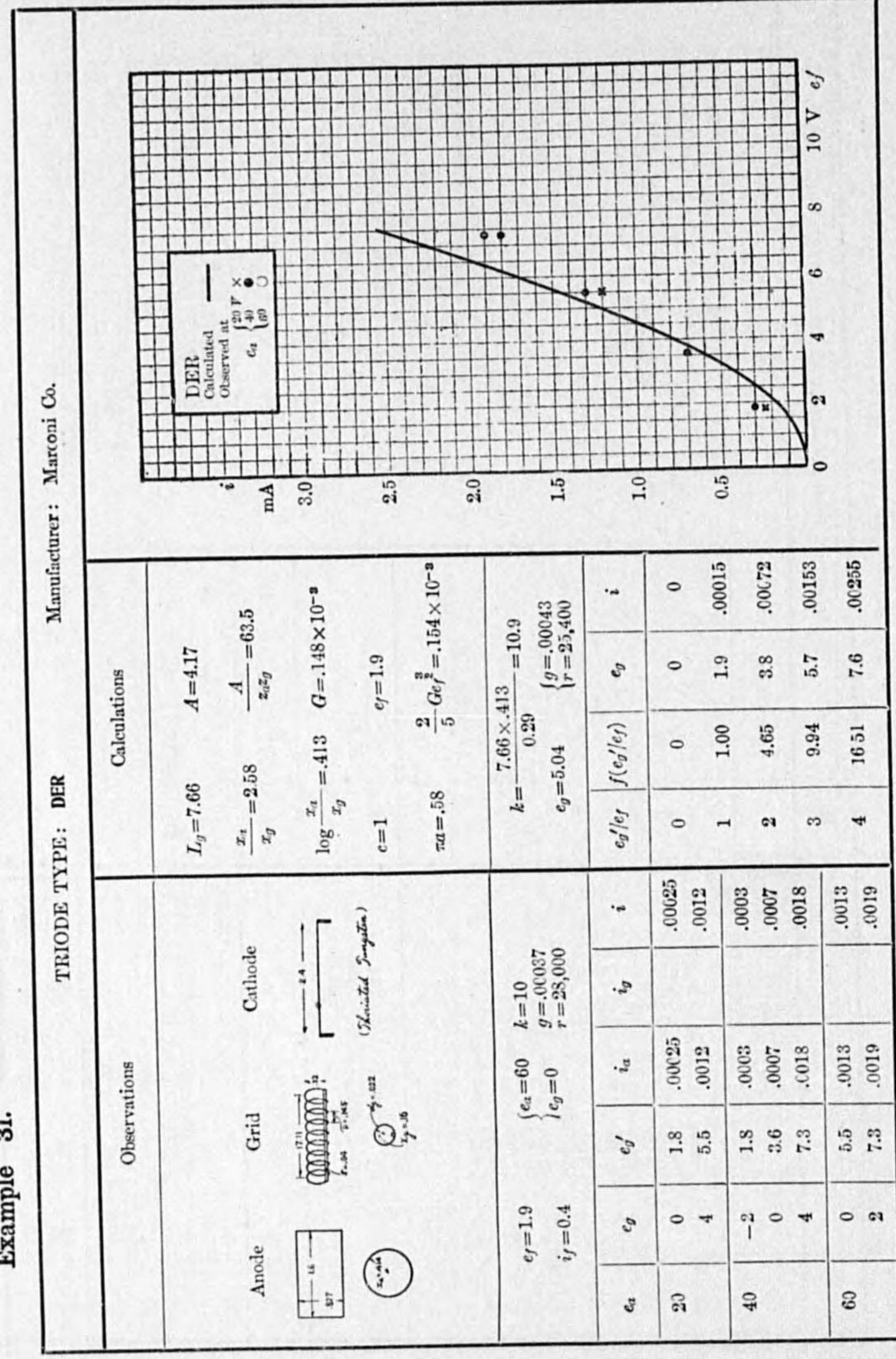
Example 29.



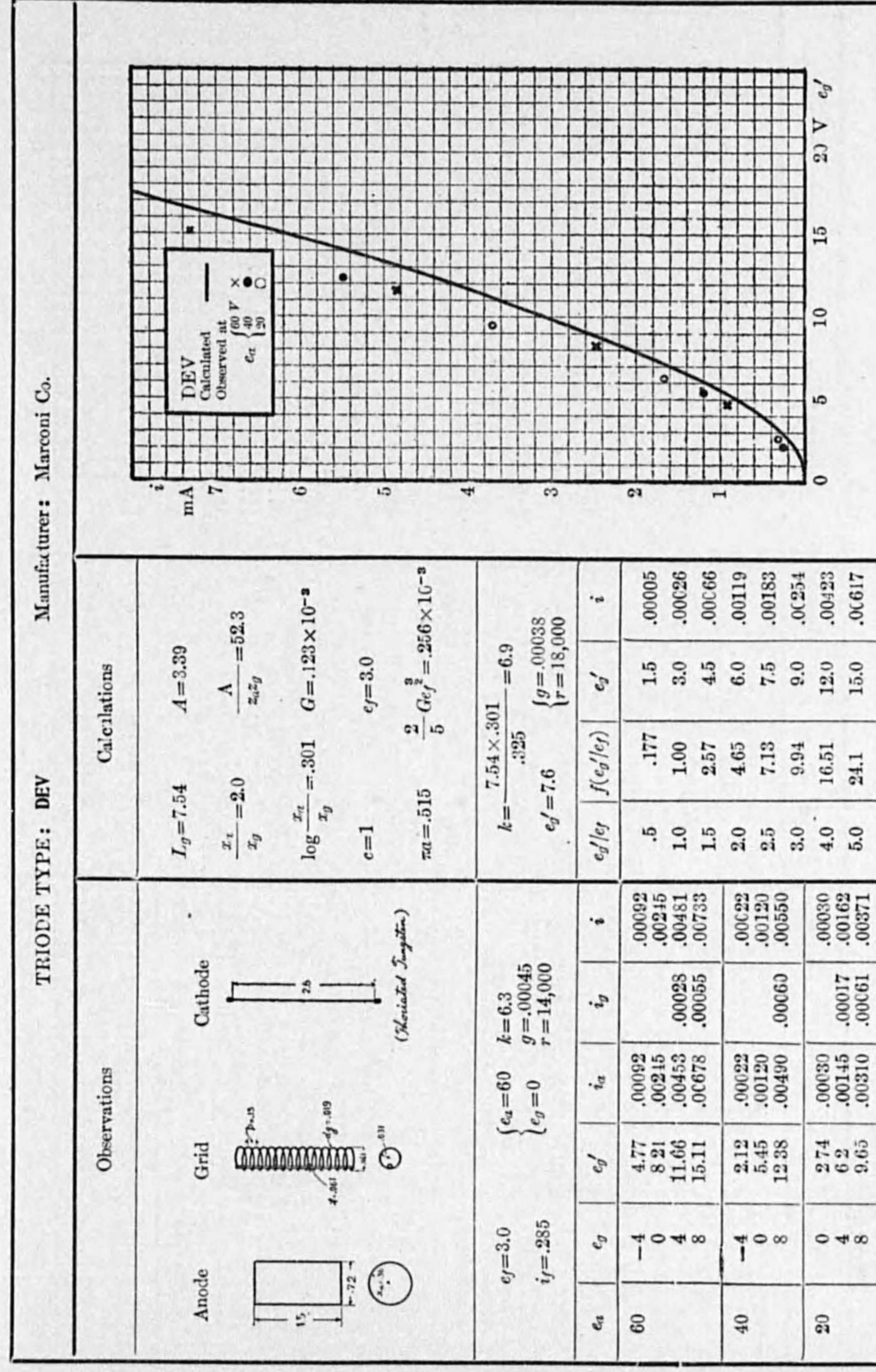
Example 30.



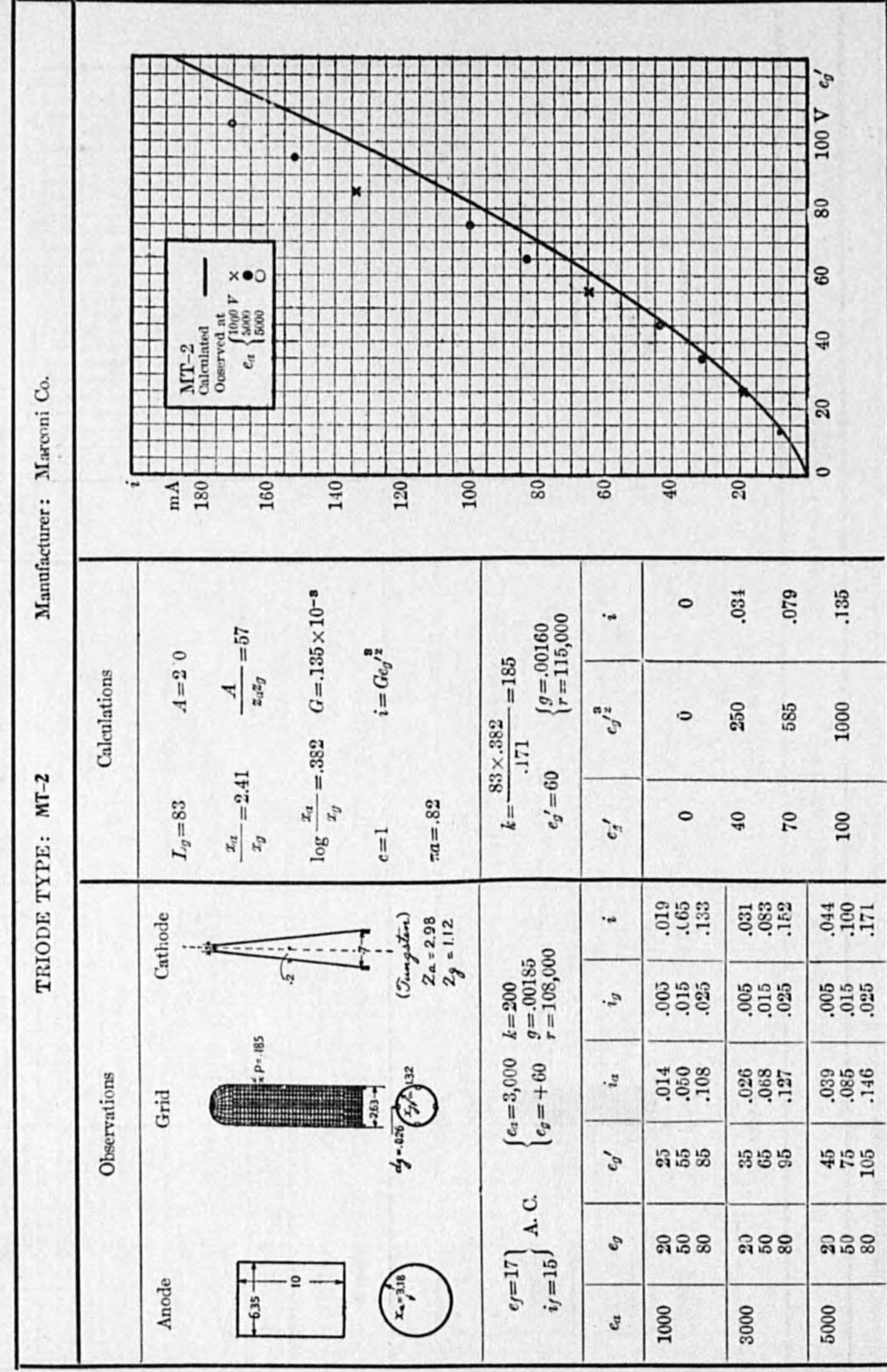
Example 31.



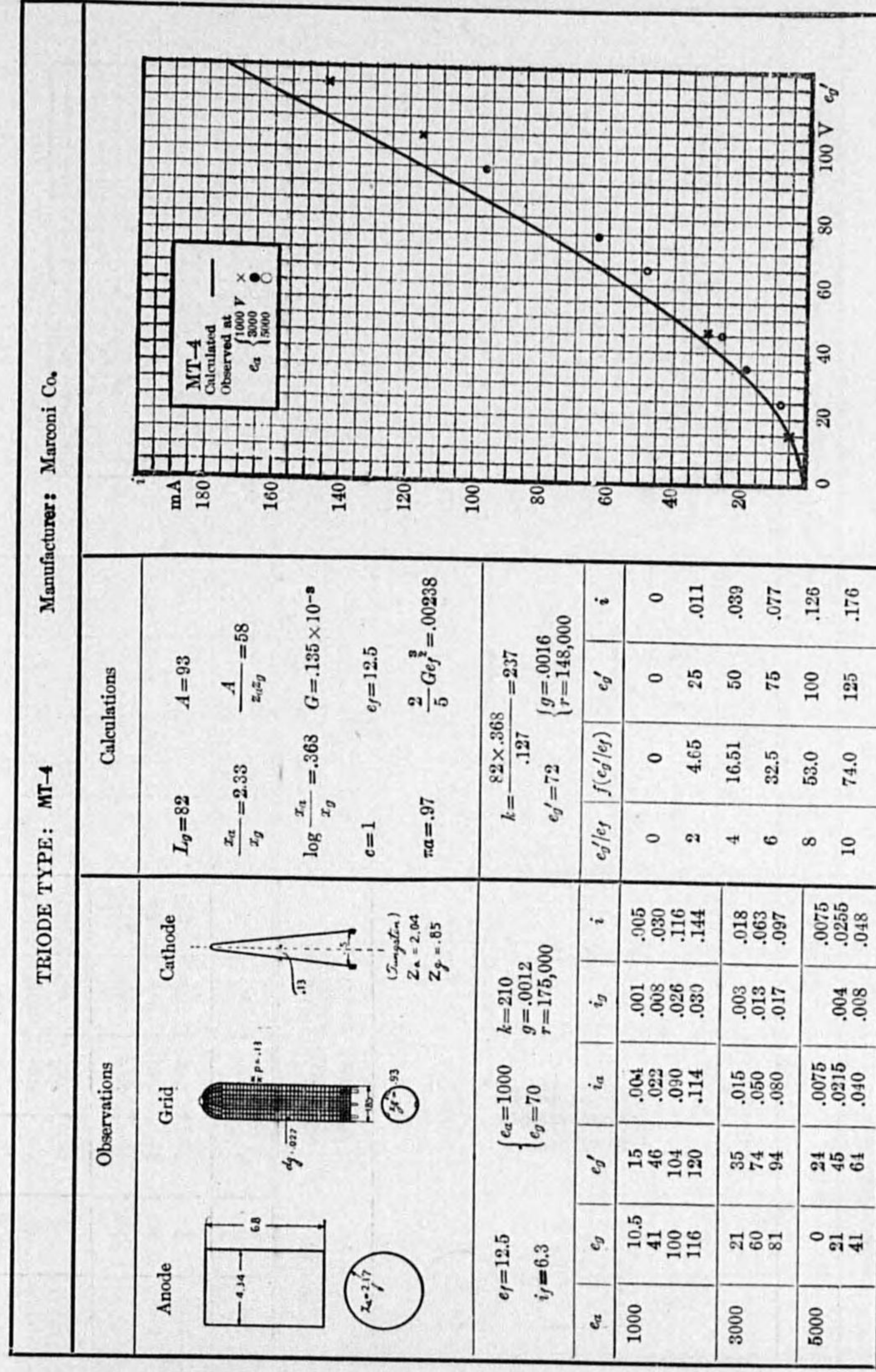
Example 32.



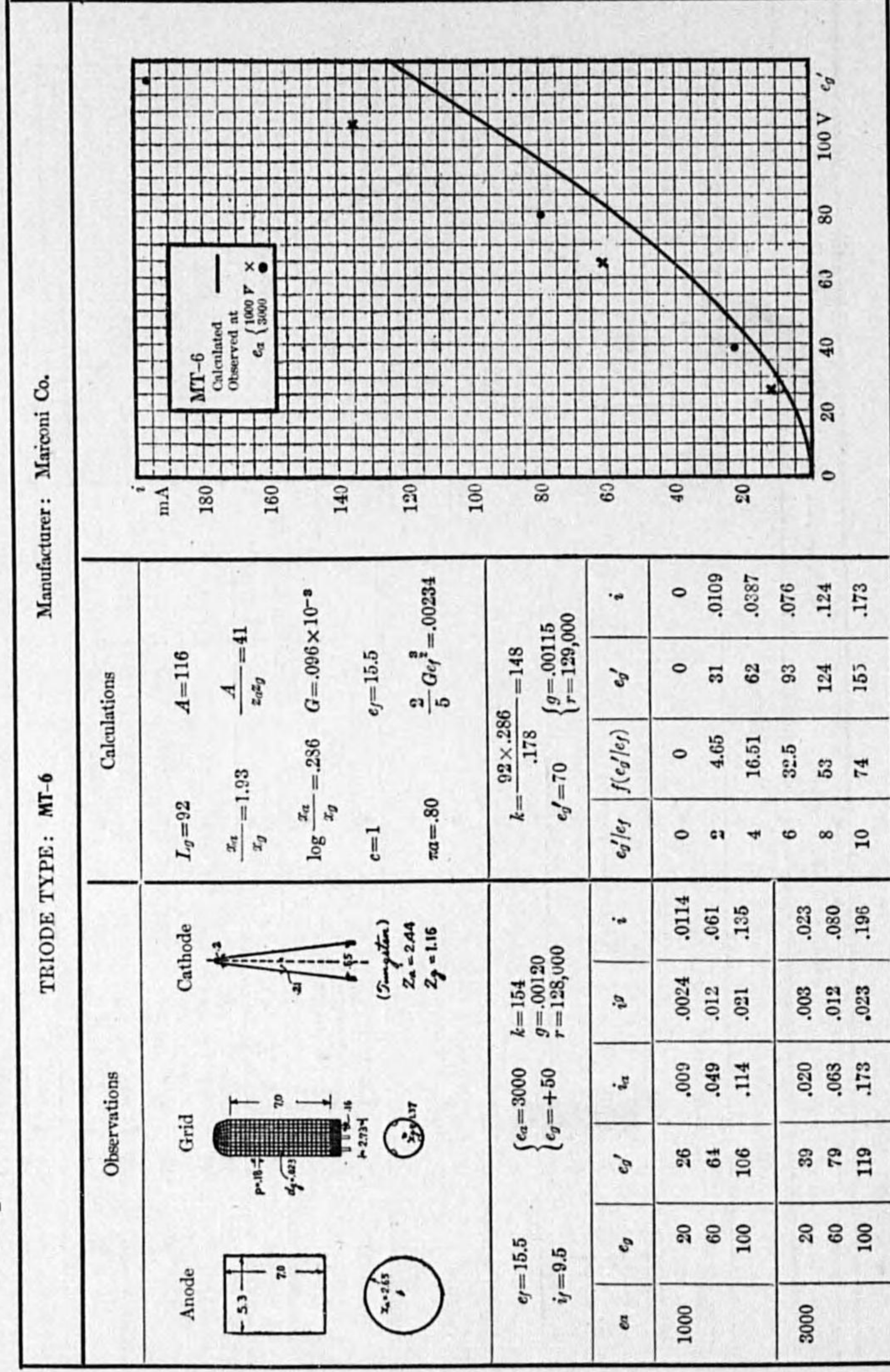
Example 37.



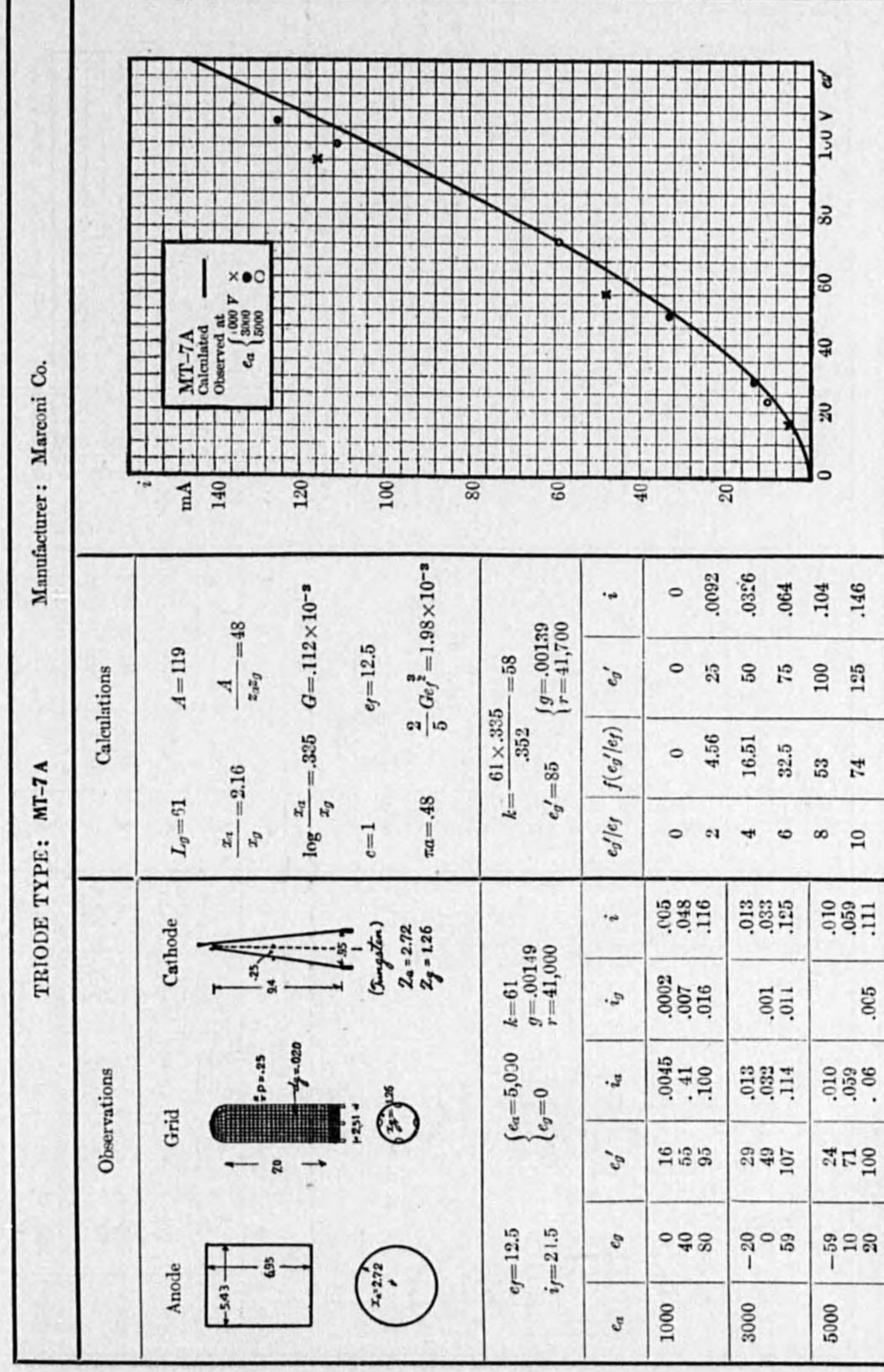
Example 38.



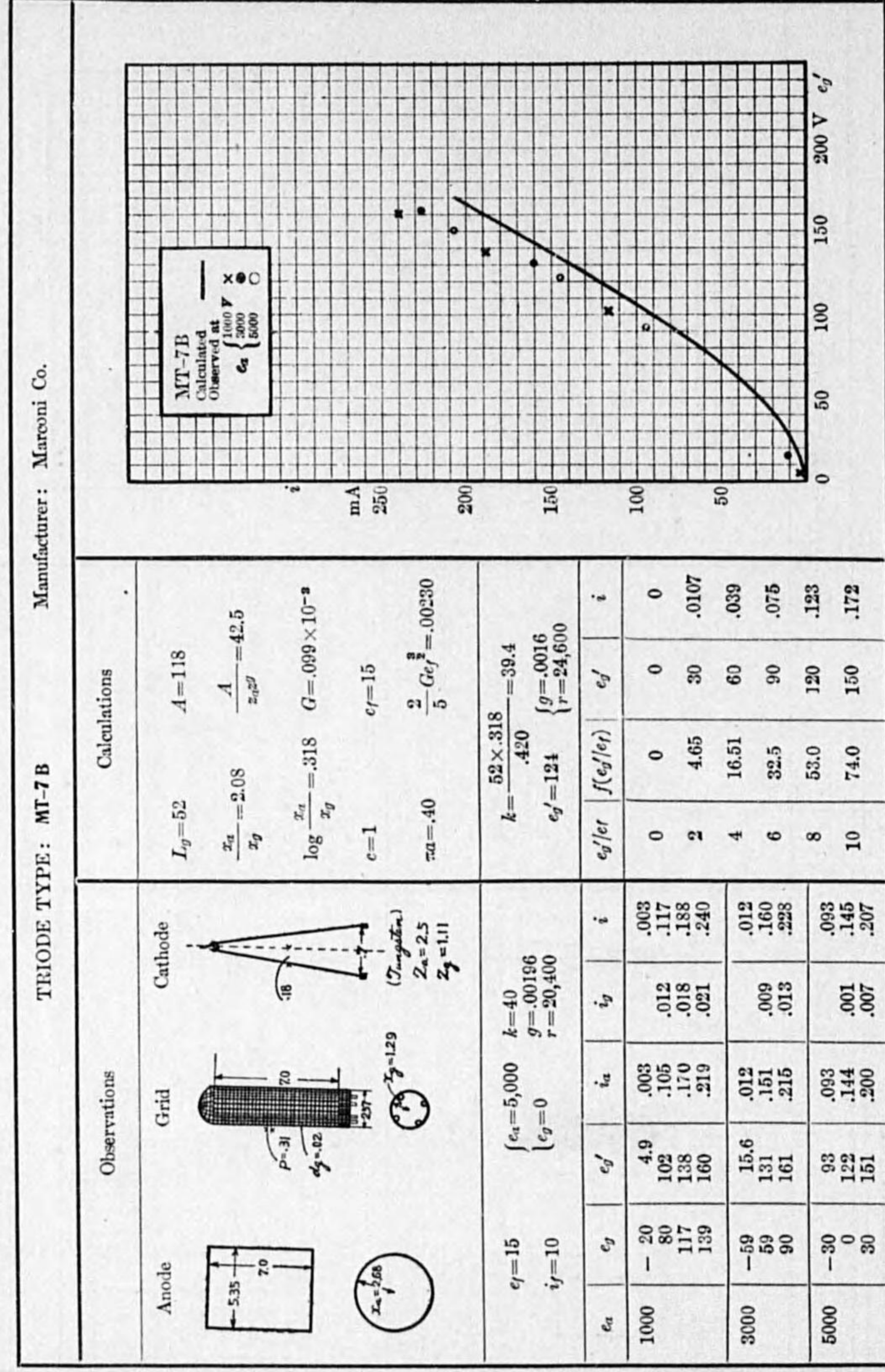
Example 39.



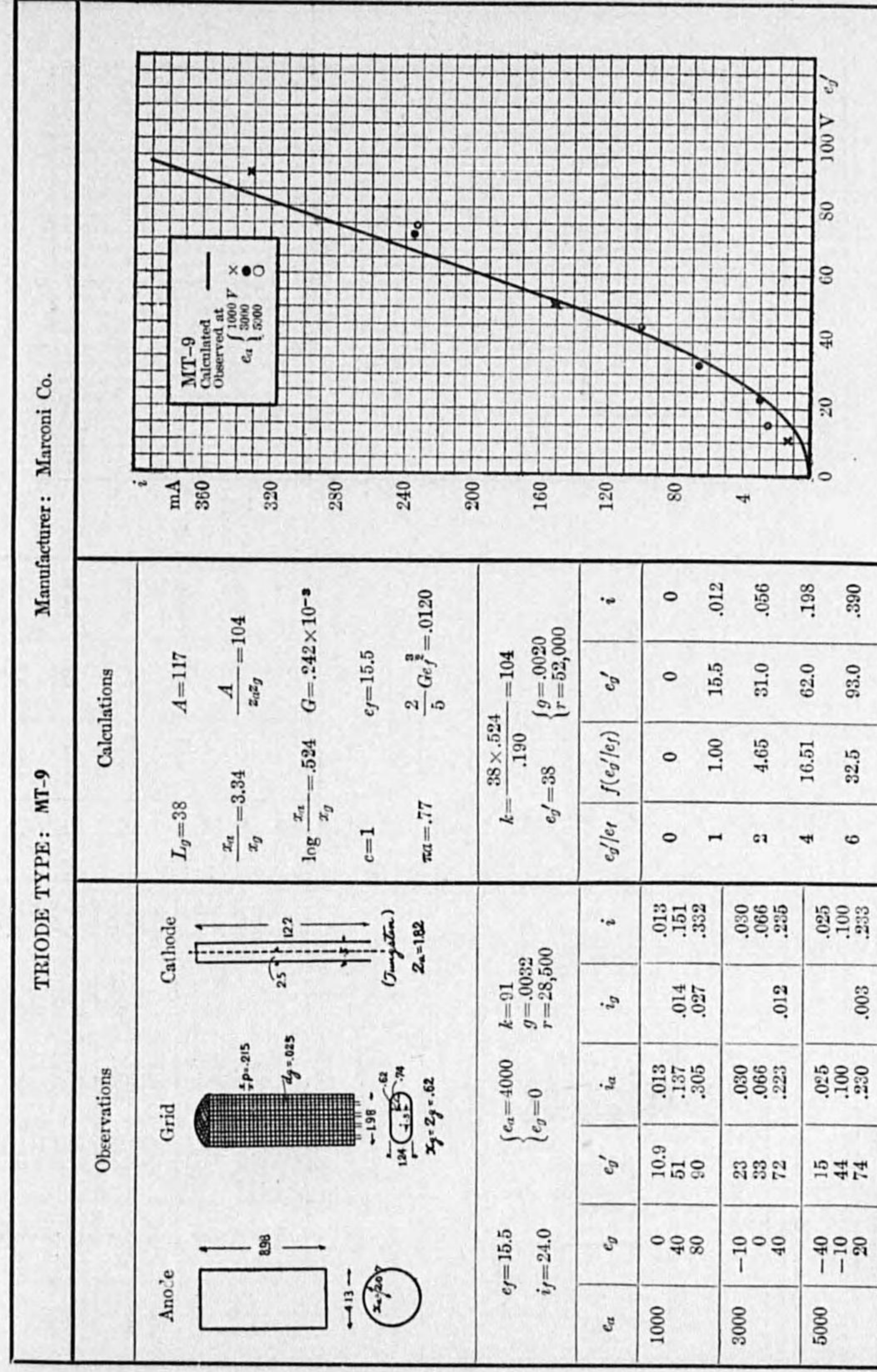
Example 40.



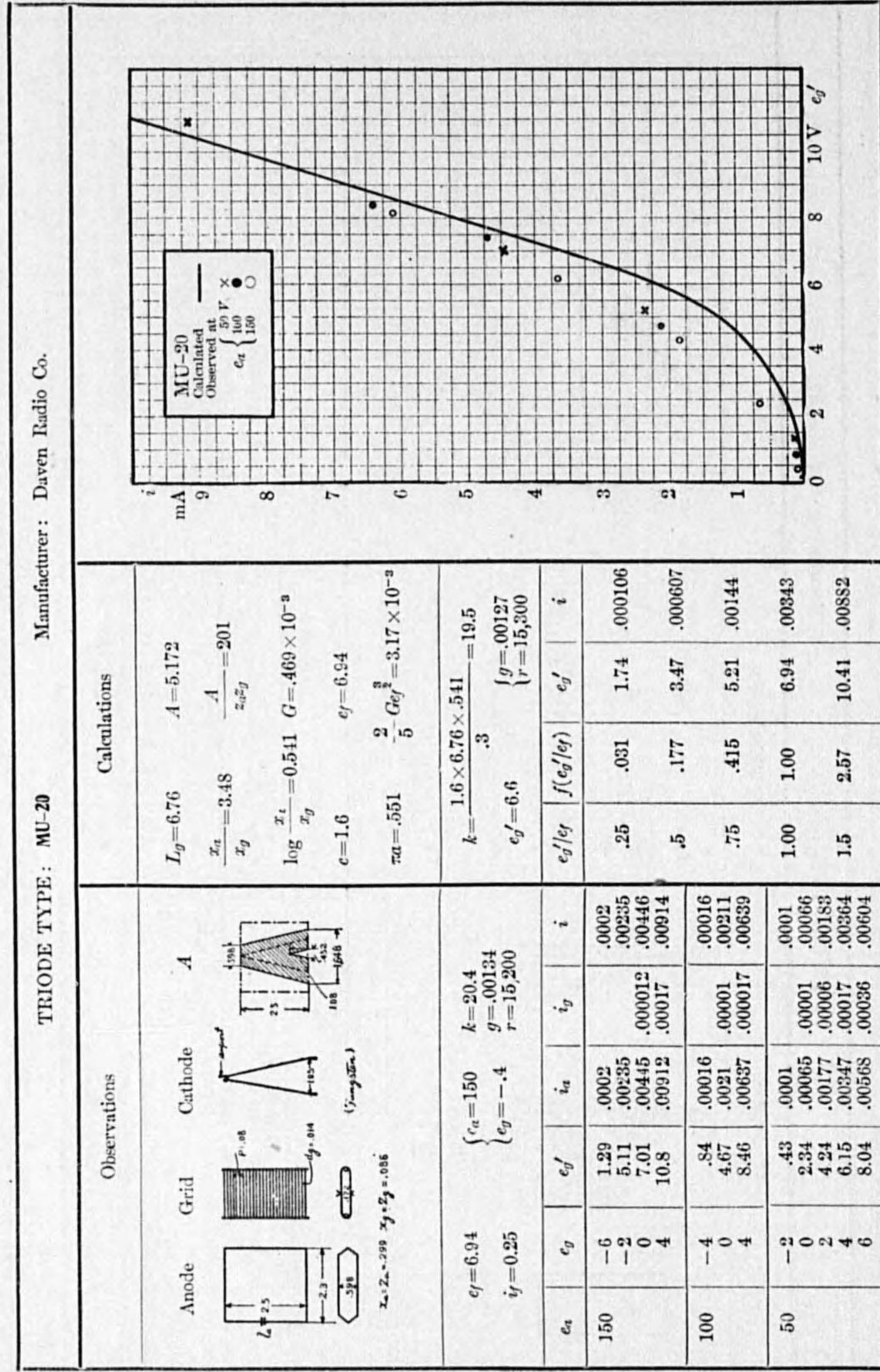
Example 41.



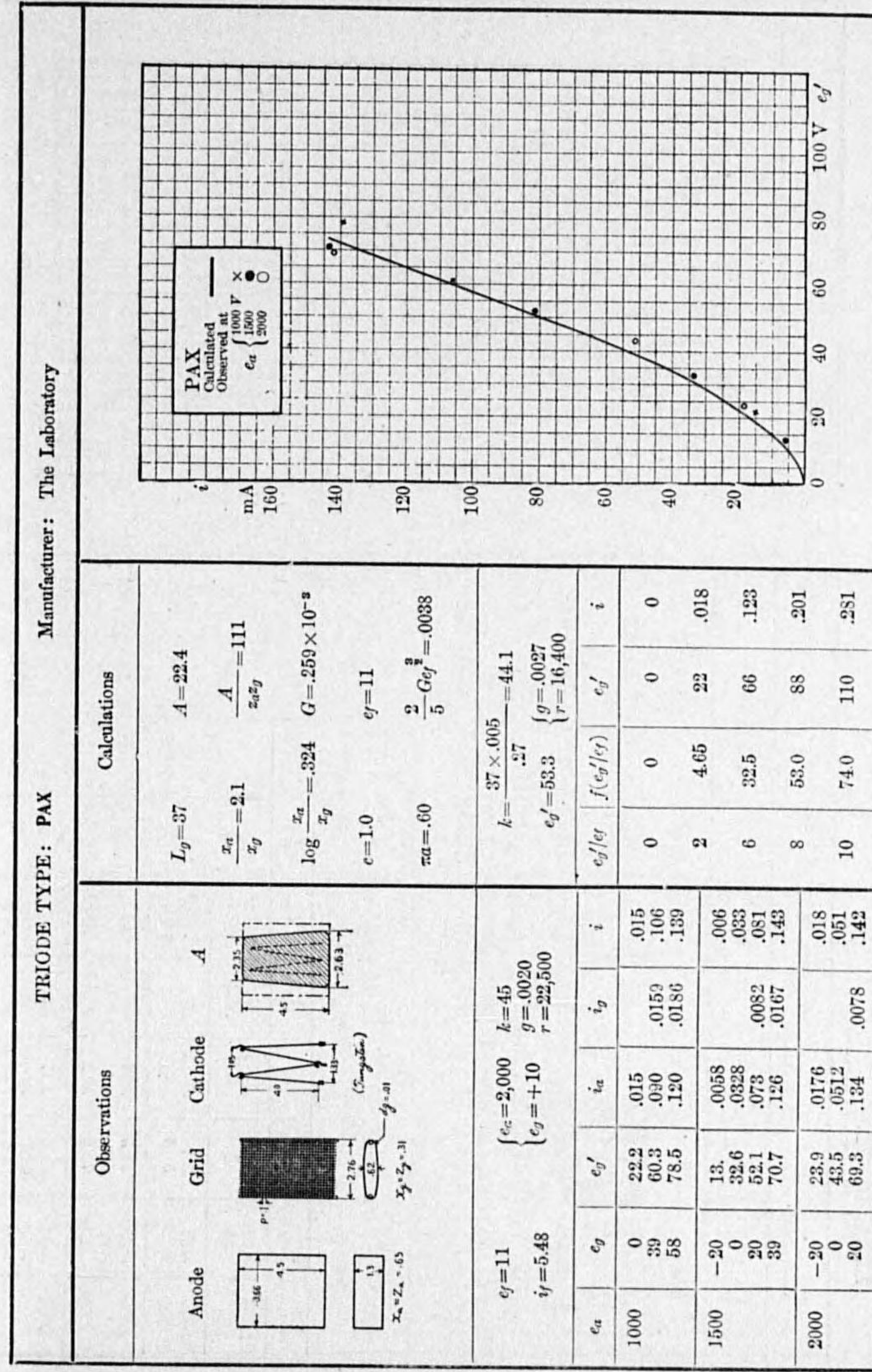
Example 42.



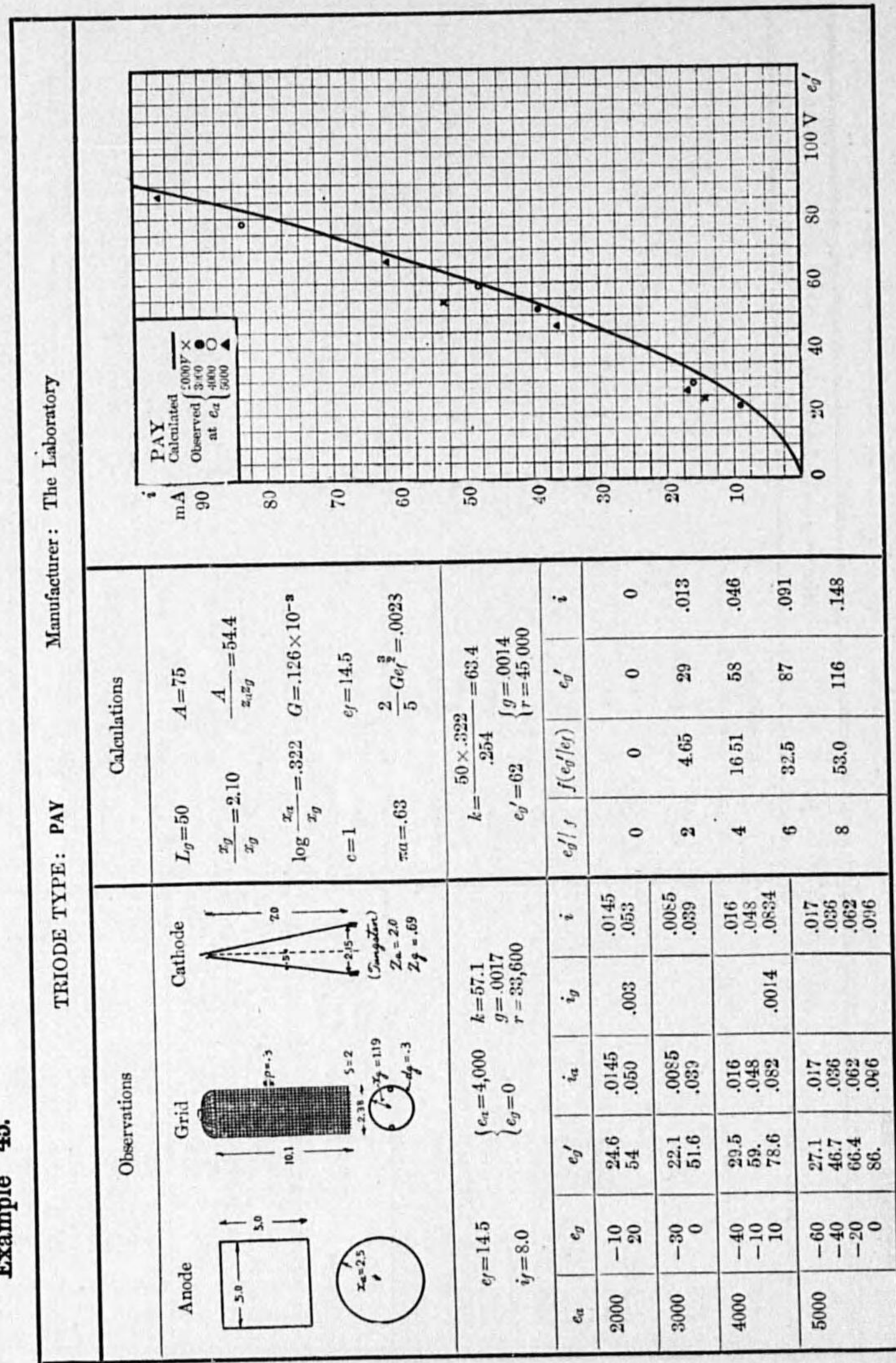
Example 43.



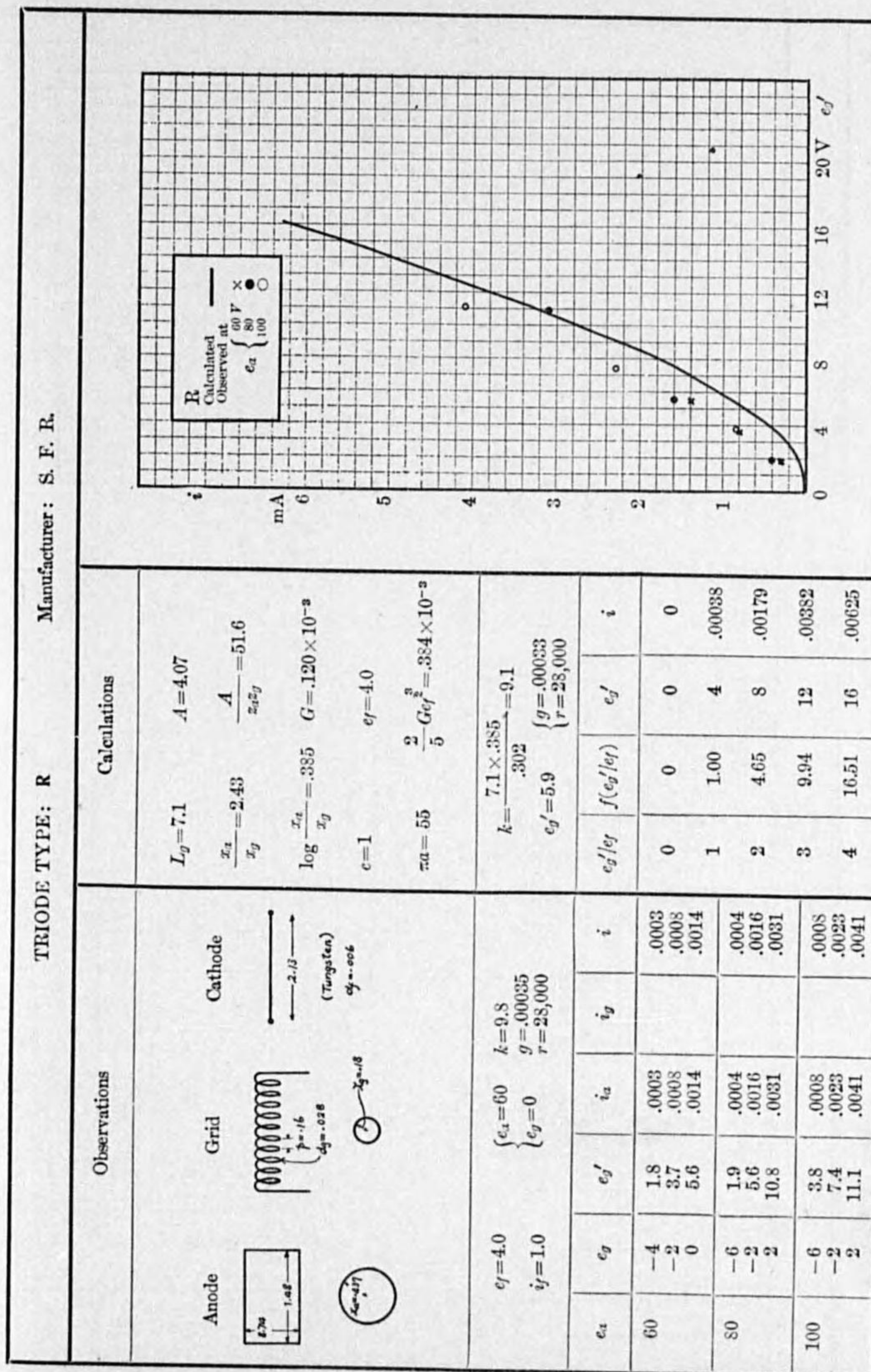
Example 44.



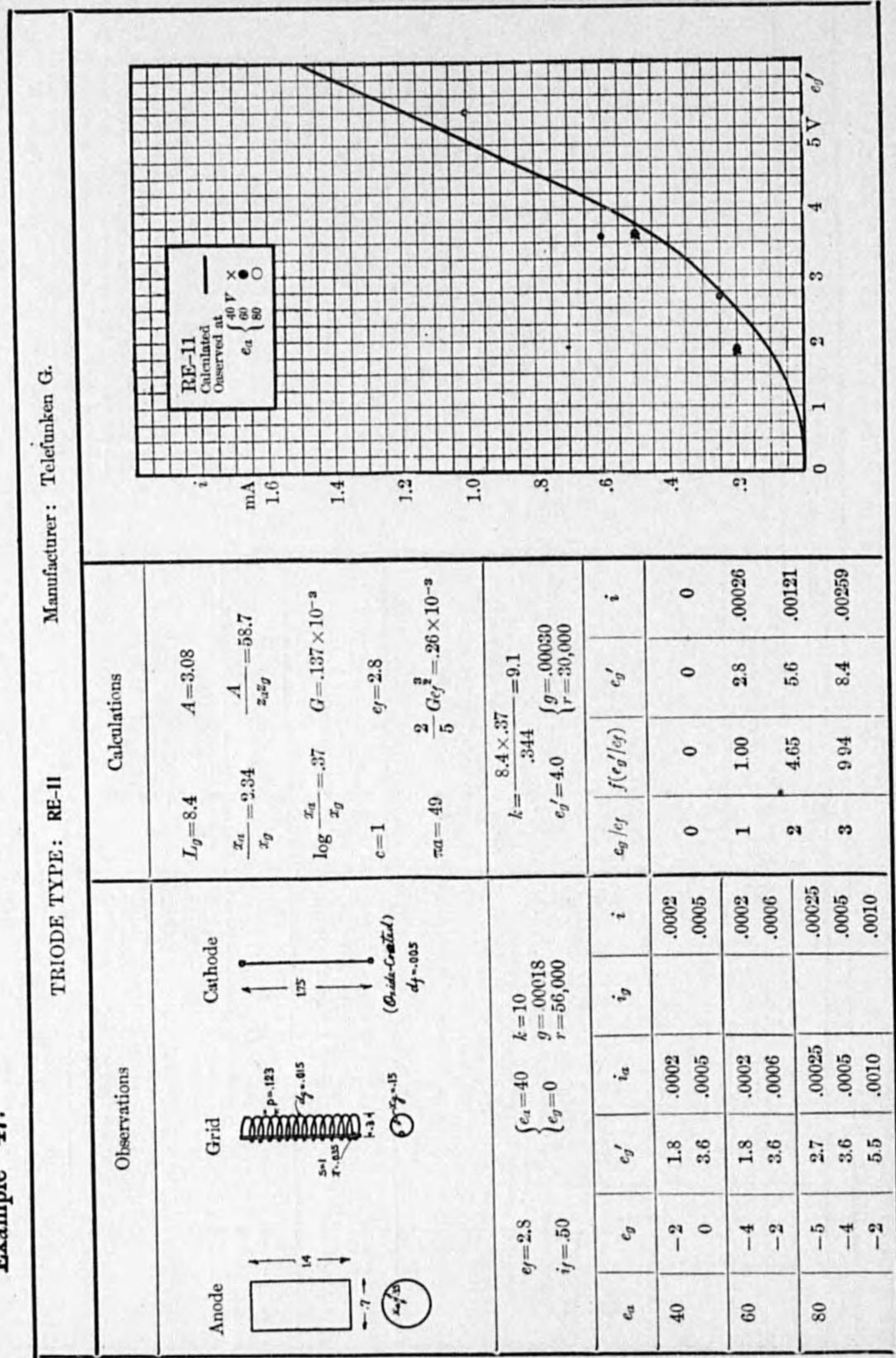
Example 45.



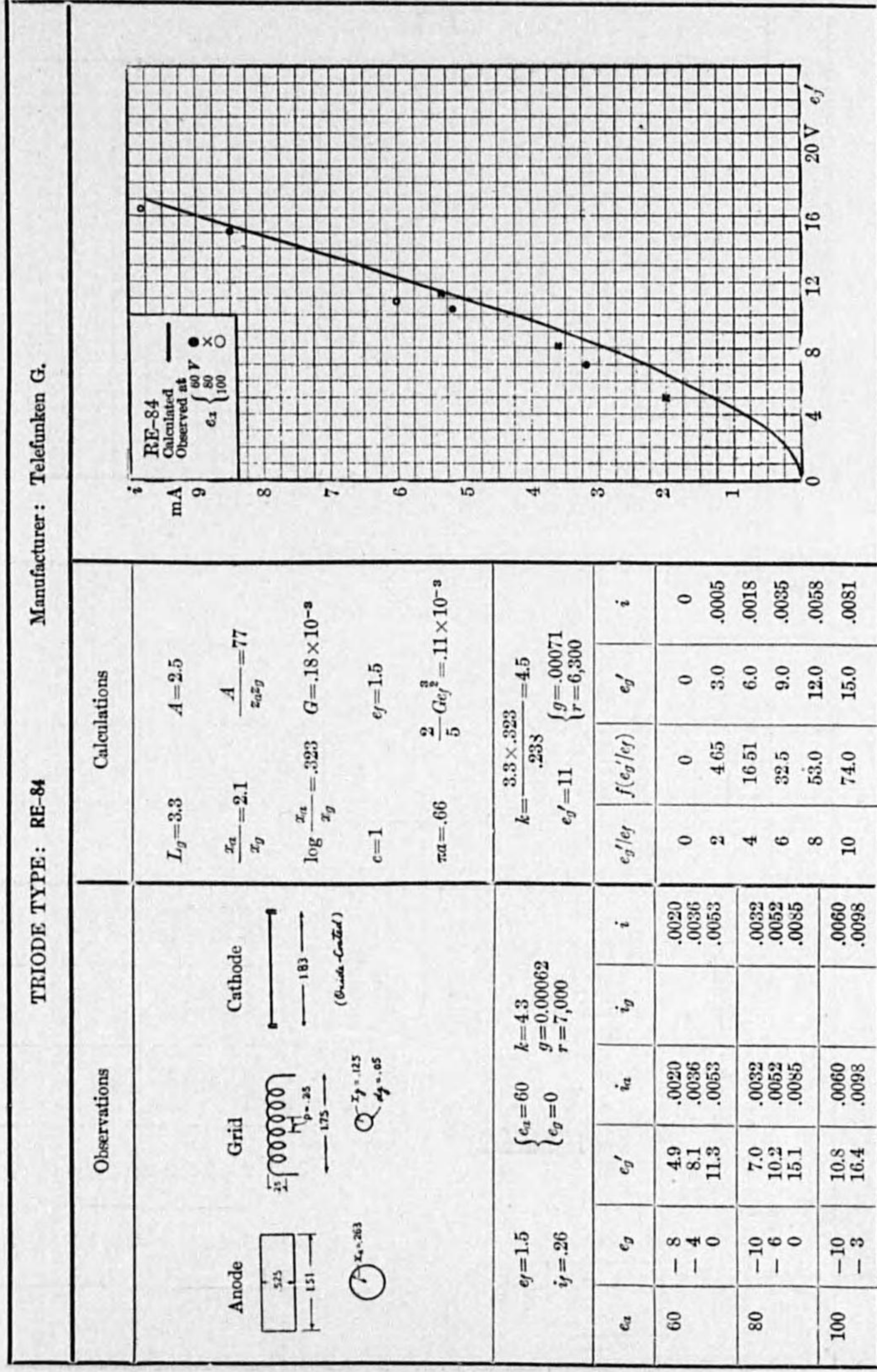
Example 46.



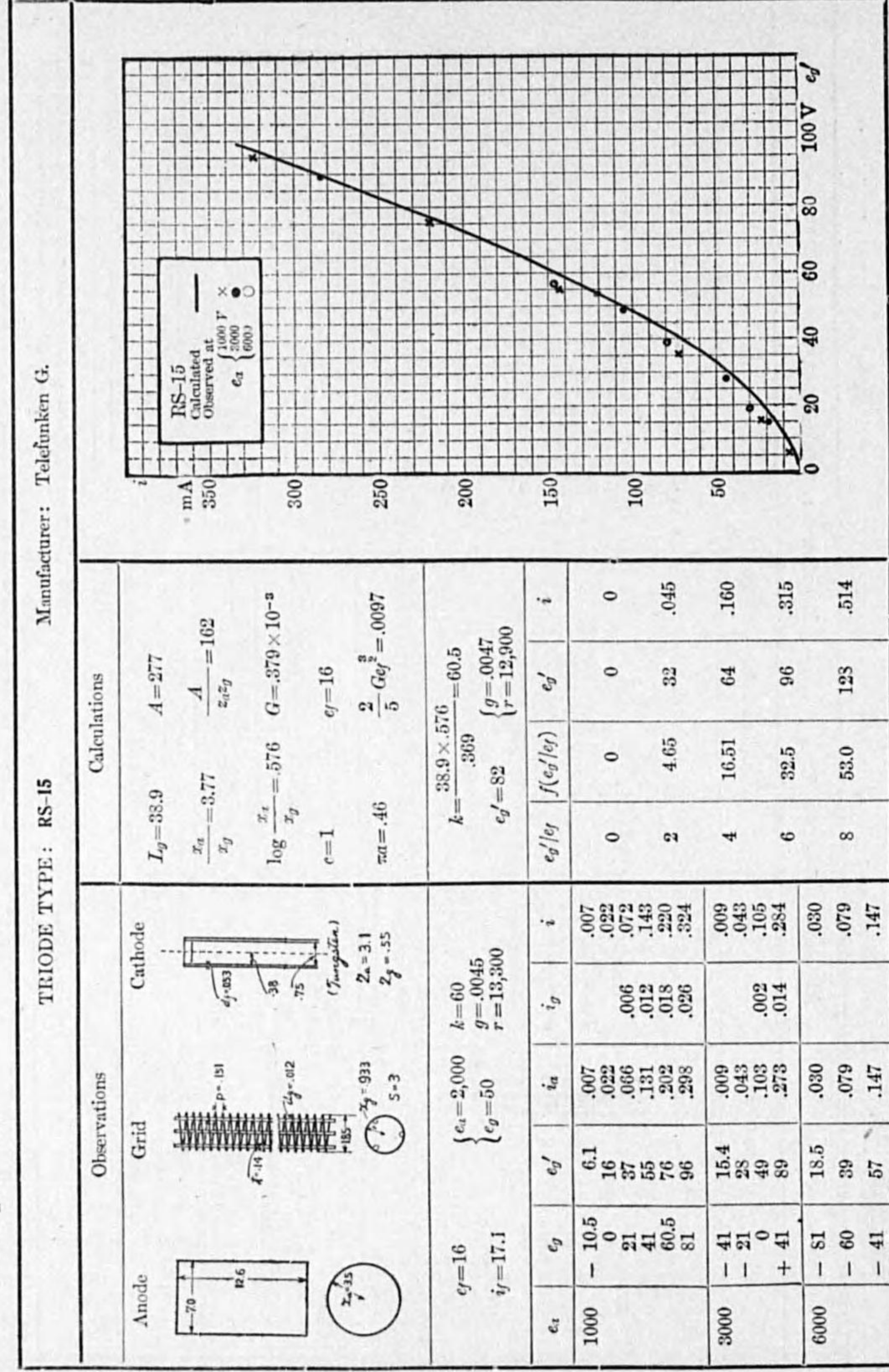
Example 47.



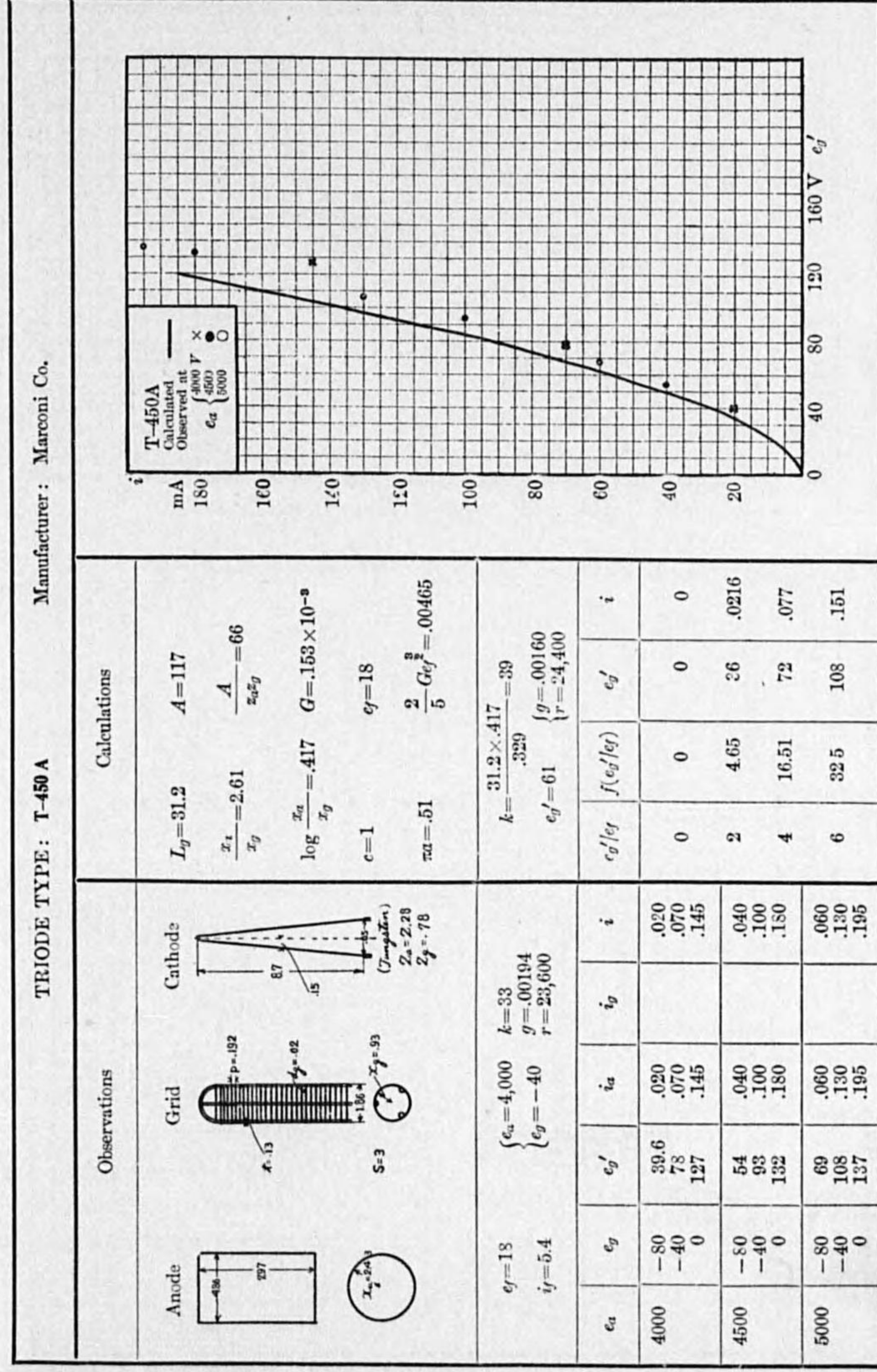
Example 48.



Example 49.

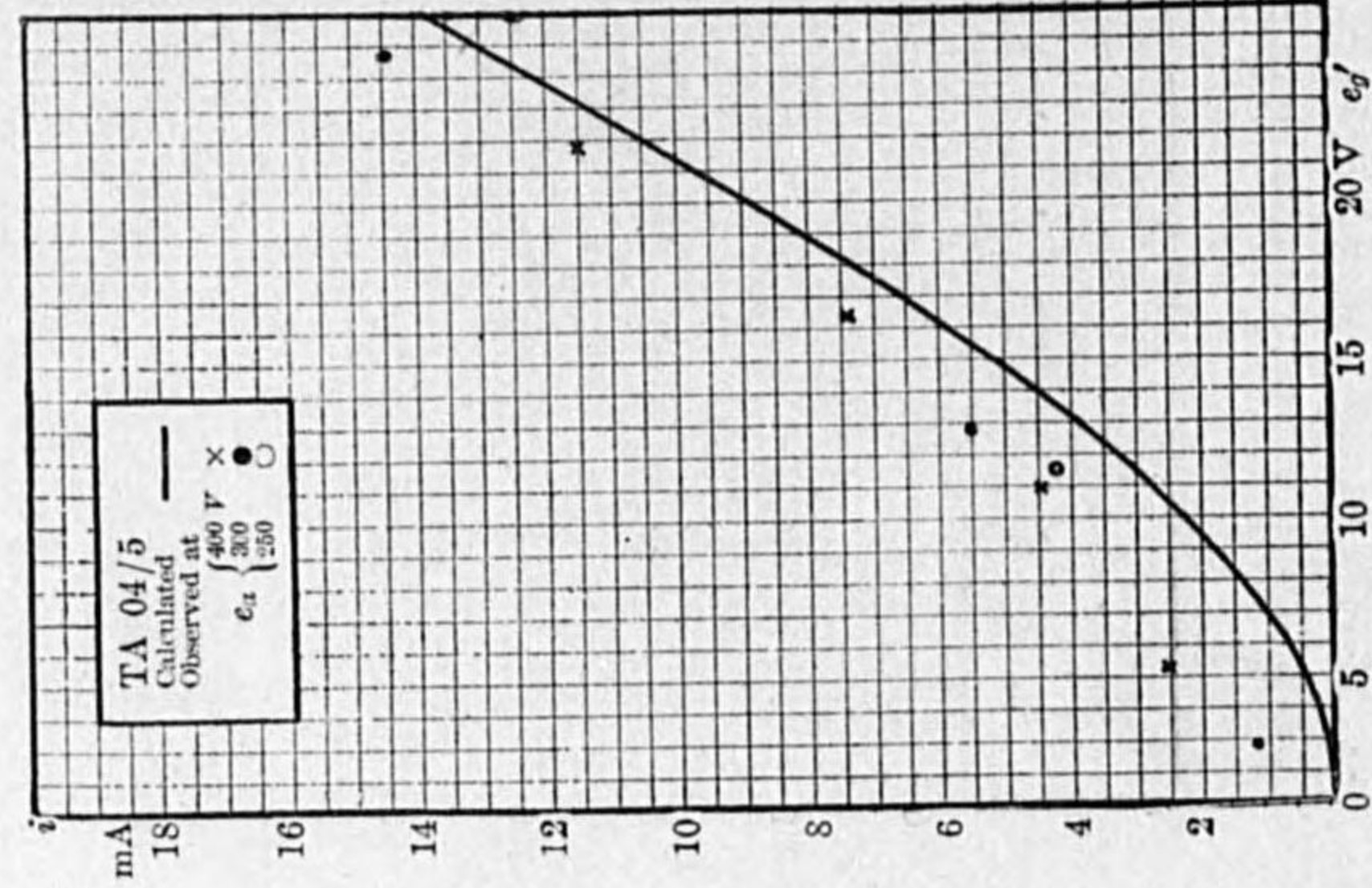


Example 50.



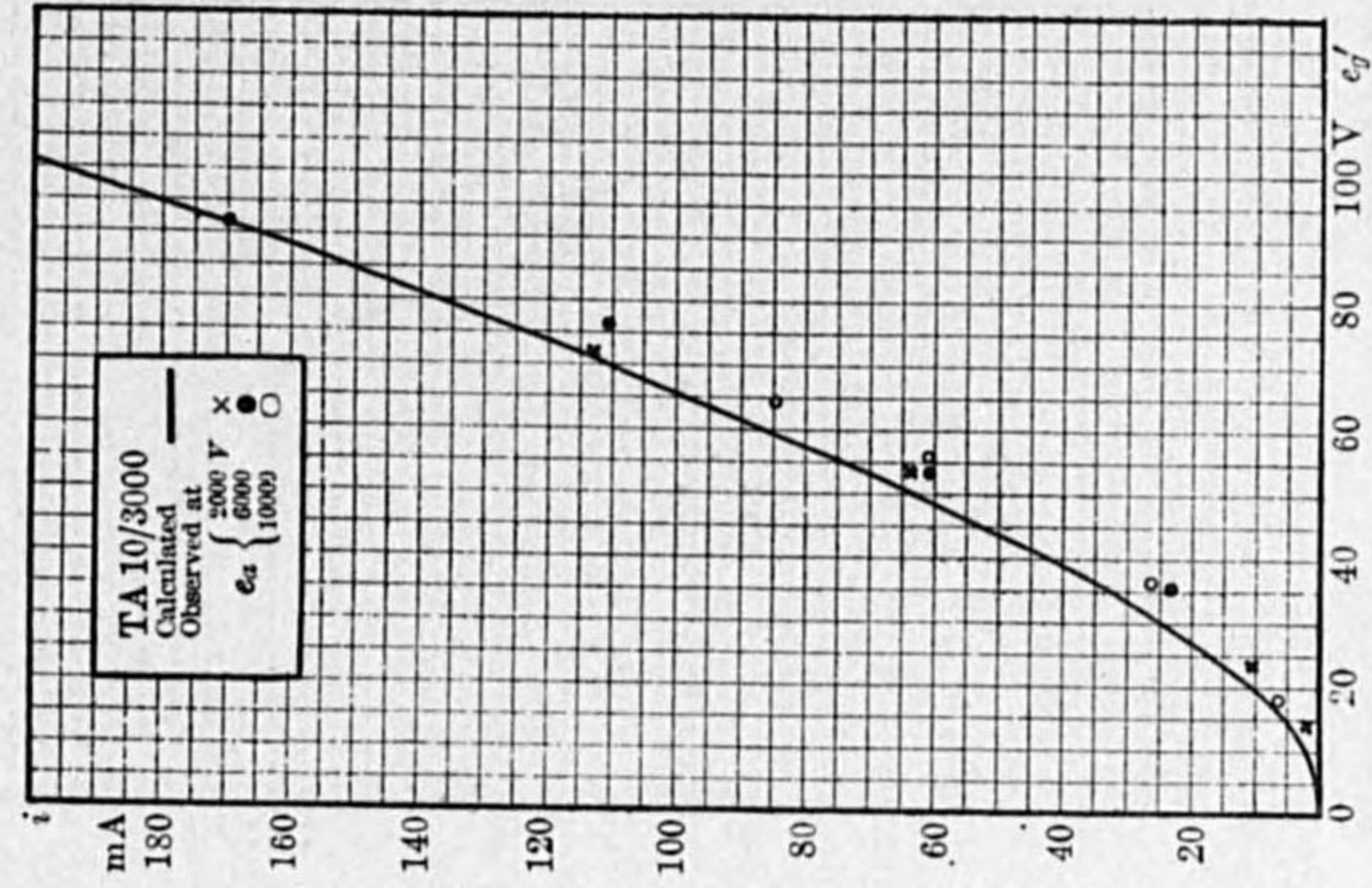
Example 51.

TRIODE TYPE: TA 04/5		Manufacturer: Philips' Lamp Works	
Observations		Calculations	
<p>Anode $e_a = 5.0$</p> <p>Grid $d_g = 0.18$</p> <p>Cathode $\chi_a = 0.50$</p>		<p>$A = 5.44$</p> <p>$\frac{x_a}{x_g} = 2.52$</p> <p>$\log \frac{x_a}{x_g} = 4.02$</p> <p>$c = 1$</p> <p>$\pi a = 59$</p> <p>$\frac{2}{5} G e_f^2 = 57 \times 10^{-8}$</p>	
<p>$e_f = 5.0$</p> <p>$i_f = 1.67$</p> <p>$e_a = 400$</p> <p>$k = 11.6$</p> <p>$g = 0.00078$</p> <p>$r = 14,900$</p>		<p>$k = \frac{8.3 \times 402}{.276} = 12$</p> <p>$e_f' = 18$</p> <p>$\left\{ \begin{array}{l} g = 0.00071 \\ r = 17,000 \end{array} \right.$</p>	
e_a	e_f	e_f'	i
400	-30	4.12	.0025
	-24	9.7	.00445
	-18	15.15	.00735
	-12	20.7	.0115
300	-24	1.75	.0012
	-12	12.8	.0055
	0	23.8	.0144
250	-6	10.3	.0042
		$f(e_f'/e_f)$	i
		.5	.000102
		1	.00057
		1.5	.00147
		2	.00266
		3	.00565
		4	.00942
		5	.0137

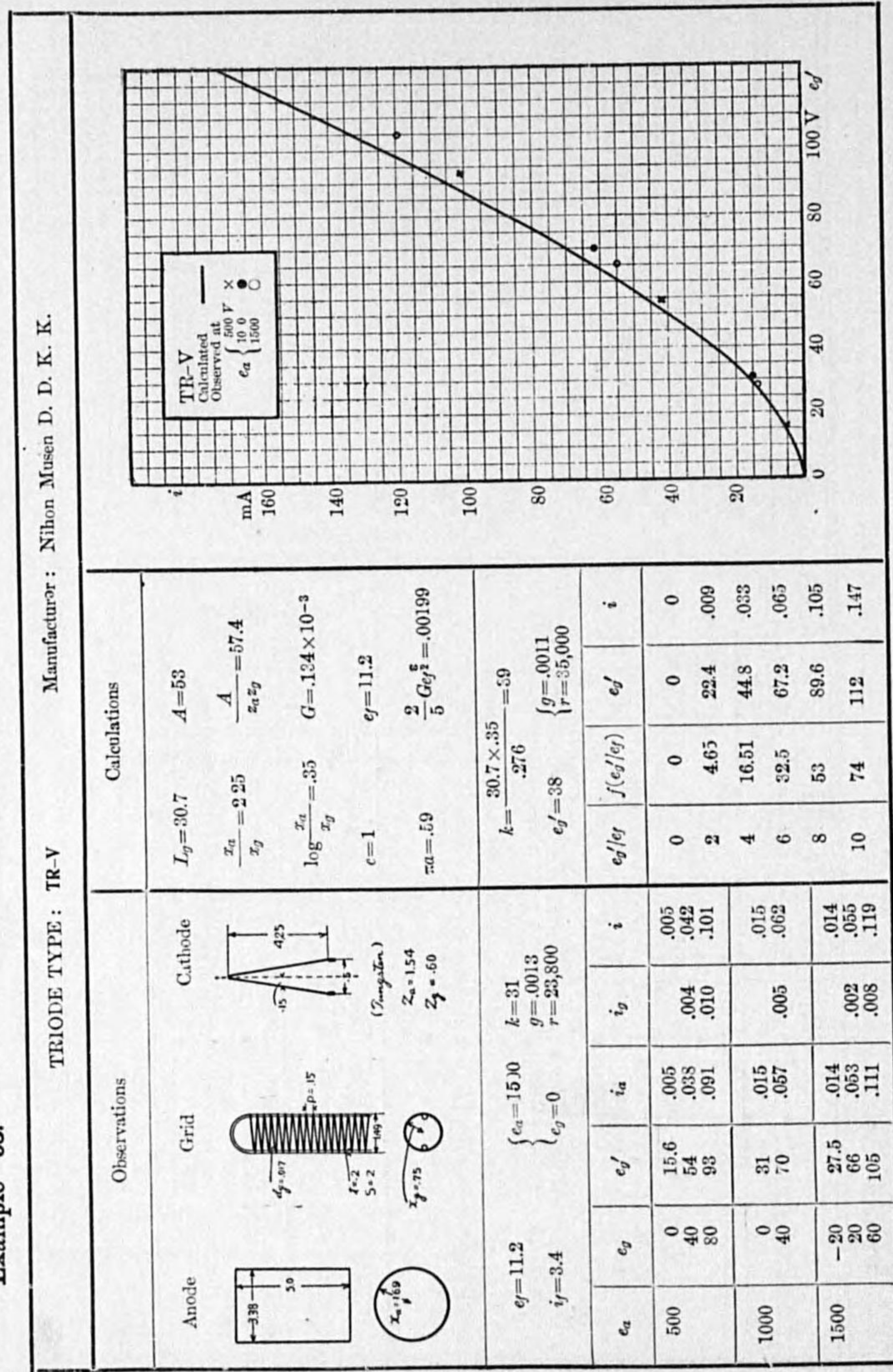


Example 52.

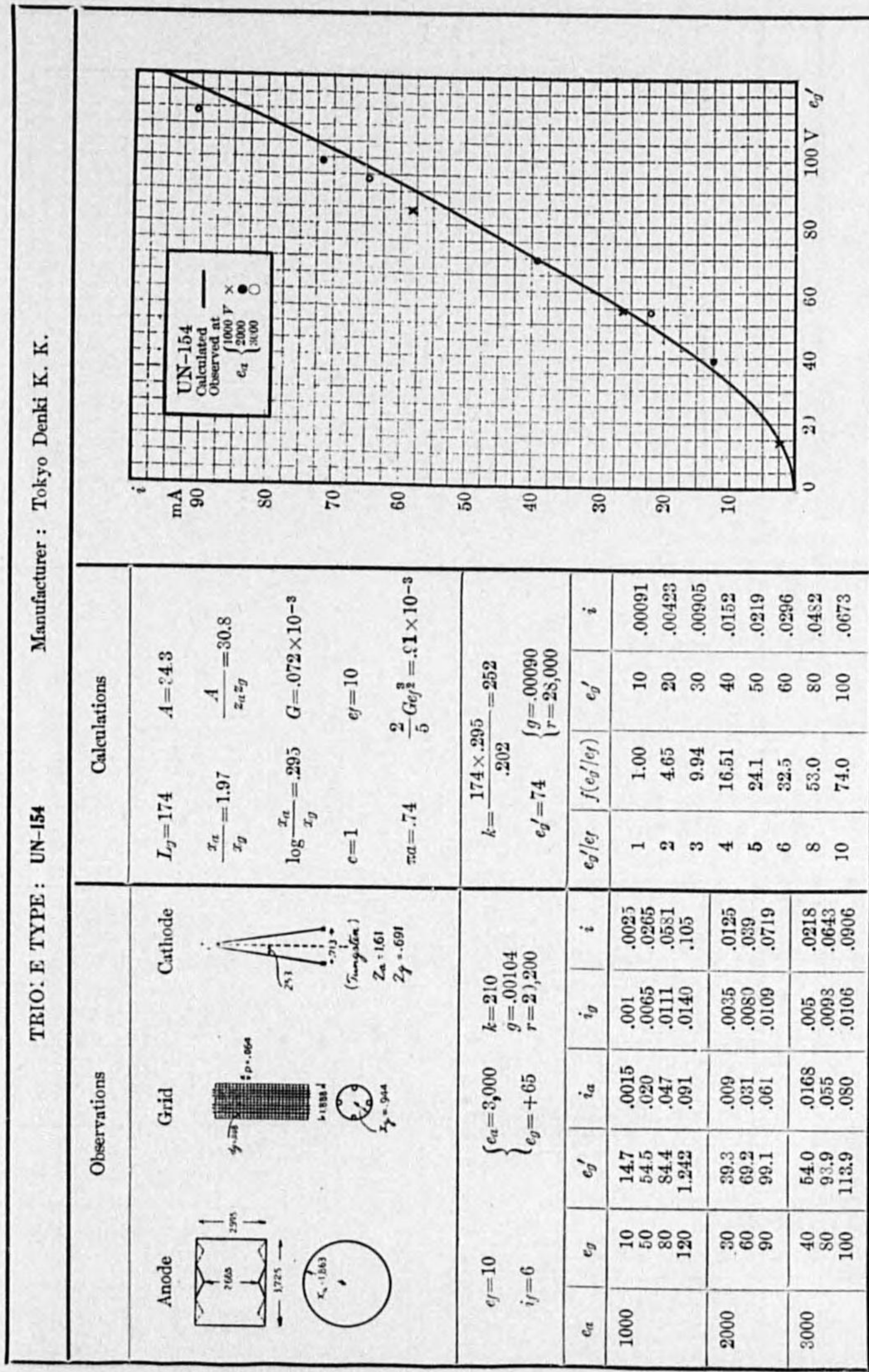
TRIODE TYPE: TA 10/3000		Manufacturer: Philips' Lamp Works	
Observations		Calculations	
<p>Anode $e_a = 13$</p> <p>Grid $d_g = 0.093$</p> <p>Cathode (Langmuir) $d_f = 0.063$</p>		<p>$A = 221$</p> <p>$\frac{x_a}{x_g} = 3.21$</p> <p>$\log \frac{x_a}{x_g} = 5.07$</p> <p>$c = 1$</p> <p>$\pi a = 63$</p> <p>$\frac{2}{5} G e_f^2 = 4.06 \times 10^{-8}$</p>	
<p>$e_f = 13$</p> <p>$i_f = 24.6$</p> <p>$e_a = 80,000$</p> <p>$k = 127$</p> <p>$g = 0.1027$</p> <p>$r = 47,000$</p>		<p>$k = \frac{70.7 \times 507}{.254} = 141$</p> <p>$e_f' = 73.4$</p> <p>$\left\{ \begin{array}{l} g = 0.0264 \\ r = 53,400 \end{array} \right.$</p>	
e_a	e_f	e_f'	i
2000	0	14.8	.002
	10	24.2	.0105
	40	52.4	.0666
	60	71.4	.1135
6000	-10	35.1	.0235
	10	53.9	.0606
	30	76.6	.1110
	50	91.7	.1700
10000	-60	17.75	.0070
	-40	36.6	.0270
	-20	55.4	.0610
	-10	64.7	.0850
		$f(e_f'/e_f)$	i
		1	.004
		2	.019
		3	.040
		4	.097
		5	.098
		6	.132
		8	.215
		10	.330



Example 53.

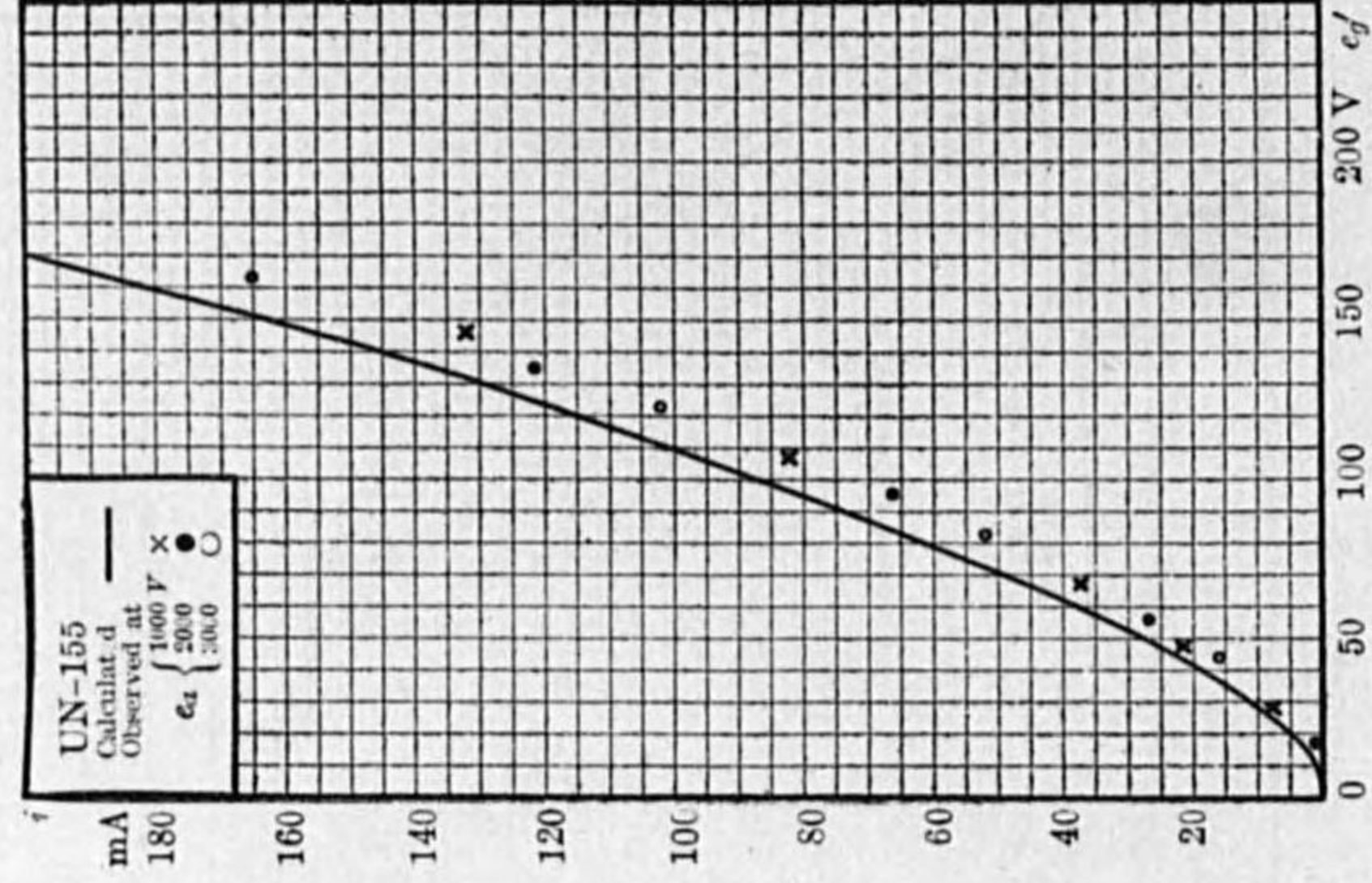


Example 54.



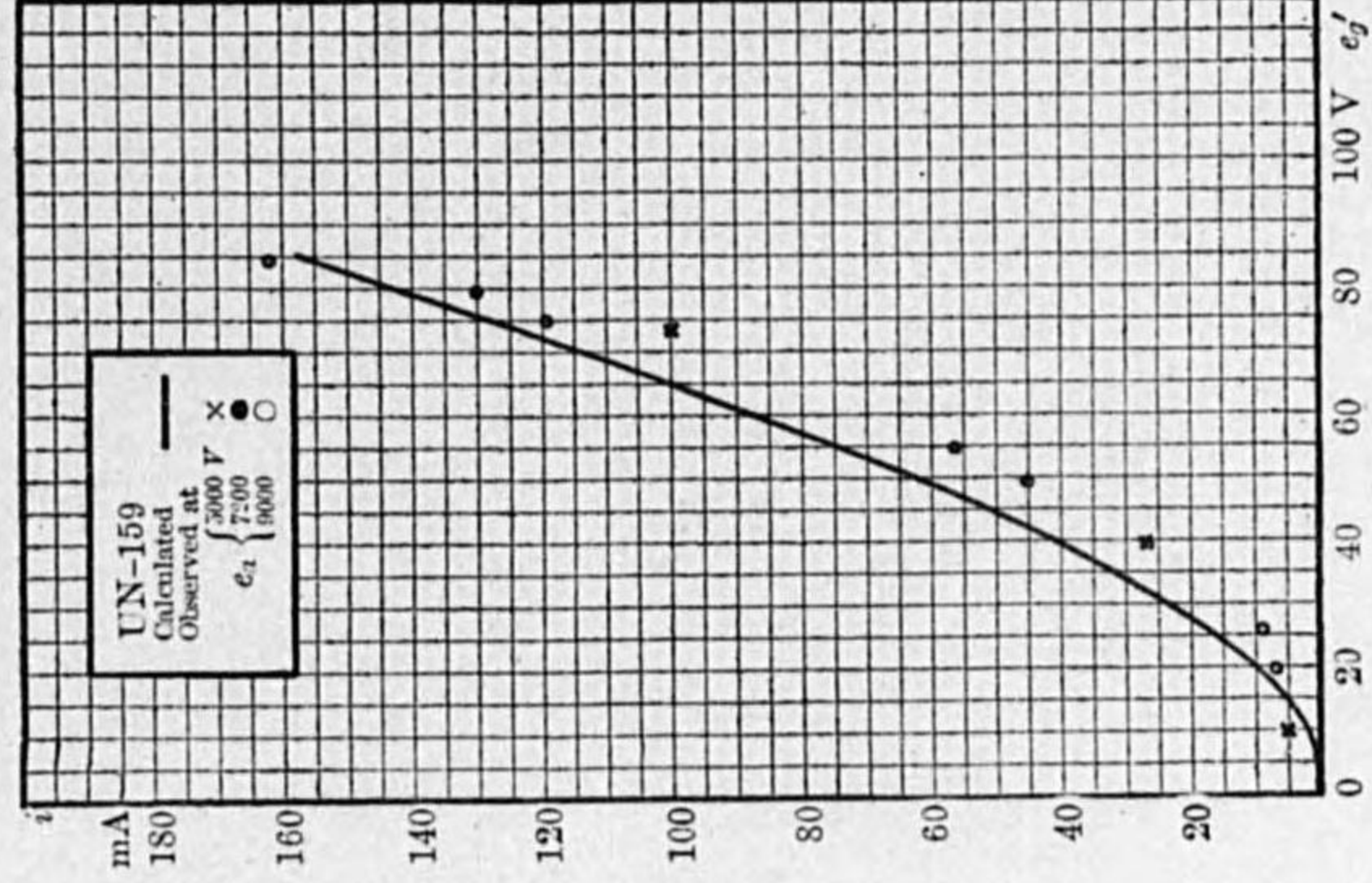
Example 55.

TRIODE TYPE : UN-155		Manufacturer : Tokyo Denki K. K.		
Observations		Calculations		
<p>Anode </p> <p>Grid </p> <p>Cathode </p>		<p>$I_g = 106$ $A = 84.6$</p> <p>$\frac{x_a}{x_g} = 1.99$ $\frac{A}{\pi a x_g} = 40.5$</p> <p>$\log \frac{x_a}{x_g} = 2.99$ $G = .9944 \times 10^{-3}$</p> <p>$c = 1$ $e_f = 12$</p> <p>$\pi a = .75$ $\frac{2}{5} C e_f^2 = .00157$</p>		
<p>$e_f = 12$ $k = 125$</p> <p>$i_f = 6$ $g = .00114$</p> <p> $r = 110,000$</p>		<p>$k = \frac{106 \times .299}{.193} = 16$</p> <p>$e_f' = 93$ $\left\{ \begin{array}{l} g = .00131 \\ r = 122,000 \end{array} \right.$</p>		
e_a	e_f	e_f'/e_f	$f(e_f'/e_f)$	i
1000	20	1	1.00	.008
	40	2	4.65	.0216
	60	3	9.94	.039
	100	4	16.51	.066
	140	5	24.1	.096
2000	0	6	32.5	.1216
	40	8	53.0	.001
	80	10	74.0	.0266
	120	15	138.0	.057
				.112
3000	20			.0135
	40			.045
	60			.084
	100			.1022
	140			.0075
				.1605

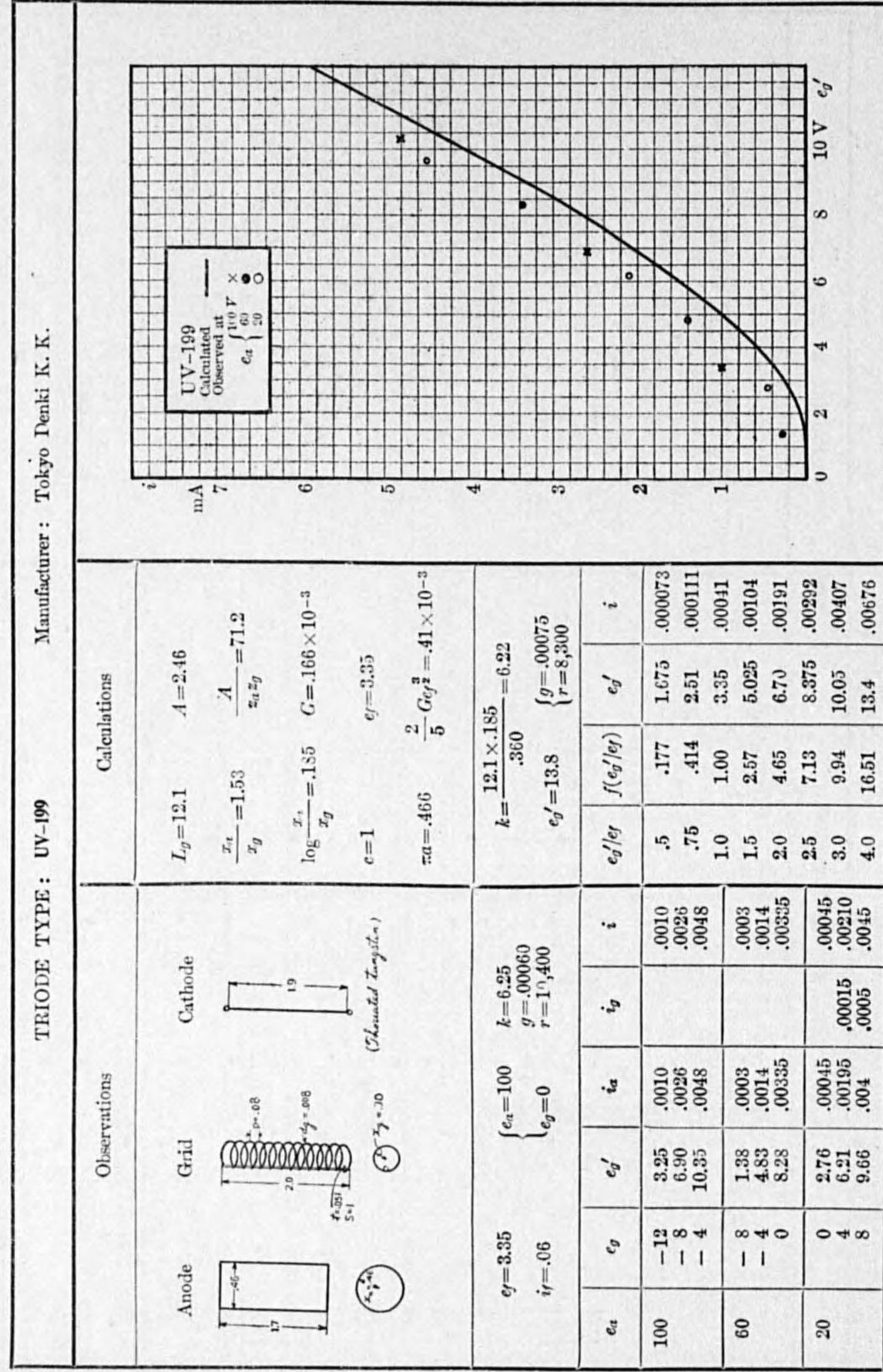


Example 56.

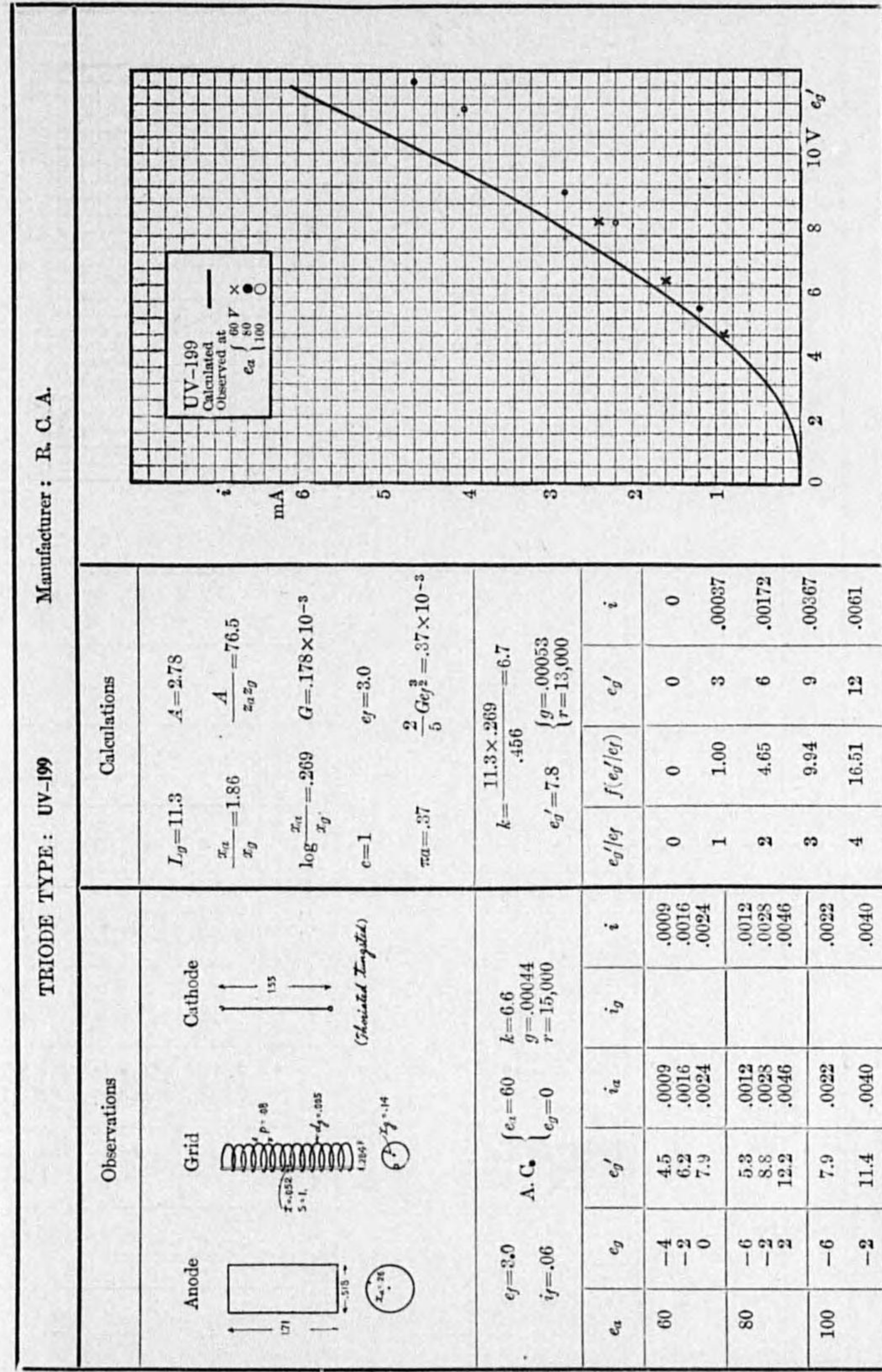
TRIODE TYPE : UN-159		Manufacturer : Tokyo Denki K. K.		
Observations		Calculations		
<p>Anode </p> <p>Grid </p> <p>Cathode </p>		<p>$I_g = 56.5$ $A = 115$</p> <p>$\frac{x_a}{x_g} = 2.32$ $\frac{A}{\pi a x_g} = 99.8$</p> <p>$\log \frac{x_a}{x_g} = 2.65$ $G = 233 \times 10^{-3}$</p> <p>$c = 1$ $e_f = 17$</p> <p>$\pi a = .71$ $\frac{2}{5} C e_f^2 = .00651$</p>		
<p>$e_f = 17$ $k = 90$</p> <p>$i_f = 23.5$ $g = .00204$</p> <p> $r = 44,100$</p>		<p>$k = \frac{56.5 \times .365}{.212} = 96$</p> <p>$e_f' = 123$ $\left\{ \begin{array}{l} g = .0037 \\ r = 26,000 \end{array} \right.$</p>		
e_a	e_f	e_f'/e_f	$f(e_f'/e_f)$	i
9000	-90	.5	.177	.005
	-60	1.0	1.00	.027
	-30	2.0	4.65	.100
7200	-60	3.0	9.94	.007
	-30	4.0	16.51	.045
	0	5.0	24.1	.130
5000	-30			.003
	0			.056
	20			.118
	30			.152



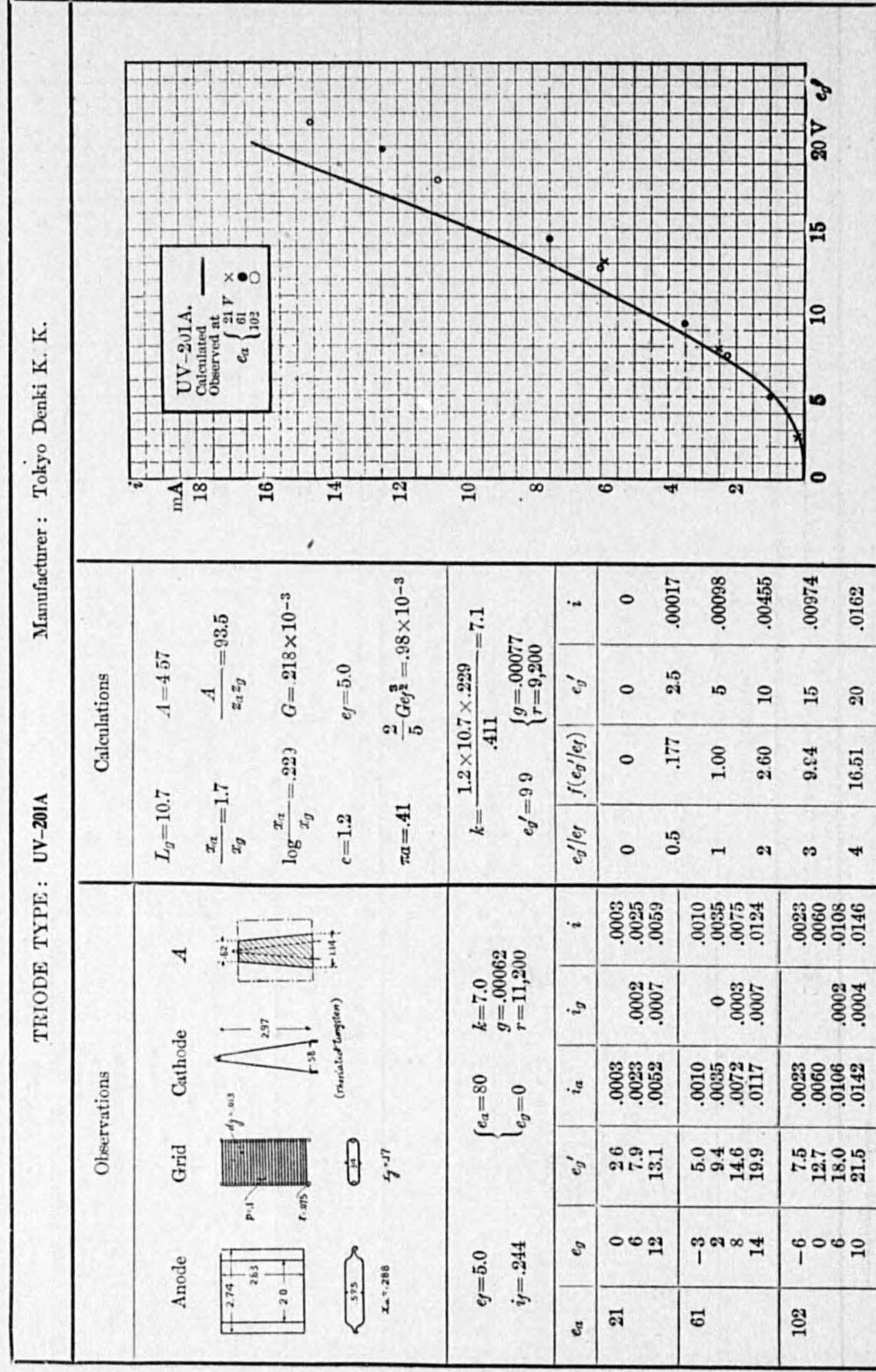
Example 57.



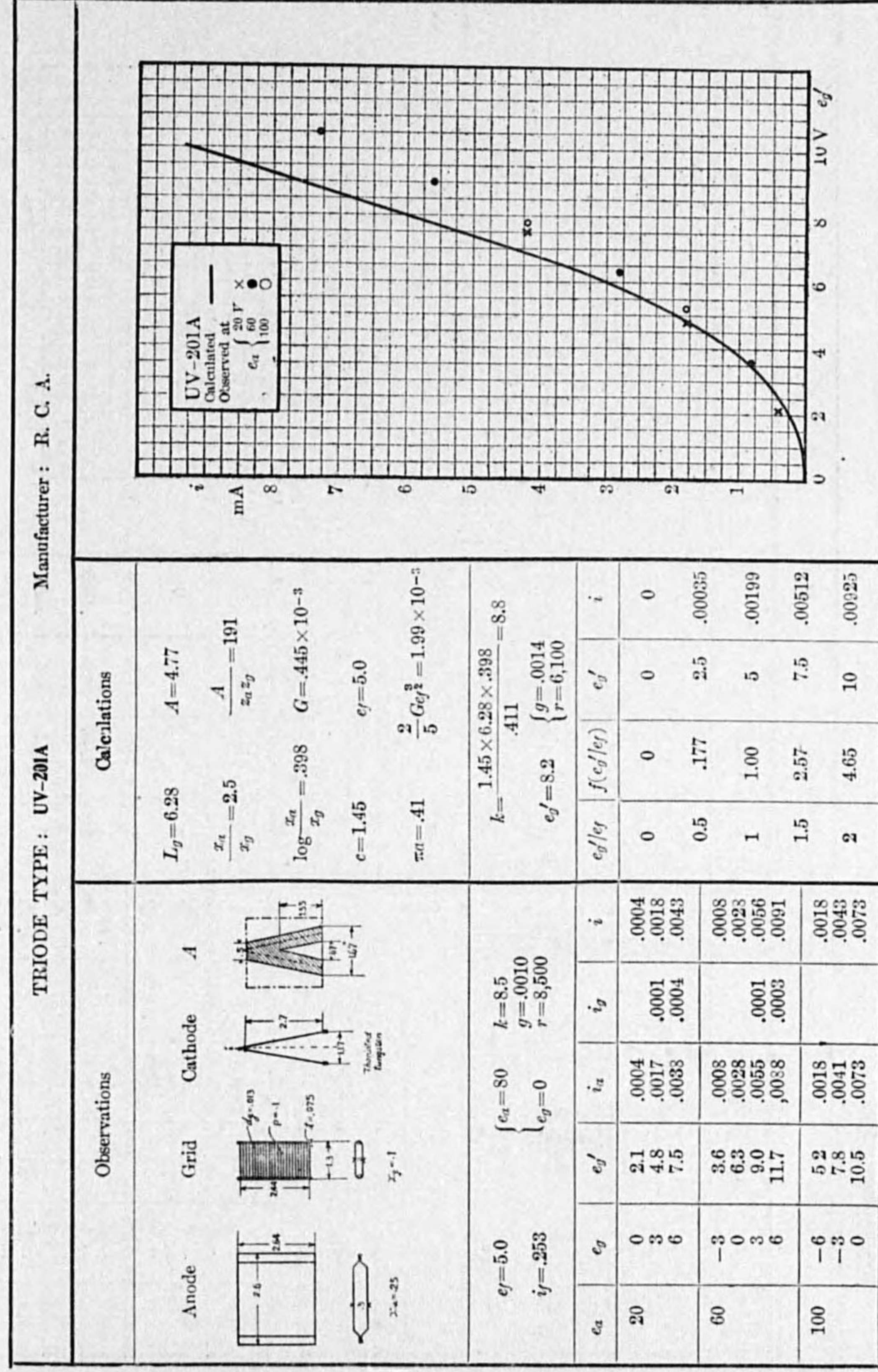
Example 58.



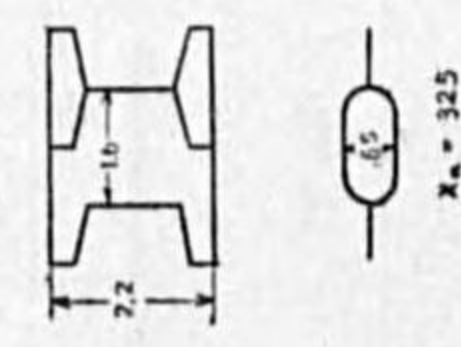
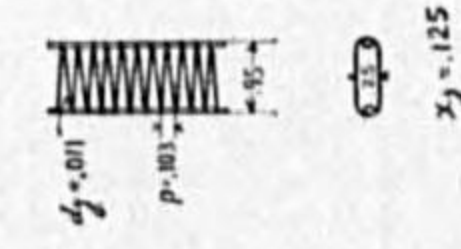
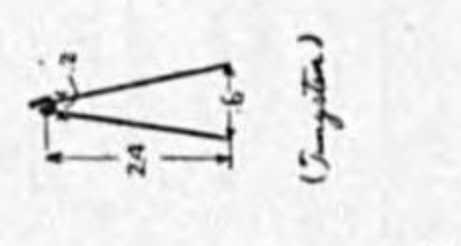
Example 59.

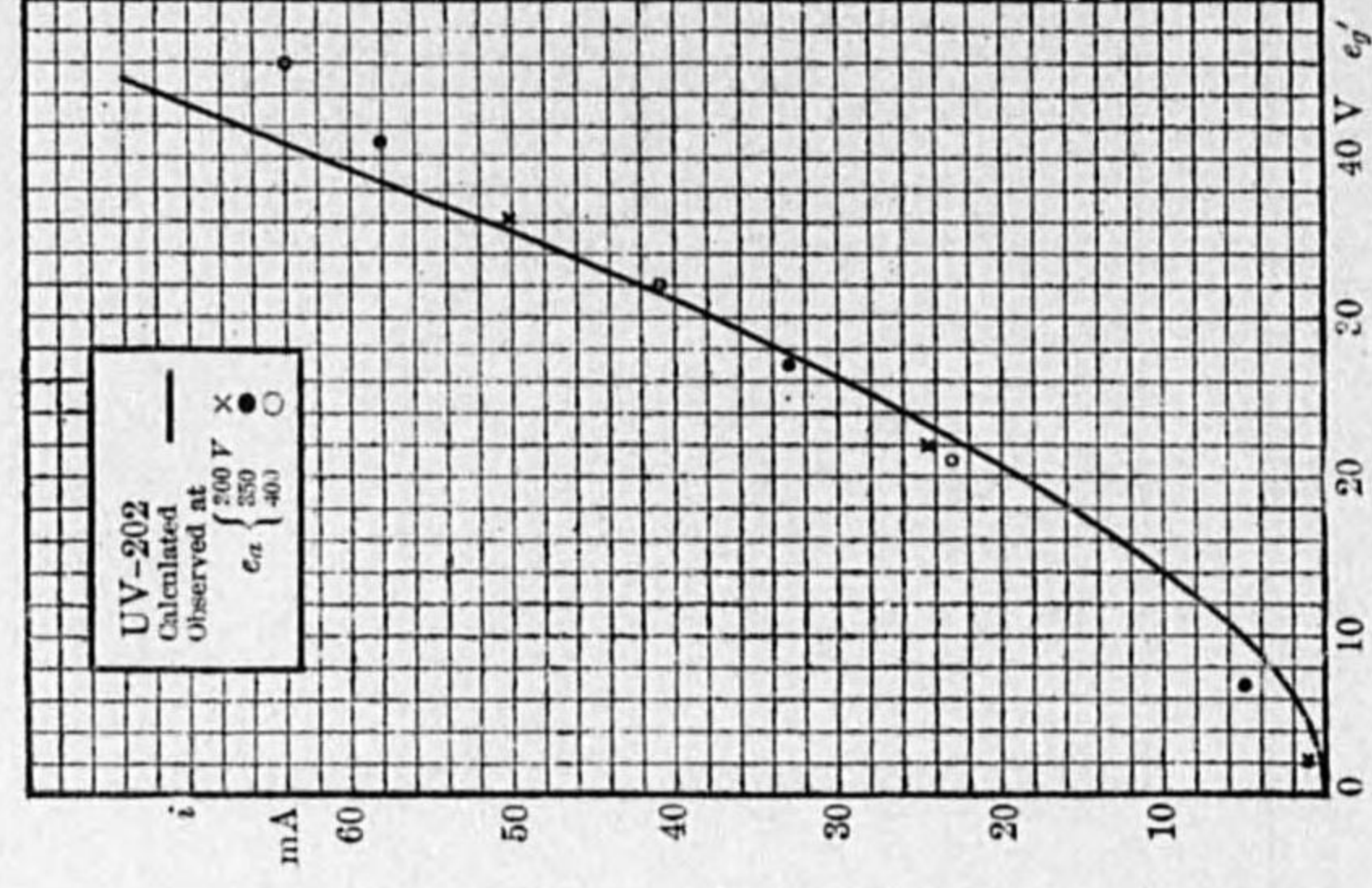


Example 60.

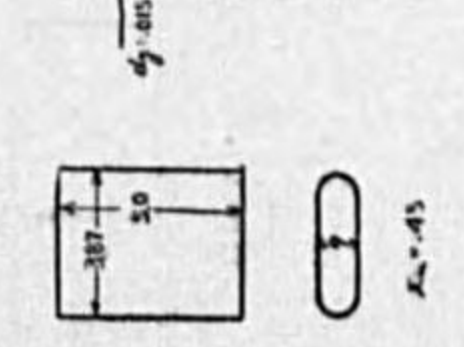
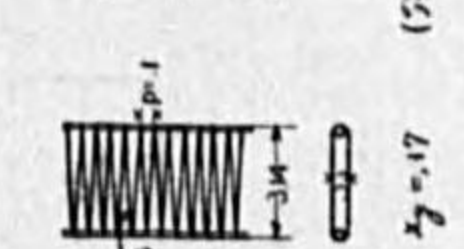
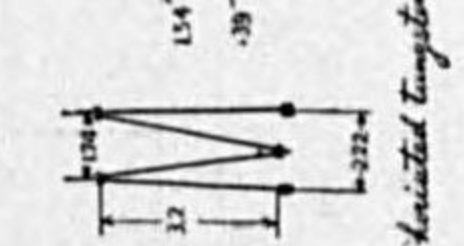


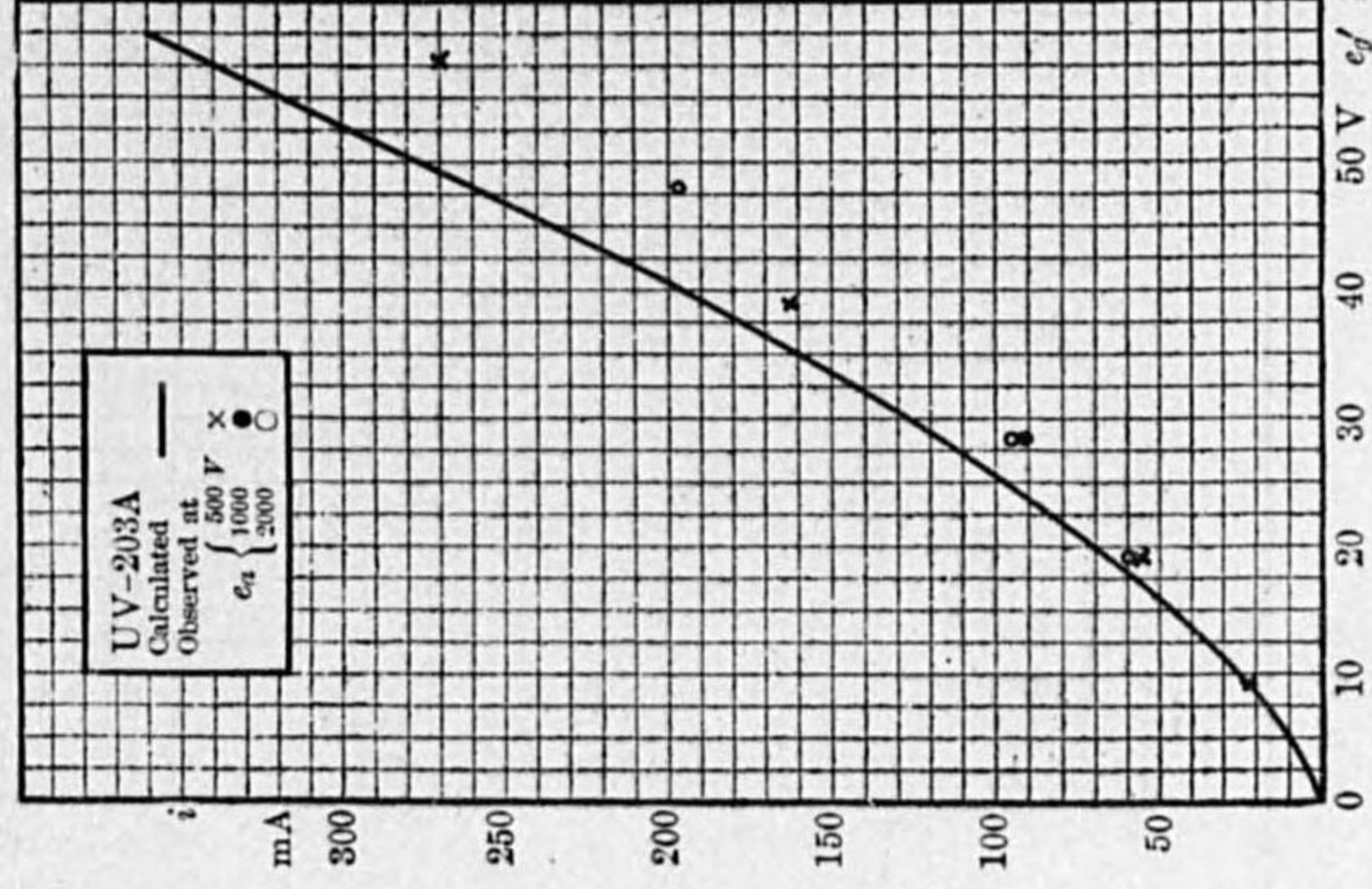
Example 61.

TRIODE TYPE: UV-202		Manufacturer: R. C. A.																																																													
Observations		Calculations																																																													
<p>Anode</p>  <p>$x_a = 325$</p>	<p>Grid</p>  <p>$r_g = 125$</p>	<p>Cathode</p>  <p>$r_c = 118$</p>	<p>$A = 4.8$</p> <p>$\frac{A}{z_a z_g} = 118$</p> <p>$G = .276 \times 10^{-3}$</p> <p>$e_f = 7.5$</p> <p>$\frac{2}{5} G e_f^2 = .00227$</p>																																																												
<p>$e_f = 7.5$</p> <p>$i_f = 2.31$</p>	<p>$\left\{ \begin{array}{l} e_a = 350 \\ e_g = -10 \end{array} \right.$</p> <p>$k = 0.3$</p> <p>$g = .0016$</p> <p>$r = 5,800$</p>	<p>$k = \frac{1.5 \times 7.6 \times .415}{.493} = 9.6$</p> <p>$e_f = 84$</p> <p>$\left\{ \begin{array}{l} g = .0017 \\ r = 5,700 \end{array} \right.$</p>	<table border="1"> <thead> <tr> <th>e_f / e_f</th> <th>$f(e_f / e_f)$</th> <th>e_f'</th> <th>i</th> </tr> </thead> <tbody> <tr> <td>0</td> <td>0</td> <td>0</td> <td>0</td> </tr> <tr> <td>1</td> <td>1.00</td> <td>7.5</td> <td>.0023</td> </tr> <tr> <td>2</td> <td>4.65</td> <td>15.0</td> <td>.0105</td> </tr> <tr> <td>4</td> <td>16.51</td> <td>30.0</td> <td>.037</td> </tr> <tr> <td>6</td> <td>32.5</td> <td>45.0</td> <td>.074</td> </tr> </tbody> </table>	e_f / e_f	$f(e_f / e_f)$	e_f'	i	0	0	0	0	1	1.00	7.5	.0023	2	4.65	15.0	.0105	4	16.51	30.0	.037	6	32.5	45.0	.074																																				
e_f / e_f	$f(e_f / e_f)$	e_f'	i																																																												
0	0	0	0																																																												
1	1.00	7.5	.0023																																																												
2	4.65	15.0	.0105																																																												
4	16.51	30.0	.037																																																												
6	32.5	45.0	.074																																																												
<table border="1"> <thead> <tr> <th>e_a</th> <th>e_g</th> <th>e_f'</th> <th>i_a</th> <th>i_g</th> <th>i</th> </tr> </thead> <tbody> <tr> <td>300</td> <td>-30</td> <td>1.9</td> <td>.003</td> <td>.024</td> <td>.003</td> </tr> <tr> <td></td> <td>-8</td> <td>22</td> <td>.024</td> <td>.049</td> <td>.024</td> </tr> <tr> <td></td> <td>8</td> <td>36</td> <td>.049</td> <td>.009</td> <td>.050</td> </tr> <tr> <td>350</td> <td>-30</td> <td>6.8</td> <td>.005</td> <td>.033</td> <td>.005</td> </tr> <tr> <td></td> <td>-8</td> <td>27</td> <td>.033</td> <td>.057</td> <td>.033</td> </tr> <tr> <td></td> <td>8</td> <td>41</td> <td>.057</td> <td>.009</td> <td>.058</td> </tr> <tr> <td>400</td> <td>-30</td> <td>21</td> <td>.023</td> <td>.041</td> <td>.023</td> </tr> <tr> <td></td> <td>-8</td> <td>31</td> <td>.041</td> <td>.009</td> <td>.041</td> </tr> <tr> <td></td> <td>8</td> <td>45</td> <td>.009</td> <td>.009</td> <td>.064</td> </tr> </tbody> </table>	e_a	e_g	e_f'	i_a	i_g	i	300	-30	1.9	.003	.024	.003		-8	22	.024	.049	.024		8	36	.049	.009	.050	350	-30	6.8	.005	.033	.005		-8	27	.033	.057	.033		8	41	.057	.009	.058	400	-30	21	.023	.041	.023		-8	31	.041	.009	.041		8	45	.009	.009	.064			
e_a	e_g	e_f'	i_a	i_g	i																																																										
300	-30	1.9	.003	.024	.003																																																										
	-8	22	.024	.049	.024																																																										
	8	36	.049	.009	.050																																																										
350	-30	6.8	.005	.033	.005																																																										
	-8	27	.033	.057	.033																																																										
	8	41	.057	.009	.058																																																										
400	-30	21	.023	.041	.023																																																										
	-8	31	.041	.009	.041																																																										
	8	45	.009	.009	.064																																																										



Example 62.

TRIODE TYPE: UV-203A		Manufacturer: R. C. A.																																																							
Observations		Calculations																																																							
<p>Anode</p>  <p>$x_a = 45$</p>	<p>Grid</p>  <p>$r_g = 17$</p>	<p>Cathode</p>  <p>$r_c = 352$</p>	<p>$A = 25.4$</p> <p>$\frac{A}{z_a z_g} = 352$</p> <p>$G = 774 \times 10^{-3}$</p> <p>$i = G e_f^2$</p> <p>$\pi a = .57$</p>																																																						
<p>$e_f = 9.5$</p> <p>$i_f = 3.25$</p>	<p>$\left\{ \begin{array}{l} e_a = 500 \\ e_g = +2 \end{array} \right.$</p> <p>$k = 25$</p> <p>$g = .0050$</p> <p>$r = 5,000$</p>	<p>$k = \frac{1.75 \times 10.7 \times .42}{.289} = 27$</p> <p>$e_f = 37$</p> <p>$\left\{ \begin{array}{l} g = .0068 \\ r = 4,000 \end{array} \right.$</p>	<table border="1"> <thead> <tr> <th>e_f'</th> <th>$e_f'^2$</th> <th>i</th> </tr> </thead> <tbody> <tr> <td>0</td> <td>0</td> <td>0</td> </tr> <tr> <td>10</td> <td>31.6</td> <td>.025</td> </tr> <tr> <td>20</td> <td>89</td> <td>.069</td> </tr> <tr> <td>30</td> <td>164</td> <td>.127</td> </tr> <tr> <td>40</td> <td>253</td> <td>.196</td> </tr> <tr> <td>50</td> <td>354</td> <td>.274</td> </tr> <tr> <td>60</td> <td>465</td> <td>.360</td> </tr> </tbody> </table>	e_f'	$e_f'^2$	i	0	0	0	10	31.6	.025	20	89	.069	30	164	.127	40	253	.196	50	354	.274	60	465	.360																														
e_f'	$e_f'^2$	i																																																							
0	0	0																																																							
10	31.6	.025																																																							
20	89	.069																																																							
30	164	.127																																																							
40	253	.196																																																							
50	354	.274																																																							
60	465	.360																																																							
<table border="1"> <thead> <tr> <th>e_a</th> <th>e_g</th> <th>e_f'</th> <th>i_a</th> <th>i_g</th> <th>i</th> </tr> </thead> <tbody> <tr> <td>500</td> <td>-10.5</td> <td>9</td> <td>.023</td> <td>.001</td> <td>.023</td> </tr> <tr> <td></td> <td>0</td> <td>19</td> <td>.056</td> <td>.008</td> <td>.057</td> </tr> <tr> <td></td> <td>21</td> <td>39</td> <td>.155</td> <td>.015</td> <td>.163</td> </tr> <tr> <td></td> <td>40</td> <td>58</td> <td>.255</td> <td>.001</td> <td>.270</td> </tr> <tr> <td>1000</td> <td>-10.5</td> <td>28.5</td> <td>.092</td> <td>.004</td> <td>.092</td> </tr> <tr> <td></td> <td>10.5</td> <td>48</td> <td>.192</td> <td>.004</td> <td>.196</td> </tr> <tr> <td>2000</td> <td>-60</td> <td>19</td> <td>.059</td> <td>.002</td> <td>.059</td> </tr> <tr> <td></td> <td>-50.5</td> <td>28.5</td> <td>.092</td> <td>.002</td> <td>.092</td> </tr> </tbody> </table>	e_a	e_g	e_f'	i_a	i_g	i	500	-10.5	9	.023	.001	.023		0	19	.056	.008	.057		21	39	.155	.015	.163		40	58	.255	.001	.270	1000	-10.5	28.5	.092	.004	.092		10.5	48	.192	.004	.196	2000	-60	19	.059	.002	.059		-50.5	28.5	.092	.002	.092			
e_a	e_g	e_f'	i_a	i_g	i																																																				
500	-10.5	9	.023	.001	.023																																																				
	0	19	.056	.008	.057																																																				
	21	39	.155	.015	.163																																																				
	40	58	.255	.001	.270																																																				
1000	-10.5	28.5	.092	.004	.092																																																				
	10.5	48	.192	.004	.196																																																				
2000	-60	19	.059	.002	.059																																																				
	-50.5	28.5	.092	.002	.092																																																				



Example 63.

TRIODE TYPE: UV-204										Manufacturer: R. C. A.			
Observations					Calculations					Graph			
Anode		Grid		Cathode		A		$I_g = 11.5$ $\frac{x_a}{x_g} = 2.5$ $\log \frac{x_a}{x_g} = .398$ $c = 1.45$ $\pi a = .575$		$A = 38.1$ $\frac{A}{\pi a x_g} = 169$ $G = .395 \times 10^{-3}$ $e_f = 11.4$ $\frac{2}{5} G e_f^2 = .00607$			
$e_f = 11.4$ $i_f = 14.75$ A. C.					$k = 26$ $g = .0048$ $r = 5,400$ $e_g = 0$					$k = 1.45 \times 11.5 \times .398 = 25.3$ $e_f = 65$ $\left\{ \begin{array}{l} g = 0.46 \\ r = 6,400 \end{array} \right.$			
e_a	e_g	e_f	i_a	i_g	i	e_f/e_g	$f(e_f/e_g)$	e_f	i				
1500	-40	17.5	.018		.018	0	0	0	0				
	-20	37	.058		.058	2	4.65	22.8	.026				
	0	56	.126		.126	4	16.51	45.6	.093				
	20	75	.210		.210	6	32.5	68.4	.182				
	-60	35.5	.048		.048	8	53.0	91.2	.298				
	-40	55	.110		.110								
	-20	74	.210		.210								

Example 64.

TRIODE TYPE: UV-206										Manufacturer: Tokyo Denki K. K.			
Observations					Calculations					Graph			
Anode		Grid		Cathode		A		$I_g = 67$ $\frac{x_a}{x_g} = 1.97$ $\log \frac{x_a}{x_g} = .294$ $c = 1$ $\pi a = 1.22$		$A = 98.6$ $\frac{A}{\pi a x_g} = 85$ $G = .198 \times 10^{-3}$ $e_f = 11.0$ $\frac{2}{5} G e_f^2 = .00285$			
$e_f = 11.0$ $i_f = 14.5$					$k = 316$ $g = .00206$ $r = 153,000$ $e_g = +20$					$k = 67 \times .294 = 230$ $e_f = 66$ $\left\{ \begin{array}{l} g = .0021 \\ r = 133,000 \end{array} \right.$			
e_a	e_g	e_f	i_a	i_g	i	e_f/e_g	$f(e_f/e_g)$	e_f	i				
6,000	-20	-1	.001		.001	0	0	0	0				
	0	19	.013		.013	2	4.65	22	.0084				
	20	39	.037	.004	.041	4	16.51	44	.030				
	29	48	.052	.006	.058	6	32.5	66	.059				
	48	67	.102	.010	.112	8	53.0	88	.096				
	-20	5.3	.003		.003								
	0	25.4	.0195	.001	.021								
	29	54	.0655	.006	.072								
	-20	11.7	.0065		.0065								
	0	32	.028	.001	.029								
	29	61	.079	.007	.086								

CHAPTER II.
**DETERMINATION OF OPERATIONS OF A TRIODE
 FROM ITS STATIC CHARACTERISTICS.**

(1) Preliminary Work.

The operations of a triode as an amplifier, oscillator, modulator, etc. can be determined from its static characteristics for a given circuit arrangement. The following descriptions are intended for rough estimation of these operating conditions, simplicity being aimed at instead of accuracy.

The static characteristic of a triode comprises two parts:—

1st. part: the anode current is determined from the equivalent grid voltage by the approximate relation,

$$i_a = G e_g'^{\frac{2}{3}}$$

2nd. part: anode current reaches saturation, and forms the upper limit of the characteristic.

The characteristic curve assumes the form as shown by a full line in Fig. 28.

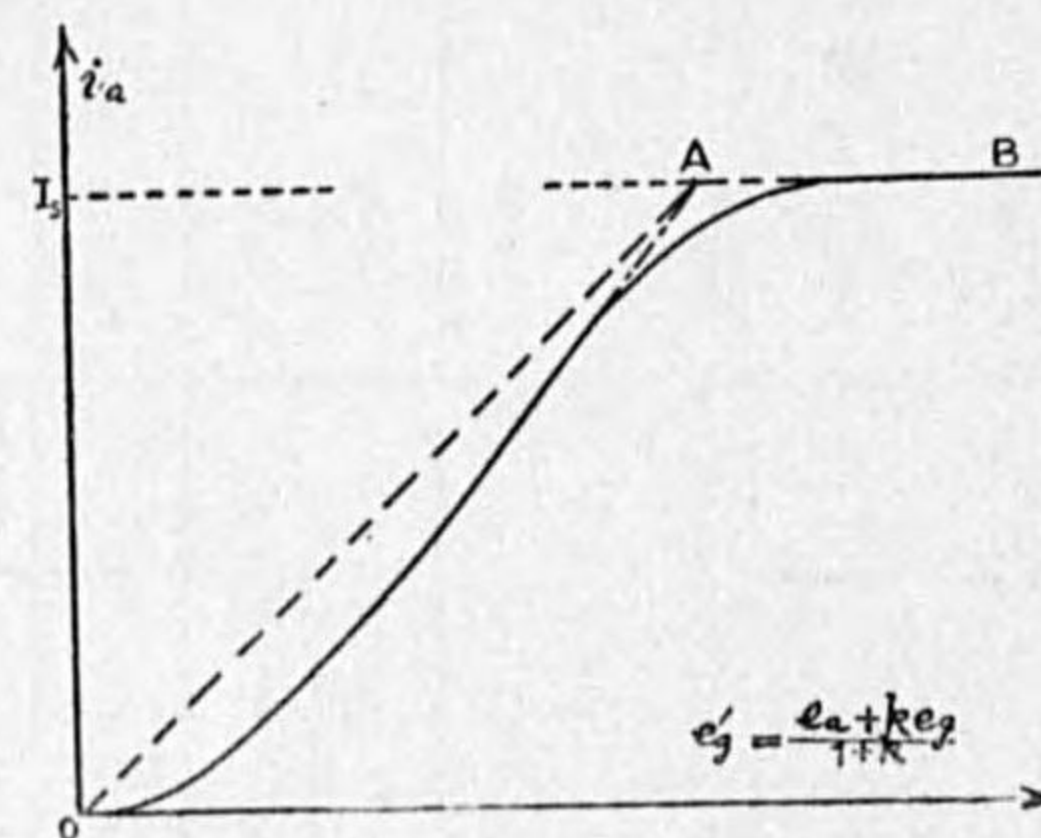


FIG. 28.

Now the 1st. part is represented as approximation by a straight line OA; in other words the anode current is assumed to be proportional to the equivalent grid voltage;

$$i_a = G' e_g' = G' \frac{e_a + k e_g}{1+k}$$

When grid voltage is zero,

$$i_a = G' \frac{e_a}{1+k} \quad \text{or} \quad \frac{e_a}{i_a} = \frac{1+k}{G'}$$

the latter corresponds to the mean anode impedance (actually resistance), so that

$$\bar{r} = \frac{1+k}{G'} \quad \text{or} \quad G' = \frac{1+k}{\bar{r}}$$

then the approximate characteristic becomes

$$i_a = \frac{e_a + k e_g}{\bar{r}} \dots \dots \dots (16)$$

The value of \bar{r} can be determined from the following relations;

$$i_a = G e_g'^{\frac{2}{3}} = G \left(\frac{e_a}{1+k} \right)^{\frac{2}{3}} \quad \text{at} \quad e_g = 0,$$

when $i_a = I_s$

$$I_s = G \left(\frac{e_a}{1+k} \right)^{\frac{2}{3}} \quad \text{or} \quad \frac{e_a}{1+k} = \left(\frac{I_s}{G} \right)^{\frac{3}{2}}$$

but it is assumed that $I_s = G' \frac{e_a}{1+k}$

$$\therefore \frac{I_s}{G'} = \left(\frac{I_s}{G} \right)^{\frac{3}{2}}$$

$$\therefore \bar{r} = \frac{1+k}{G'} = \frac{1+k}{I_s^{\frac{1}{3}} G^{\frac{2}{3}}}$$

$$\text{or} \quad (1+k)^3 = G^2 \bar{r}^3 I_s \dots \dots \dots (17)$$

This gives a relation among the parameters of a triode, from which \bar{r} can be obtained.

From equation (16)

$$\frac{i_a}{I_s} = \frac{e_a + k e_g}{\bar{r} I_s} \dots \dots \dots (18)$$

This is the simplest and universal representation of the triode characteristic, in which the anode current is expressed in the unit of I_s and voltages in the unit of $\bar{r}I_s$. (Fig. 29)

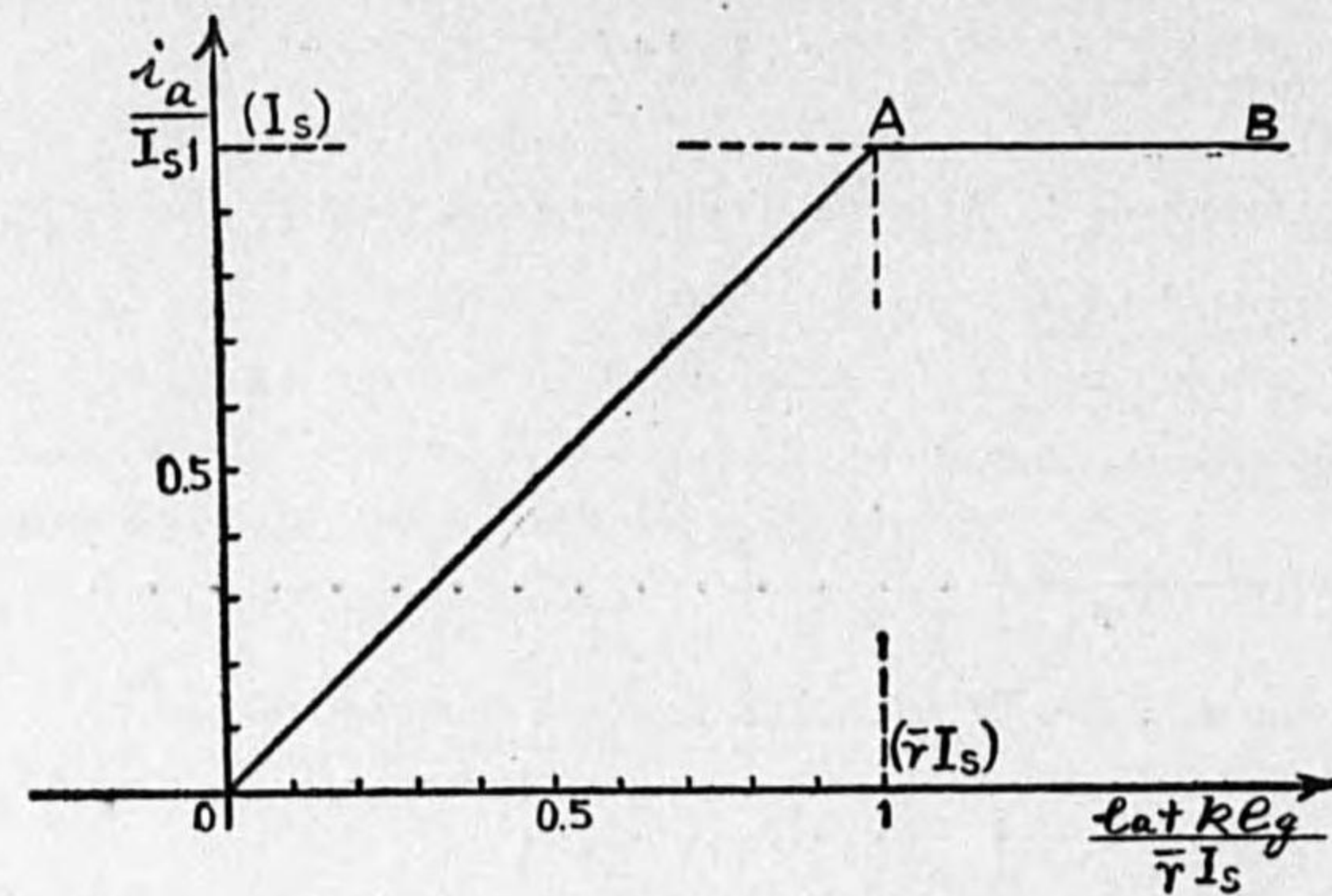


FIG. 29.

Let E_g = grid steady voltage,
 E_a = anode steady voltage,
 ε_g = grid alternating voltage, maximum value,
 ε_a = anode alternating voltage, maximum value,

positive directions being taken in the direction of direct current. Put a load in anode circuit, which may be considered to act as a resistance \mathcal{R} at the operating frequency. (Fig. 30)

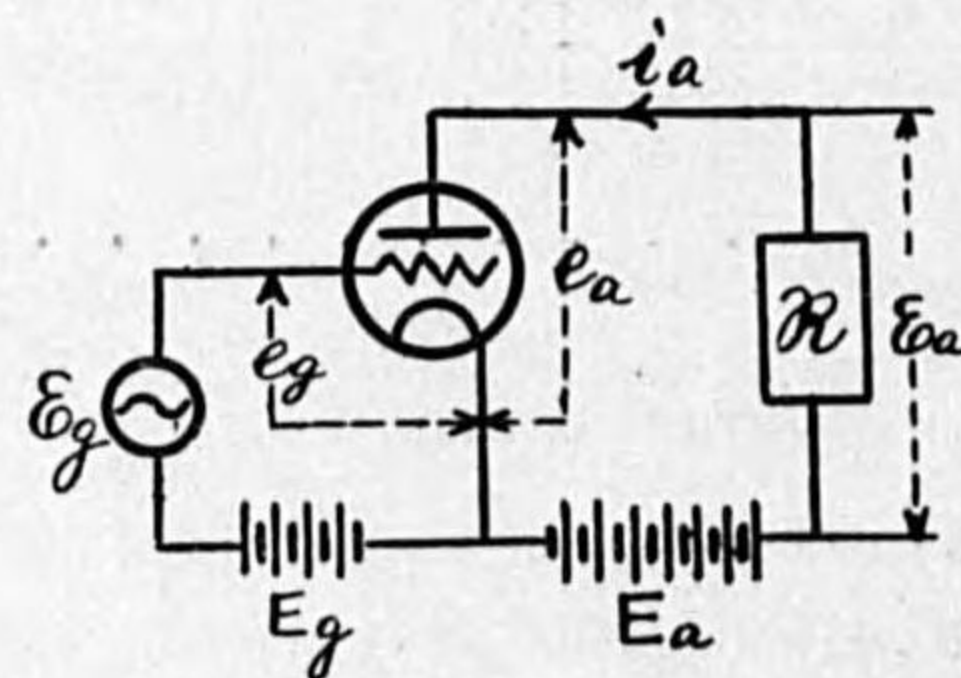


FIG. 30.

Then in optimum operating conditions ε_g and ε_a are always in opposite phase, because when e_g is positive, i_a increases and the voltage drop on \mathcal{R} augments in such a direction as to reduce the direct anode voltage, and thus e_a becomes low.

If the instantaneous value of grid voltage be represented by

$$e_g = E_g + \varepsilon_g \cos \theta,$$

anode voltage will be

$$e_a = E_a - \varepsilon_a \cos \theta,$$

and for a given tube the instantaneous value of anode current will be determined by

$$\begin{aligned} e_a + k e_g &= E_a - \varepsilon_a \cos \theta + k(E_g + \varepsilon_g \cos \theta) \\ &= E_a + k E_g + (k \varepsilon_g - \varepsilon_a) \cos \theta \end{aligned}$$

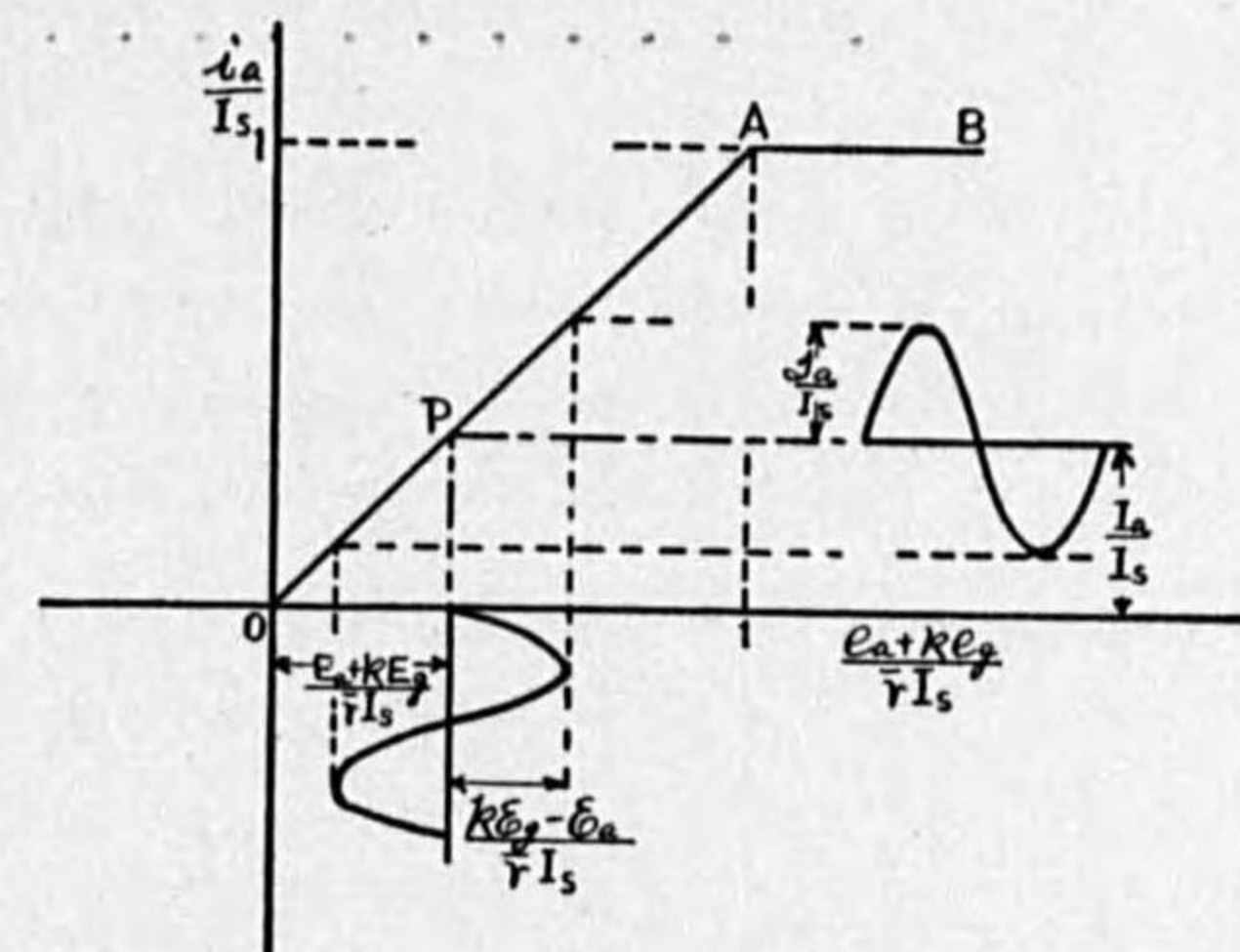


FIG. 31.

Thus in Fig. 31, a steady voltage $\frac{E_a + kE_g}{\bar{r}I_s}$ determines the working point P on the characteristic and the alternating component $\frac{k\varepsilon_g - \varepsilon_a}{\bar{r}I_s}$ gives the amplitude of oscillation, the working point being the center. The variation of anode current due to this oscillating voltage is sinusoidal when the amplitude of voltage is small, but becomes distorted when it is very large.

Let I_a = mean value or direct current component of anode current,
 \mathcal{I}_a = fundamental a. c. component of anode current, in maximum value,
 positive direction being taken as that of d. c.,
 then in the undistorted range,

$$\frac{i_a}{I_s} = \frac{k\mathcal{E}_g - \mathcal{E}_a}{\bar{r}I_s} \cos \theta + \frac{E_a + kE_g}{\bar{r}I_s} = \frac{\mathcal{I}_a}{I_s} \cos \theta + \frac{I_a}{I_s}$$

or $I_a = \frac{E_a + kE_g}{\bar{r}}$ and $\mathcal{I}_a = \frac{k\mathcal{E}_g - \mathcal{E}_a}{\bar{r}}$.

In the range of distorted wave form,

$$\frac{I_a}{I_s} = M \frac{k\mathcal{E}_g - \mathcal{E}_a}{\bar{r}I_s} \dots \dots \dots (19)$$

$$\frac{\mathcal{I}_a}{I_s} = F \frac{k\mathcal{E}_g - \mathcal{E}_a}{\bar{r}I_s} \dots \dots \dots (20)$$

in which M and F are the factors to be multiplied to the undistorted amplitude of oscillation in order to obtain the mean and fundamental components of the distorted wave form, and are functions of the two quantities u and v that are determined by the amplitude of oscillation and the position of the working point, as shown in Fig. 33.

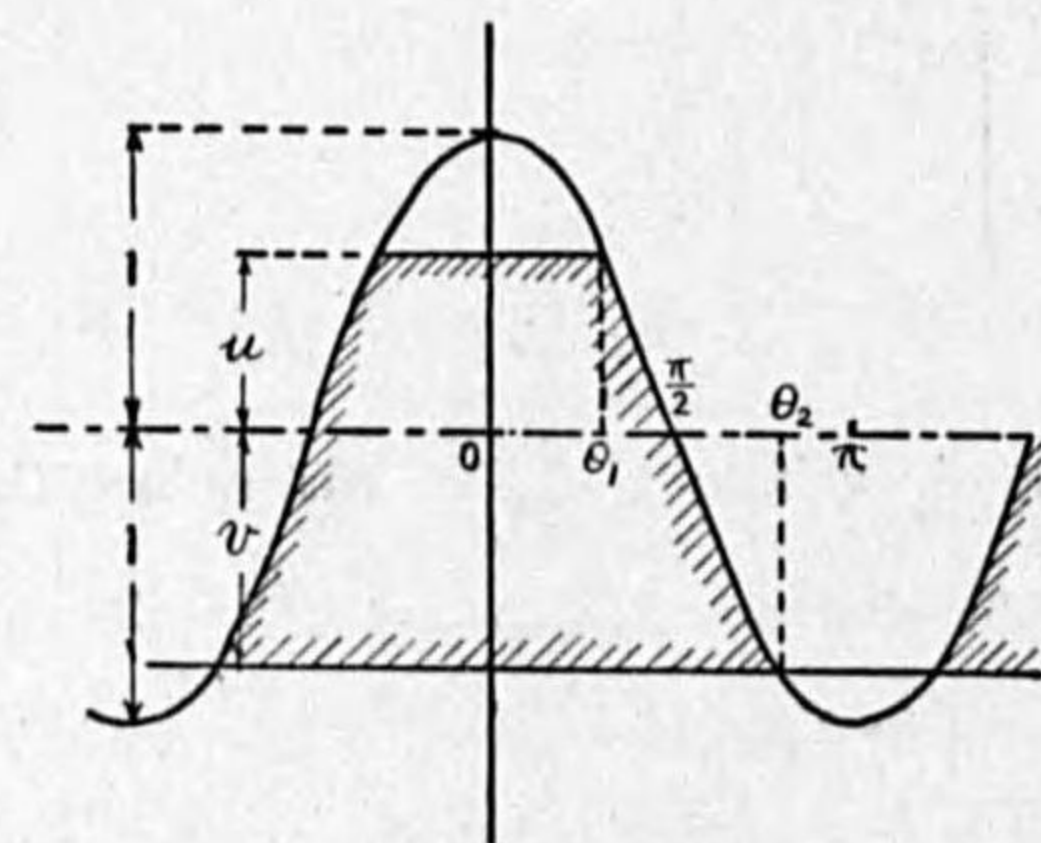


FIG. 32.

Analysis of the Distorted Wave Form.

Let a sinusoidal wave $\cos \theta$ as shown in Fig. 32 have an amplitude of unity. This wave is limited at the positive direction by an amount u and in the negative direction by v , and the negative limiting line is taken as datum.

Let $u = \cos \theta_1$, and $v = \cos \theta_2$

When these wave forms come in repetition, mean value becomes

$$M = \frac{1}{\pi} \left\{ \int_{\theta_1}^{\theta_2} (v + \cos \theta) d\theta + (u+v)\theta_1 \right\}$$

$$= \frac{1}{\pi} (v\theta_1 - \sin \theta_1) + \frac{1}{\pi} (v\theta_2 + \sin \theta_2)$$

$$= M_1 + M_2$$

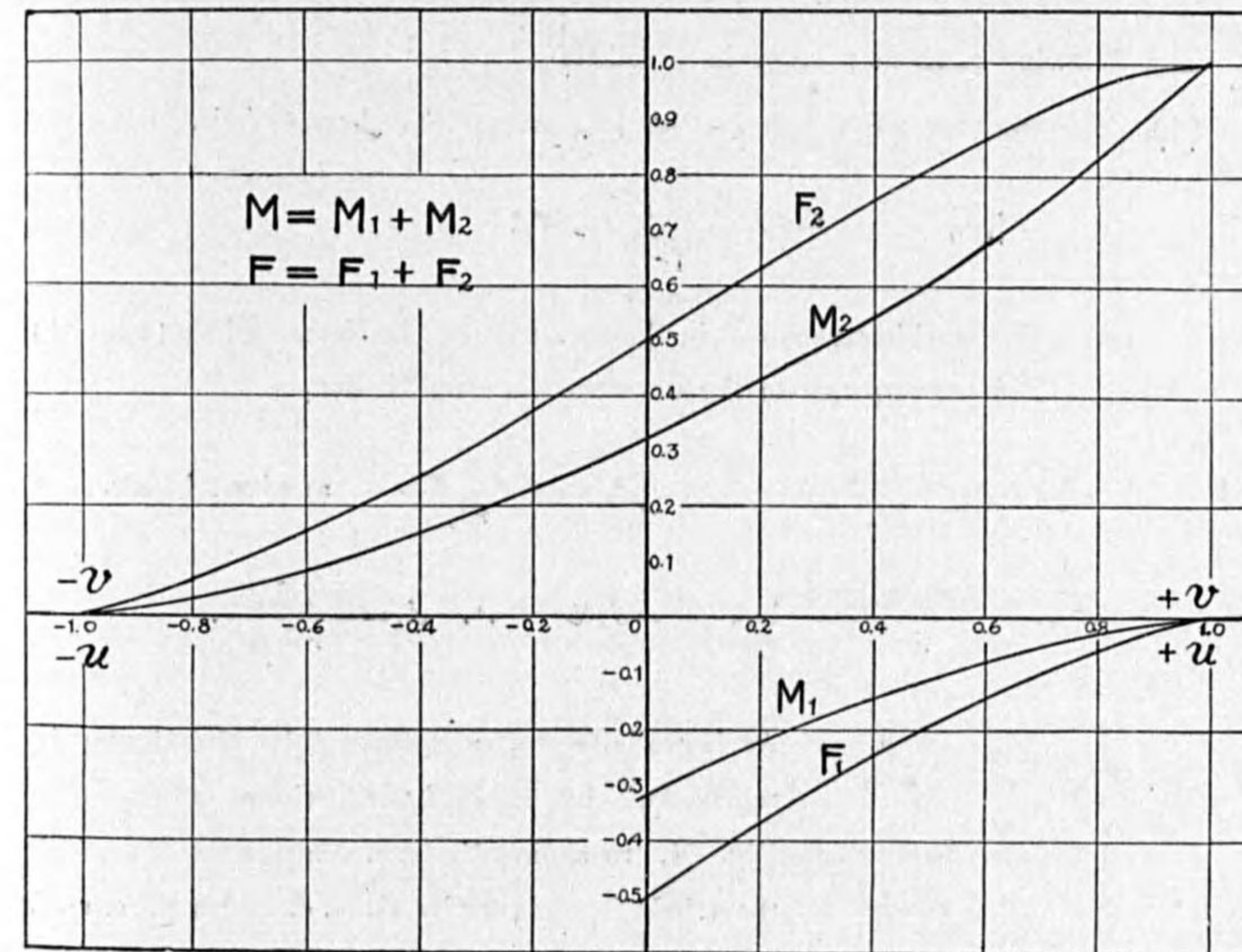


FIG. 33.

and fundamental amplitude becomes

$$F = \frac{2}{\pi} \left\{ \int_0^{\theta_1} (u+v) \cos \theta \, d\theta + \int_{\theta_1}^{\theta_2} (v + \cos \theta) \cos \theta \, d\theta \right\}$$

$$= \frac{1}{\pi} \left(2u \sin \theta_1 - \theta_1 - \frac{1}{2} \sin 2\theta_1 \right) + \frac{1}{\pi} \left(2v \sin \theta_2 + \theta_2 + \frac{1}{2} \sin \theta_2 \right)$$

$$= F_1 + F_2$$

Fig. 33 shows the values of M 's and F 's for various values of u and v .

For the anode current of a triode in operation, the undistorted amplitude is $\frac{k\epsilon_g - \epsilon_a}{\bar{r}I_s}$, and so in order to obtain the mean value or the d. c. component of anode current this amplitude must be multiplied by M corresponding to u and v determined by the relative conditions of working point and amplitude of oscillation. In the same way the fundamental component of anode current is obtained by multiplying the undistorted amplitude $\frac{k\epsilon_g - \epsilon_a}{\bar{r}I_s}$ by the value of F corresponding to u and v .

The following cases may occur in practice ;

- (1) The working point rests on the 1st. part of the characteristic.

i. e.,
$$0 < \frac{E_a + kE_g}{\bar{r}I_s} < 1$$

- (a) The working range is in the 1st. part of the characteristic (Fig. 31)
This corresponds to the distortionless amplification,

and
$$\frac{I_a}{I_s} = \frac{E_a + kE_g}{\bar{r}I_s} \quad \frac{J_a}{I_s} = \frac{k\epsilon_g - \epsilon_a}{\bar{r}I_s} \quad \text{as given before.}$$

or
$$J_a = \frac{k\epsilon_g - \epsilon_a}{\bar{r}} \quad \text{but } \epsilon_a = J_a R \quad \therefore J_a = \frac{k\epsilon_g}{\bar{r} + R}.$$

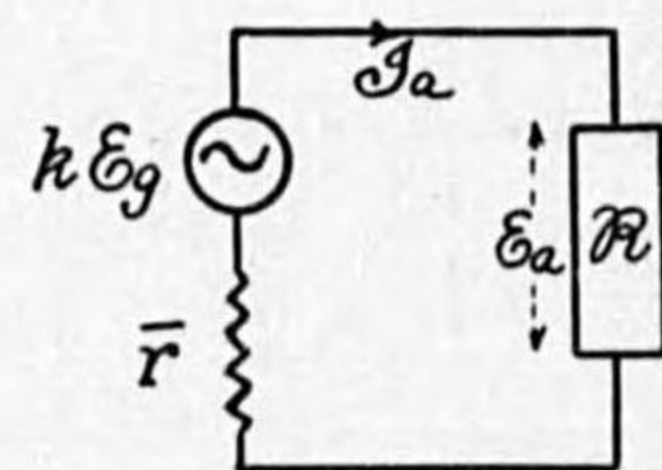


FIG. 34.

As is well known, a vacuum tube circuit may be represented by an equivalent circuit as shown in Fig. 34, regarding the a. c. components, in which the triode is replaced by an a. c. source of e. m. f. $k\epsilon_g$ and of internal resistance \bar{r} .

- (b) The working range outsteps the 1st. part.

- (i) When the working point is in the middle of the 1st. part (Fig. 35),

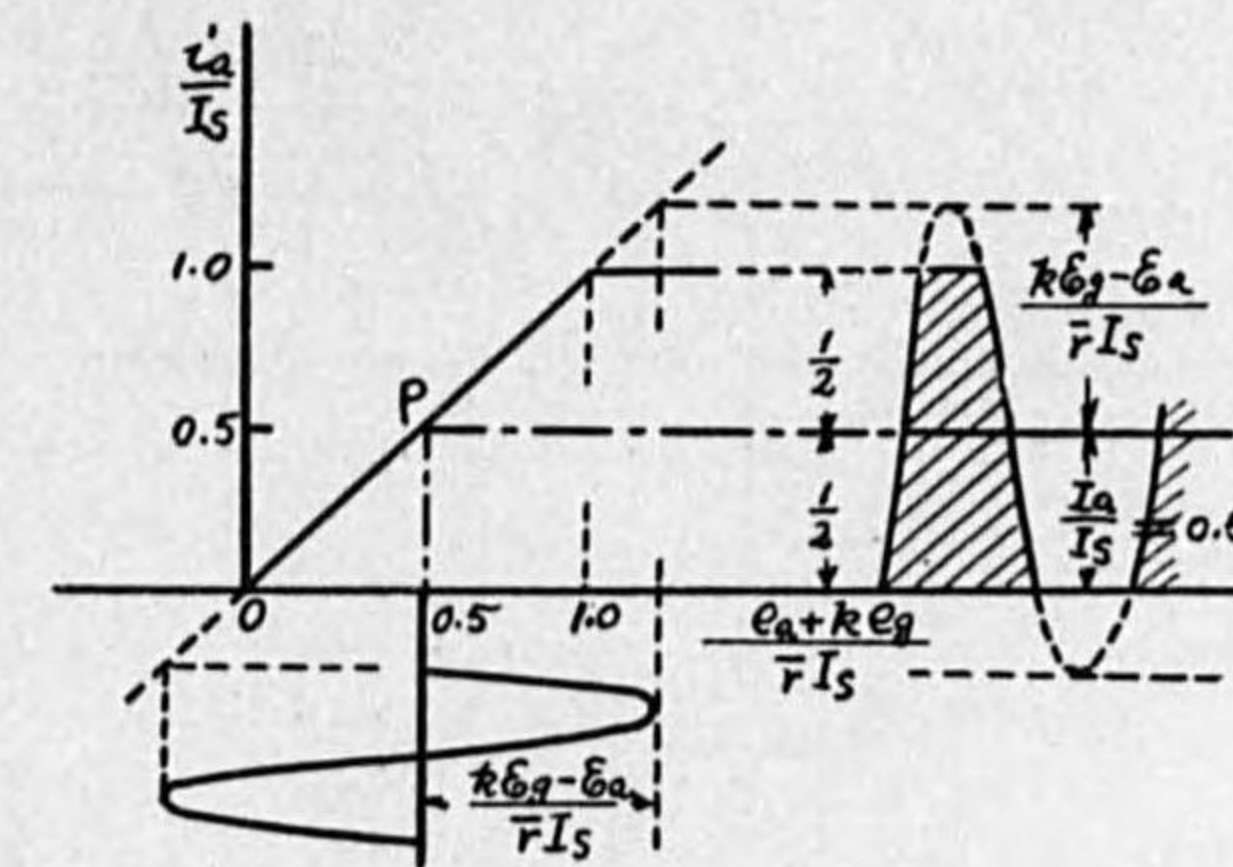


FIG. 35.

i. e.
$$\frac{E_a + kE_g}{\bar{r}I_s} = 0.5 \quad \text{and} \quad \frac{k\epsilon_g - \epsilon_a}{\bar{r}I_s} > 0.5$$

then
$$u = v = \frac{1}{2} \cdot \frac{\bar{r}I_s}{k\epsilon_g - \epsilon_a}$$

- (ii) When the working point is below the middle point,

i. e.
$$\frac{E_a + kE_g}{\bar{r}I_s} < 0.5$$

- 1° Working range reaches the zero anode current (Fig. 36),

i. e.
$$\frac{k\epsilon_g - \epsilon_a}{\bar{r}I_s} > \frac{E_a + kE_g}{\bar{r}I_s}$$

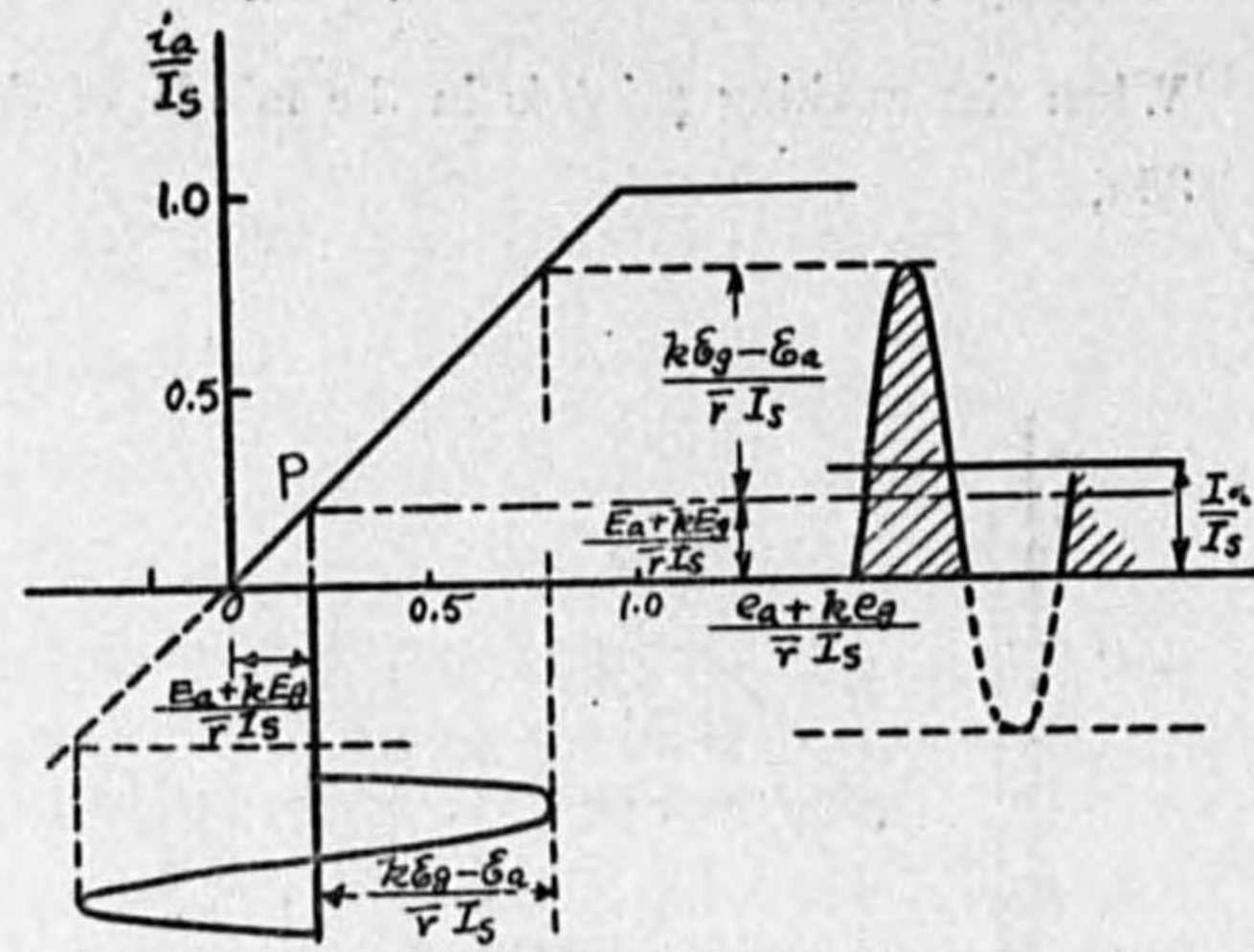


FIG. 36.

Here $u=1$, $v = \frac{E_a + kE_g}{kE_g - E_a}$.

2° Working range reaches saturation (Fig. 37),

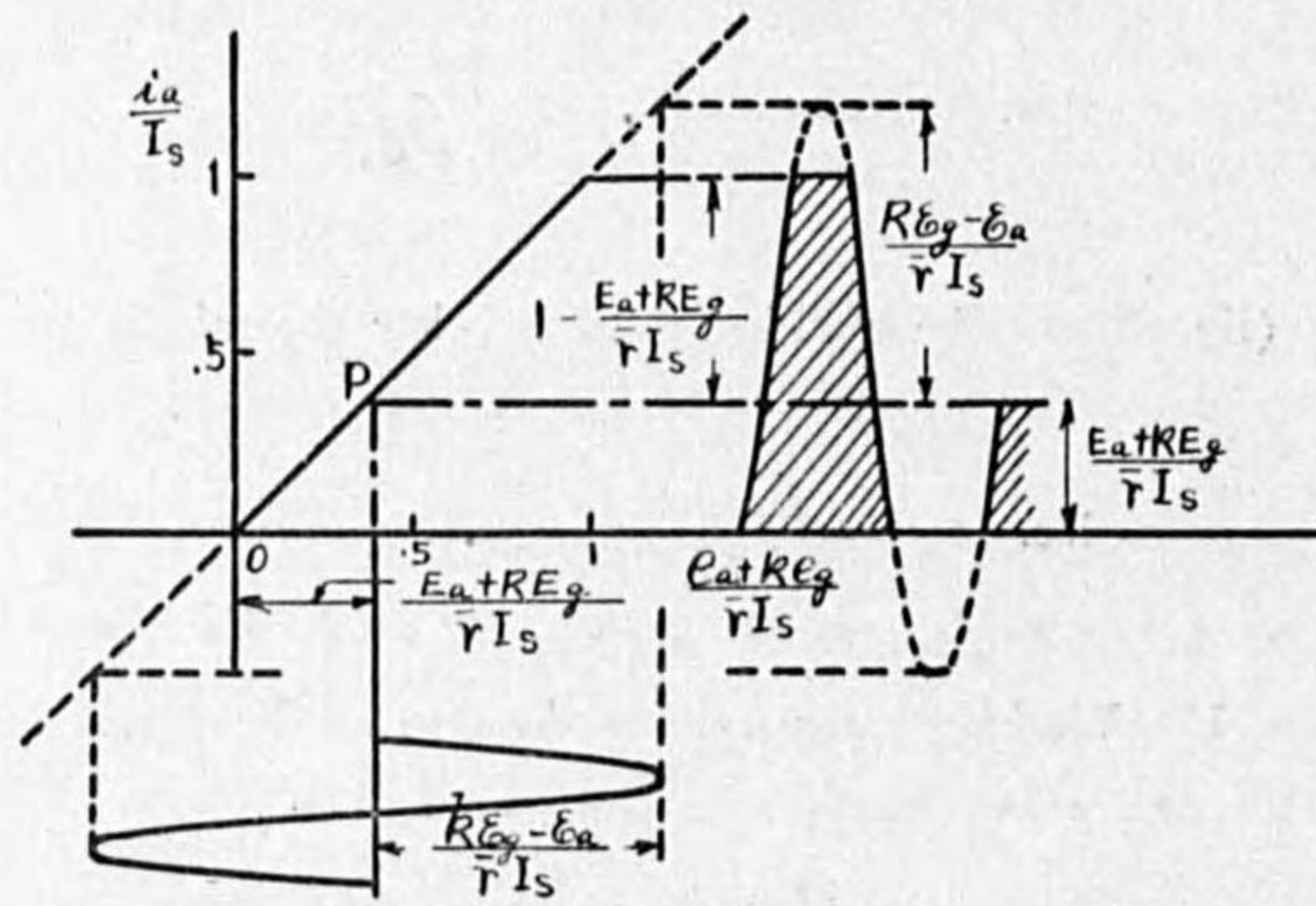


FIG. 37.

i. e. $\frac{kE_g - E_a}{rI_s} > 1 - \frac{E_a + kE_g}{rI_s}$.

$u = \frac{rI_s - (E_a + E_g)}{kE_g - E_a}$, $v = \frac{E_a + kE_g}{kE_g - E_a}$.

(iii) When the working point is above the middle point,

i. e. $\frac{E_a + kE_g}{rI_s} > 0.5$

1° Working point reaches saturation (Fig. 38),

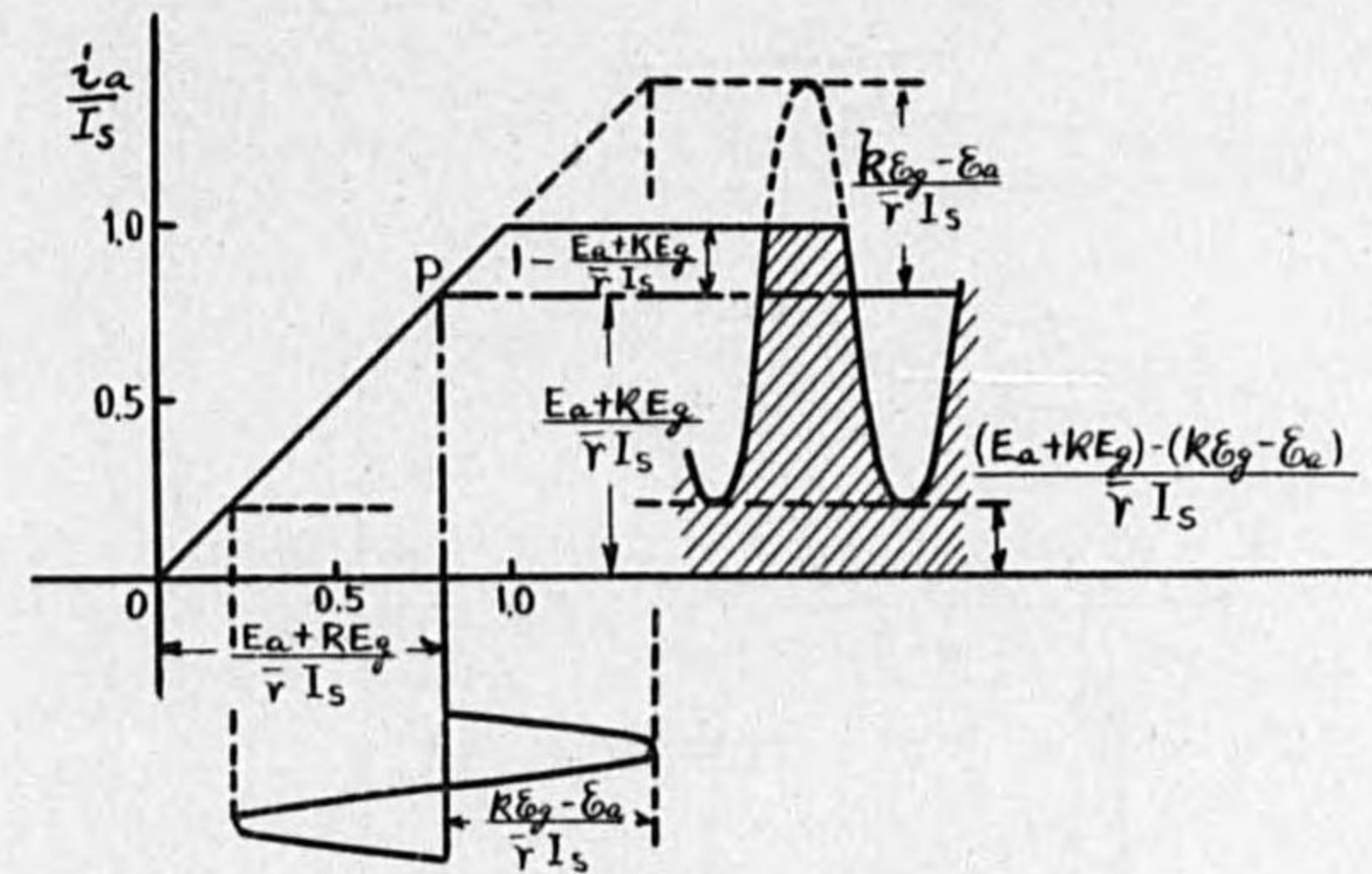


FIG. 38.

i. e. $\frac{kE_g - E_a}{rI_s} > 1 - \frac{E_a + kE_g}{rI_s}$

$u = \frac{rI_s - (E_a + kE_g)}{kE_g - E_a}$, $v = 1$

and $\frac{(E_a + kE_g) - (kE_g - E_a)}{rI_s}$ must be added to the resulting mean

value in order to obtain $\frac{I_a}{I_s}$.

2° Working point reaches zero current (Fig. 39),

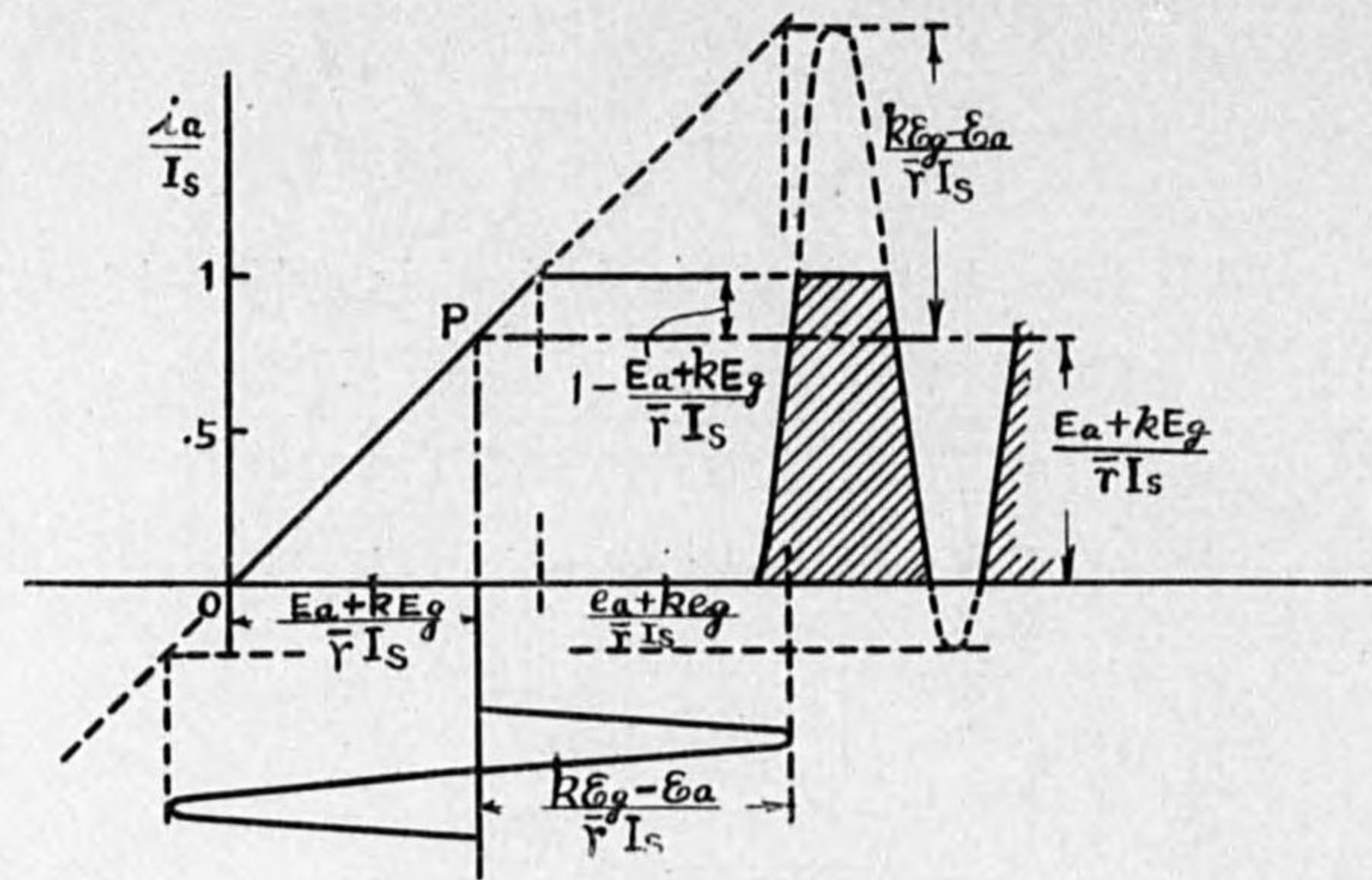


FIG. 39.

i. e.
$$\frac{kE_g - E_a}{rI_s} > \frac{E_a + kE_g}{rI_s}$$

$$u = \frac{rI_s - (E_a + kE_g)}{kE_g - E_a}, \quad v = \frac{E_a + kE_g}{kE_g - E_a}$$

(2) The working point is in the negative side,

i. e.
$$\frac{E_a + kE_g}{rI_s} < 0$$

This corresponds to the condition $E_a + kE_g < 0$ i. e. $-kE_g > E_a$ or the negative grid bias is so high as to entirely suppress the anode current. High efficiency operation of a power amplifier or an oscillator corresponds to this case.

(a) Peak voltage is limited within the 1st. part (Fig. 40),

i. e.
$$0 < \frac{(kE_g - E_a) + (E_a + kE_g)}{rI_s} < 1.$$

$$u = 1, \quad v = \frac{E_a + kE_g}{kE_g - E_a} \quad (\text{which is negative}).$$

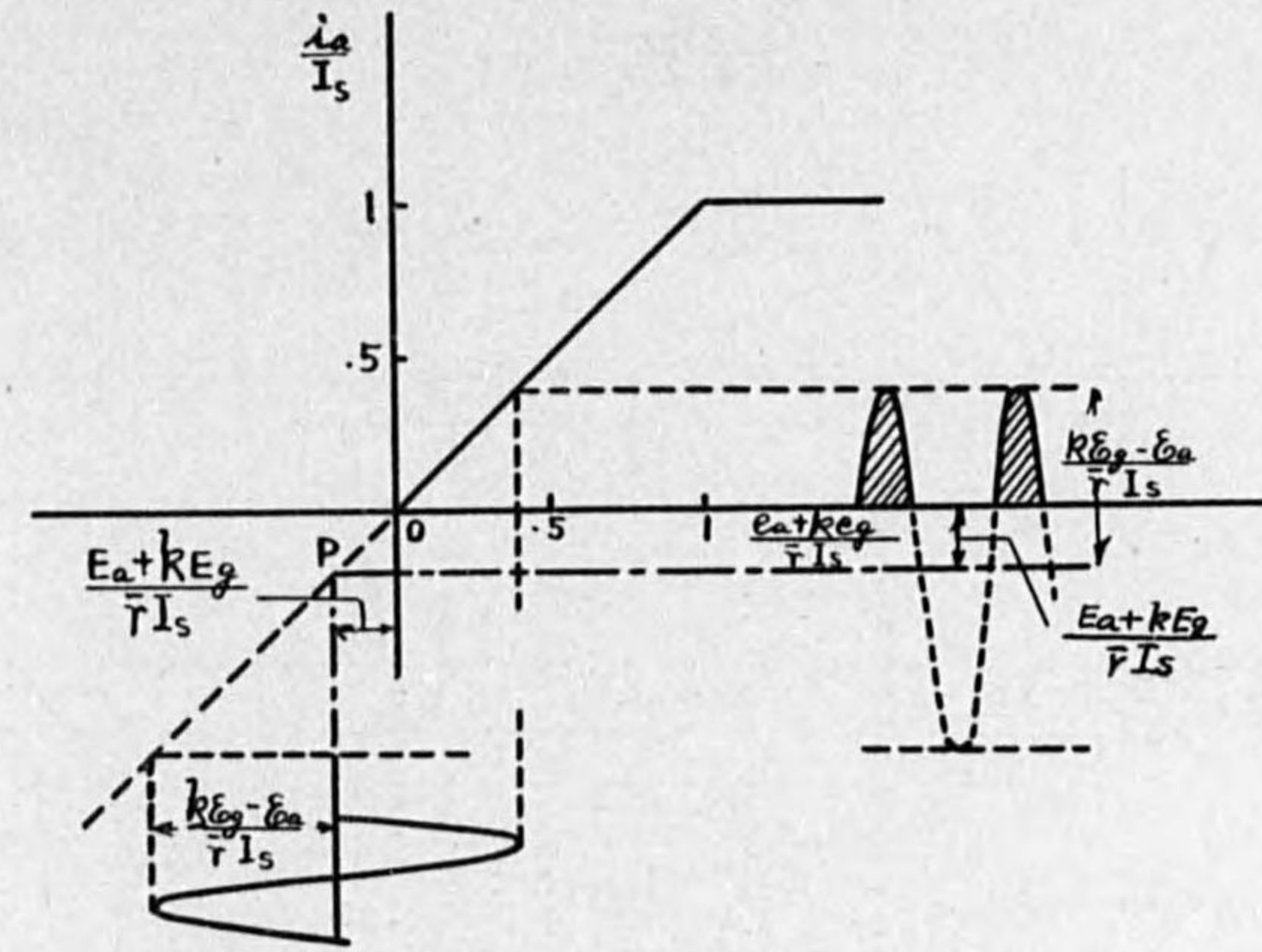


FIG. 40.

(b) Peak voltage outsteps the 1st. part (Fig. 41),

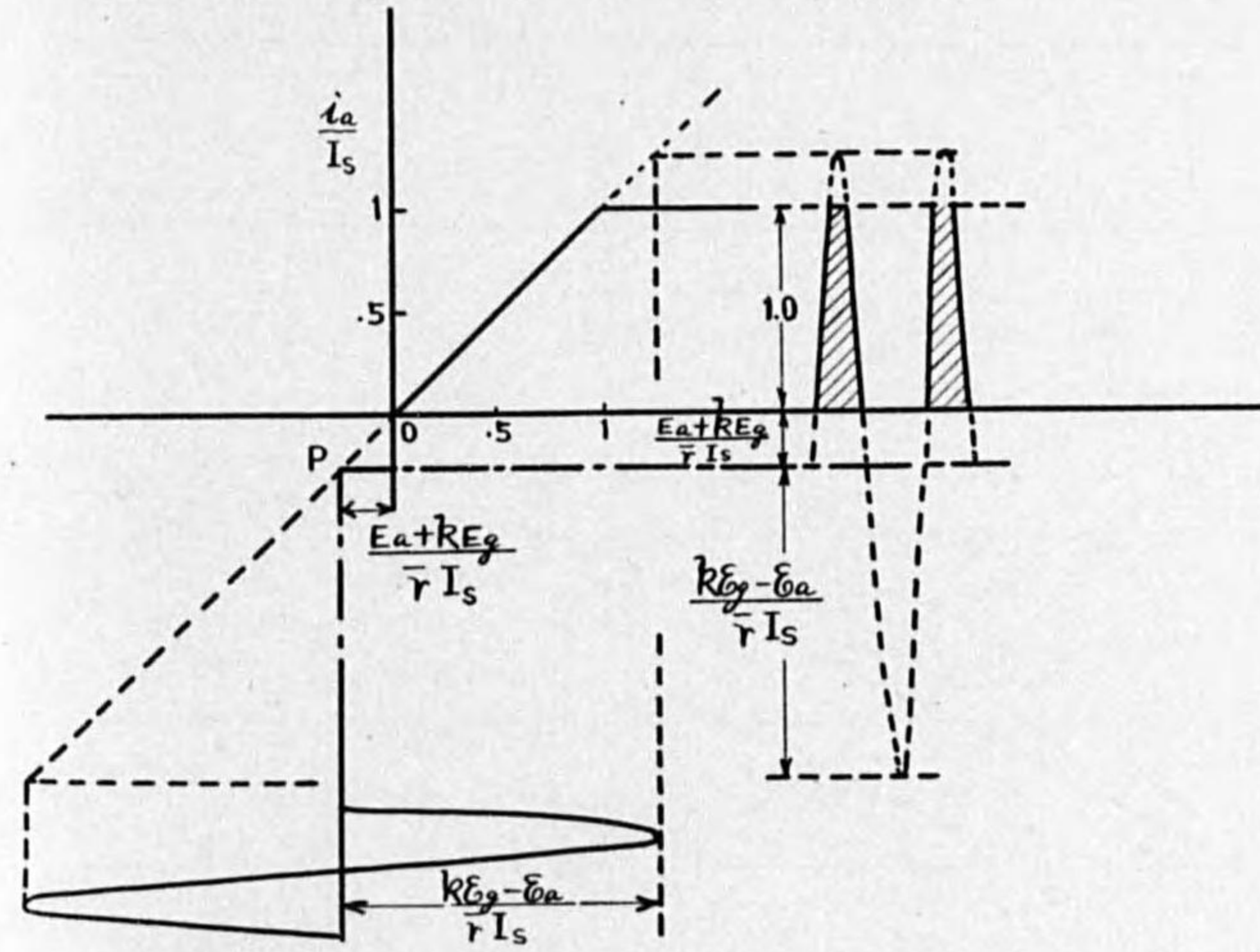


FIG. 41.

i. e. $\frac{(k\epsilon_g - \epsilon_a) + (E_a + kE_g)}{\bar{r}I_s} > 1.$
 $u = \frac{\bar{r}I_s - (E_a + kE_g)}{k\epsilon_g - \epsilon_a}, \quad v = \frac{E_a + kE_g}{k\epsilon_g - \epsilon_a}$ (which is negative)

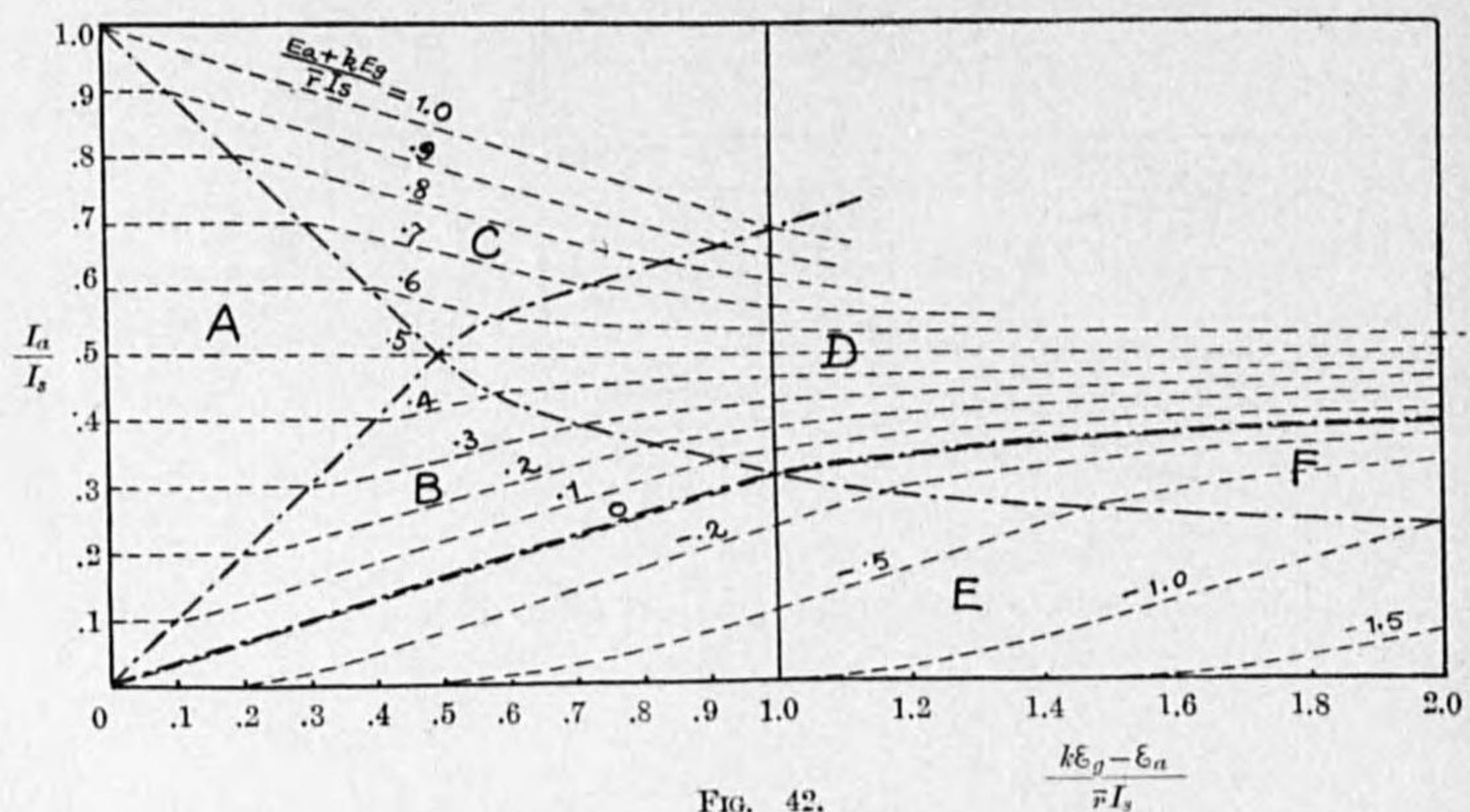


FIG. 42.

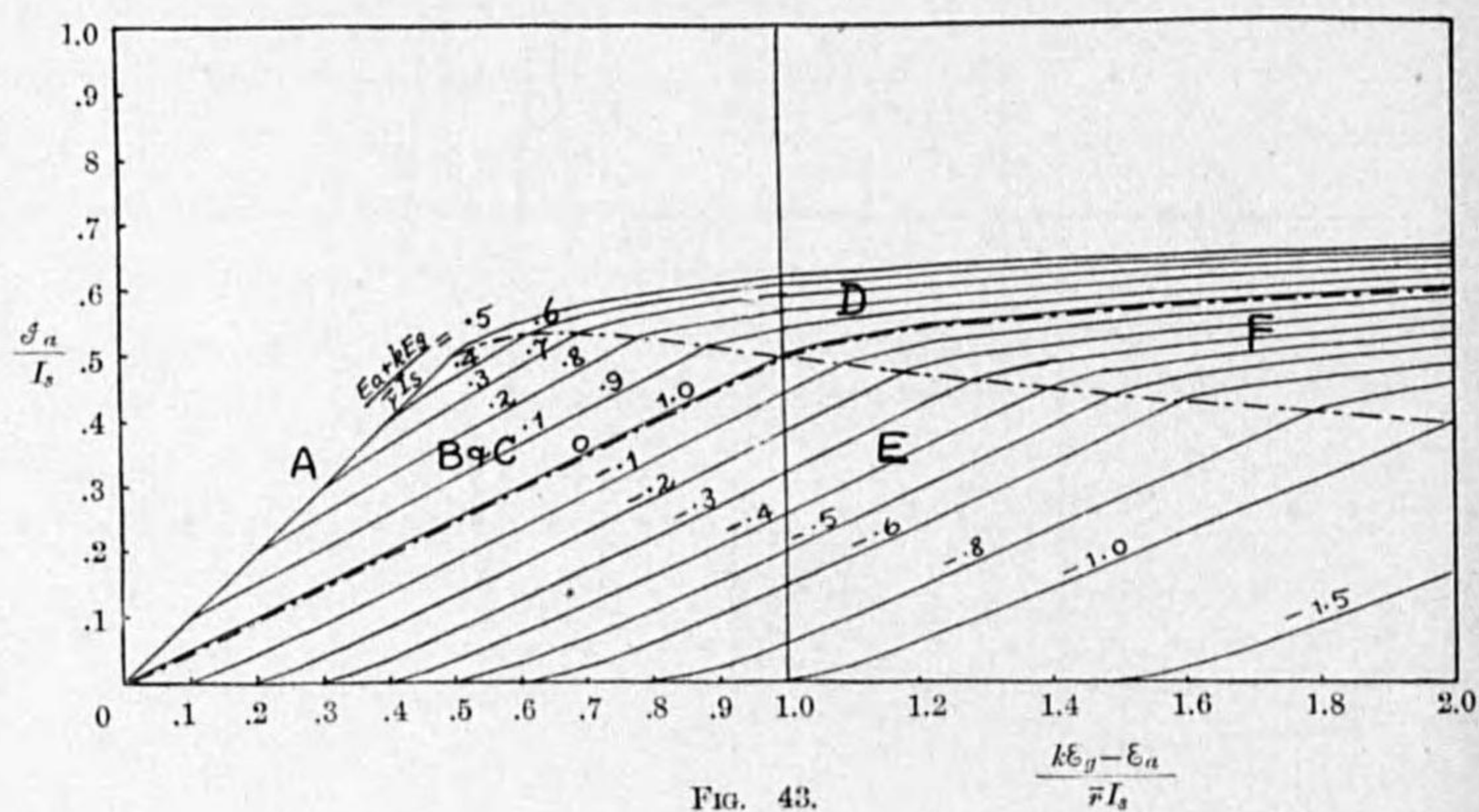


FIG. 43.

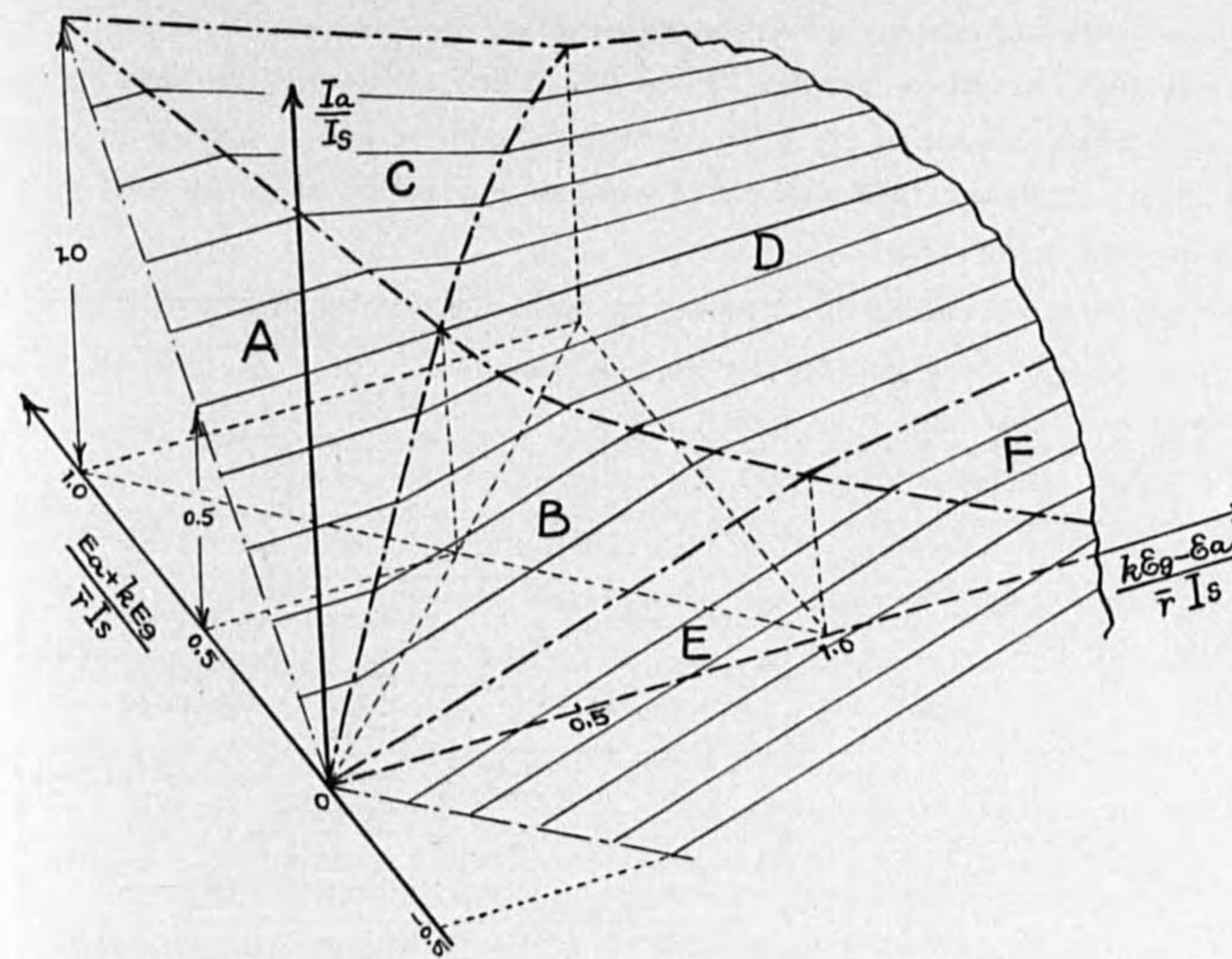


FIG. 44.

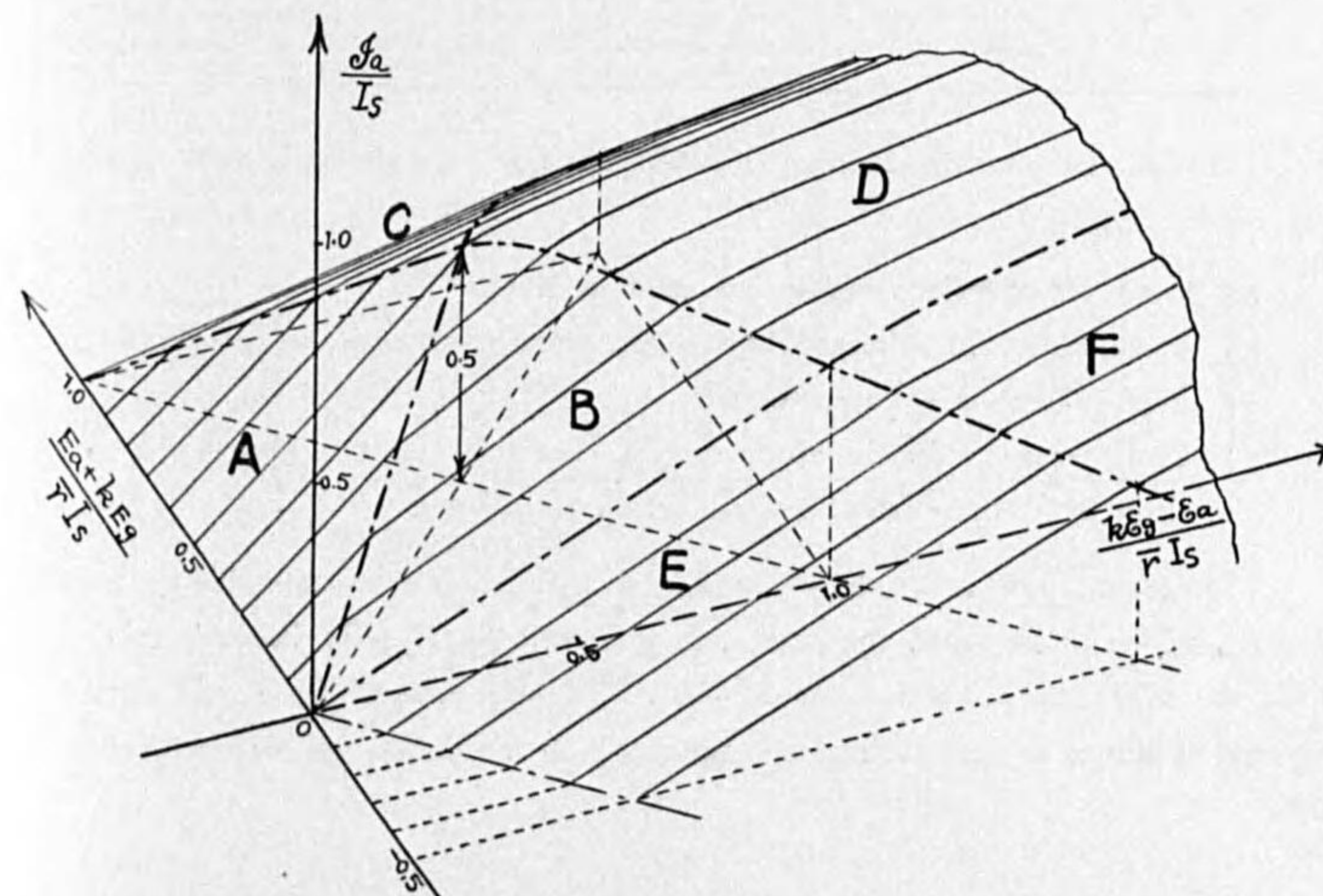


FIG. 45.

The results of calculations on the above given operating conditions are summarized in diagrams shown in Figs. 42 and 43. These curves give the d. c. and a. c. values of anode current at any given operating condition, and is universally applicable to any particular tube as long as voltages are expressed in the unit of $\bar{v}I_s$, and currents in the unit of I_s .

These dynamic characteristic curves represent the surfaces illustrated in Fig. 44 (d. c. component $\frac{I_a}{I_s}$) and Fig. 45 (a. c. component $\frac{I_a'}{I_s}$). The two characteristic surfaces comprise the following six regions of practical importance;

Regions	Working point	Anode current	Practical value
A	On the slope of characteristics.	Not limited.	Distortionless amplification.
B	Ditto.	Limited by zero-line.	Self-oscillation practicable and effectively subjected to modulation.
C	Ditto.	Limited by saturation, D. C. component is relatively high.	Ditto, but lower efficiency of operation.
D	Ditto.	Limited by both zero-line and saturation.	Self-oscillation or amplification with large power.
E	At zero anode current with highly negative grid.	Lower portion entirely suppressed, upper portion not being limited.	Distortionless amplification of modulated waves.
F	Ditto.	Ditto, upper portion being limited by saturation. D. C. component is relatively low.	Self-oscillation or amplification with large power at high efficiency. (Impulse excitation)

It should be remembered that this diagram has been derived under the following assumptions:-

- static characteristic curves are straight lines,
- anode and grid voltages vary in sine wave form and just in opposite phase,
- grid current is not appreciable,
- load connected in the anode circuit does not produce appreciable voltage drop by direct current as well as by harmonics.

Thus the diagram is not strictly applicable when there is considerable grid current flowing, which arises when the maximum grid voltage $E_g + \mathcal{E}_g$ becomes comparable with the minimum anode voltage $E_a - \mathcal{E}_a$. In such a case the anode alternating current attains a drooping characteristic at high excitation as shown in Fig. 46.

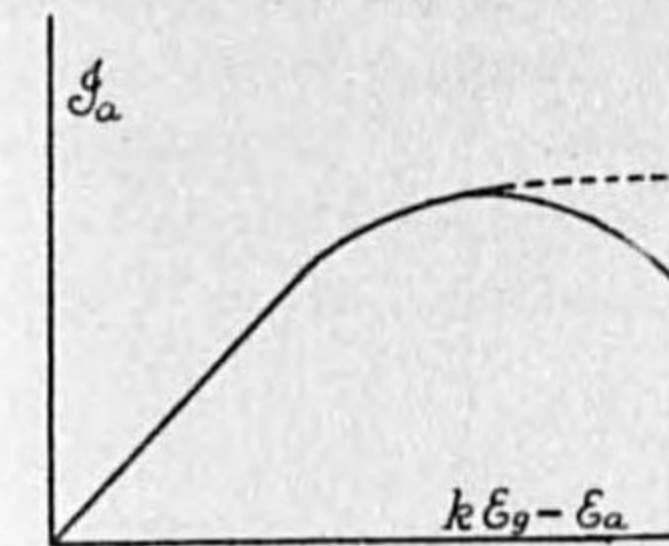


FIG. 46.

The diagram also gives erroneous results if it is applied to a case of very small amplitude of oscillation, as the curves have been derived with the mean anode resistance which is a little different from the differential resistance at lower part of characteristics. More accurate results can be obtained in such a case by deriving the particular value of anode resistance from the given static characteristics at the given voltages, the solution being made by the principle of the equivalent circuit shown in Fig. 34. But the diagram may be serviceable for studying at least qualitatively the various working conditions of a triode even if it is not strictly applicable.

Experimental Verification.

The dynamic characteristic curves were obtained by experiment in the following way.

A triode was used as a radio-frequency power amplifier in a circuit shown in Fig. 47.

A parallel resonance circuit with an inductance L and a capacity C was connected to the anode, and was adjusted to resonance at the frequency of the impressed grid voltage. A non-inductive resistance R' and a hot-wire ammeter were inserted in the resonance circuit in order to

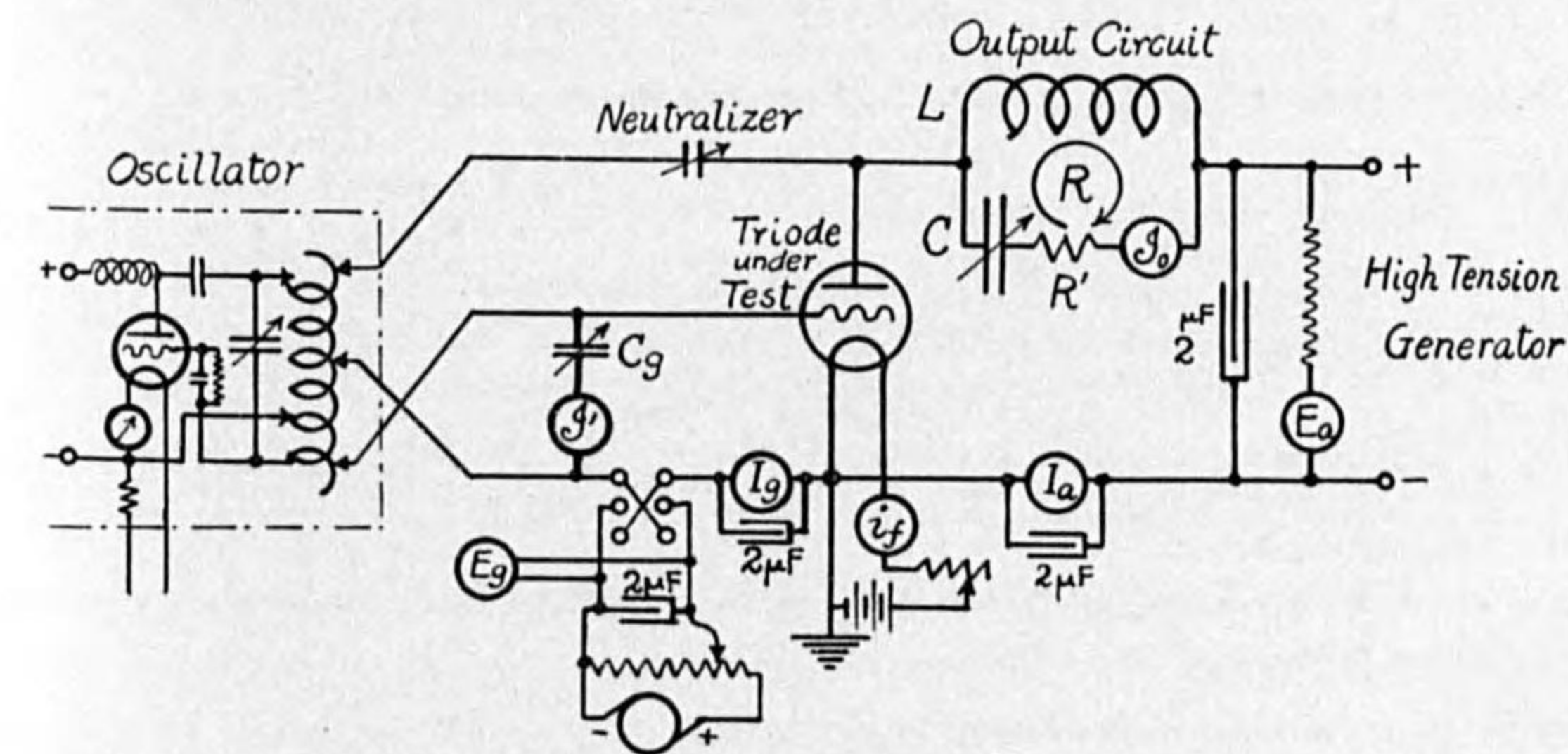


FIG. 47.

vary the resonance impedance as well as to obtain output power. The grid alternating voltage was impressed by a local oscillator, and a condenser C_g being shunted to the grid, the grid voltage was calculated from its capacity and the current passing through it. Neutralization was effected by a small capacity inserted between the anode and one end of the local oscillator inductance, and by this means regenerative action due to the inter-electrode capacity of the tube was eliminated.

The frequency was kept at

$$\omega = 2\pi f = 3 \times 10^6 \quad (\lambda = 628 \text{ m})$$

and at this frequency the resistance of the resonance circuit excluding R' was 3.0 ohms.

First the tube characteristics were taken and the constants k , I_s , \bar{r} and $\bar{r}I_s$ were calculated, \bar{r} being taken to comply with equation (17).

During the experiment, under constant filament current to give the predetermined I_s value, E_a and E_g were varied and at each step of variation, \mathcal{J}_0 and I_a were observed with variation of \mathcal{J}' and C_g . Then calculations were made as follows,

$$\epsilon_a = \frac{\mathcal{J}_0}{\omega C} \quad \mathcal{R} = \frac{L}{CR} = \frac{1}{\omega^2 C^2 R}$$

in which $R = R' + 3.0$

$$\mathcal{J}_a = \frac{\epsilon_a}{\mathcal{R}} \quad \epsilon_g = \frac{\mathcal{J}'}{\omega C_g}$$

Hence $\frac{k\epsilon_g - \epsilon_a}{\bar{r}I_s}$ could be calculated for each value of $\frac{E_a + kE_g}{\bar{r}I_s}$, and $\frac{\mathcal{J}_a}{I_s}$ and $\frac{I_a}{I_s}$ were plotted against $\frac{k\epsilon_g - \epsilon_a}{\bar{r}I_s}$ to obtain the dynamic characteristic curves.

All the alternating quantities are expressed in maximum values.

Example 67. Triode type UV-204.

Operated at $e_f = 8.5$ $i_f = 12.2$ $\mathcal{R} = 27,100$ $E_a = 1500$ to 2500 .

Static characteristics are shown in Fig. 48, from which we obtain

$$I_s = 0.071 \quad \bar{r} = 17,200 \quad \bar{r}I_s = 1,220 \quad k = 25$$

The resulting curves are shown in Fig. 49, which are in conformity to the theoretical diagram in the main.

Example 68. Triode type RS-15.

Static characteristics are shown in Fig. 50.

$$e_f = 13.3 \quad i_f = 15.8$$

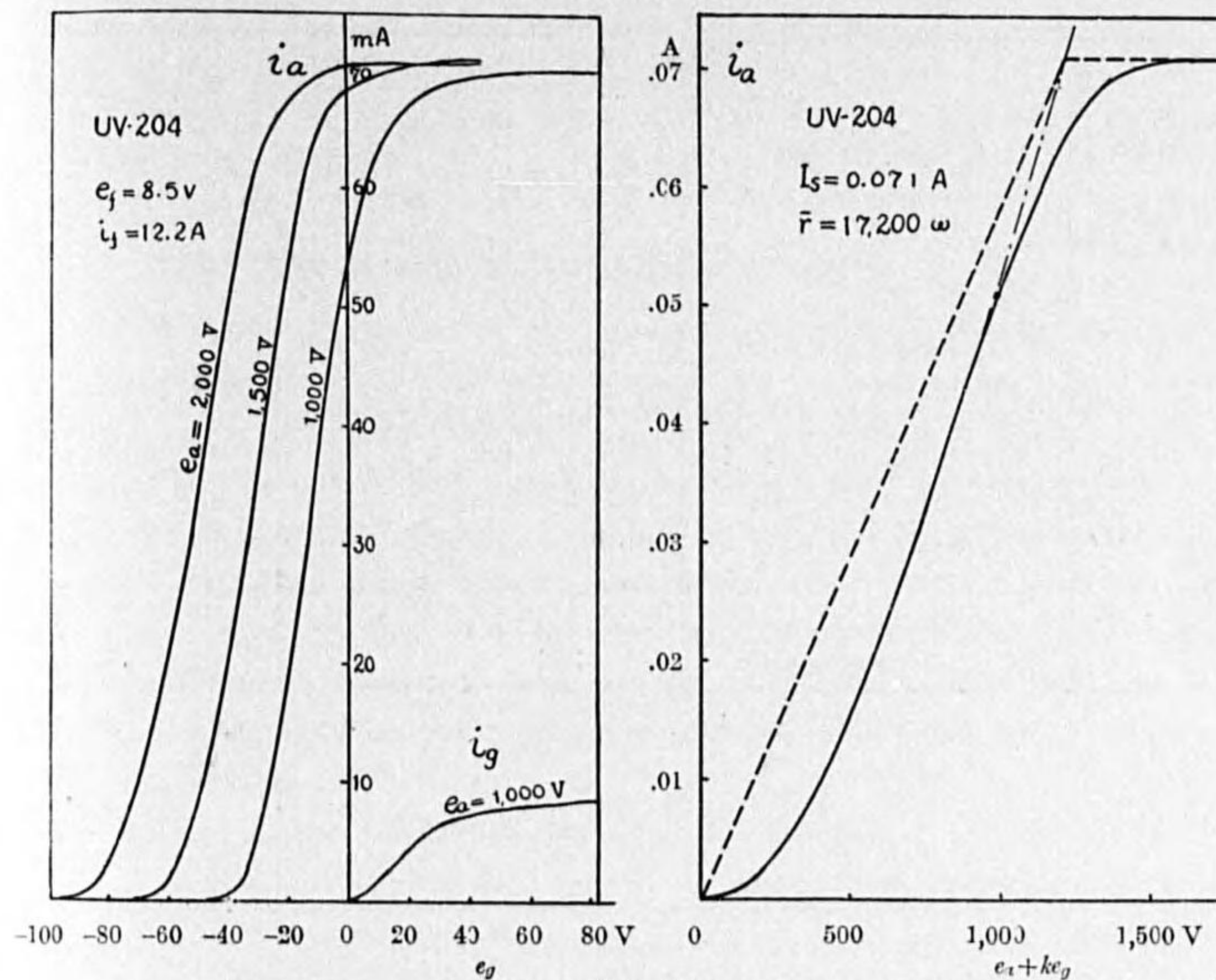


FIG. 48.

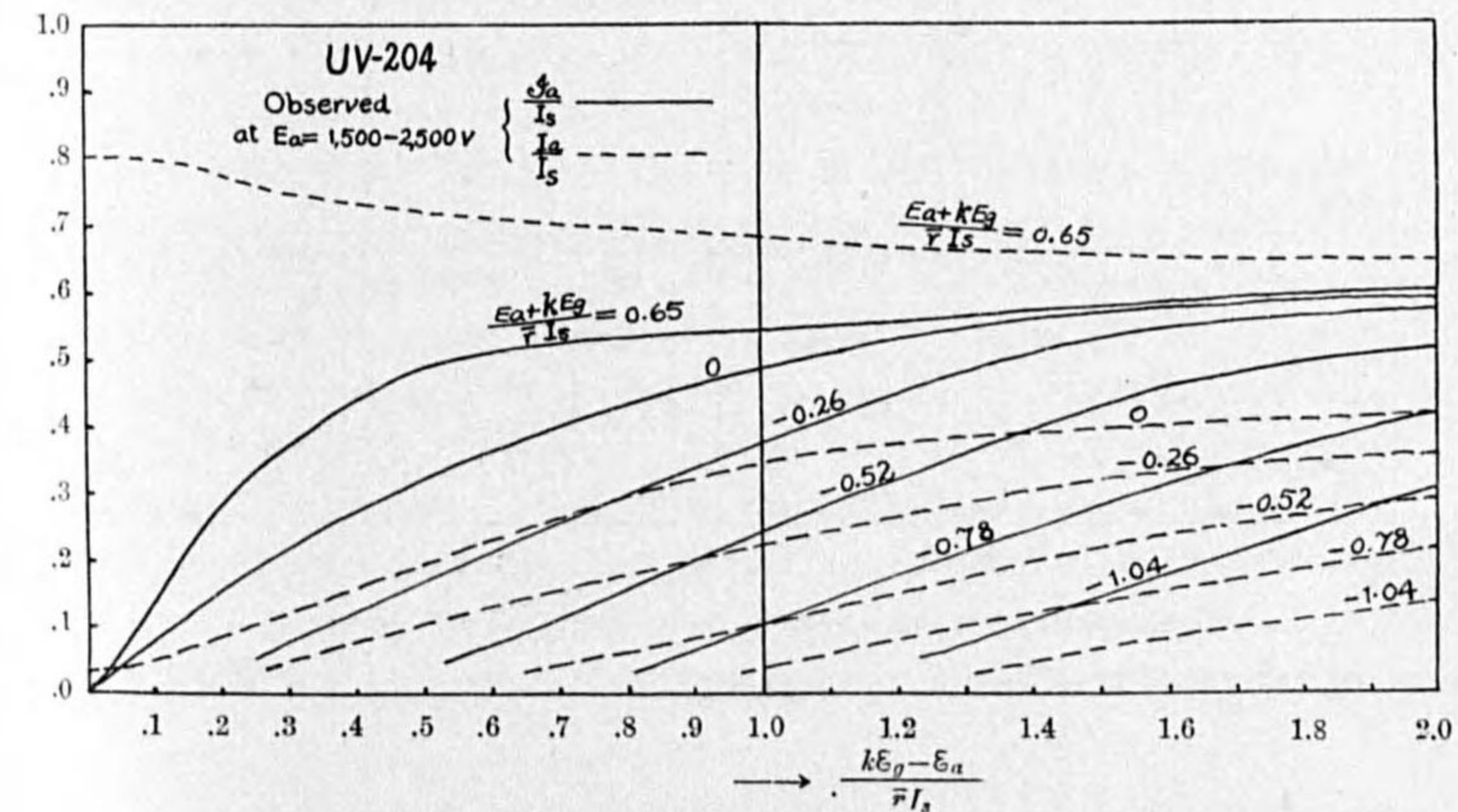


FIG. 49.

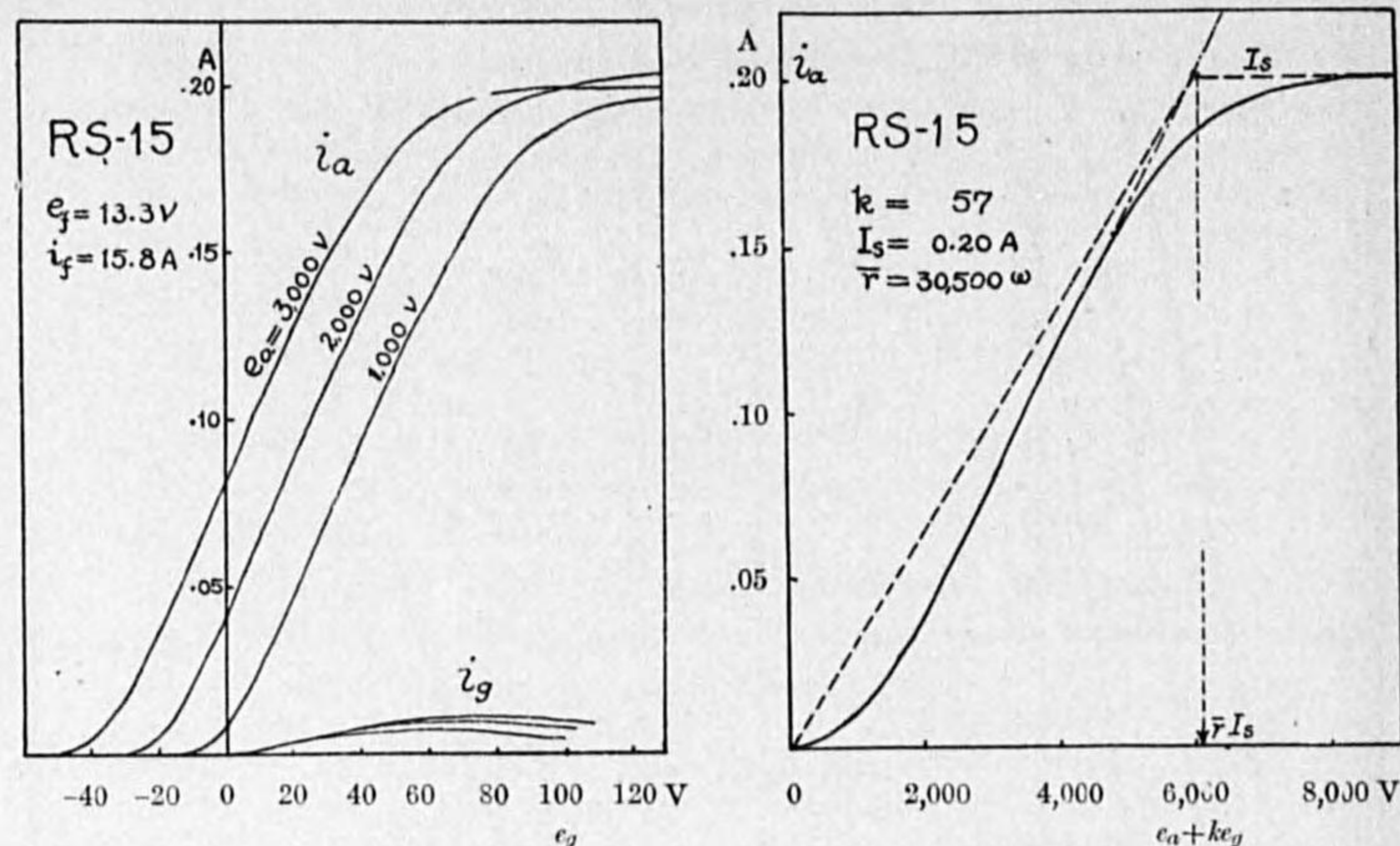


FIG. 50.

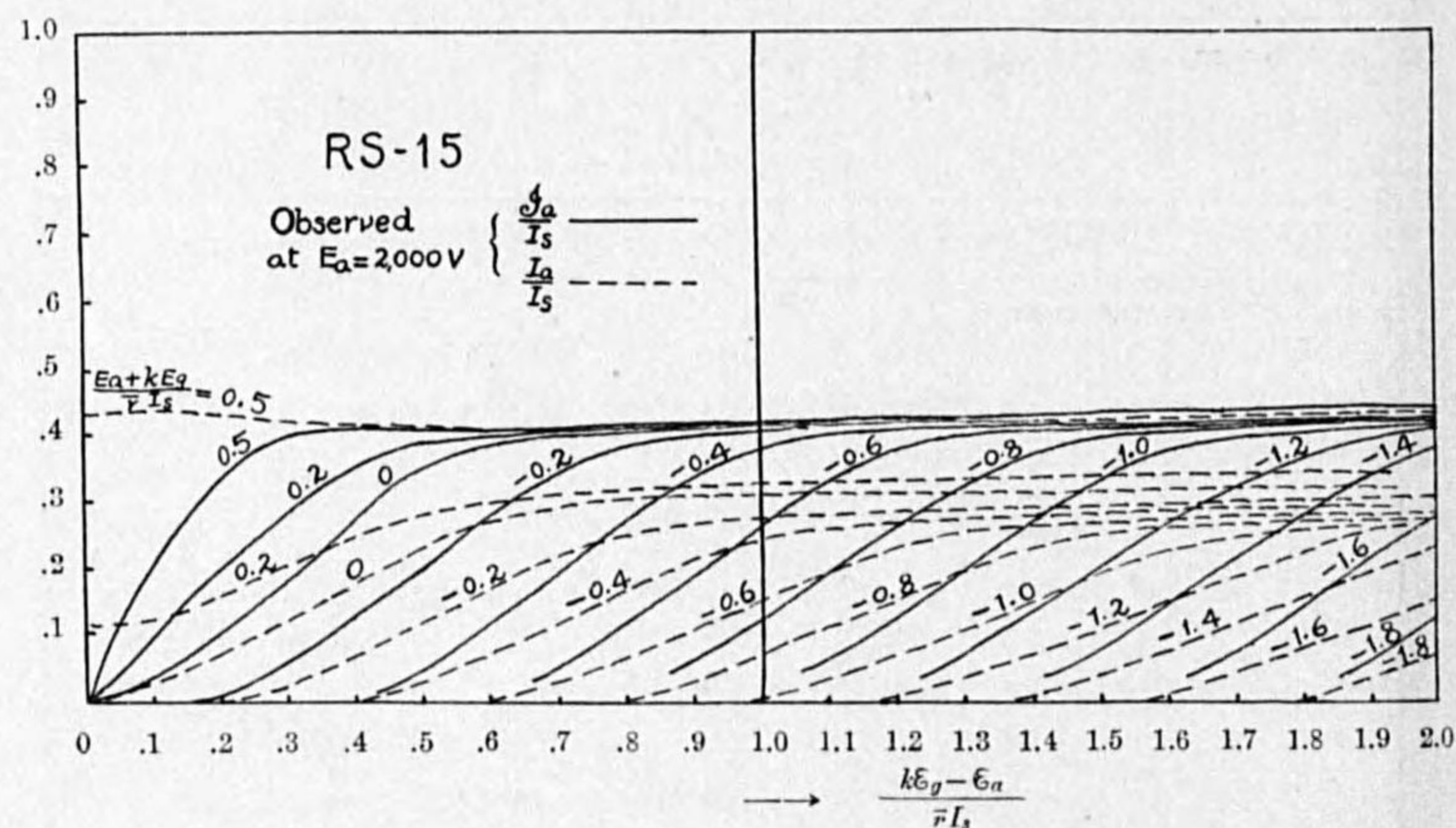


FIG. 51.

$$I_s = 0.200 \quad k = 57 \quad \bar{r} = 30,500 \quad \bar{r}I_s = 6,100$$

tested at $E_a = 2,000$ (the normal anode voltage of the tube is 4,000).

The result is shown in Fig. 51. Currents are rather low compared with the theoretical curves, but the general tendency is in agreement with them.

(2) The Dynamic Characteristic Diagram.

In CHART I annexed to this paper, the above given dynamic characteristics are reproduced with its left side extended to another diagram in which the ordinates give currents in the unit of I_s , and the abscissae give voltages in the unit of $\bar{r}I_s$. In this part of the diagram a group of straight lines starting at the origin represent the external impedance \mathcal{R} in the unit of internal resistance \bar{r} , and hyperbolas give the contour lines of equal power.

This diagram, which is to be called the "Dynamic Characteristic Diagram," is applicable to any triode, if its parameters k , \bar{r} , and I_s are known and if currents, voltages, resistances and powers are expressed in the units of I_s , $\bar{r}I_s$, \bar{r} , and $\bar{r}I_s^2$ respectively.

The use of the diagram is explained in the following.

A vacuum tube of saturation current I_s , amplification constant k , and mean anode impedance \bar{r} , which are all known, is used as an amplifier with an anode circuit impedance \mathcal{R} , and its operating conditions are to be predicted. First calculate the unit quantities $\bar{r}I_s$ and $\bar{r}I_s^2$ from the given unit quantities \bar{r} and I_s , and express all the quantities in these units. In the following explanations quantities expressed in these manner are taken instead of actual values.

Let anode voltage be E_a and grid bias be E_g . Calculate $E_a + kE_g$ and the corresponding dynamic characteristic curve of I_a and \mathcal{I}_a are found on the diagram. For graphical evaluation of this, E_a and kE_g (E_g is considered to be negative) are taken on the left side abscissa such as the points a and b in Fig. 52. Draw a line at b with inclination of 45° to intersect the vertical line through a at point c , then the ordinate of c represents $E_a + kE_g$ and the corresponding characteristic curves of I_a and \mathcal{I}_a are obtained as the lines def and oeg in the figure. Line oh is drawn to represent the given external impedance. For a given grid exciting voltage \mathcal{E}_g , calculate $k\mathcal{E}_g$, and take this quantity on the right side abscissa such as the point i ; from i a straight line is drawn parallel to the resistance line oh and

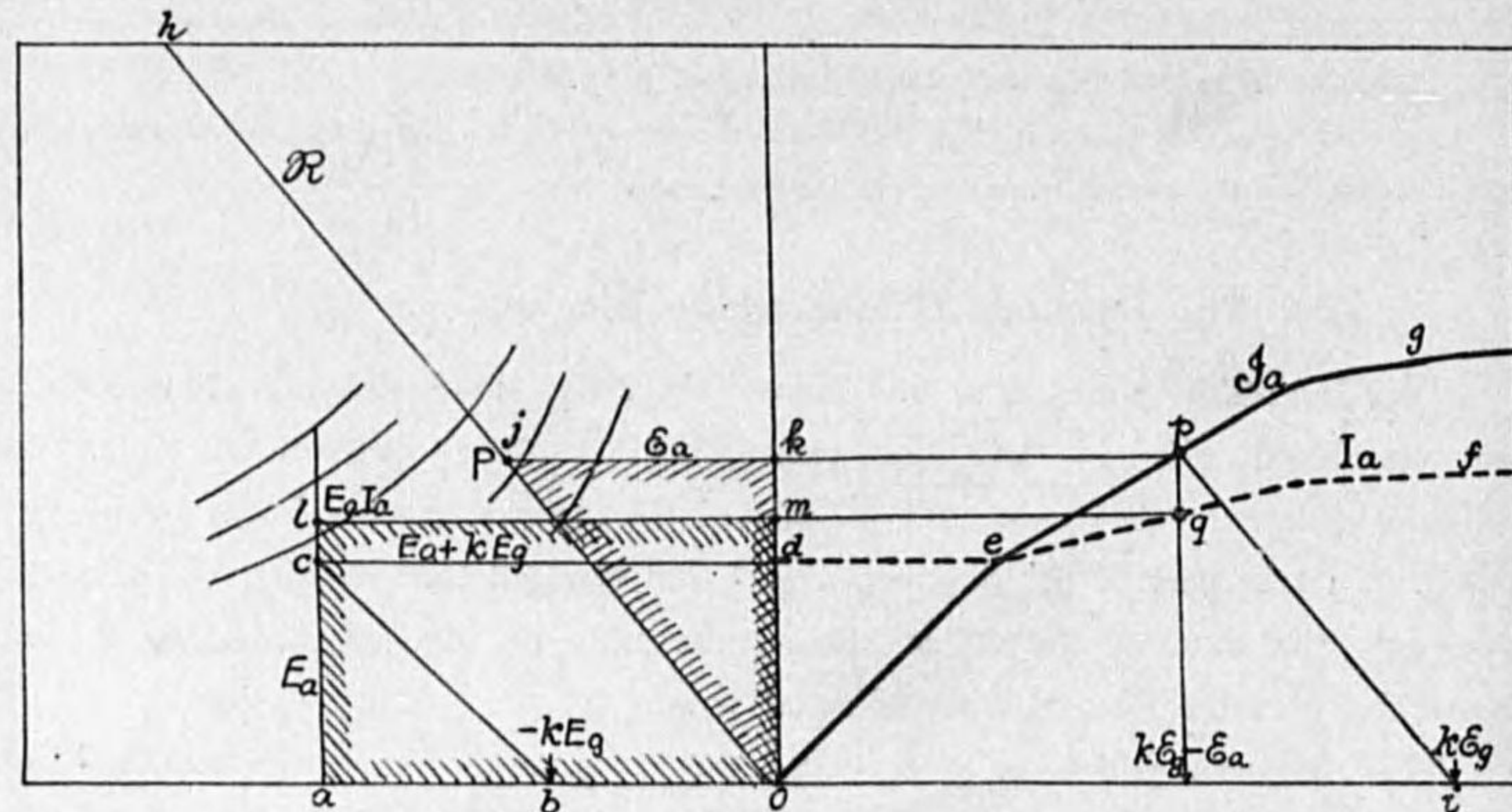


FIG. 52.

let this line intersect with the dynamic line oeg at p ; then this gives the working point on the dynamic characteristic. The reason is as follows; the ordinate represents \mathcal{I}_a , and let a level line through p intersect with the oh line at j and with the ordinate axis at k , then $\overline{ok} = \mathcal{I}_a$ and $\tan \angle jok = \mathcal{R}$. Therefore $\overline{jk} = \mathcal{I}_a \mathcal{R} = \mathcal{E}_a$. But $\overline{pj} = \overline{oi} = k\mathcal{E}_g$, and thus abscissa of the point p is $\overline{pk} = \overline{pj} - \overline{jk} = k\mathcal{E}_g - \mathcal{E}_a$, and is in conformity with that the dynamic characteristic curves have been expressed by the abscissa of $k\mathcal{E}_g - \mathcal{E}_a$.

The area of the triangle $\triangle ojk$ gives $\frac{1}{2}\mathcal{E}_a \mathcal{I}_a$ or $\frac{1}{2}\mathcal{I}_a^2 \mathcal{R}$ and represents the power output, which can be read by means of the power contour hyperbolas numbered at the top. The steady component I_a is obtained by drawing a line vertically from point p to intersect with the I_a dynamic line at a point q . A level line through q intersects with the vertical line through a at l , and with the ordinate axis at m . The rectangular area $omla$ is $E_a I_a$ and represents the input power to the tube, which can be read from the position of the point l on the contour hyperbolas numbered at the left end. The efficiency of conversion can be calculated from the two power values.

When the triode is used as a self-oscillator, the grid voltage \mathcal{E}_g is in definite relation to the anode voltage \mathcal{E}_a as determined from the circuit conditions.

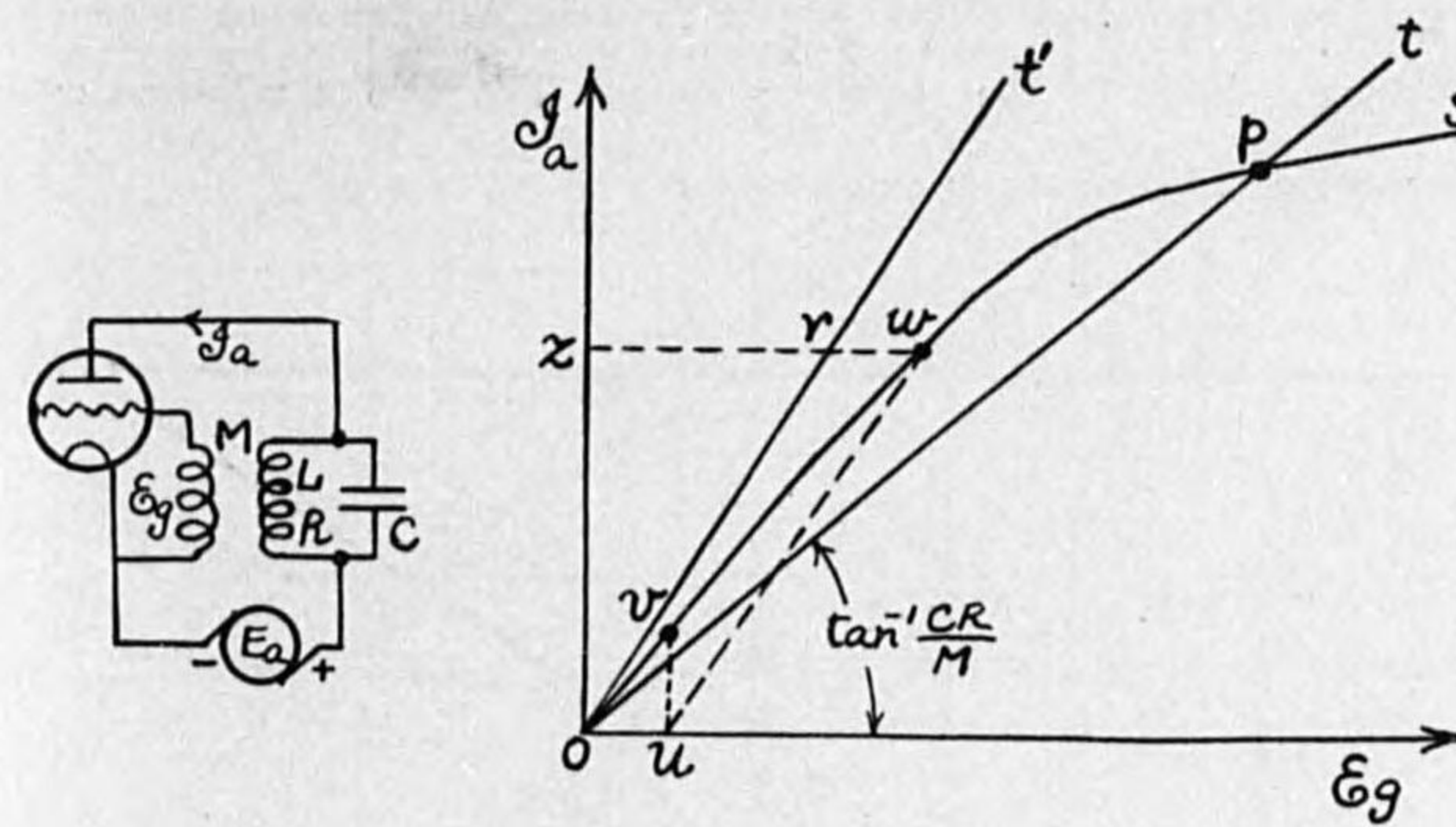


FIG. 53.

In an example shown in Fig. 53, \mathcal{I}_a is determined from \mathcal{E}_g by a dynamic line ops , while \mathcal{I}_a and external impedance $\mathcal{R} = \frac{L}{CR}$ determine $\mathcal{E}_a = \mathcal{I}_a \frac{L}{CR}$ and this induces an e. m. f. $\mathcal{E}_g = \mathcal{E}_a \frac{M}{L}$ in the grid circuit. Hence $\frac{\mathcal{I}_a}{\mathcal{E}_g} = \frac{CR}{M}$ is a straight line, the inclination of which is $\tan^{-1} \frac{CR}{M}$ as shown by a line ot in Fig. 53. Thus the dynamic characteristic curve ops gives the relation in which \mathcal{I}_a is determined by \mathcal{E}_g from the tube characteristics, while the excitation line ot gives the relation in which \mathcal{E}_g is determined by \mathcal{I}_a from circuit conditions. Then the point of intersection p shall be the working point of the self-oscillator. If the coupling becomes loose, the excitation line is shifted to left and finally will not intersect with the dynamic line, and in this case oscillation cannot be produced.

The regeneration can be explained in the same diagram. When regeneration is applied, anode circuit is coupled to grid circuit but not so close as to produce oscillation, such as a line ot' in Fig. 53. If the regenerative connection is not made, for a certain grid voltage such as \overline{ou} , the anode current is \overline{uv} . But on regenerative condition, a line is to be drawn from the point u parallel to the line ot' and the intersecting point w on the characteristic gives the working point. The reason is that the level line from w intersecting with ot' at r and with the ordinate axis at z repre-

sents the grid excitation which is the sum of the originally impressed voltage $\overline{ou} = \overline{rw}$ and the voltage induced by the anode current \overline{oz} . The ratio of regenerative amplification to non-regenerative one is expressed by $\frac{\overline{oz}}{uv}$.

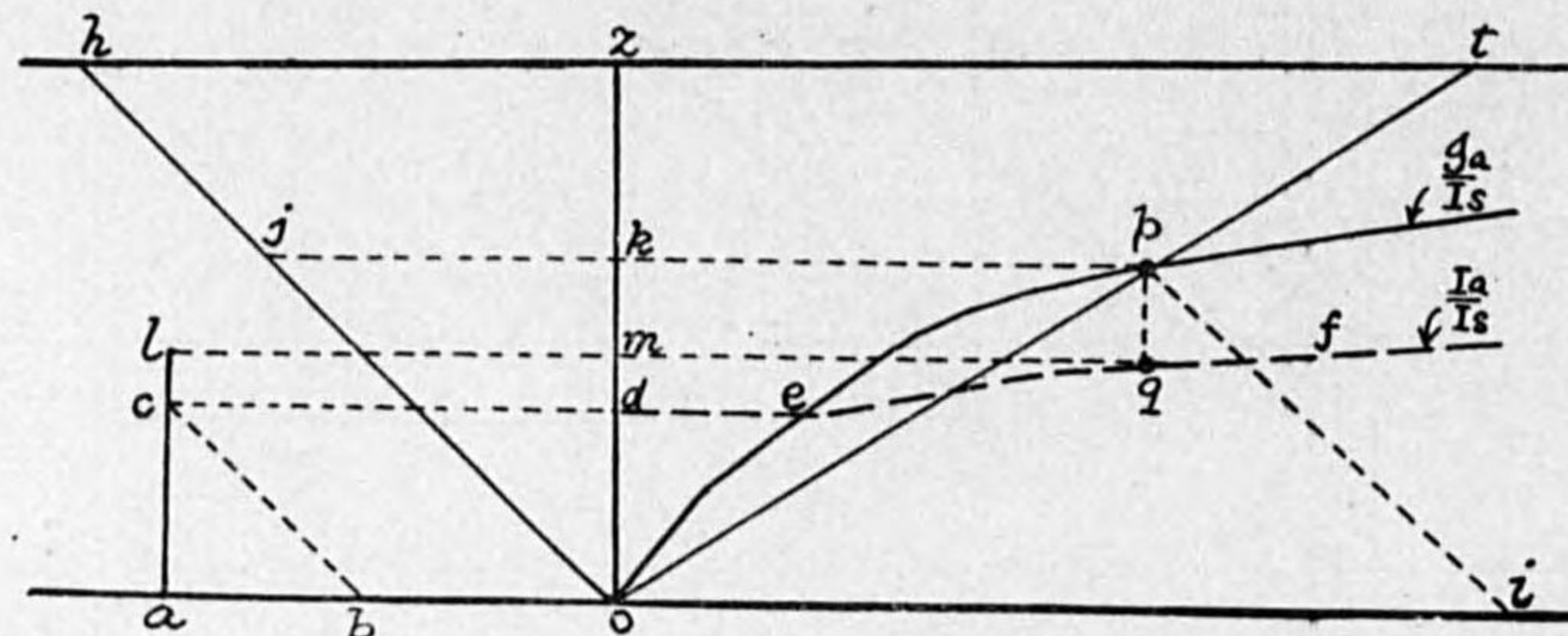


FIG. 54.

Now these ideas can be applied to the dynamic characteristic diagram in the following way (Fig. 54). Comparing the figure with Fig. 53, resistance line oh corresponds to the ordinate axis of Fig. 53, and the abscissa representing kE_g corresponds to that of Fig. 53. The excitation line ot in Fig. 53 is obtained in Fig. 54 by taking the quantity $\frac{kE_g}{f_a}$ from the point h to the right on the level line as a

point t , and by connecting this point to the origin; in other words $\frac{kE_g}{f_a} - R$

shall be taken on right abscissa as \overline{zt} in order to obtain the excitation line ot . The point of intersection of the excitation line with the dynamic characteristic curve gives the working point p and all the other quantities can be derived in the same way as explained before. In CHART I, $\left(\frac{kE_g}{f_a}\right)_c$ means that the relation is to be derived from the circuit conditions.

The modulation of a self-oscillating tube consists in altering the anode or grid steady voltage with audio frequency, hence producing the corresponding variations in the amplitude of oscillation. This means the variation of $E_a + kE_g$, other things being equal.

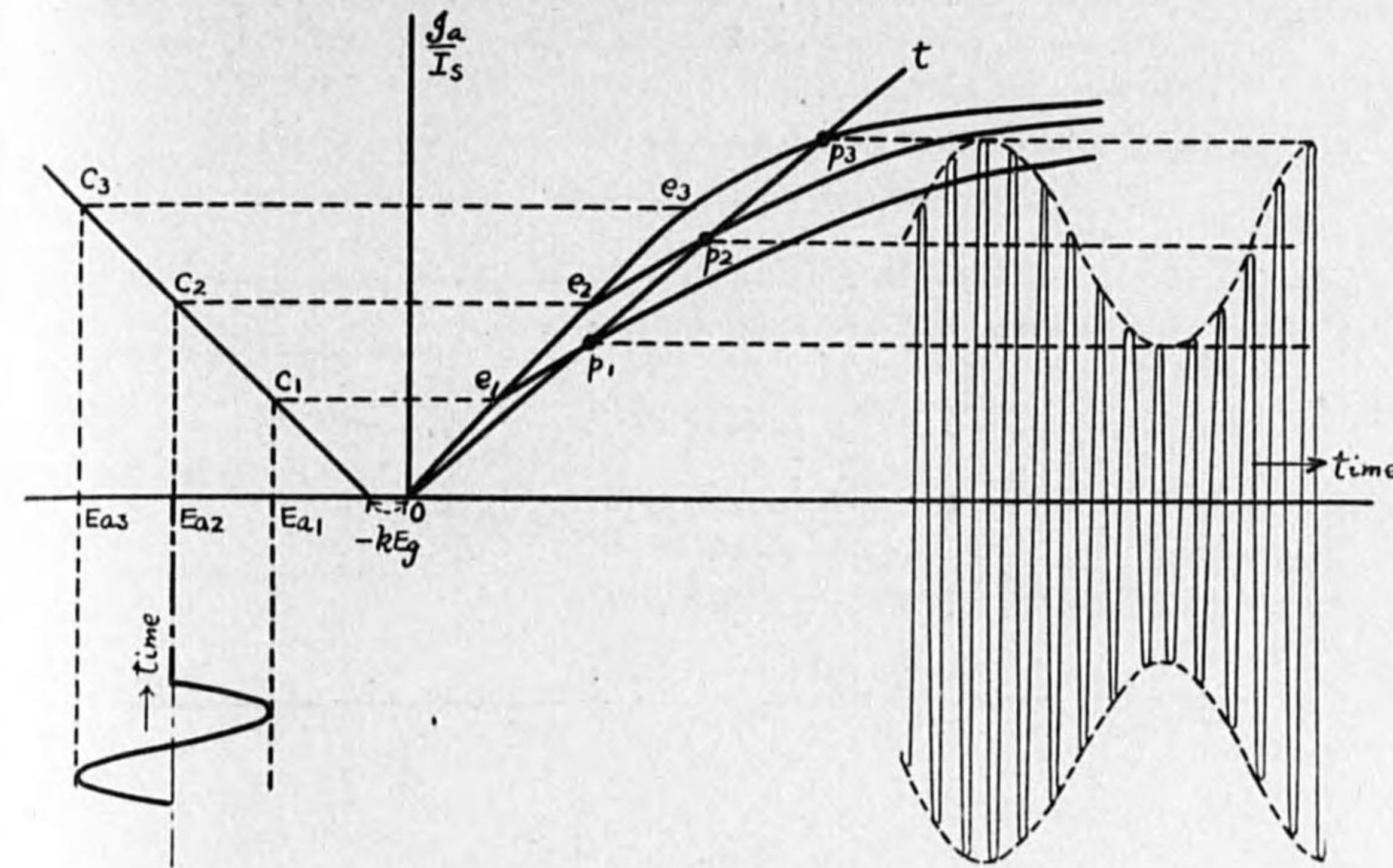


FIG. 55.

Thus, for example, if anode voltage E_a is varied in sinusoidal wave form as shown in Fig. 55, $E_a + kE_g$ will vary accordingly and the dynamic characteristic curve is shifted up and down. The excitation line ot remaining unvaried, the working point p must travel on the ot line and the oscillating current I_a varies its amplitude in accordance with the variation of the anode voltage.

Applications of the dynamic characteristic diagram are further illustrated by the following examples.

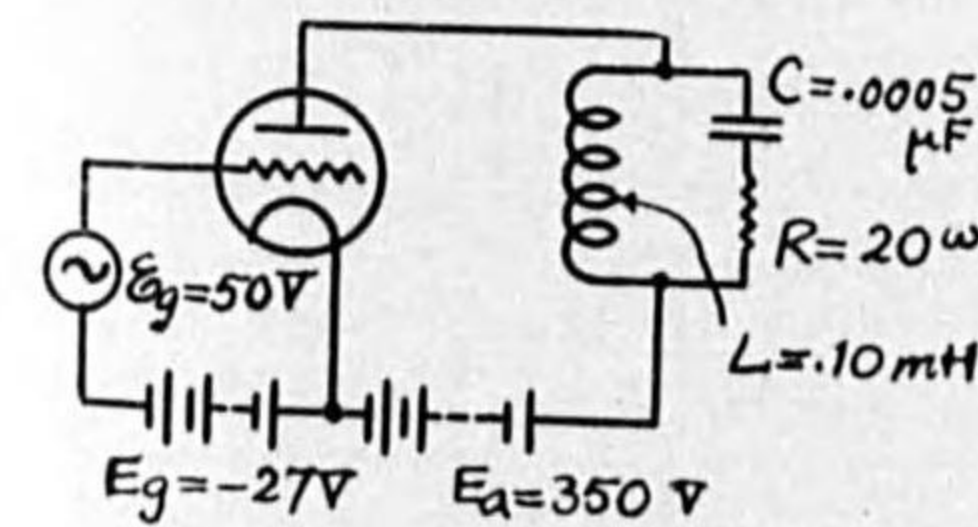


FIG. 56.

Example 69. A triode type UX-210 has a characteristic represented by the following quantities at a certain filament voltage.

$$k=7.5 \quad \bar{r}=5,000 \omega \quad I_s=0.20 \text{ A}$$

Its working conditions in the following cases are required.

(a) R. F. Amplifier.

The relation determined from the circuit condition;

$$\frac{\epsilon_a}{\epsilon_g} = \frac{\omega I_a}{\omega L_g} = \frac{I_a}{L_g} \quad \epsilon_a = \mathcal{J}_a \mathcal{R}$$

$$\therefore \frac{\mathcal{J}_a \mathcal{R}}{\epsilon_g} = \frac{I_a}{L_g} \quad \therefore \frac{k \epsilon_g}{\mathcal{J}_a} = \frac{k \mathcal{R} L_g}{I_a} \approx 9,240$$

hence $\frac{k \frac{\epsilon_g}{\mathcal{J}_a} - \mathcal{R}}{\bar{r}} = 1.27$

The procedure to obtain the working points p and q are illustrated in Fig. 59.

The results obtained from the diagram;

$$\mathcal{J}_a = 0.55 I_s = 0.11 \text{ A.} \quad I_a = 0.43 I_s = 0.086 \text{ A.}$$

$$\epsilon_a = 0.32 \bar{r} I_s = 320 \text{ V.}$$

Output $P = \frac{1}{2} \epsilon_a \mathcal{J}_a = 17.6 \text{ W.}$ Input $E_a I_a = 30.1 \text{ W.}$

Closed circuit current $= \sqrt{P/R} = 0.94 \text{ A. effective.}$

Efficiency $\eta = 0.58$ $k \epsilon_g = 1.04 \bar{r} I_s = 1,040$ $\epsilon_g = 139 \text{ V.}$

In actual case, power output will be slightly reduced due to partial consumption for the grid excitation.

Example 70. A triode type VM-100 has a rating as shown in the following table. Its optimum operating conditions used as power amplifier and oscillator in various cases are to be studied.

e_f	i_f	I_s	Permissible anode loss	E_a	k	\bar{r}
12.0 V.	24.0 A.	1.50 A.	1,000 W.	10,000 V.	75	28,000 ω

$$\bar{r} I_s = 42,000 \text{ V} \quad \bar{r} I_s^2 = 63,000 \text{ W} \quad \frac{E_a}{\bar{r} I_s} = 0.24$$

(a) Distortionless Amplifier or Modulator.

Connect a non-inductive resistance of \mathcal{R} ohms as a load to the anode circuit. (Fig. 60.) When the tube is used as a modulator, this resistance corresponds to the equivalent a. c. resistance of the oscillator to be modulated. In order to avoid the d. c. potential drop in \mathcal{R} , a choke coil and a blocking condenser are inserted, which is considered to give no appreciable effect on the value of the output impedance.

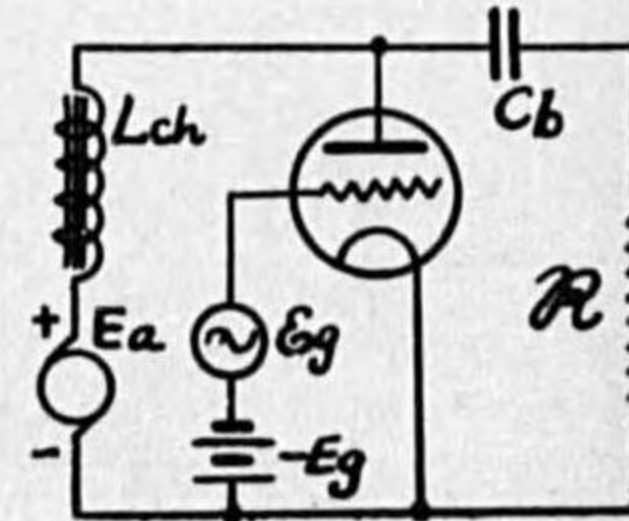


FIG. 60.

The distortionless amplification requires the conditions:—

1° That the working point rests in the region A or on the $\frac{\mathcal{J}_a}{I_s}$ characteristic line AO in Fig. 61, which represents lower portion of the dynamic characteristic diagram.

2° That the grid current is not appreciable, i. e. $E_g + \epsilon_g \leq 0$

3° That the minimum anode current does not come on the curved part of the static characteristic curves, i. e. $I_a - \mathcal{J}_a > \epsilon I_s$, ϵ being a small quantity,

For the maximum available power output, we take

$$E_g + \epsilon_g = 0 \quad \text{and} \quad I_a - \mathcal{J}_a = 10 \text{ mA} = 0.0067 I_s$$

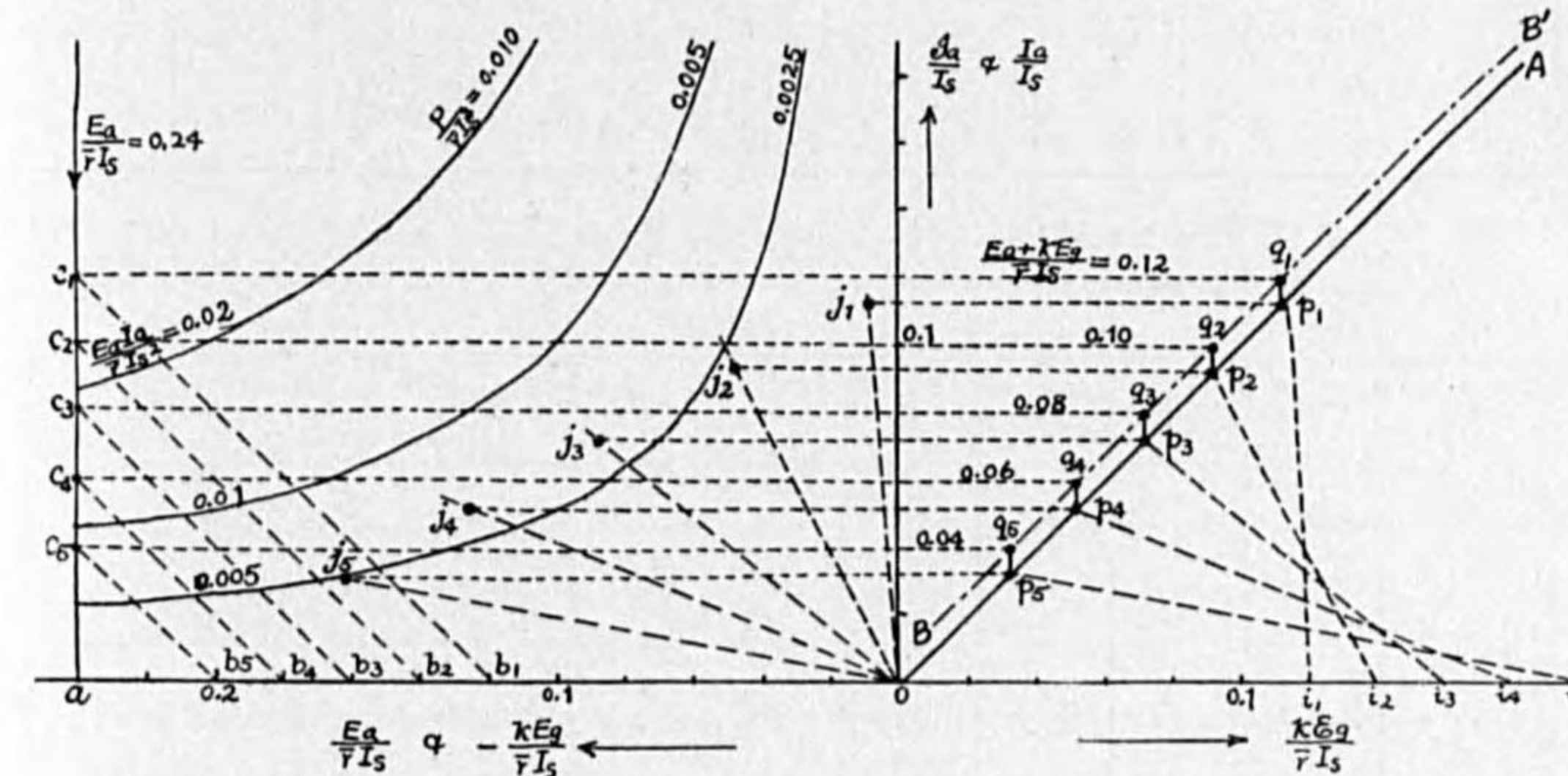


FIG. 61.

$\frac{E_a}{\bar{r} I_s} = 0.24$ comes to a point a , in Fig. 61, and the condition $E_g + \epsilon_g = 0$ or $-k E_g = k \epsilon_g$ requires that $\overline{ob} = \overline{oi}$ in Fig. 52. Another condition $\frac{I_a}{I_s} - \frac{\mathcal{J}_a}{I_s} = 0.0067$ requires that the working point on the $\frac{I_a}{I_s}$ characteristics should rest on the line BB' in Fig. 61, which is taken above the line OA by an amount 0.0067.

Assume several values of $\frac{k E_g}{\bar{r} I_s}$, such as b_1, b_2, b_3 , etc. in Fig. 61, and from them $\frac{E_a + k E_g}{\bar{r} I_s}$ can be determined such as c_1, c_2, c_3 , etc., and the working points are obtained on each $\frac{I_a}{I_s}$ line such as q_1, q_2, q_3 , etc., while working points on $\frac{\mathcal{J}_a}{I_s}$ line are such as p_1, p_2, p_3 , etc. $\frac{k \epsilon_g}{\bar{r} I_s}$ should be taken as equal to $-\frac{k E_g}{\bar{r} I_s}$ and the points i_1, i_2, i_3 , etc., taken

in such a way are connected to p_1, p_2, p_3 , etc. The resistance lines should be drawn from the origin parallel to these lines $i_1 p_1, i_2 p_2, i_3 p_3$ and the working points on the left side diagram are obtained such as j_1, j_2, j_3 , etc. These determine power output P and a. c. anode voltage ϵ_a . On the other hand e_1, e_2, e_3 , etc., give power inputs. All the quantities thus obtained are in the following table.

$\frac{E_a}{\bar{r}I_s}$	$\frac{kE_g}{\bar{r}I_s}$	$\frac{k\epsilon_g}{\bar{r}I_s}$	$\frac{I_a}{I_s}$	$\frac{I_a}{I_s}$	$\frac{\epsilon_a}{\bar{r}I_s}$	$\frac{\mathcal{R}}{\bar{r}}$	$\frac{P}{\bar{r}I_s^2}$	$\frac{E_a I_a}{\bar{r}I_s^2}$	η
0.24	-0.12	0.12	0.12	0.112	0.008	0.072	0.00045	0.028	0.016
	-0.14	0.14	0.10	0.092	0.047	0.51	0.0022	0.024	0.093
	-0.16	0.16	0.08	0.072	0.086	1.19	0.0032	0.019	0.167
	-0.18	0.18	0.06	0.052	0.125	2.40	0.0032	0.013	0.242
	-0.20	0.20	0.04	0.032	0.130	4.07	0.0025	0.0089	0.28

The above quantities given in actual values are as follows and the powers are plotted in curves in Fig. 62.

E_a	kE_g	E_g	ϵ_g	I_a	I_a	ϵ_g	\mathcal{R}	P	$E_a I_a$	η
10,000 V	V	V	V	A	A	V	ω	W	W	%
	-5040	-67	67	.180	.168	336	2,020	28	1,760	1.6
	-5880	-78	78	.150	.138	1,970	14,300	140	1,510	9.3
	-6720	-90	90	.120	.108	3,610	33,400	198	1,200	16.7
	-7560	-100	100	.090	.078	5,250	67,200	198	820	24
-8400	-112	112	.060	.048	5,470	114,000	157	560	28	

In order to obtain maximum power output from the tube, the resistance \mathcal{R} must be chosen such that $\mathcal{R} = 2\bar{r} = 56,000$ as shown in Fig. 62. This complies with the theory⁽⁹⁾ that, for maximum output of distortionless amplification, the output impedance should be twice the anode impedance. In Fig. 62 the input to the tube is also plotted. In actual operating condition, when the tube is not amplifying alternating power, the

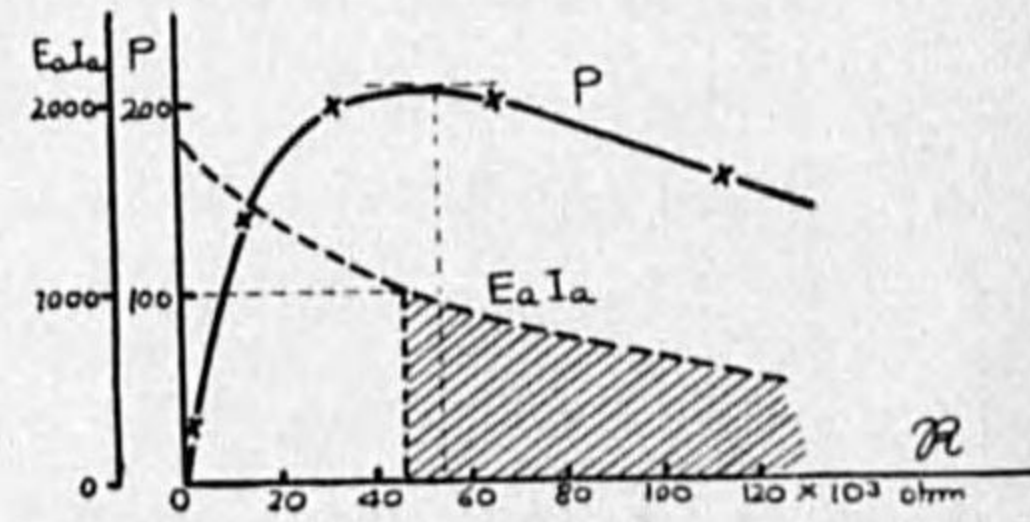


FIG. 62.

(9) E. W. Kellogg: J. I. E. E. p. 490, May, 1925.

total input power $E_a I_a$ is dissipated at the anode. As the anode loss permissible is 1,000 watts, the safe working range must be in the hatched part of Fig. 62. The efficiency of power conversion increases with the increase of \mathcal{R} .

The above discussion is based on the condition that the grid input voltage ϵ_g can be obtained at any convenient amount. If this quantity be previously given, the solution will be somewhat different, and the maximum power output can be obtained at $\mathcal{R} = \bar{r}$ or at an output circuit impedance equal to the anode impedance, which is a well-known fact. But in this case the condition of distortionless amplification is disregarded, otherwise the anode voltage should be raised above normal value. Fig. 63 and the following table show this relation.

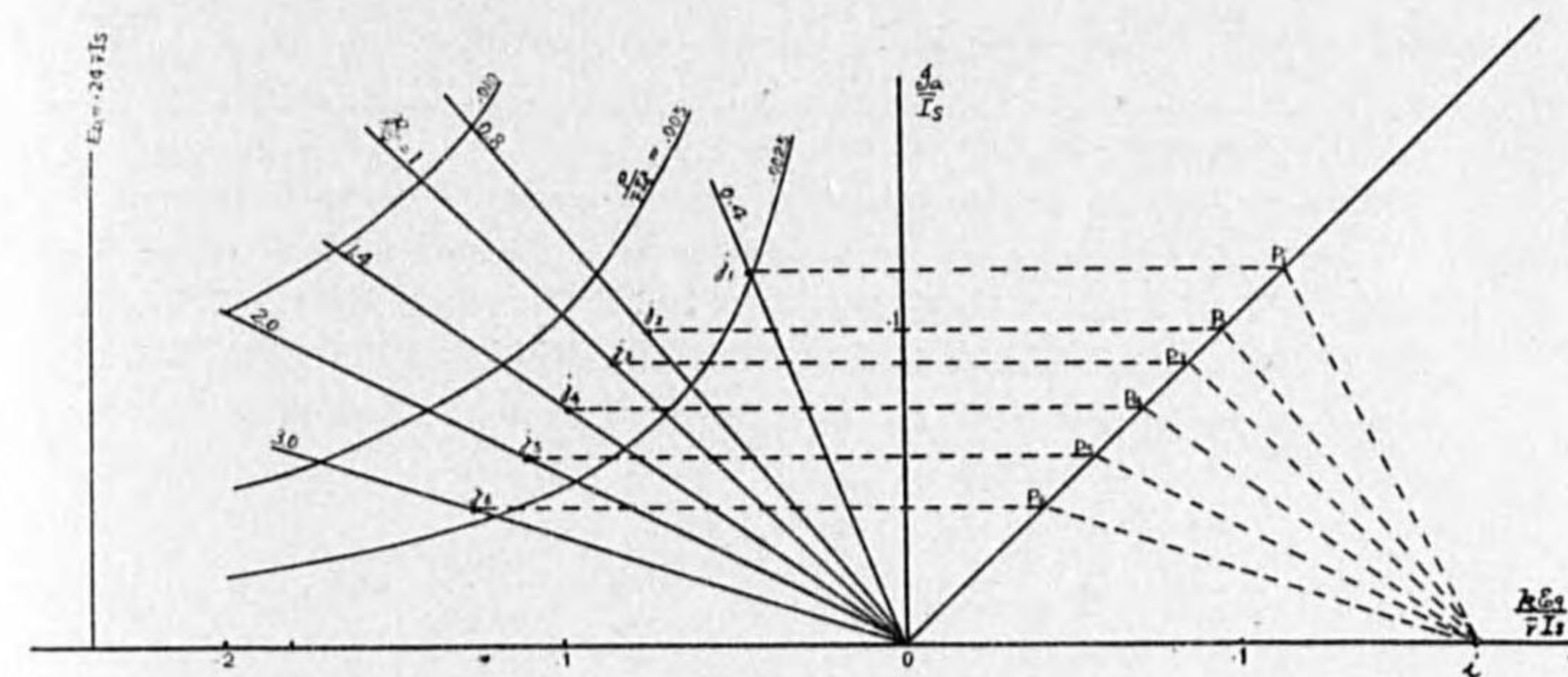


FIG. 63.

$\frac{E_a}{\bar{r}I_s}$	$\frac{\mathcal{R}}{\bar{r}}$	$\frac{P}{\bar{r}I_s^2}$	\mathcal{R}	P
$\frac{E_a}{\bar{r}I_s} = .24$ $\frac{k\epsilon_g}{\bar{r}I_s} = 0.17$ ($E_a = 10,000$ $\epsilon_g = 95$)	0.4	.0026	11,200	164
	0.8	.0035	22,400	220
	1.0	.0038	23,000	240
	1.4	.0035	39,200	220
	2.0	.0028	56,000	176
	3.0	.0021	84,000	132

(b) Oscillator for Radio-telegraph Transmission.

The tube is used as a radio-telegraph transmitter and a maximum power output is required to be obtained at the highest possible efficiency, with a circuit as shown in Fig. 64.

The antenna circuit is assumed to have the constants; $L=0.32\text{mH}$ $C=.0023\mu\text{F}$ $R=10\omega$. Output circuit impedance can be adjusted by taking taps on the inductance, but first consider the case of maximum impedance such as

$$\bar{R} = \frac{L}{CR} = 13,900\omega$$

hence $\frac{\bar{R}}{\bar{r}} = 0.50$

and $\frac{E_a}{\bar{r}I} = 0.24$ as before.

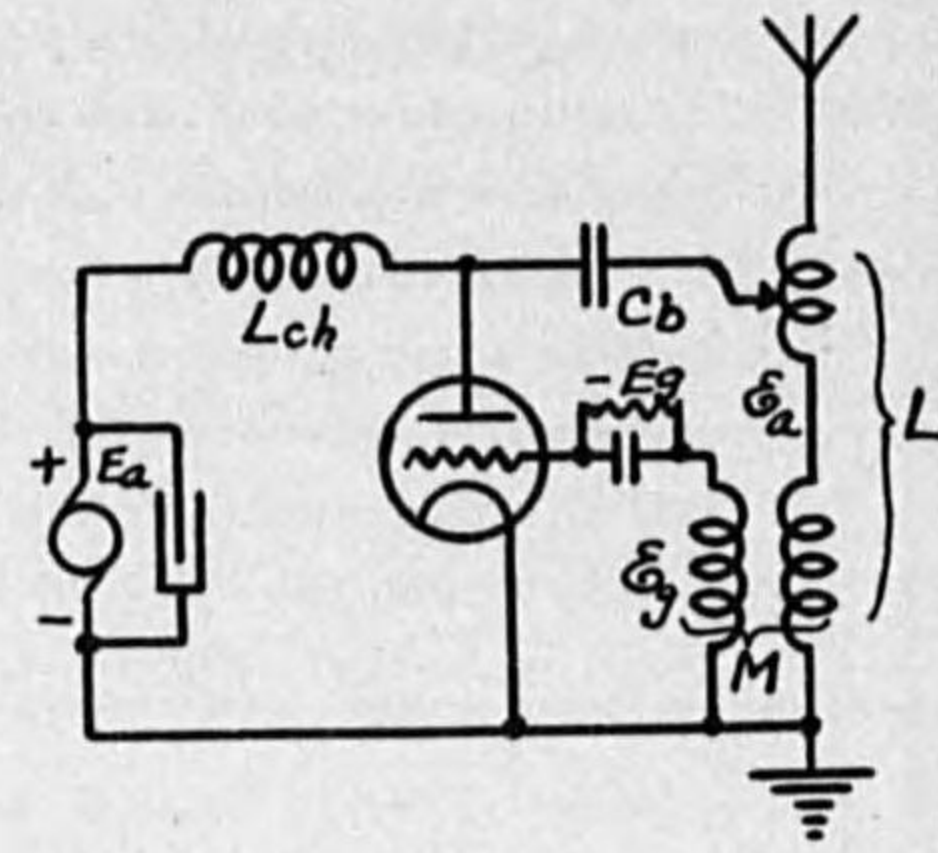


FIG. 64.

It is understood that the choke and the blocking condenser are designed to exert no appreciable effect on the total impedance.

For giving maximum power output as an oscillator, the anode minimum voltage $E_a - \epsilon_a$ should be equal or slightly higher than the maximum grid voltage $E_g + \epsilon_g$. This is because for too low ϵ_a , the utilisation of E_a is low, while for too high ϵ_a , $E_a - \epsilon_a$ is low, and, appreciable current flows in the grid and anode power is reduced. Thus let $E_a - \epsilon_a = E_g + \epsilon_g$

$$\text{or } \frac{\epsilon_g}{\bar{r}I_s} = \frac{E_a}{\bar{r}I_s} - \frac{\epsilon_a}{\bar{r}I_s} - \frac{E_g}{\bar{r}I_s}$$

If $\frac{E_a + kE_g}{\bar{r}I_s}$ be assumed, $\frac{kE_g}{\bar{r}I_s} = \frac{E_a + kE_g}{\bar{r}I_s} - \frac{E_a}{\bar{r}I_s}$ can be derived and hence $\frac{E_g}{\bar{r}I_s}$ too, and again assuming $\frac{\epsilon_a}{\bar{r}I_s}$, $\frac{\epsilon_g}{\bar{r}I_s}$ can be derived by the above given relation.

On the other hand, for the assumed value of $\frac{\epsilon_a}{\bar{r}I_s}$, working point p can be determined on the dynamic characteristics and $\frac{k\epsilon_g}{\bar{r}I_s}$ or $\frac{\epsilon_g}{\bar{r}I_s}$ is known. Thus we can finally find such $\frac{\epsilon_a}{\bar{r}I_s}$ value as to give equal $\frac{\epsilon_g}{\bar{r}I_s}$ on both the cases and this is the required optimum condition.

The two procedures for deriving $\frac{\epsilon_g}{\bar{r}I_s}$ are shown in the following table.

$\frac{\epsilon_a}{\bar{r}I_s}$	$\frac{I_a}{I_s}$	$\frac{E_a + kE_g}{\bar{r}I_s}$	$\frac{k\epsilon_g}{\bar{r}I_s}$	$\frac{\epsilon_g}{\bar{r}I_s}$	$\frac{kE_g}{\bar{r}I_s}$	$\frac{E_g}{\bar{r}I_s}$	$\frac{\epsilon_g}{\bar{r}I_s}$	Difference $\frac{\epsilon_g}{\bar{r}I_s}$
		0.4	0.70	0.0093	0.16	0.00214	0.0179	0.0086
		0.2	0.85	0.0113	0.04	0.00053	0.0194	0.0081
0.22	0.45	0	1.12	0.0149	-0.24	-0.0032	0.0232	0.0083
		-0.2	1.32	0.0176	-0.44	-0.0059	0.0259	0.0083

In the above table both the values of $\frac{\epsilon_g}{\bar{r}I_s}$ do not coincide each other, and their difference is constant as shown in the last column. So there is no necessity of calculating for more than one value of $\frac{E_a + kE_g}{\bar{r}I_s}$.

Thus $\frac{E_a + kE_g}{\bar{r}I_s} = 0.40$ being assumed, the following results are obtained for further variation of $\frac{\epsilon_a}{\bar{r}I_s}$.

$\frac{\epsilon_a}{\bar{r}I_s}$	$\frac{\epsilon_g}{\bar{r}I_s}$ from the diagram	$\frac{\epsilon_g}{\bar{r}I_s} = \frac{E_a}{\bar{r}I_s} - \frac{\epsilon_a}{\bar{r}I_s} - \frac{E_g}{\bar{r}I_s}$
0.20	0.0080	0.0379
0.22	0.0093	0.0179
0.23	0.0096	0.0079

From this we get the working point to give equal $\frac{\epsilon_g}{\bar{r}I_s}$ by interpolation:

$$\frac{\epsilon_a}{\bar{r}I_s} = 0.228 \quad \frac{\epsilon_g}{\bar{r}I_s} = 0.0095 \quad \frac{k\epsilon_g}{\bar{r}I_s} = 0.712 \quad \text{at} \quad \frac{E_a + kE_g}{\bar{r}I_s} = 0.40$$

and $\frac{I_a}{I_s} = 0.458, \quad I_a = 0.69 \text{ A.} \quad P = \frac{1}{2} \epsilon_a I_a = 3,290 \text{ W.}$

Input depends on $\frac{I_a}{I_s}$ which in turn depends on $\frac{E_a + kE_g}{\bar{r}I_s}$ as shown in the following table.

$\frac{\epsilon_a}{\bar{r}I_s}$	$\frac{I_a}{I_s}$	$\frac{E_a + kE_g}{\bar{r}I_s}$	$\frac{k\epsilon_g}{\bar{r}I_s}$	$\frac{\epsilon_g}{\bar{r}I_s}$	$\frac{kE_g}{\bar{r}I_s}$	$\frac{I_a}{I_s}$	$\frac{E_a I_a}{\bar{r}I_s^2}$	η
		0.40	0.71	0.0096	0.16	0.47	0.113	0.46
		0.20	0.87	0.0116	0.04	0.32	0.077	0.67
0.228	0.458	0	1.14	0.0152	-0.24	0.24	0.057	0.91
		-0.20	1.34	0.0179	-0.44	0.24	0.057	0.91
		-1.00	2.37	0.0316	-1.24	0.24	0.057	0.91

Then at a constant output of $P=3.29 \text{ KW}$, the efficiency can be raised up to 91% with increase of the negative grid bias and exciting voltage. If the tube is separately excited, or used as a power amplifier, the optimum condition will be,

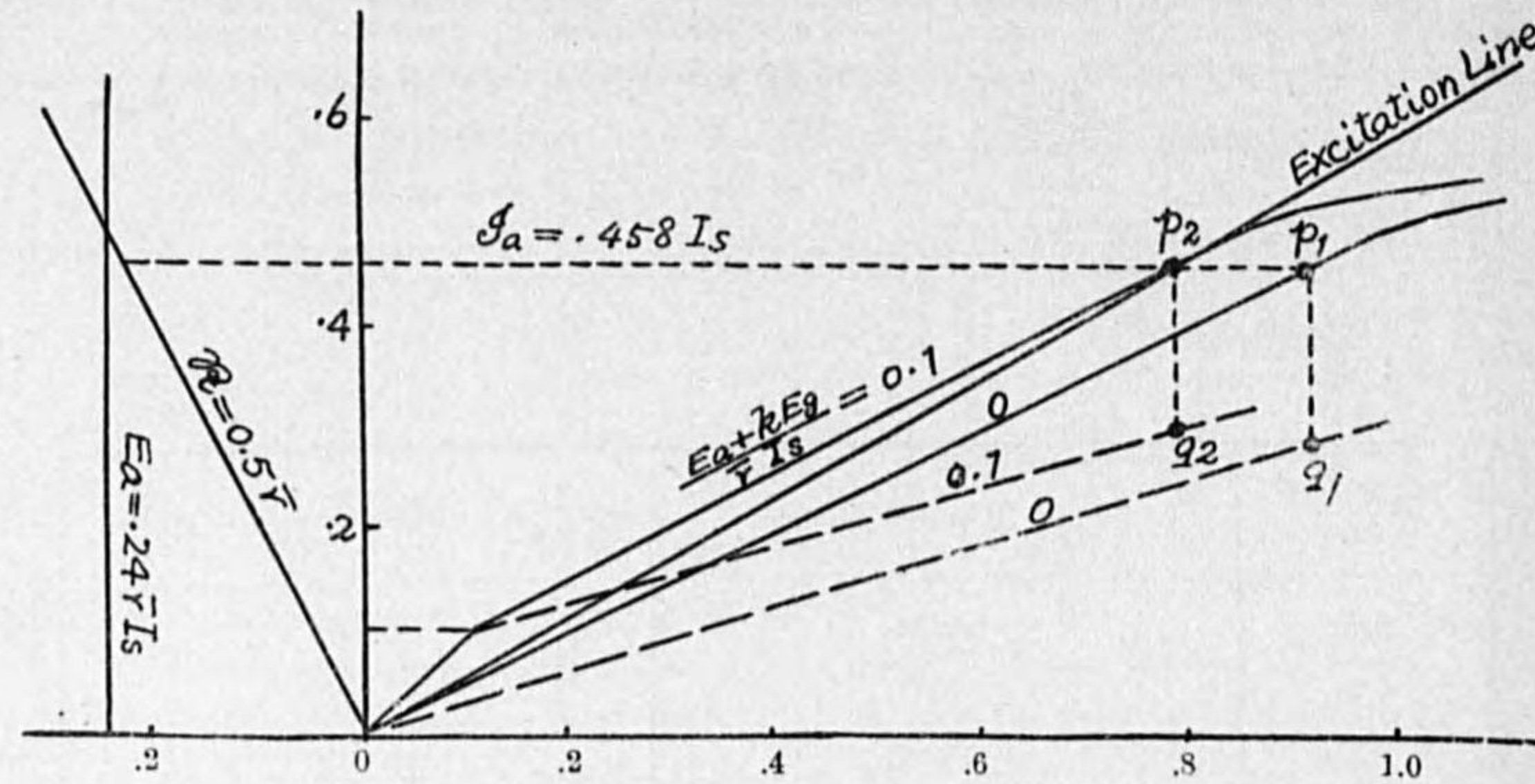


FIG. 65.

$$\frac{E_a + kE_g}{\bar{r}I_s} = 0 \quad \frac{kE_g}{\bar{r}I_s} = -0.24$$

$$kE_g = -10,100 \quad E_g = -135 \text{ V.} \quad I_a = 0.36 \text{ A.}$$

The working points are shown in Fig. 65 as points p_1 and q_1 . If the tube is used as a self-oscillator, the excitation line must intersect with the $\frac{I_a}{I_s}$ line at the value of $\frac{I_a}{I_s} = 0.458$. The above given working points do not fulfill this condition and another pair of working points such as follows must be taken; (p_2 and q_2 in Fig. 65)

$$\frac{E_a + kE_g}{\bar{r}I_s} = 0.1 \quad \frac{kE_g}{\bar{r}I_s} = -0.14 \quad kE_g = -5,800 \quad E_g = -77.4$$

$$I_a = 0.28I_s = 0.42 \text{ A.}$$

Input $E_a I_a = 4,200 \text{ W.}$ Loss = 1,000 W. $\eta = 78\%$

Part of the output given above is consumed for the grid excitation. If this grid loss is neglected, the antenna current will be

$$I_o = \sqrt{\frac{P}{R}} = 17.9 \text{ A. effective value.}$$

The oscillation circuit must be so arranged as to fulfill the following condition;

$$kE_g = 1.01 \bar{r}I_s = 4,250 \text{ V.}$$

or $E_g = 57 \text{ V}$ must be induced by the antenna current of $I_o = 17.9 \text{ A.}$ eff. = 25.3 A. max

But $E_g = \omega M I_o \quad \omega = \frac{1}{\sqrt{CL}} = 1.17 \times 10^6,$

then $M = \frac{E_g}{\omega I_o} = 1.93 \times 10^{-6} \text{ H.}$

In actual case greater value of M will be required in order to meet the grid loss.

The grid bias voltage $-E_g$ can be obtained by the adjustment of the grid leak resistance, the potential drop produced on it by the grid current being E_g .

This type of tube is usually operated at the input of 3 to 4 KW and the conversion efficiency of about 80% in C. W. transmitter.

(c) Self-Oscillator for Radio-telephone Transmission.

A radio-telephone transmitter is constructed by adding a modulator tube to the circuit shown in Fig. 64. (constant current system). The working condition of the oscillator tube is required.

As the modulation of the output radio-frequency current should effectively be done, the working point must be at such a point p shown in Fig. 66, when the tube is oscillating without modulation.

$$E_a = 0.24 \bar{r}I_s \quad E_a + kE_g = 0.15 \bar{r}I_s \quad I_a = 0.26I_s = 0.39 \text{ A.}$$

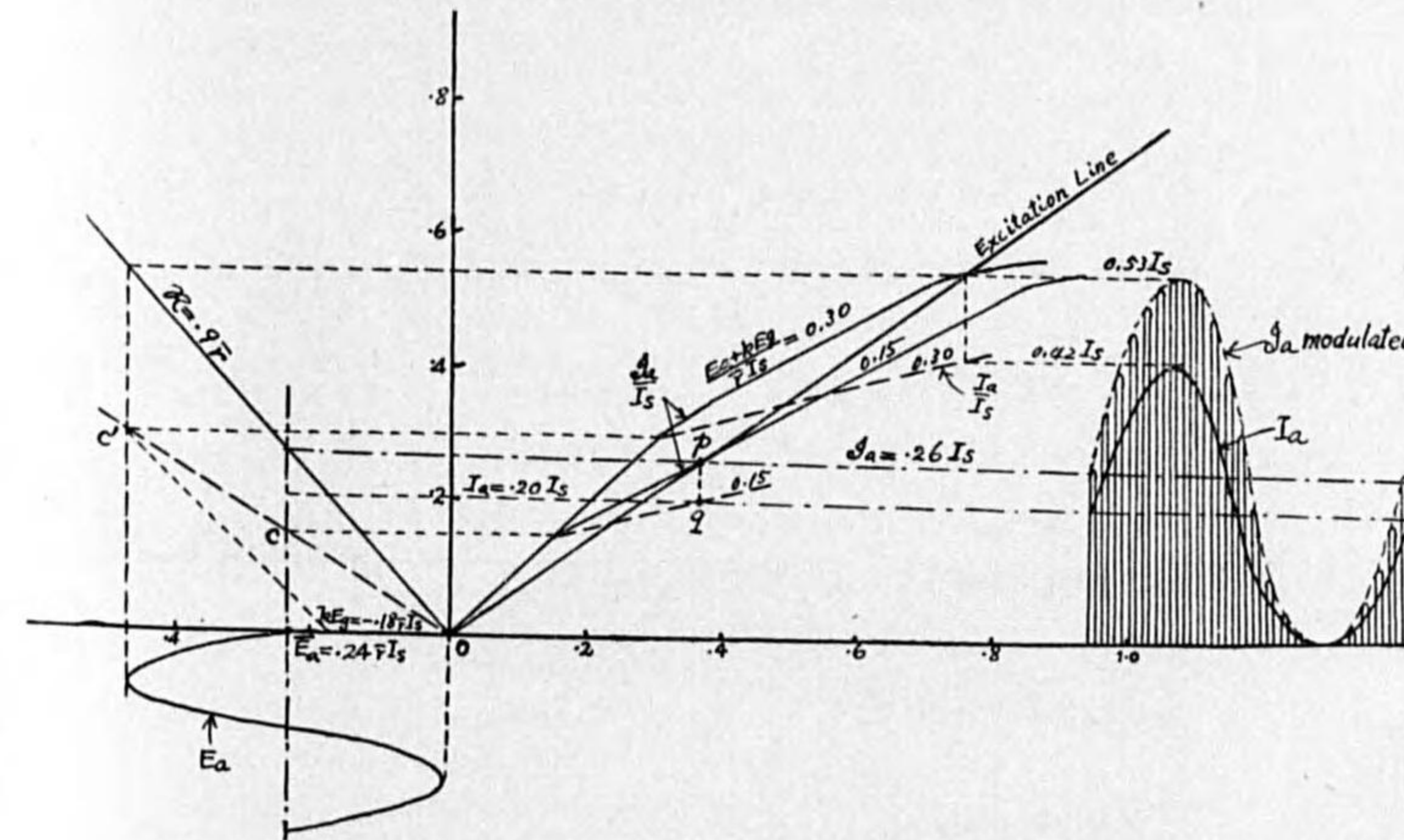


FIG. 66.

CHAPTER III.

THE DESIGN OF TRIODES.

(1) Working Points on the Dynamic Characteristic Diagram.

The design of a triode to satisfy specified conditions can be accomplished in the following way, which shows a typical case where the use of the triode is indicated and its power output is given.

Optimum working points can always be found on the dynamic characteristic diagram for any particular use of a triode. This has been explained in the last chapter, and here it will suffice to give a table showing these optimum conditions that the writer conceives to be appropriate.

Use of Triode	$\frac{E_a + kE_g}{\bar{r}I_s}$	$\frac{I_a}{I_s}$	$\frac{\mathcal{R}}{\bar{r}}$
Low power amplifier.	0.3~0.5	0.2~0.4	1.0
Distortionless power amplifier and modulator.	0.3~0.5	0.2~0.4	2.0
Oscillator or power amplifier for radio-telegraphy.	-1.0	0.55	1.0
Self-oscillator for radio-telephony.	0.3	0.35	1.2
Power amplifier for radio-telephony, amplifying modulated waves.	0	0.25	1.0
Ditto, amplifying C. W. and being subjected to modulation.	0	0.25	1.4

If the above three quantities are decided, the followings may be directly obtained from the diagram:—

$$\frac{P}{\bar{r}I_s^2}, \quad \frac{kE_g}{\bar{r}I_s}, \quad \frac{E_a}{\bar{r}I_s}, \quad \frac{I_a}{I_s}.$$

$\frac{E_a}{\bar{r}I_s}$ can roughly be estimated according to the use of the tube, and from this the approximate values of $\frac{E_a I_a}{\bar{r}I_s^2}$ and η can be found.

(2) Saturating Voltage and Saturation Current.

For a given power output P , $a = \frac{P}{\bar{r}I_s^2}$ having been known, $\bar{r}I_s^2$ can be obtained and next comes an important problem of splitting $\bar{r}I_s^2$ into the saturating voltage $\bar{r}I_s$ and the saturation current I_s , i.e. $\bar{r}I_s^2 = \bar{r}I_s \times I_s$.

If one of any other operating conditions, such as anode voltage E_a or anode circuit impedance \mathcal{R} , is given at the same time, the solution is simple, as $\frac{E_a}{\bar{r}I_s}$ or $\frac{\mathcal{R}}{\bar{r}}$ has already been determined.

If this is not the case, most precise considerations must be taken for this from technical and economical points of view, especially in the design of standard types of tubes. The general considerations of the two alternatives, high $\bar{r}I_s$ tube or low $\bar{r}I_s$ tube for a given power output are as follows:

	High $\bar{r}I_s$ tube	Low $\bar{r}I_s$ tube	Remarks
Anode voltage	high	low	Anode voltage must be within a practicable limit from standpoint for insulations of the tube and other apparatuses.
Saturation current	low	high	
Cathode power consumption	little	large	Lower filament power is preferable as overall operating efficiency becomes higher and anode radiating area can also be reduced.
Internal and external impedances	high	low	
Amplification constant	high	low	

Anode power conversion efficiency is not very different as it is principally determined from the working points, but in a higher voltage tube anode voltage is more completely utilized and net efficiency will be a little higher than lower voltage tube.

This problem involves not only the economy of the tube itself but also that of apparatus with which the tube is to be used, such as output circuits, anode source of power, amplifiers preceding the tube under consideration, etc. The practicable

limits in the values of E_a , \mathcal{R} , and cathode heating power should also be taken into consideration.

Regarding the oscillatory power output of a triode, following consideration is sometimes necessary. Output P somewhat larger than the required amount has to be taken as the designing basis in order to take effect of the grid current into account which were not done in the derivation of the dynamic characteristic diagram. The grid current affects the power output in two ways; first it reduces the anode current and hence the output, and secondly it absorbs some portion of the output in case of self-oscillators. An increase of P , 10 or 20% above the required value, will generally be sufficient, according as the tube is used as a power amplifier or a self-oscillator.

(3) Amplification Constant.

From equation (17),

$$(1+k)^3 = G^2 \bar{r} I_s$$

and $P = a \bar{r} I_s^2$

hence $(1+k)^3 = \left(\frac{Ga}{P} \right)^2 (\bar{r} I_s)^3 \dots \dots \dots (21)$

G is not so much different with the type of tubes and is of the order of 10^{-4} as shown in the following table.

Tubes		No. of tubes examined	G	
Anode voltage	Electrode		Range	Average
6000-10,000	cylinder	14	.08-.4 x 10 ⁻³	0.15 x 10 ⁻³
200-5,000	cylinder	8	.08-.4 x 10 ⁻³	0.17 x 10 ⁻³
"	plane	15	.15-.9 x 10 ⁻³	0.38 x 10 ⁻³
below 100	cylinder	10	.12-.5 x 10 ⁻³	0.18 x 10 ⁻³
"	plane	5	.28-.5 x 10 ⁻³	0.33 x 10 ⁻³

Total average; G for plane electrodes, 0.35×10^{-3}
 G for cylindrical electrodes, 0.16×10^{-3}

G , a , and P having been known, k is in definite relation to $\bar{r} I_s$ as given by equation (21), and so once $\bar{r} I_s$ is determined, k can be directly derived.

In case of oscillators, self or separately-excited, power lost in the excitation depends on the value of k . In a self-excited oscillator, this power is converted from the output of the tube and too much exciting power results in the lowering of net output and overheating of the grid. In a separately-excited oscillator or power amplifier, the grid loss is to be supplied from the preceding tube. In these cases the value of k will be estimated as follows; for the most favorable operation at a given anode voltage, the minimum anode voltage $E_a - \mathcal{E}_a$ must be nearly equal to the maximum grid voltage $\mathcal{E}_g + E_g$ (E_g is usually negative), and this requires that

$$E_a - \mathcal{E}_a = E_g + \mathcal{E}_g$$

or $\frac{E_a}{\bar{r} I_s} - \frac{\mathcal{E}_a}{\bar{r} I_s} = \left(\frac{k E_g}{\bar{r} I_s} + \frac{k \mathcal{E}_g}{\bar{r} I_s} \right) \frac{1}{k}$

hence $k = \frac{\frac{k \mathcal{E}_g}{\bar{r} I_s} + \frac{E_a + k E_g}{\bar{r} I_s} - \frac{E_a}{\bar{r} I_s}}{\frac{E_a}{\bar{r} I_s} - \frac{\mathcal{E}_a}{\bar{r} I_s}} \dots \dots (22)$

in which all quantities except $\frac{E_a}{\bar{r} I_s}$ are already known. Thus if k is given,

$\frac{E_a}{\bar{r} I_s}$ can be accurately determined and $\frac{E_a I_a}{\bar{r} I_s^2}$ and η are accordingly known.

For a rough estimation of the grid excitation loss in the above working condition, the grid current may be assumed to have a triangular wave-form as shown in Fig. 68, and its peak value to reach $\frac{1}{2} I_s$ in a severe case of excitation. The results of calculations are as follow.

Grid current d. c. component

$$I_g = \mu I_s$$

Material	Allowable loss, watt/cm ²
Nickel	$w=3$
Molybdenum	5
Tungsten	8
Water-cooled copper anode	20

The filament heating power W_f must also be considered, as some portion of it will dissipate through the anode. Suppose q part of the filament power is radiated through the anode, then

$$A \geq \frac{W_a + qW_f}{w}$$

q depends on the degree at which the filament is hidden in the anode, and in ordinary cases in which anode is open on both ends, q may be taken as about 0.5. The writer deems it reasonable to take the effective area A explained in Chapter I, instead of the actual area, in the above expression.

Examples in the existing tubes ($q=0.5$ being assumed and W_a being the test anode loss):

Nickel anode tubes					Molybdenum anode tubes				
Type	W_a	W_f	A	w	Type	W_a	W_f	A	w
211-A	65	30	34	2.4	MS-III	50	32	16	4.1
MT-1	150	54	43	4.1	MT-7A	1000	310	119	9.7
MT-2	600	250	200	3.6	MT-9	1500	370	117	14.4
MT-4	200	79	93	2.6	UV-204	250	170	38	8.8
UV-203A	100	31	25	4.6	UV-206	300	160	99	3.9

For anode voltages less than 4,000 V, plane anode is preferable, while for higher voltages cylindrical one is more convenient.

In high voltage tubes grid voltage also becomes high with respect to the cathode, and appreciable distance must be kept between grid and cathode in order to avoid severe electrostatic attraction. On the other hand, in low voltage tubes x_g can be reduced, and if the cathode is made of W-shaped filament arranged in a plane, A may be greatly increased without difficulty in construction.

The order of x_a in the existing tubes are as follows;

Receiving tubes } E_a below 100 V. }	$x_a=0.2-0.5$ cm.
$E_a=100-1,000$ V.	0.3-1.0 cm.
$E_a=1,000-10,000$ V.	0.6-3.5 cm.

The actual anode surface area should be made as effective as possible in order to reduce the mass of the anode and hence to minimize the adsorbed gas evolving in the evacuation process, as well as from economical point of view. The plate should be as thin as mechanically allowable, but not so thin as to avoid free conduction of heat, otherwise local over-heating or melting may occur at accidental overload of the anode.

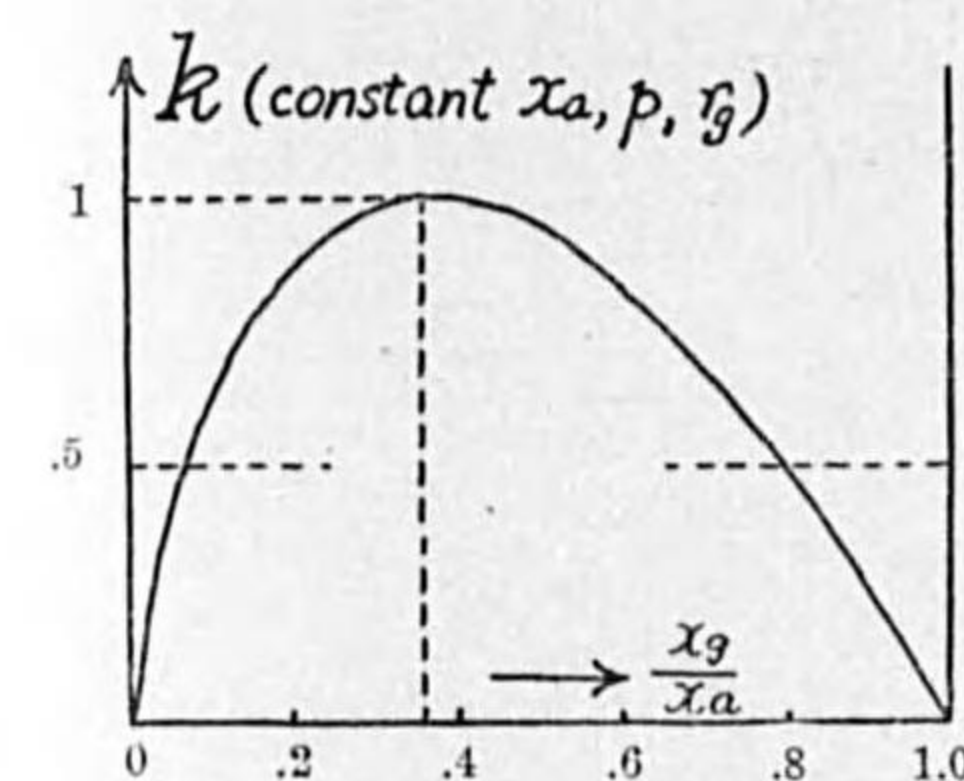


FIG. 70.

The anode area A , anode-to-cathode distance x_a or z_a , and the span l_f of the filament must be in conformity with one another to give the predetermined value of G by the expression,

$$G = 2.33 \times 10^{-6} \frac{A}{z_a z_g}$$

The grid construction is determined from amplification constant. When x_a is given and other dimensions p and d_g remain unvaried, k is maximum at $x_g = 0.4x_a$ (Fig. 70). It is therefore advisable to take as $x_g = 0.4x_a$ in order to reduce the mass of the grid as well as to minimize the effect of non-uniformity of x_g on the value of k .

Thus

$$\frac{k}{\log \frac{x_a}{x_g}} = \frac{k}{0.4} = \frac{cL_g}{\log \coth \pi a}$$

TABLES II, III, and IV on pages 160-161 are to be referred to for the calculation and the following table shows the ranges of actual values of L_g and πa in existing tubes. It is interesting to note that L_g and k are of equal magnitude in average.

k	Range of L_g	Range of πa
3	2-7	0.25-0.50
5	3-12	
8	4-17	
10	5-20	0.30-0.60
15	7-28	
20	8-35	
25	10-40	
30	11-45	
40	14-60	
50	16-70	0.35-0.74
60	19-80	
80	23-100	
100	28-120	0.40-0.90
150	40-200	
300	60-300	0.55-1.20

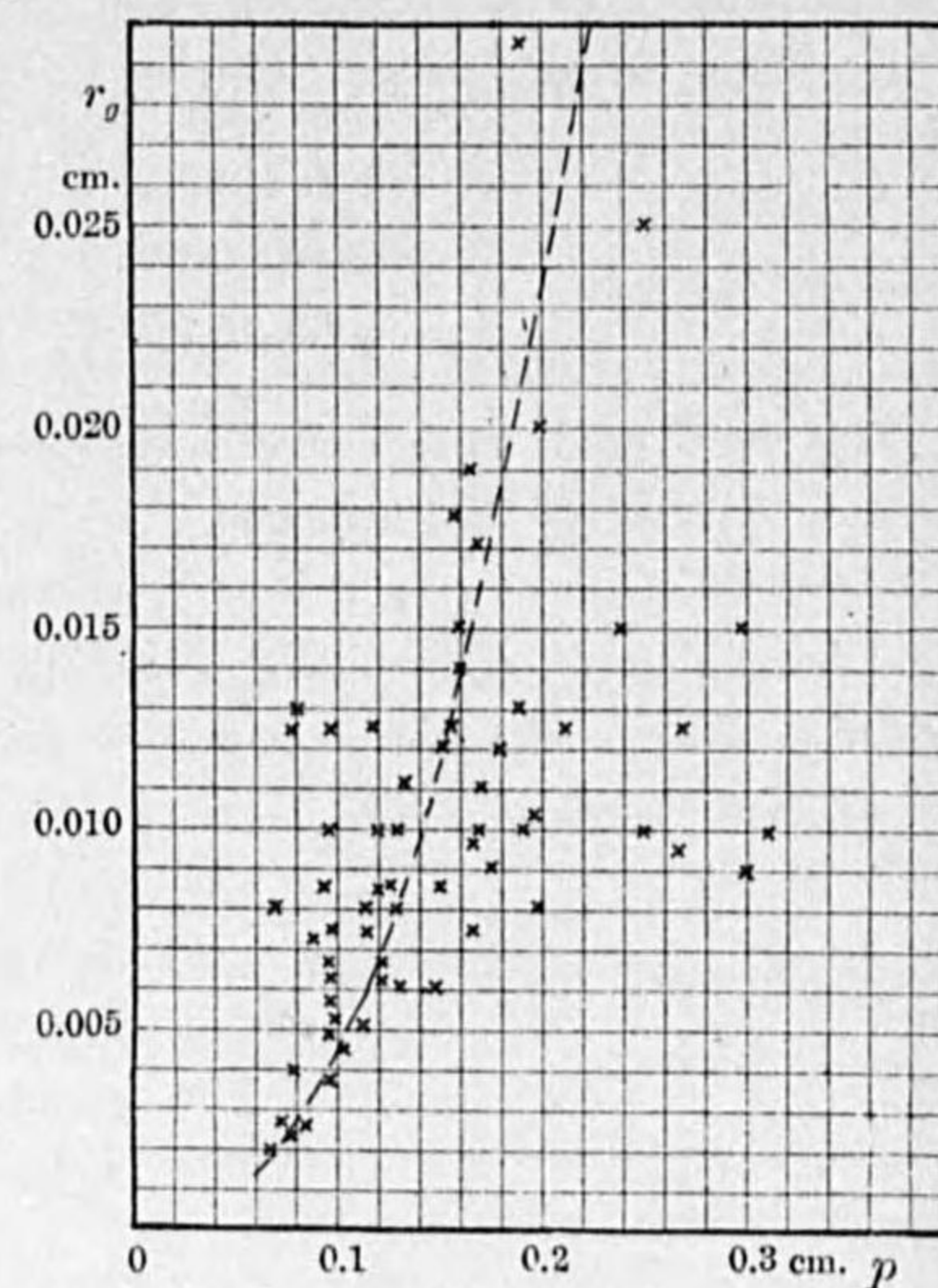


FIG. 71.

L_g and πa having been determined, the next problem is to determine p and d_g . This means whether to use thick wires at broad pitch or to use thin wires closely arranged.

It is preferable to take πa small in order to reduce the mass of the grid and to facilitate evacuation. This is effected by thin grid wires at comparatively narrow pitch, but in extreme cases mechanical rigidity of grid will be lost and deformation or break down will occur during operation by the heating of grid due to either the radiated heat from other electrodes or the grid loss.

Materials best suited for grid are molybdenum and nickel, but the latter has a remarkable effect of secondary emission and often causes the "blocking" of power oscillators.

The pitch p of grid wires exerts a most remarkable effect on k . Fig. 71 shows actual values of p and r_g in existing tubes, from which general tendency can be observed.

(5) Design of the Cathode.

Design of a tungsten cathode to give the required emission I_s can be accomplished by means of the CHART II annexed to this paper. It is preferable to design the filament to give a slightly higher value of emission than desired in order to give allowance for the discrepancies which might take place.

For a strict estimation of the filament life L , which is the life of the tube in ideal case, an economical condition must be dealt with in such a way that the total running cost of a tube is a minimum for a given power output. This condition is given by the following relations;

Total cost per watt output per hour

$$T = \frac{C_t}{PL} + \left(\frac{1}{\eta} + \frac{W_f}{P} \right) C_p$$

in which C_t = cost of the tube.

C_p = cost of power per watt hour.

On the other hand, for the filament of a certain diameter the life L depends on its temperature, which in turn is determined at what filament efficiency $\frac{I_s}{W_f}$ it is operated, thus

$$L = \phi \left(\frac{W_f}{I_s} \right)^\sigma$$

Minimum of the operating cost T occurs at a life

$$L_{opt} = \phi^{\frac{1}{1+\sigma}} \left(\frac{\sigma C_t}{C_p I_s} \right)^{\frac{\sigma}{1+\sigma}}$$

For tungsten filaments, the two constants σ and ϕ are of the following orders.

$$\sigma \doteq 2.6$$

d_f	ϕ
for $i_f=3$ A	0.0010
8	0.0048
20	0.037

It is general practice to take 2,000 to 5,000 hours, as the order of reasonable life, except for special cases in which the life must be sacrificed for other conditions.

Determination of filament dimensions by means of the chart is explained in the following

table. This chart has been worked out by Kato⁽¹⁰⁾ from the data given by Forsythe and Worthing⁽¹¹⁾ and the life is assumed to be the time in which 10% of the initial diameter of the filament is lost by evaporation.

l = total length of the filament,

l' = effective length of the filament, that is, the length which will give the emission I_s , if it be at a uniform temperature equal to that on its middle portion.

$l = l' + m\Delta l$. Δl = length of a cooled end.

m = no. of leads and anchored points.

e_f = terminal voltage of the filament,

e_f' = potential drop on the effective length l' ,

$e_f = e_f' + m\Delta e_f$ Δe_f = voltage at a cooled end.

$\frac{e_f}{l} = \frac{e_f'}{l'}$ approximately.

r_f = radius of the filament,

L = life of the filament.

I_s = total emission.

Given quantities	Procedure to obtain other quantities
l, r_f, i_f	Chart IIa, from r_f and i_f $L, \left(\frac{e_f'}{l'}\right), \left(\frac{I_s}{l'}\right)$ Chart IIc, from r_f and i_f $\Delta l, \Delta e_f$ $l' = l - m\Delta l$ $I_s = \left(\frac{I_s}{l'}\right)l'$ $e_f = \left(\frac{e_f'}{l'}\right)l' + m\Delta e_f$

(10) N. Kato: "Graphs for the Design of Bright-Emitting Tungsten Filament," Circulars of the Electrotechnical Laboratory, No. 50, April, 1928

(11) W. E. Forsythe and A. G. Worthing: Astrophysical J., 61. p. 146, 1925.

Given quantities	Procedure to obtain other quantities
l, e_f, I_s	Assume $\Delta e_f = 1$, $\left(\frac{I_s}{e_f'}\right) = \frac{I_s}{e_f - m\Delta e_f}$, $\left(\frac{l'}{e_f'}\right) = \left(\frac{l}{e_f}\right)$ Chart IIb, from $\left(\frac{l'}{e_f'}\right)$ and $\left(\frac{I_s}{e_f'}\right)$, i_f, r_f, l Chart IIc, Δe_f assured.
l, r_f, e_f	$\left(\frac{e_f'}{l'}\right) = \frac{e_f}{l}$, Chart IIa, from r_f and $\left(\frac{e_f'}{l'}\right)$, $I_s, i_f, \left(\frac{I_s}{l'}\right)$ Chart IIc, from i_f and r_f $\Delta l, \Delta e_f$ $l' = l - m\Delta l$, $I_s = \left(\frac{I_s}{l'}\right)l'$
r_f, i_f, I_s	Chart IIa, from i_f and r_f $L, \left(\frac{e_f'}{l'}\right), \left(\frac{I_s}{l'}\right)$ Chart IIc, from i_f and r_f $\Delta l, \Delta e_f$ $l' = \frac{I_s}{\left(\frac{I_s}{l'}\right)}$, $l = l' + m\Delta l$, $e_f = \left(\frac{e_f'}{l'}\right)l' + m\Delta e_f$
r_f, e_f, I_s	Assume $\Delta e_f = 1$, $\left(\frac{I_s}{e_f'}\right) = \frac{I_s}{e_f - m\Delta e_f}$. Chart IIb, from r_f and $\left(\frac{I_s}{e_f'}\right)$, $i_f, \left(\frac{l'}{e_f'}\right), L$ Chart IIc, $\Delta l, \Delta e_f$ assured $l' = \left(\frac{l'}{e_f'}\right)(e_f - m\Delta e_f)$, $l = l' + m\Delta l$
r_f, e_f, L	Chart IIb, from r_f and L $i_f, \left(\frac{l'}{e_f'}\right), \left(\frac{I_s}{e_f'}\right)$ Chart IIc, from r_f and i_f , $\Delta l, \Delta e_f$ $e_f' = e_f - m\Delta e_f$, $I_s = \left(\frac{I_s}{e_f'}\right)e_f'$, $l' = \left(\frac{l'}{e_f'}\right)e_f'$
e_f, i_f, I_s	Assume $\Delta e_f = 1$, $\left(\frac{I_s}{e_f'}\right) = \frac{I_s}{e_f - m\Delta e_f}$ Chart IIb, from i_f and $\left(\frac{I_s}{e_f'}\right)$, $r_f, L, \left(\frac{l'}{e_f'}\right)$ Chart IIc, from i_f and r_f $\Delta l, \Delta e_f$ assured $l = \left(\frac{l'}{e_f'}\right)(e_f - m\Delta e_f) + m\Delta l$

Given quantities	Procedure to obtain other quantities
e_f, i_f, L	Chart IIb, from i_f and L $r_f, \left(\frac{I_s}{e_f'}\right), \left(\frac{l'}{e_f'}\right)$ Chart IIc, from i_f and r_f $\Delta e_f, \Delta l$ $e_f' = e_f - m\Delta e_f, I_s = \left(\frac{I_s}{e_f'}\right)e_f', l = \left(\frac{l'}{e_f'}\right)e_f' + m\Delta l$
i_f, I_s, L	Chart IIa, from i_f and L $r_f, \left(\frac{I_s}{l'}\right), \left(\frac{e_f'}{l'}\right)$ Chart IIc, from i_f and r_f $\Delta e_f, \Delta l$ $l' = \frac{I_s}{\left(\frac{I_s}{l'}\right)}, l = l' + m\Delta l, e_f' = \left(\frac{e_f'}{l'}\right)l', e_f = e_f' + m\Delta e_f$
e_f, I_s, L	Assume $\Delta e_f = 1, \left(\frac{I_s}{e_f'}\right) = \frac{I_s}{e_f - m\Delta e_f}$ Chart IIb, from L and $\left(\frac{I_s}{e_f'}\right)$ r_f, i_f, l' Chart IIc, from i_f and r_f $\Delta l, \Delta e_f$ assured $l = l' + m\Delta l$

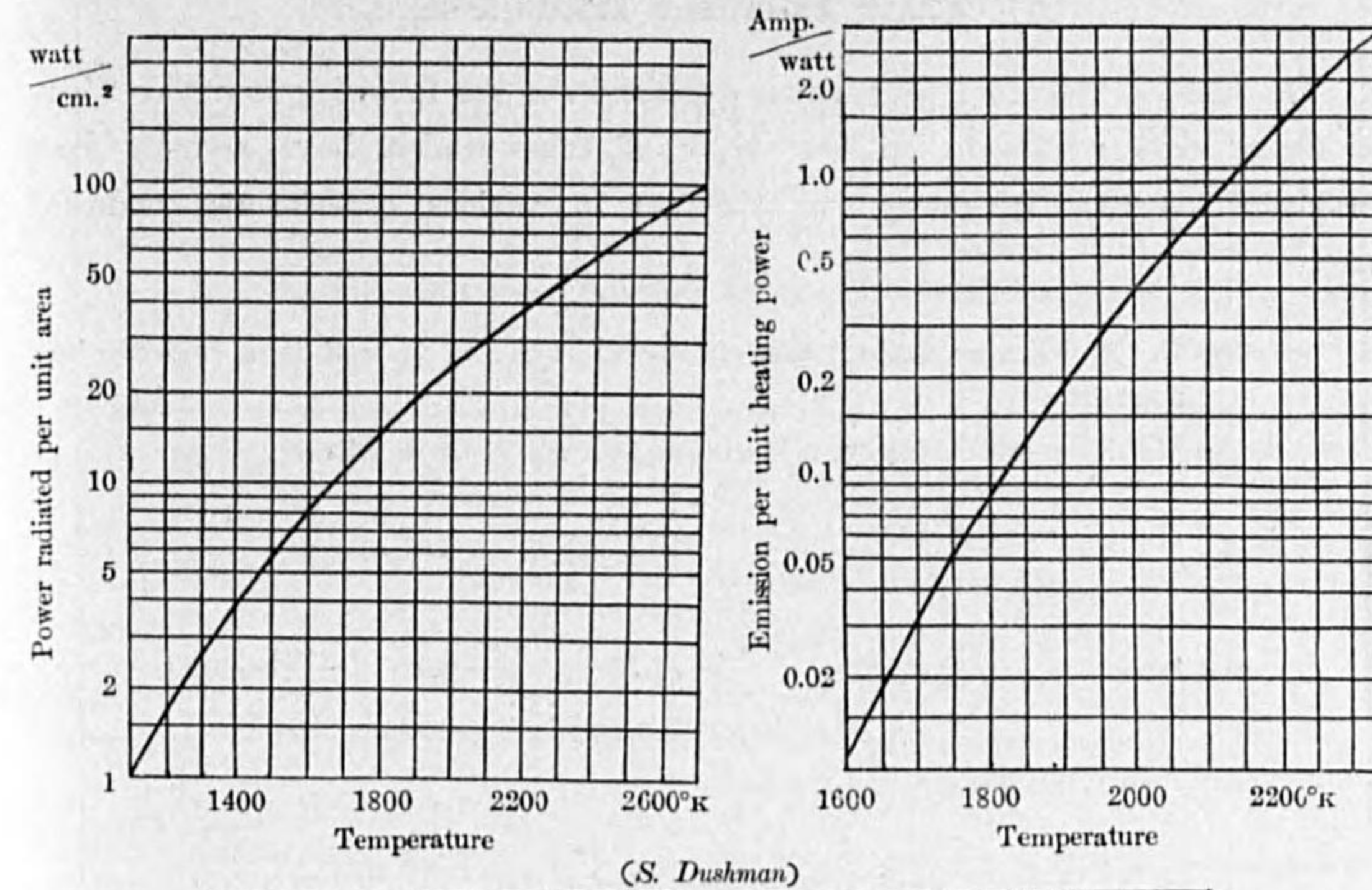
The filament efficiency which is usually expressed by milliamperes per watt, can be increased with increase of the filament diameter, because the working temperature of a thicker filament can be made higher than that of a thinner one without shortening its life. But in an extreme case of the former the filament becomes too short to obtain the required anode effective area. On the other hand, a thin filament suffers from the unevenly heated effect of superposed anode current and the life will be shorter, especially when a direct current is used for the heating. In this respect the filament current should be larger than 30 times the working anode current I_a .

The design of thoriated tungsten filaments can not be considered accurately, as the emission is very much affected by the degree of activation and the residual gas, but the curves shown in Fig. 72, which were taken from the data published by Dushman⁽¹²⁾ and Sano⁽¹³⁾, will be of use in obtaining general conception on this type of filament.

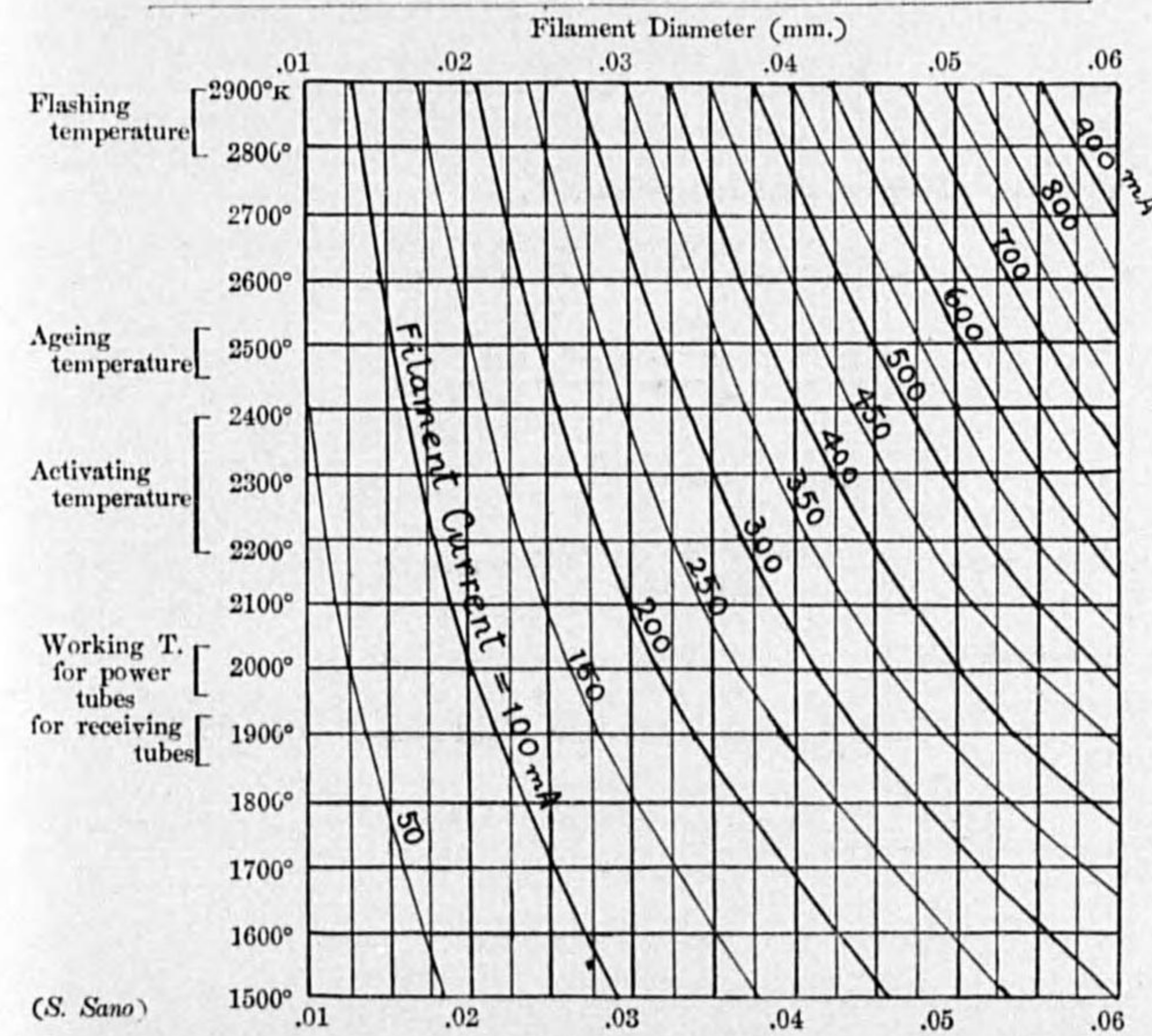
(12) S. Dushman: Phys. Rev., June 1927, p. 857.

(13) S. Sano: "Properties of a Thoriated Tungsten Filament etc.," Circular of the Electrotechnical Laboratory No. 43, Feb., 1927.

Fig. 72. Operation of Thoriated Tungsten Filament.



(S. Dushman)



(S. Sano)

(6) Examples on the Triode Design.

The design procedure is further explained in the following examples where the design data are given on four types of tubes which have actually been constructed at the Laboratory for the use in various experiments conducted there.

Example 71. To design an oscillator tube of 250 watt output to be used in a radio-telephone transmitter.

The working points on the dynamic characteristics are chosen as follows;

$$\frac{E_a + kE_g}{\bar{r}I_s} = 0.30 \quad \frac{\mathcal{E}_a}{I_s} = 0.35 \quad \frac{\mathcal{R}}{\bar{r}} = 1.20$$

and hence
$$\frac{P}{\bar{r}I_s^2} = 0.075 \quad \frac{\mathcal{E}_a}{\bar{r}I_s} = 0.43 \quad \frac{I_a}{I_s} = 0.32 \quad \frac{k\mathcal{E}_g}{\bar{r}I_s} = 0.80$$

As $P = 250$,
$$\bar{r}I_s^2 = \frac{250}{0.075} = 3,340$$

Assume $\frac{E_a}{\bar{r}I_s} = 0.45$ which is taken slightly higher than $\frac{\mathcal{E}_a}{\bar{r}I_s}$,

then
$$\frac{E_a I_a}{\bar{r}I_s^2} = 0.144 \quad \eta = \frac{P}{E_a I_a} = \frac{0.075}{0.144} = 0.52$$

The grid loss being considered by equation (23),

$$\frac{kE_g}{\bar{r}I_s} = \frac{E_a + kE_g}{\bar{r}I_s} - \frac{E_a}{\bar{r}I_s} = -0.15$$

$$\frac{-E_g}{\mu\mathcal{E}_g} = \frac{-kE_g}{\bar{r}I_s} \cdot \frac{\bar{r}I_s}{k\mathcal{E}_g} = \frac{0.15}{0.80} = 0.188$$

$$\mu = 0.109 \quad \nu = 0.095$$

hence
$$k \geq \frac{0.095 \times 0.80 + 0.109 \times 0.15}{0.144 - 0.075} \times 10 = 13.4$$

In equation (21),

$$\alpha = \frac{P}{\bar{r}I_s^2} = 0.075 \quad P = 250 \quad \text{and assume} \quad G = 0.35 \times 10^{-9}$$

then
$$\frac{G\alpha}{P} = 1.05 \times 10^{-7}$$

and
$$(1+k)^3 = \left(\frac{G\alpha}{P}\right)^2 (\bar{r}I_s)^5$$

$$= 1.10 \times 10^{-14} (\bar{r}I_s)^5$$

or
$$\bar{r}I_s = \sqrt[5]{\frac{(1+k)^3}{1.10} \times 10^{14}}$$

Let three values of k larger than 13.4 be assumed and further calculations are made as follows;

k	$\bar{r}I_s$	$I_s = \frac{\bar{r}I_s^2}{\bar{r}I_s}$	$\frac{E_a}{\bar{r}I_s}$ by Eqn. (22)	E_a	I_a	$E_a I_a$	η	\bar{r}	\mathcal{R}	approximate filament power
15	3,260	1.02	0.471	1,540	0.33	510	0.49	3,200	3,800	* 200
20	3,840	0.87	0.462	1,770	0.28	500	0.50	4,400	5,300	* 175
25	4,360	0.77	0.457	1,990	0.25	500	0.50	5,700	6,800	* 150

* based on 5 mA/watt.

The anode voltage up to 2,000 V can be obtained from a d. c. generator with convenience. Overall efficiency including the filament loss is improved with increase of k , and the filament power becomes less appreciable compared with the anode loss.

So that $k=25$ is to be taken,

then $E_a = 2,000 \quad \mathcal{R} = 6,800 \quad \bar{r} = 5,700 \quad I_s = 0.77$

Molybdenum plate is to be used with the effective area:

$$A = \frac{250 + 150 \times 0.5}{5} = 65$$

Let $x_g = 0.4 \quad x_a$ then $\frac{A}{x_a x_g} = \frac{160}{x_a^2}$

$$G = 0.35 \times 10^{-9} \quad \text{as assumed before,}$$

$$\therefore 2.33 \times 10^{-9} \times \frac{160}{x_a^2} = 0.35 \times 10^{-9}$$

$$\therefore x_a = 1.00 \quad x_g = 0.40$$

Dimensions of the grid is determined from

$$\frac{k}{\log \frac{x_a}{x_g}} = \frac{cI_g}{\log \coth \pi a}$$

in which $k=25$, $\log \frac{x_a}{x_g}=0.40$ $e=1.7$ (W-shaped filament)

Grid is to be formed of a system of parallel wires.

Assume $I_g=25$ 20 15

then $\log \coth \pi a=0.680$ 0.545 0.408

from Table IV $\pi a=0.22$ 0.30 0.39

$\pi a = \frac{I_g r_g}{x_g}$ $\therefore r_g=0.0040$ 0.0060 0.010

Take $I_g=15$ and $r_g=0.010$, as thinner wires are liable to deformation,

then $p = \frac{2\pi r_g}{I_g} = 0.17$

Design of the filament;

tungsten is to be used, and assume the life to be

$$L=2,000.$$

Working anode current $I_a=0.25$ $\therefore i_f > 30 I_a=7.5$

Take $i_f=10$.

From Chart IIa,

$$r_f=0.017 \quad \frac{I_s}{\nu}=0.07 \quad \frac{e_f'}{\nu}=0.89$$

and from Chart IIc,

$$\Delta e_f=1.05 \quad \Delta l=1.2$$

Filament is designed with 20% increase of I_s , or

$$I_s=0.77 \times 1.2=0.90$$

then $\nu = \frac{I_s}{\left(\frac{I_s}{\nu}\right)} = 13$

If th's effective length of the filament is divided into sections arranged in four rows, anode effective area can be obtained as

$$A = (2x_d \nu + 4\pi x_a^2) \times 2 = 77$$

which shows that the required value of $A=65$ can be easily obtained.

$$\nu=13 \quad \Delta l=1.2 \quad m=5$$

(number of leads=2, and number of anchored points=3)

Total length $l=13+5 \times 1.2=19$

and $e_f' = \left(\frac{e_f'}{\nu}\right) \times \nu = 11.6$

$$e_f = e_f' + m \Delta e_f = 11.6 + 5.3 = 16.9$$

The dimensions of the tube will be such as shown in Fig. 73, and rating of the tube as follows;

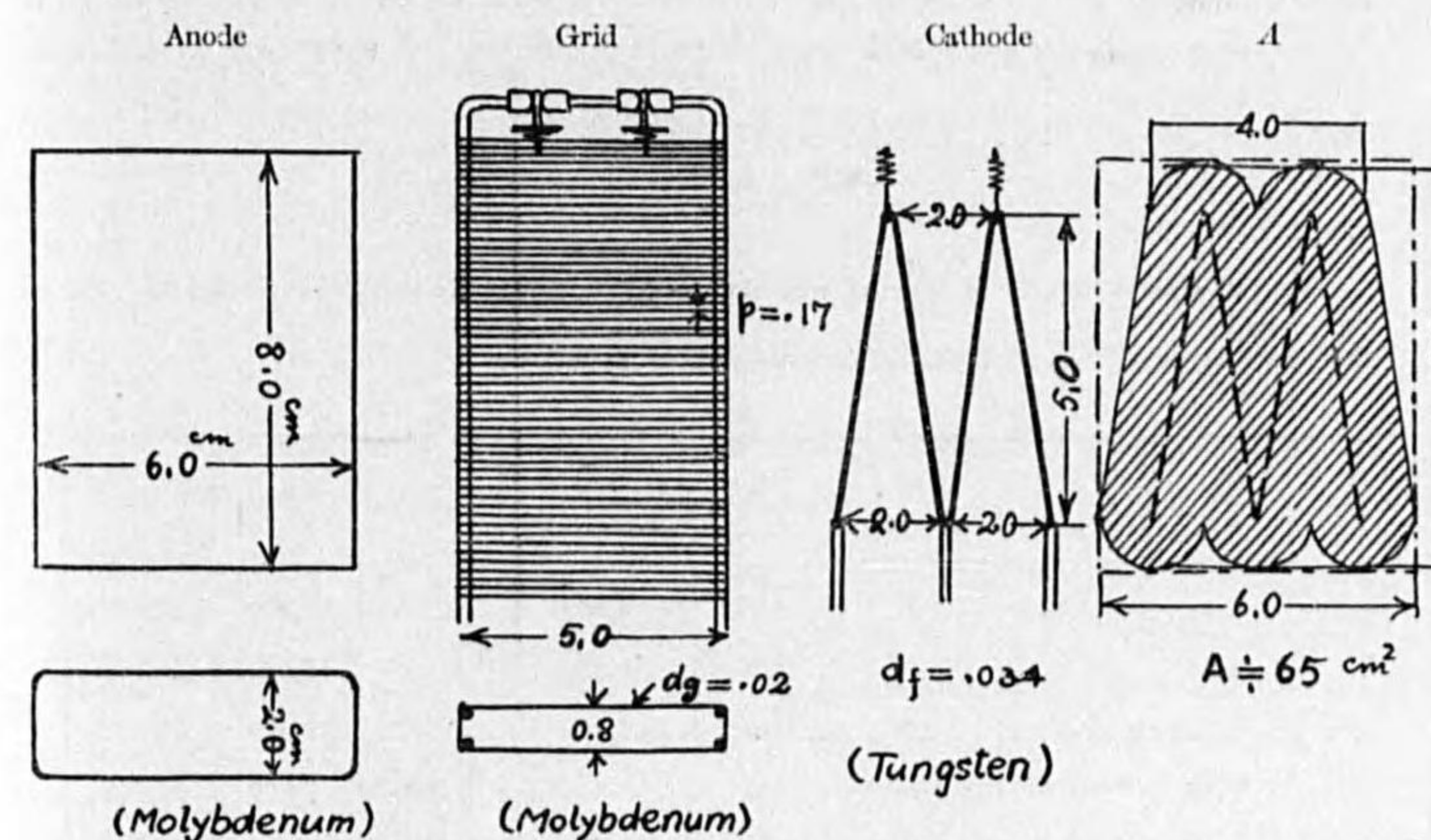


FIG. 73.

$$e_f=17 \text{ V} \quad i_f=10 \text{ A}$$

$$E_a=2,000 \text{ V} \quad P=250 \text{ W} \quad E_a I_a=500 \text{ W}$$

$$\eta=50\% \quad E_g=-27 \text{ V}$$

$$k=25 \quad \bar{r}=5,700 \quad \bar{R}=6,800$$

A well-known type of tube UV-204, which was originally put on the market by the Radio Corporation of America, has the rating of 250 watt output to be used in a radio telephone transmitter, and is similar in this respect to the tube under consideration. The dimensions of the tube are as shown in Fig. 5 on page 17 and ratings of the tube are as follows:

$$e_f = 11 \text{ V} \quad i_f = 14.75 \text{ A} \quad k = 20.$$

$$E_a = 2,000 \text{ V} \quad P = 250 \text{ W} \quad I_a = 0.25 \text{ A} \quad E_a I_a = 500 \text{ W}$$

Example 72. Design data of a triode type PAM, manufactured at the Laboratory.

Given Conditions: the tube is to be used in radio-frequency measurements as an oscillator.

Anode voltage: up to 1,000 V.

Power output: 30 W.

Filament current: about 3 A.

Design: Working points on the dynamic characteristic diagram are chosen as follows, so as to give the largest power with the least possible distortion of wave form in self-exciting condition:

$$\frac{E_a + kE_g}{\bar{r}I_s} = 0.50 \quad \frac{E_a}{I_s} = 0.58 \quad \frac{I_a}{I_s} = 0.50$$

Output circuit impedance $\frac{\bar{r}}{\bar{r}}$ is not determinable from the required conditions, and so their several values are tried for further calculations as follows:

$\frac{\bar{r}}{\bar{r}}$	$\frac{E_a}{\bar{r}I_s}$	$\frac{P}{\bar{r}I_s^2}$	$\bar{r}I_s^2$ ($P=30$)	$\frac{E_a}{\bar{r}I_s}$	$\bar{r}I_s$ ($E_a=1000$)	I_s	\bar{r}	\bar{r}
0.6	0.34	0.10	300	0.35	2,860	0.105	27,300	16,400
1.0	0.58	0.17	177	0.60	1,670	0.106	15,800	15,800
1.5	0.87	0.25	120	0.90	1,110	0.107	10,400	15,600
2.0	1.16	0.34	89	1.20	835	0.107	7,800	15,600

Higher $\frac{\bar{r}}{\bar{r}}$ gives lower $\bar{r}I_s^2$, and the tube may be of lower power capacity.

Take $\frac{\bar{r}}{\bar{r}} = 2.0$, then $\bar{r} = 7,800$ $I_s = 0.107$ $\bar{r}I_s = 835$ $\bar{r}I_s^2 = 89$

Assume $G = 0.35 \times 10^{-3}$

then from equation (17),

$$(1+k)^2 = G^2 \bar{r}^2 I_s = 6,440$$

$$k = 17.6$$

Working conditions predicted from these data:

$$\text{power input} = \frac{E_a}{\bar{r}I_s} \times \frac{I_a}{I_s} \bar{r}I_s^2 = 53.5 \text{ W}$$

$$\begin{aligned} \text{power output} &= 30 \text{ W} \\ \text{loss} &= 23.5 \text{ W} \\ \text{efficiency} &= 56\% \end{aligned}$$

Filament is designed, taking slightly higher emission than required,

thus $I_s = 0.15 \text{ A}$

let $i_f = 3 \text{ A}$ as given and $L = 2,000$ hours

then from Chart IIa,

$$r_f = 0.0077 \text{ cm} \quad \frac{I_s}{\nu} = 0.015 \quad \text{and} \quad \frac{e_f'}{\nu} = 1.18$$

and from Chart IIc, $\Delta l = 0.8$ $\Delta e_f = 1.05$

Filament is spanned in W-shape, $m = 5$ (no. of leads = 2, no. of anchored points = 3)

$$\text{then} \quad l' = \frac{I_s}{\left(\frac{I_s}{\nu}\right)} = 10 \quad l = l' + m\Delta l = 14 \text{ cm}$$

$$e_f' = \left(\frac{e_f'}{\nu}\right)\nu = 11.8 \quad e_f = e_f' + m\Delta e_f = 17 \text{ V} \quad W_f = e_f i_f = 51 \text{ W}$$

The nearest radius of filament obtainable is $r_f = 0.0085$ and this is to be actually used.

Molybdenum plate being used, its anode area:

$$A > \frac{W_a + 0.5 W_f}{5} = 7 \text{ cm}^2$$

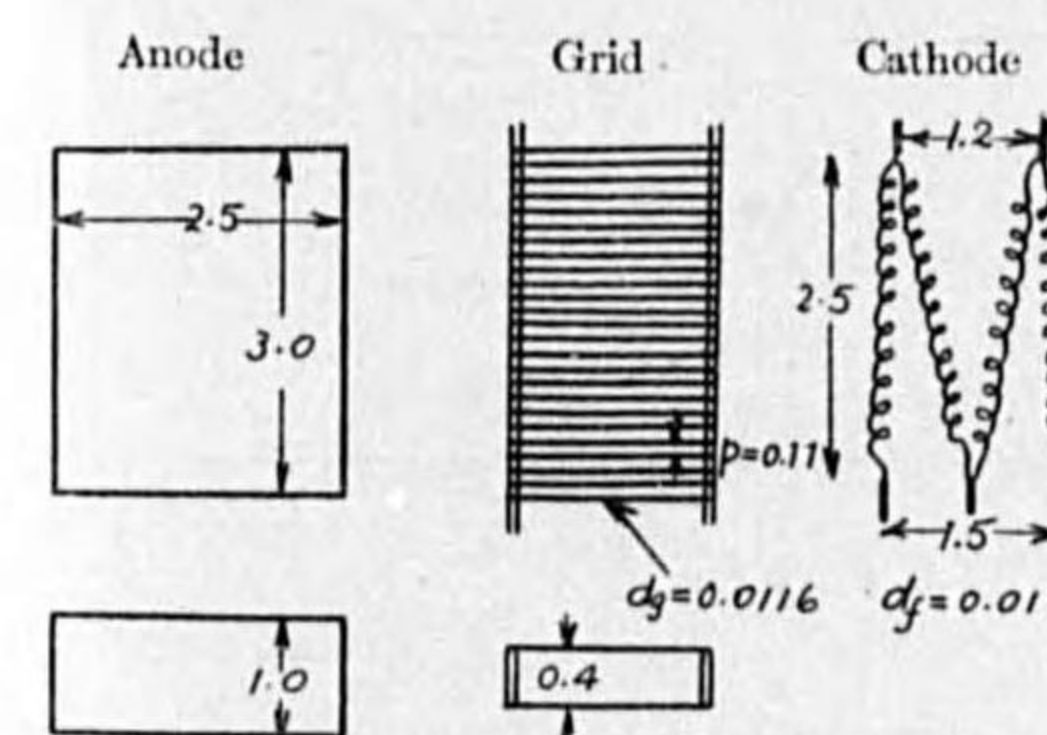


FIG. 74 (PAM)

If the filament length of 14 cm is spanned straight in W-shape, the anode area becomes unnecessarily large, so that filament is curled into spiral and spanned in W-shaped as shown in Fig. 74.

Anode area taken in accordance with this arrangement of filament becomes,

$$A = 2 \times 3.0 \times 2.5 = 15 \text{ cm}^2$$

This curling of filament results in slight reduction of emission and so the total length is increased to $l = 20$ cm.

Let $x_a = 0.5 \text{ cm}$ and $x_g = 0.2 \text{ cm}$ ($z_a = x_a$, $z_g = x_g$)

$$\text{then} \quad G = 2.33 \times 10^{-6} \frac{A}{x_a x_g} = 0.35 \times 10^{-3}$$

which is consistent with the previously assumed value.

$$k=17.6 \text{ and } \log \frac{x_a}{x_g}=0.4 \quad \frac{cI_g}{\log \coth \pi a}=44.$$

Grid being formed of parallel wires,

$$c=1.5 \quad I_g \frac{2\pi r_g}{p} = \frac{1.26}{p} \quad \pi a = \frac{\pi d_g}{p} \quad \frac{I_g}{\log \coth \pi a} = 29$$

Taking different values of p ,

p	I_g	$\log \coth \pi a$	πa	d_g	r_g
0.07	18.0	0.62	0.25	0.0056	0.0028
0.10	12.6	0.43	0.39	0.0124	0.0062
0.15	8.4	0.29	0.57	0.0271	0.0135

Tungsten filaments actually obtainable are of diameters:

$$0.007 \quad 0.012 \quad 0.016 \quad 0.020 \quad 0.025 \quad 0.030$$

Taking the nearest diameter, $d_g=0.012$ then $p=0.10$

Tubes of this type were actually constructed at the Laboratory with dimensions shown in Fig. 74, photograph of a completed tube being shown in Fig. 75 (facing page 158).

Test data:

Filament characteristics,

e_f	i_f	I_s
16.0 V	2.85 A	0.013 A
17.0	2.95	0.029
18.0	3.05	0.058
19.2	3.15	0.150

Normal operating condition, $e_f=19.5$ V. $i_f=3.2$ A.

Static characteristics are shown in Fig. 76.

Parameters; at $e_a=500$ and $e_g=0$,

$$k=11 \quad g=0.00160 \quad r=6,650$$

Its optimum condition as a self-oscillator, the circuit being adjusted to give maximum power with reasonable efficiency is:—

$$E_a=950 \text{ V.}$$

$$\text{Power input, anode d. c. } I_a=0.080 \text{ A.}$$

$$\text{power } E_a I_a=76 \text{ W.}$$

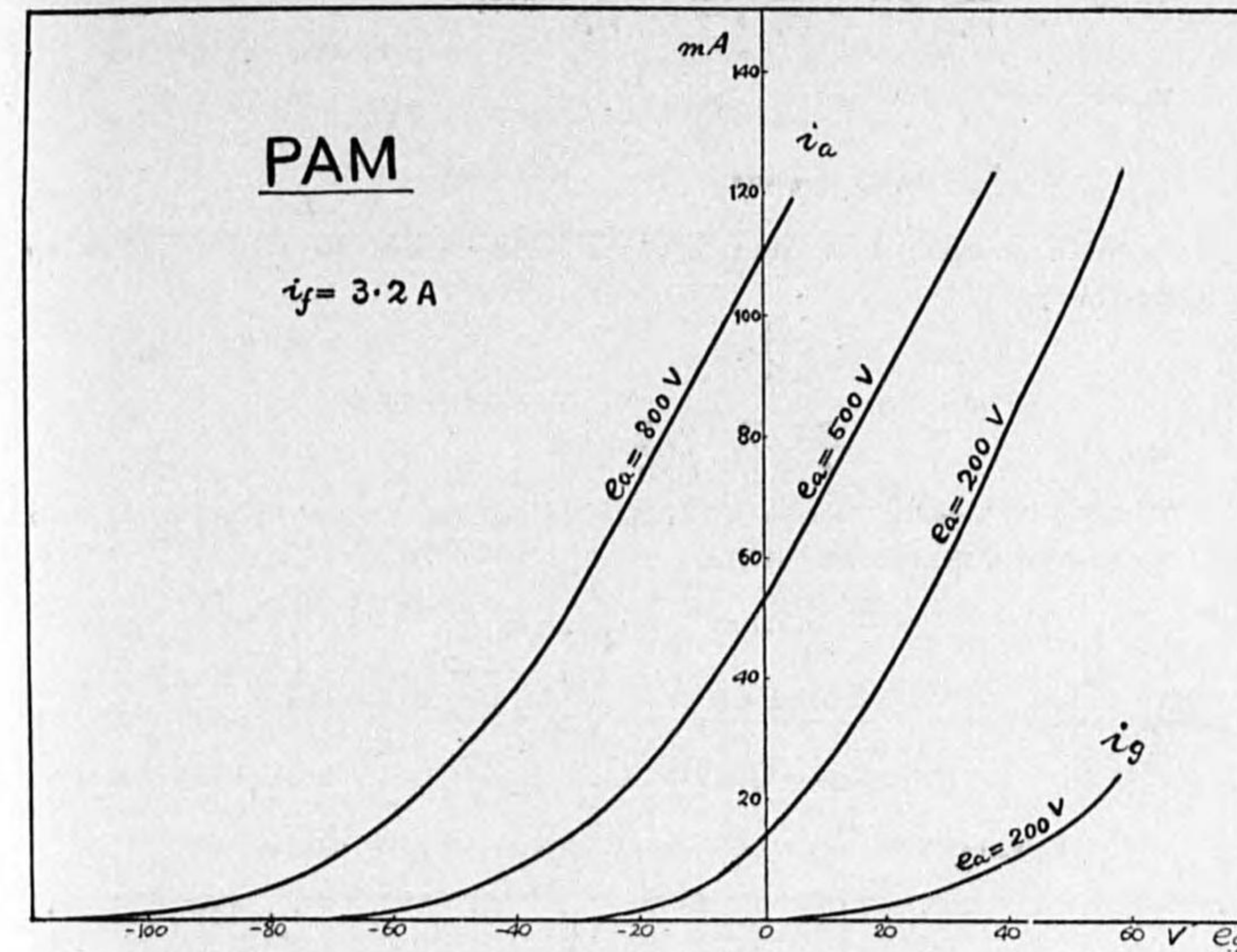


FIG. 76.

Power output, closed circuit current $I_o=2.65$ A eff.

closed circuit resistance $R=6.0\omega$

power $I_o^2 R=42$ W

Efficiency, $\eta=55\%$ Loss=34 W

Anode loss test: no defects were found at 80 W. loss for 5 min.

Example 73. Design data of a triode type PAK, manufactured at the Laboratory.

Given conditions: the tube is to be used as an oscillator in a radio-telephone transmitter of 100 watt output, and also to be used as a modulator in the same transmitter. Anode voltage is up to 3,000 V (this is the rated voltage of a direct current generator installed at the Laboratory)

Design: working points on the dynamic characteristic diagram when operating as an oscillator:

$$\frac{E_a+kE_g}{\bar{r}I_s}=0.30 \quad \frac{I_a}{I_s}=0.35 \quad \frac{\bar{r}}{\bar{r}}=1.2$$

$$\text{then } \frac{\epsilon_a}{\bar{r}I_s} = 0.42 \quad \frac{I_a}{I_s} = 0.31 \quad \frac{P}{\bar{r}I_s^2} = 0.074$$

$$\text{Taking } \frac{E_a}{\bar{r}I_s} = 0.50$$

$$\frac{E_a I_a}{\bar{r}I_s^2} = 0.155 \quad \eta = 0.48$$

Equivalent alternating-current resistance of the oscillator against the modulator will be approximately

$$\mathcal{R}_t = \frac{E_a}{I_a}$$

$$\text{or } \frac{\mathcal{R}_t}{\bar{r}} = \frac{E_a}{\bar{r}I_s} \bigg/ \frac{I_a}{I_s} = 1.61$$

If, single tube is used as the modulator in the constant-current system of modulation, the working condition of the modulator will be

$$\frac{E_a}{\bar{r}I_s} = 0.50 \quad \frac{\mathcal{R}_t}{\bar{r}} = 1.61$$

In order that the modulation may be accomplished without distortion,

$$\epsilon_a < E_a \quad \text{and so } \frac{\mathcal{J}_a}{I_s} < 0.30 \quad \text{and } \frac{E_a + kE_g}{\bar{r}I_s} > \frac{\mathcal{J}_a}{I_s} \quad \text{at maximum amplitude.}$$

Trying various values of the maximum allowable amplitude of anode current,

$\frac{\mathcal{J}_a}{I_s}$	$\frac{E_a + kE_g}{\bar{r}I_s}$	$\frac{kE_g}{\bar{r}I_s}$	$\frac{k\epsilon_g}{\bar{r}I_s}$	$\frac{\epsilon_a}{\bar{r}I_s}$	Degree of Modulation $\approx \frac{\epsilon_a}{E_a}$
0.30	0.32	-0.18	0.78	0.48	0.96
0.25	0.27	-0.23	0.65	0.40	0.80
0.20	0.22	-0.28	0.52	0.32	0.64
0.15	0.17	-0.33	0.39	0.24	0.48
0.10	0.12	-0.38	0.26	0.16	0.32

The grid voltage must not be positive at any instant, so that

$$-E_g > \epsilon_g \quad \text{or} \quad -\frac{kE_g}{\bar{r}I_s} > \frac{k\epsilon_g}{\bar{r}I_s}$$

thus the amplitude of anode current must be limited to about 0.15 in the table and the distortionless limit of modulation is 50%.

Anode loss in this working condition is

$$\frac{W_a}{\bar{r}I_s^2} = \frac{E_a}{\bar{r}I_s} \cdot \frac{E_a + kE_g}{\bar{r}I_s} = 0.50 \times 0.17 = 0.085 \quad \left(\frac{I_a}{I_s} = \frac{E_a + kE_g}{\bar{r}I_s} \right)$$

If two tubes are used as the modulator, they can be replaced by single a tube of the following parameters in considering the operation:

$$\text{saturation current } I_s' = 2I_s$$

$$\text{anode impedance } \bar{r}' = \frac{1}{2} \bar{r}$$

$$\text{amplification constant } k' = k$$

$$\text{Then } \bar{r}'P = \bar{r}I_s \quad \bar{r}'I_s'^2 = 2\bar{r}I_s^2$$

and the working conditions are

$$\text{anode voltage } \frac{E_a}{\bar{r}'I_s'} = \frac{E_a}{\bar{r}I_s} = 0.50$$

$$\text{anode circuit impedance } \frac{\mathcal{R}_t}{\bar{r}'} = \frac{2\mathcal{R}_t}{\bar{r}} = 3.22$$

In order that there is no distortion,

$$\epsilon_a < E_a \quad \text{and} \quad \frac{\mathcal{J}_a}{I_s'} < 0.15 \quad \frac{E_a + k'E_g}{\bar{r}'I_s'} > \frac{\mathcal{J}_a}{I_s'}$$

Taking various amplitudes of anode current,

$\frac{\mathcal{J}_a}{I_s'}$	$\frac{E_a + k'E_g}{\bar{r}'I_s'}$	$\frac{k'E_g}{\bar{r}'I_s'}$	$\frac{k'\epsilon_g}{\bar{r}'I_s'}$	$\frac{\epsilon_a}{\bar{r}'I_s'}$	Degree of Modulation
0.15	0.17	-0.33	0.63	0.48	0.96
0.12	0.14	-0.36	0.50	0.39	0.78
0.09	0.11	-0.39	0.33	0.29	0.58
0.06	0.08	-0.42	0.25	0.19	0.38

In order that $-E_g > \epsilon_g$, $\frac{\mathcal{J}_a}{I_s'}$ must be within about 0.10, which gives 64% as the maximum distortionless modulation obtainable.

$$\text{Total anode loss, } \frac{W_a'}{\bar{r}'I_s'^2} = 0.50 \times 0.12 = 0.06 \quad W_a' = 2W_a \quad \bar{r}'I_s'^2 = 2\bar{r}I_s^2$$

$$\text{Anode loss per tube } \frac{W_a}{\bar{r}I_s^2} = 0.06$$

Thus compared with the single tube operation, the two-tube system gives 30% higher degree of distortionless modulation with 30% lower anode loss per tube.

The design is further proceeded as follows;

$$\frac{E_a}{\bar{r}I_s} = 0.50 \quad \text{and} \quad E_a = 3,000 \quad \therefore \bar{r}I_s = 6,000$$

Considering effects of grid current, 20% higher value of power output is taken as the designing basis,

$$P=120 \quad \frac{P}{\bar{r}I_s^2}=0.074 \quad \therefore \bar{r}I_s^2=1,620$$

$$I_s = \frac{\bar{r}I_s^2}{\bar{r}I_s} = 0.27 \quad \bar{r} = 22,000$$

Design of the cathode:

assume $L=2,000$ and take 5 A tungsten filament which has a diameter of $d_f=0.0235$ or $r_f=0.0118$

From Chart II a, $\frac{e_f'}{V}=0.97 \quad \frac{I_s}{V}=0.025 \quad i_f=5.7$

and from Chart II c, $\Delta l=1.0 \quad \Delta e_f=1.05$

Filament is to be spanned in W-form, thus $m=5$

$$I_s=0.27 \quad l' = I_s \left(\frac{L}{V} \right) = 10.8 \quad l = l' + m\Delta l = 15.8$$

$$e_f' = \left(\frac{e_f'}{V} \right) V = 10.5 \quad e_f = e_f' + m\Delta e_f = 15.5$$

Summarizing the filament data,

$$l=16 \text{ cm} \quad d_f=0.0235 \text{ cm}$$

$$e_f=15.5 \text{ V} \quad i_f=5.7 \text{ A} \quad W_f=88 \text{ W}$$

Smallest value of x_g practically attainable being taken,

$$x_g=0.3 \quad \text{and} \quad x_a=0.7$$

Anode loss

$$W_a=0.081 \bar{r}I_s^2=130 \text{ W}$$

Anode area required,

$$A = \frac{130+44}{5} = 35 \text{ cm}^2$$

Taking a molybdenum plate of 3.5×4.5 cm. as the anode,

$$A = 2 \times 3.5 \times 4.5 = 32 \text{ cm}^2$$

$$\text{and} \quad G = 2.33 \times 10^{-8} \times \frac{32}{0.7 \times 0.3} = 0.35 \times 10^{-8}$$

From equation (17),

$$(1+k)^2 = G^2 \bar{r}^2 I_s = 0.35 \times 10^8 \quad k=69$$

Design of the grid:

$$\log \frac{x_a}{x_g} = 0.4 \quad c=1.7 \quad I_g = \frac{1.8}{p} \quad \log \coth \pi a = \frac{I_g}{102}$$

p	I_g	$\log \coth \pi a$	πa	d_g
0.08	23.5	0.23	0.63	0.018
0.10	18.8	0.18	0.79	0.025
0.11	17.1	0.17	0.84	0.030

Tungsten wire of the nearest diameter is $d_g=0.017$ and hence $p=0.08$

Working conditions of the tube are predicted as follows:

As an oscillator,

$$E_a=3,000 \text{ V} \quad P=100 \text{ W}$$

$$R=1.2 \bar{r}=26,500 \omega$$

$$I_a=0.31 I_s=0.084 \text{ A}$$

$$E_a I_a=250 \text{ W} \quad \eta=0.48$$

As a modulator, single tube operation,

$$E_a=3,000 \text{ V} \quad I_a=0.17 I_s=0.046 \text{ A}$$

$$E_a I_a=140 \text{ W} \quad E_g=-29 \text{ V} \quad \epsilon_g \leq 29 \text{ V} \quad \text{modulation} \leq 50 \%$$

Ditto, two tube operation,

$$E_a=3,000 \text{ V} \quad I_a \text{ per tube}=0.032 \text{ A}$$

$$E_a I_a \text{ per tube}=96 \text{ W} \quad E_g=-33 \text{ V}$$

$$\epsilon_g \leq 33 \text{ V} \quad \text{modulation} \leq 65 \%$$

One of the tubes constructed at the Laboratory is shown in Fig. 77 (photograph facing page 153), of which the dimensions are shown in Fig. 78.

Test data: Characteristics were obtained as shown in Fig. 79.

Working test was made at the anode voltage $E_a=2,450$ V, the tube being operated in its full power:

$$I_a=0.165 \text{ A} \quad \text{Input } E_a I_a=400 \text{ W}$$

$$\text{Oscillatory current } I_o=4.7 \text{ A} \quad \text{Resistance}=11 \omega$$

$$\text{Output}=250 \text{ W} \quad \text{Efficiency } \eta=0.62$$

$$\text{Wavelength}=1,400 \text{ m.}$$

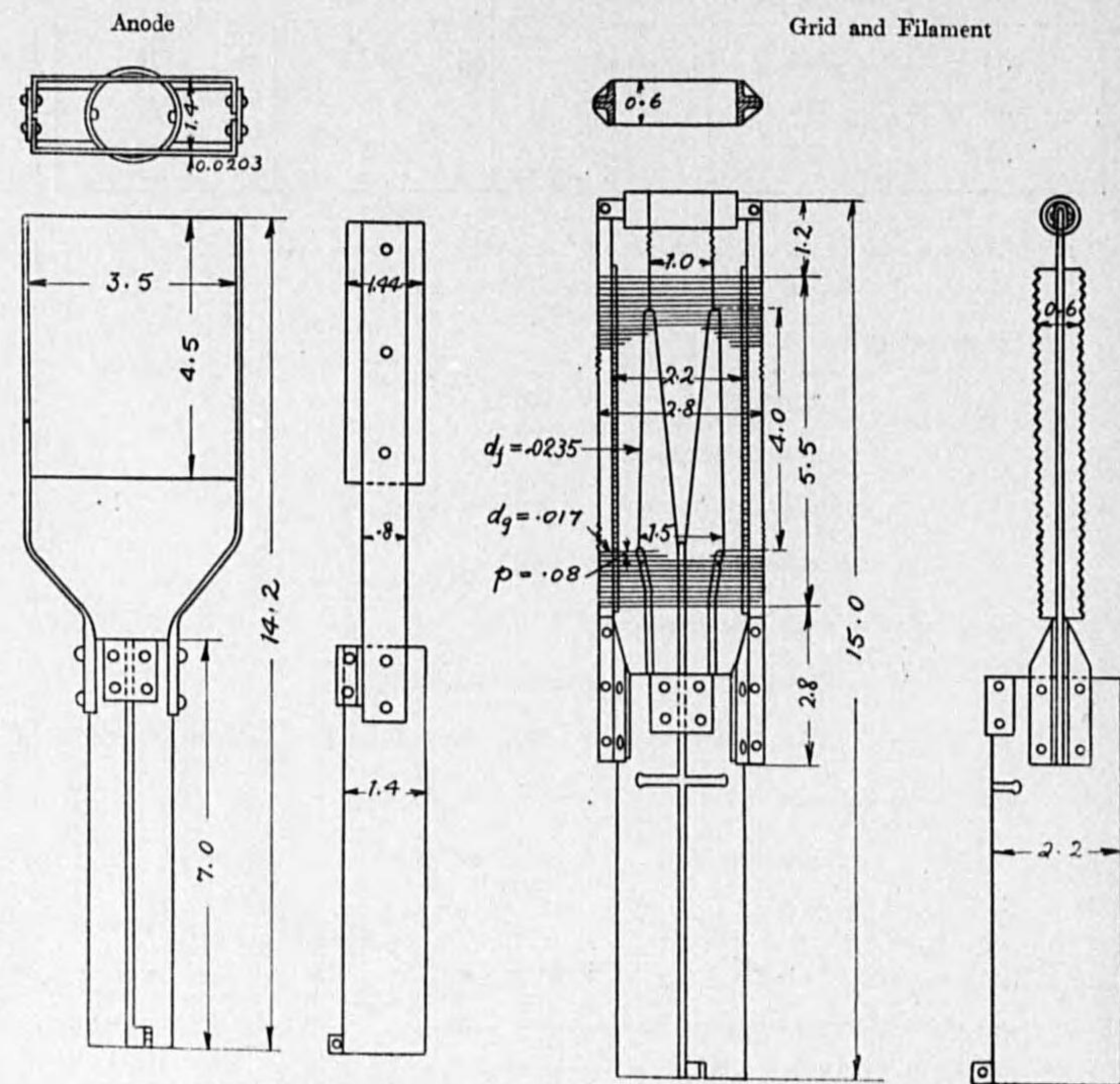


FIG. 78 (PAK)

When the tube is used as an oscillator in a radiophone transmitter, the working anode current must be lower than the above value so as to permit further increase in case of modulation. If 60% modulation is attained at peak oscillatory current of 4.7 A as in the above data, the carrier amplitude will be $\frac{4.7}{1.6} = 2.9$ A and the power output $(2.9)^2 \times 11 = 93$ W. If the anode voltage is raised up to 3,000 V, the power output over 100 W will be obtained.

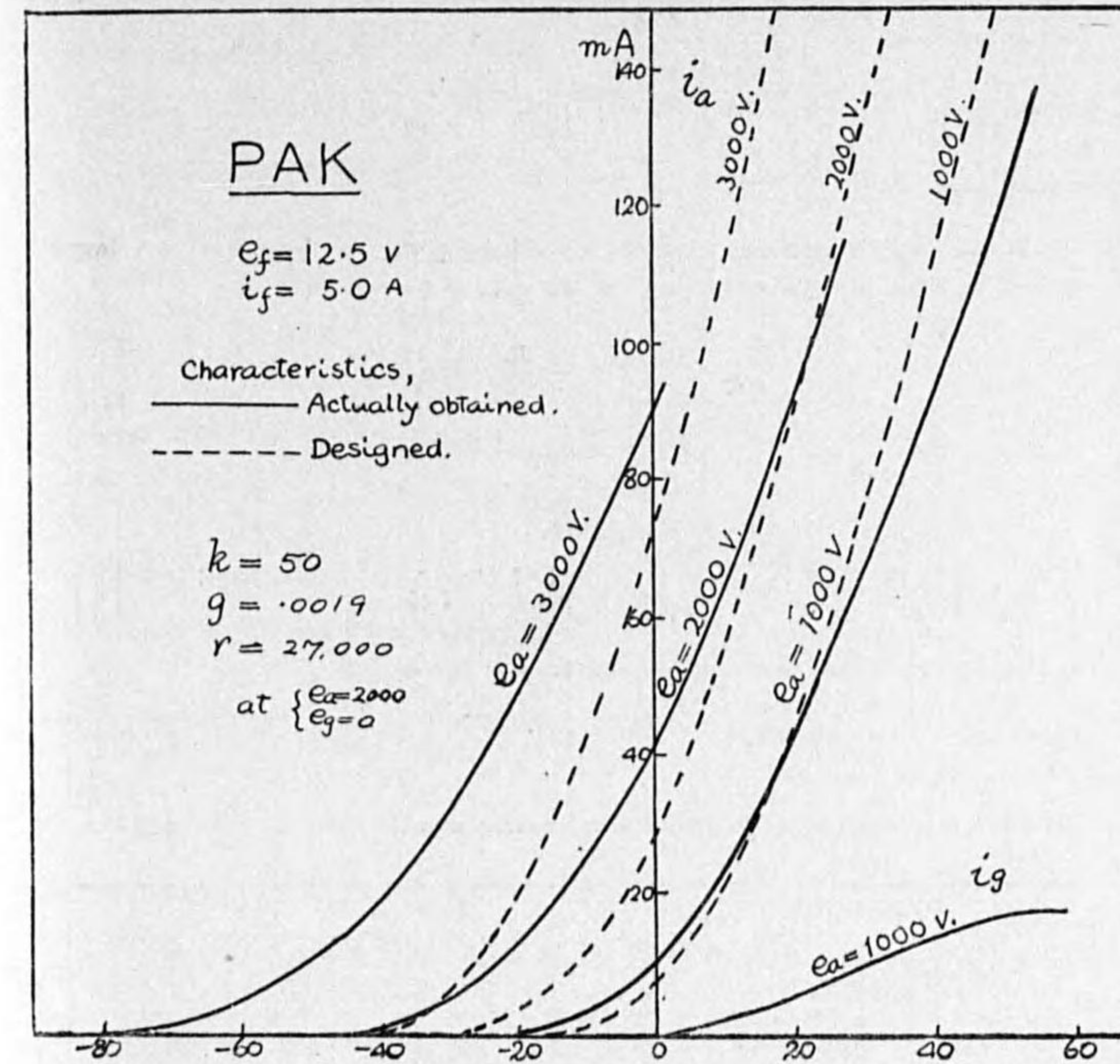


FIG. 79.

Example 74. Design data of a triode type PBN, manufactured at the Laboratory.

Given conditions: The tube is to be used as a radio-telephone power amplifier, modulated wave being impressed on the grid.

Output at the carrier amplitude, $P = 1$ KW.

Anode voltage $E_a = 10,000$ V.

Distortionless range of modulation, 80 %.

Design: Linear amplification of radio-frequency amplitude is obtained at

$$\frac{E_a + kE_g}{rI_s} = 0$$

Take $\frac{R}{\bar{r}}=1.0$ and let the 80% modulated anode current reach $\frac{I_a'}{I_s}=0.50$, then at the carrier amplitude,

$$\frac{I_a'}{I_s} = \frac{1}{1.8} \cdot \frac{I_a'}{I_s} = 0.28 \quad \frac{E_a}{\bar{r}I_s} = \frac{I_a'}{I_s} \cdot \frac{R}{\bar{r}} = 0.28$$

$$\frac{I_a}{I_s} = 0.18 \quad \frac{P}{\bar{r}I_s^2} = 0.039 \quad P=1,000 \quad \therefore \bar{r}I_s^2 = 25,600$$

In order that the maximum amplitude of oscillating power may be obtained at a favorable working condition, as explained on page 129, the value of k should be

$$k = \frac{\frac{kE_g'}{\bar{r}I_s} + \frac{E_a + kE_g}{\bar{r}I_s} - \frac{E_a}{\bar{r}I_s}}{\frac{E_a}{\bar{r}I_s} - \frac{E_a'}{\bar{r}I_s}} \dots \dots \dots (22)$$

and

$$k \geq 10 \frac{\sqrt{\frac{kE_g'}{\bar{r}I_s} - \mu} \frac{kE_g}{\bar{r}I_s}}{\frac{E_a I_a'}{\bar{r}I_s^2} - \frac{P'}{\bar{r}I_s^2}} \dots \dots \dots (23)$$

working condition at the maximum amplitude being as follows,

$$\frac{E_a'}{\bar{r}I_s} = 0.50 \quad \frac{kE_g'}{\bar{r}I_s} = 1.50 \quad \frac{P'}{\bar{r}I_s^2} = 0.125 \quad \frac{I_a'}{I_s} = 0.32$$

The values of k which meet the requirements will vary with the value of $\frac{E_a}{\bar{r}I_s}$ as follows:

$\frac{E_a}{\bar{r}I_s}$	Equation (22)			Equation (23)						
	Numerator	Denominator	k	$\frac{kE_g'}{\bar{r}I_s}$	$-\frac{E_g}{\bar{r}I_s}$	ν	μ	$\sqrt{\frac{kE_g'}{\bar{r}I_s} - \mu}$	$\frac{kE_g}{\bar{r}I_s}$	Limit of k
0.51	0.99	0.01	99	-0.51	0.34	.087	.097	.130	-.049	47
0.52	0.98	0.02	49	-0.52	0.34	.087	.097	.130	-.050	43
0.54	0.96	0.04	24	-0.54	0.36	.086	.095	.129	-.051	38

The results are plotted in Fig. 80, from which it is known that $\frac{E_a}{\bar{r}I_s}$ must be less than 0.523 and k be higher than 43.

Take $\frac{E_a}{\bar{r}I_s} = 0.515$ then $k=67$
 As $E_a=10,000$ $\bar{r}I_s=19,400$
 $I_s = \frac{\bar{r}I_s^2}{\bar{r}I_s} = 1.32$ $\bar{r}=14,700$

From equation (17)

$$G^2 = \frac{(1+k)^2}{\bar{r}^2 I_s} = 7.53 \times 10^{-8}$$

$$G = 0.274 \times 10^{-4}$$

Design of the cathode:

Let $I_s = 1.4$ A

and take $L = 5000$

and $r_f = 0.0325$

(25 A tungsten filament)

From Chart II a,

$$\frac{e_f'}{\nu} = 0.55 \quad \frac{I_s}{\nu} = 0.08 \quad i_f = 27$$

and from Chart II c, $\Delta l = 1.5$ $\Delta e_f = 1.05$

Filament is to be spanned in V-shape, $m = 3$

$$\nu = \frac{I_s}{\left(\frac{I_s}{\nu}\right)} = 17.5 \quad l = \nu + m\Delta l = 22$$

$$e_f' = \left(\frac{e_f'}{\nu}\right)\nu = 9.65 \quad e_f = e_f' + m\Delta e_f = 12.8$$

$$W_f = 460$$

Water-cooled type is to be adopted, as the anode loss is rather high as 1.4 KW, and also for the convenience of using the tube at still higher power for other purposes.

Anode area required:

$$A > \frac{1400 + 460}{20} = 92 \text{ cm}^2$$

Available copper tube has an inner diameter of 4 cm, so that $x_a = 2.0$; and let $x_j = 1.0$.

Actual area obtainable:

$$A = 2\pi x_a \cdot \frac{l}{2} = 138 \text{ cm}^2$$

Assume $x_a = 1.7$ and $x_j = 0.7$, as the filament is in V-shape.

Taking the above obtained value of A ,

$$G = 2.33 \times 10^{-6} \frac{A}{x_a^2 x_j} = 0.27 \times 10^{-4}$$

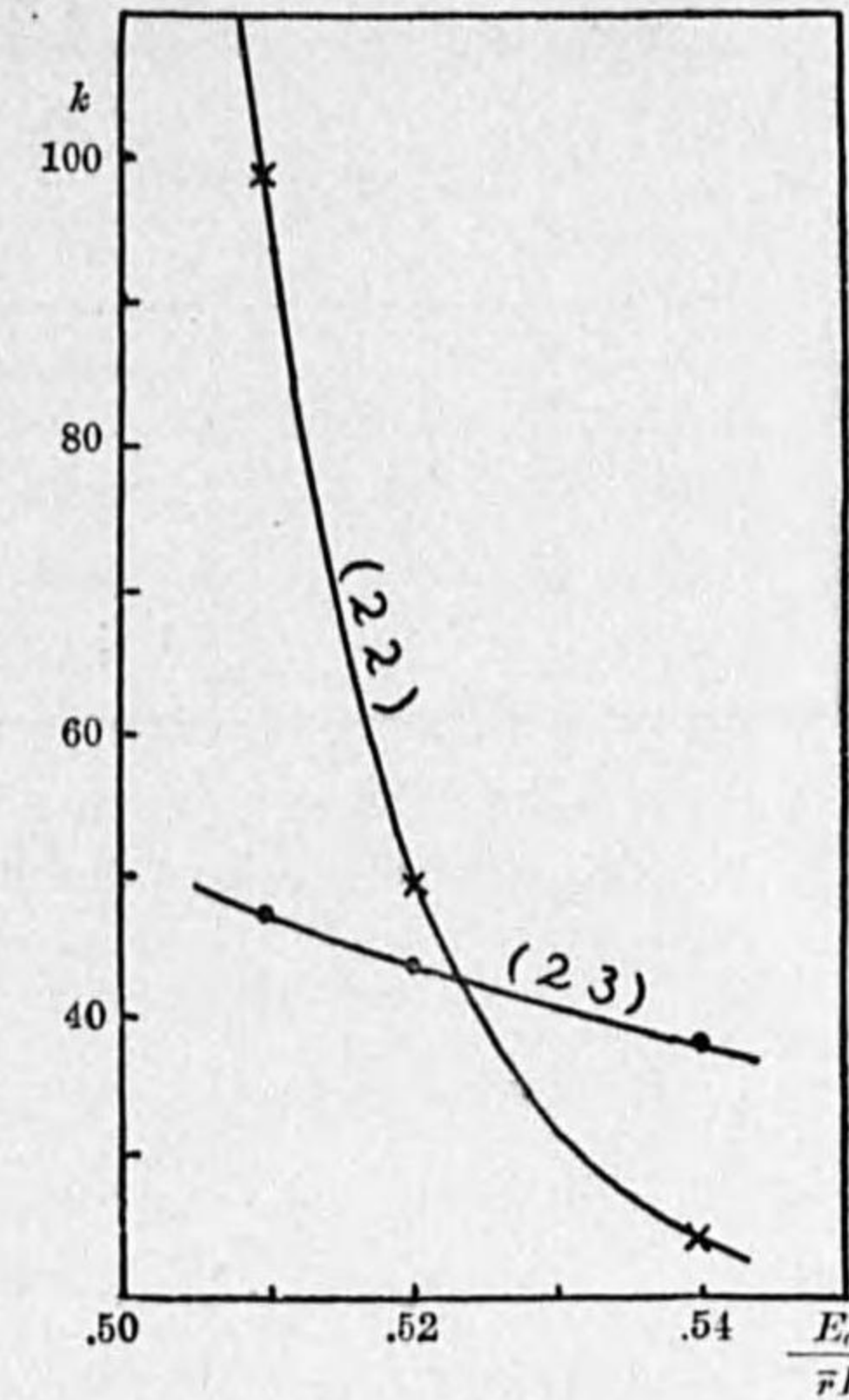


FIG. 80.

which is consistent with that previously derived from parameters.

Design of the grid: molybdenum wire mesh is to be used.

$$k=67 \quad \log \frac{x_a}{x_g} = 0.301 \quad L_g = \frac{4\pi x_g}{p} = \frac{12.6}{p} \quad \log \coth \pi a = \frac{L_g}{67} \times 0.301$$

p	L_g	$\log \coth \pi a$	πa	r_g	d_g
0.2	63	0.283	0.58	0.0092	0.018
0.3	42	0.189	0.77	0.018	0.036
0.4	31	0.141	0.91	0.029	0.058

Nearest available mesh of $p=0.3$ and $d_g=0.030$ is to be used.

Working conditions predicted from the design data:

$$\bar{r}=14,700 \quad I_s=1.32 \quad \bar{r}I_s=19,400 \quad \bar{r}I_s^2=25,600$$

At the carrier amplitude, i.e. when not modulated:

Power input	$E_a I_a = 0.515 \times 0.18 \times 25,600 = 2,370$ W
Power output	$P = 1,000$ W
Efficiency	$\eta = 0.42$ Loss = 1,370 W
Anode currents	$\mathcal{I}_a = 0.28 \times 1.32 = 0.37$ A $I_a = 0.18 \times 1.32 = 0.24$ A
Grid excitation	$k \epsilon_g = 0.85 \times 19,400 = 16,500$ $\epsilon_g = 246$ V
Grid bias voltage	$k E_g = -E_a = -10,000$ $E_g = -150$ V

At the maximum amplitude of modulated wave amplification, or on the full-power working condition:

Power input	$E_a I_a' = 0.515 \times 0.32 \times 25,600 = 4,200$ W
Power output	$P' = 0.125 \times 25,600 = 3,200$ W
Efficiency	$\eta = 0.76$ Loss = 1,000 W
Anode currents	$\mathcal{I}_a' = 0.50 \times 1.32 = 0.66$ A $I_a = 0.32 \times 1.32 = 0.42$ A

A tube actually constructed is shown in Fig. 81 (photograph facing page 158), its dimensions being shown in Fig. 82.

Test data: Static characteristics actually obtained are shown in Fig. 83, together with those predicted from the design data.

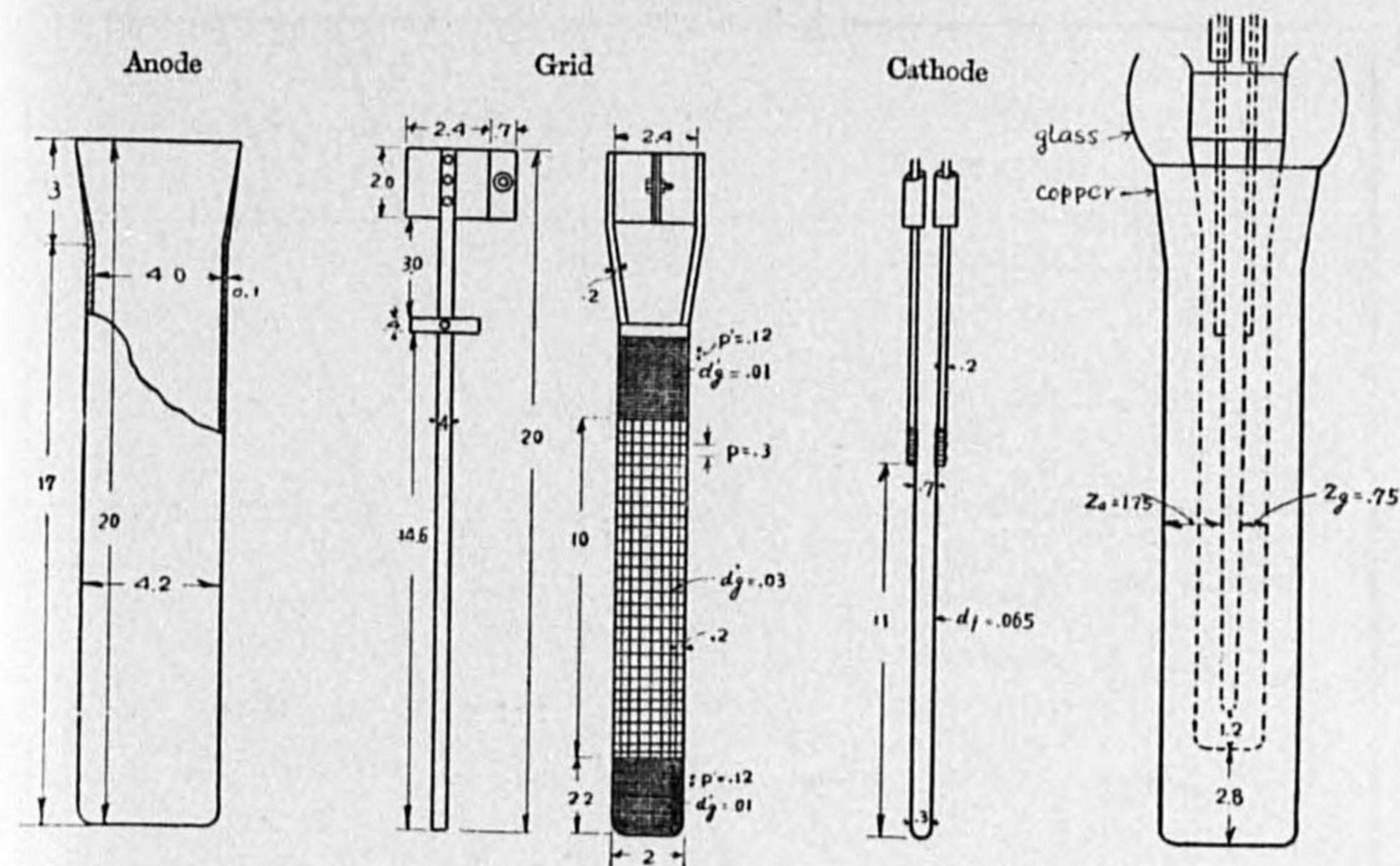


FIG. 82. (PBN)

Working test; the tube was operated as a self-oscillator and adjusted to give full power, the result was as follows:

Filament,	$e_f = 13.2$ V	$i_f = 24.7$ A
Power input,	$E_a = 9,600$ V	$I_a = 0.52$ A
	$E_a I_a = 5,000$ W	
Power output,	oscillatory current	$\mathcal{I}_o = 31.6$ A eff.
	resistance	$R = 3\omega$
	$P = 3,000$ W	
Efficiency	$\eta = 0.60$	
Grid current	$I_g = 0.035$ A	
Grid leak	$R_g = 20,000 \omega$	$E_g = -700$ V

The tube has not yet been submitted to its proper use, but the characteristics actually obtained show that it meets the requirements for a radiophone power amplifier giving the rated power output.

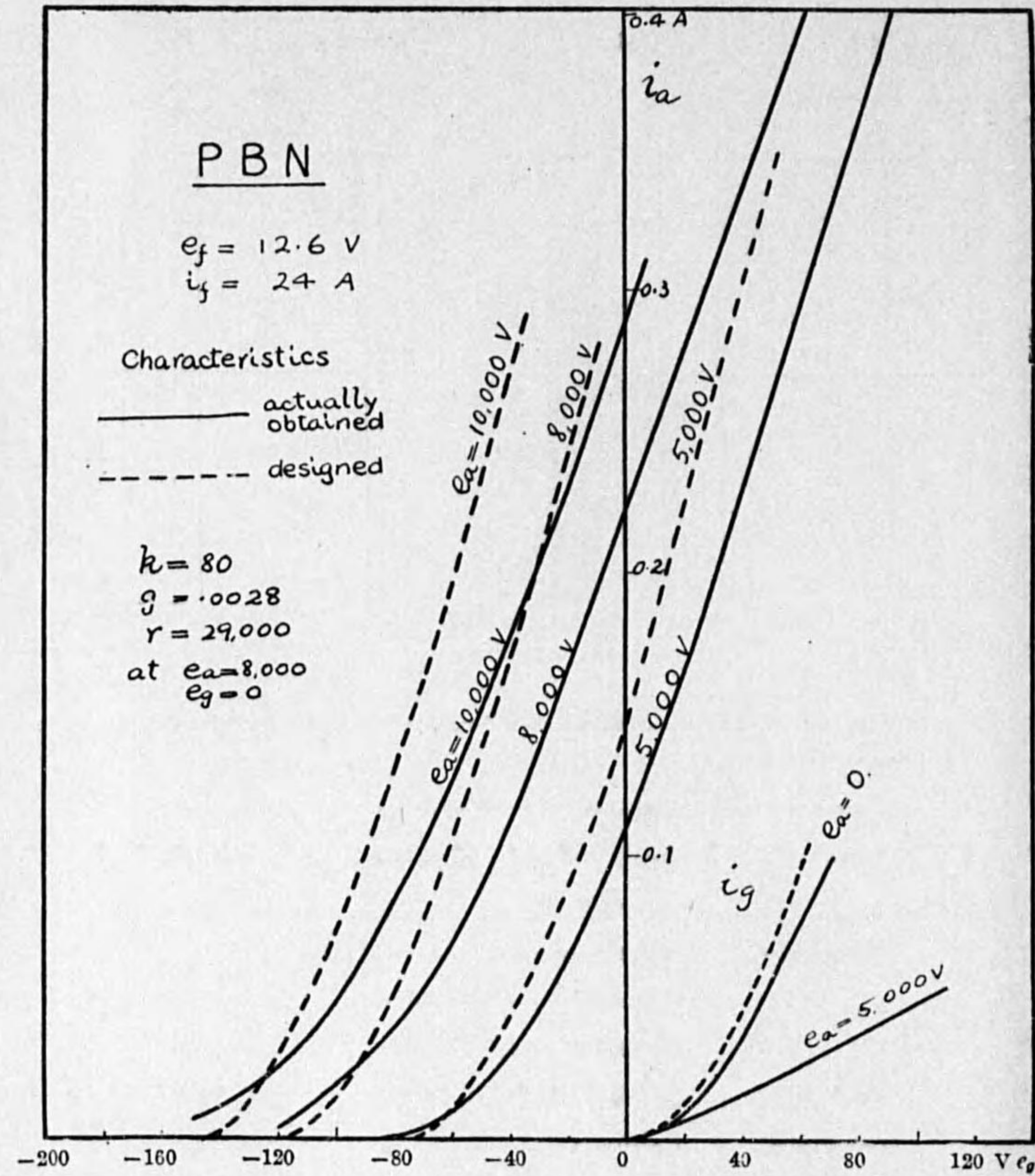


Fig. 83.

SUMMARY.

(1) Calculations on Vacuum Tubes.

A. Diode characteristics:

$$i_a = G e_a^{\frac{3}{2}} \quad \text{for } e_f = 0 \text{ or } e_a \gg e_f$$

$$i_a = \frac{2}{5} G e_f^{\frac{3}{2}} \cdot f\left(\frac{e_a}{e_f}\right) \quad (\text{TABLE I})$$

$$G = 2.33 \times 10^{-6} \frac{A}{x_a^2}$$

B. Triode characteristics:

$$i = i_a + i_g = \frac{2}{5} G e_f^{\frac{3}{2}} \cdot f\left(\frac{e_g'}{e_f}\right) \quad (\text{TABLE I})$$

$$e_g' = \frac{e_a + k e_g}{1 + k}$$

$$G = 2.33 \times 10^{-6} \frac{A}{x_a x_g}$$

$$e_g < 0: i_a = i$$

$$e_a \gg e_g > 0: i_a = \frac{i}{1 + 1.5 a \sqrt{\frac{e_g}{e_a}}}$$

C. Triode parameters:

$$k = \frac{c L_g \log \frac{x_a}{x_g}}{\log \coth \pi a} \quad (\text{TABLES II, III \& IV})$$

$$g = 1.5 G \frac{k}{1+k} \left(\sqrt{\frac{e_g'}{e_f}} - \frac{1}{4} \cdot \frac{e_f}{\sqrt{e_g'}} \right)$$

$$r = \frac{k}{g}$$

$$(1+k)^3 = G^2 \bar{r}^3 I_s$$

D. Saturation current I_s is calculated by CHART II for a tungsten filament.

E. Operating conditions are determined by the dynamic characteristic diagram shown in CHART I.

$\frac{e_g'}{e_f}$	$f\left(\frac{e_g'}{e_f}\right)$
0	0
0.25	0.031
0.50	0.177
0.75	0.414
1.00	1.00
1.5	2.57
2.0	4.65
2.5	7.13
3.0	9.94
4.0	16.51
5.0	24.1
6.0	32.5
8.0	53.0
10	74.0
15	138
20	211
40	622
$\frac{e_a}{e_f}$	$f\left(\frac{e_a}{e_f}\right)$

Cylindrical-electrode tubes; $c=1$		
Plane-electrode tubes, grid of a mesh; $c=1$		
Plane-electrode tubes, grid of parallel wires;		
	c	
$\frac{x_a}{x_g}$	Filament	
	W-shaped	V-shaped
1	1.0	1.0
2	1.5	1.3
3	1.9	1.6
4	2.4	1.9
5	2.8	2.1

Grid construction	L_g	πa
Wires parallel to the filament	n	$\frac{nd_g}{2x_g}$ or $\frac{I_g r_g}{x_g}$
Parallel wires or spiral, no support	$\frac{2\pi x_g}{p}$	$\frac{\pi d_g}{p}$ or $\frac{I_g r_g}{x_g}$
Ditto, with supports in the stream of electron	$\frac{2\pi x_g}{p} + s\left(1 - \frac{t}{p}\right)$	$\frac{(L_g - s)d_g + st}{2x_g}$
Square mesh, with or without support	$\frac{4\pi x_g}{p} \left(1 - \frac{r_g}{p}\right)$	$\frac{\pi d_g}{p} \left(2 - \frac{d_g}{p}\right)$ or $\frac{I_g r_g}{x_g}$
These are equally applicable to tubes of cylindrical or plane electrodes.		

πa	$\log \coth \pi a$	Difference per 0.01 of πa
0.10	1.002	29,
0.20	0.714	17,
0.30	0.542	12,2
0.40	0.420	8,5
0.50	0.335	6,6
0.60	0.269	5,1
0.70	0.218	4,0
0.80	0.178	3,0
0.90	0.145	2,7
1.00	0.118	2,2
1.10	0.096	1,6
1.20	0.080	1,5
1.30	0.065	

(2) The Design of a Triode.

Design procedure;

1) The working points are determined on the dynamic characteristic diagram, CHART I, so as to satisfy the specified working conditions. (Refer to the table on page 126.)

The following quantities will then be determined:—

$$a = \frac{P}{\bar{r}I_s^2}, \quad \frac{\mathcal{E}_a}{\bar{r}I_s}, \quad \frac{J_a}{I_s}, \quad \frac{I_a}{I_s}, \quad \frac{k\mathcal{E}_g}{\bar{r}I_s},$$

$$\frac{E_a + kE_g}{\bar{r}I_s}, \quad \frac{\mathcal{R}}{\bar{r}}.$$

Approximately determined:—

$$\frac{E_a}{\bar{r}I_s}, \quad \frac{E_a I_a}{\bar{r}I_s^2}, \quad \eta, \quad \frac{kE_g}{\bar{r}I_s}.$$

2) If power output P is given, $\bar{r}I_s^2$ is known; $\bar{r}I_s^2$ is then split into $\bar{r}I_s$ and I_s , considering the practicable limits of E_a , \mathcal{R} , W_f , etc. as well as economical conditions.

3) A value of G being assumed (refer to the table on page 128), k is known from

$$(1+k)^3 = \left(\frac{Ga}{P}\right)^2 (\bar{r}I_s)^5 \quad \text{or} \quad (1+k)^3 = G^2 \bar{r}^3 I_s.$$

At a full-power working condition of power amplifier or oscillator, the following relations should be considered for the evaluation of k ;

$$k = \frac{\frac{k\mathcal{E}_g}{\bar{r}I_s} + \frac{E_a + kE_g}{\bar{r}I_s} - \frac{E_a}{\bar{r}I_s}}{\frac{E_a}{\bar{r}I_s} - \frac{\mathcal{E}_a}{\bar{r}I_s}}$$

and

$$k \geq 10 \frac{\nu \frac{k\mathcal{E}_g}{\bar{r}I_s} - \mu \frac{kE_g}{\bar{r}I_s}}{\frac{E_a I_a}{\bar{r}I_s^2} - \frac{P}{\bar{r}I_s^2}}$$

in which ν and μ are given in Fig. 69 on page 130.

Calculations have to be tried for several values of k or G , and the most favorable one be selected among them.

4) Dimensions of the Electrodes.

a) Effective anode area

$$A \geq \frac{W_a + qW_f}{w} \quad (\text{Refer to page 132})$$

b) Distance between electrodes must satisfy the relations:

$$x_g \doteq 0.4 x_a$$

$$G = 2.33 \times 10^{-6} \frac{A}{z_a x_g^2}$$

c) Grid construction is determined by

$$\frac{k}{\log \frac{x_a}{x_g}} = \frac{cL_g}{\log \coth \pi a}$$

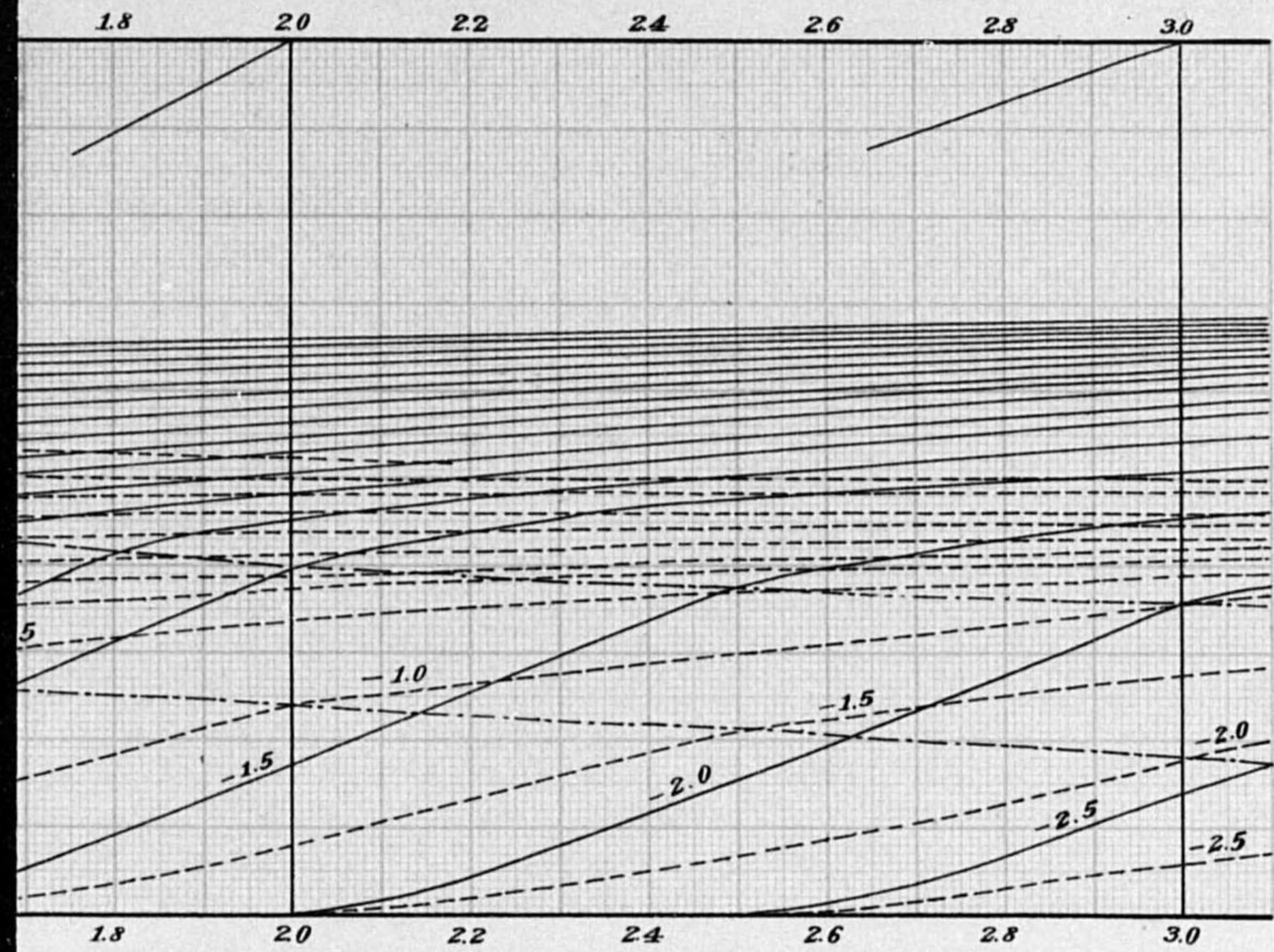
(Refer to the table on page 134 and TABLES II, III and IV)

p , d_g , etc. are finally determined.

d) Cathode is designed by means of CHART II for tungsten giving a slightly higher value for I_s than required.

The design procedure as shown above is for a typical case, and alterations will be needed according to the specified conditions.

—(the end)—



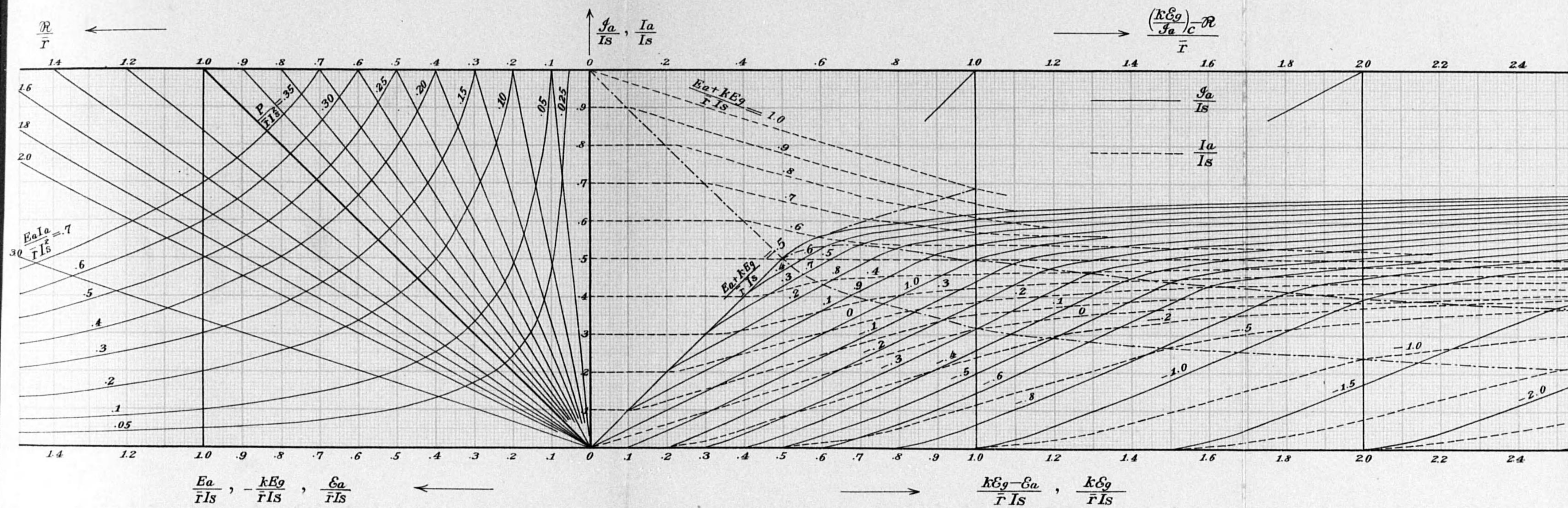


CHART I. DYNAMIC CHARACTERISTIC DIAGRAM

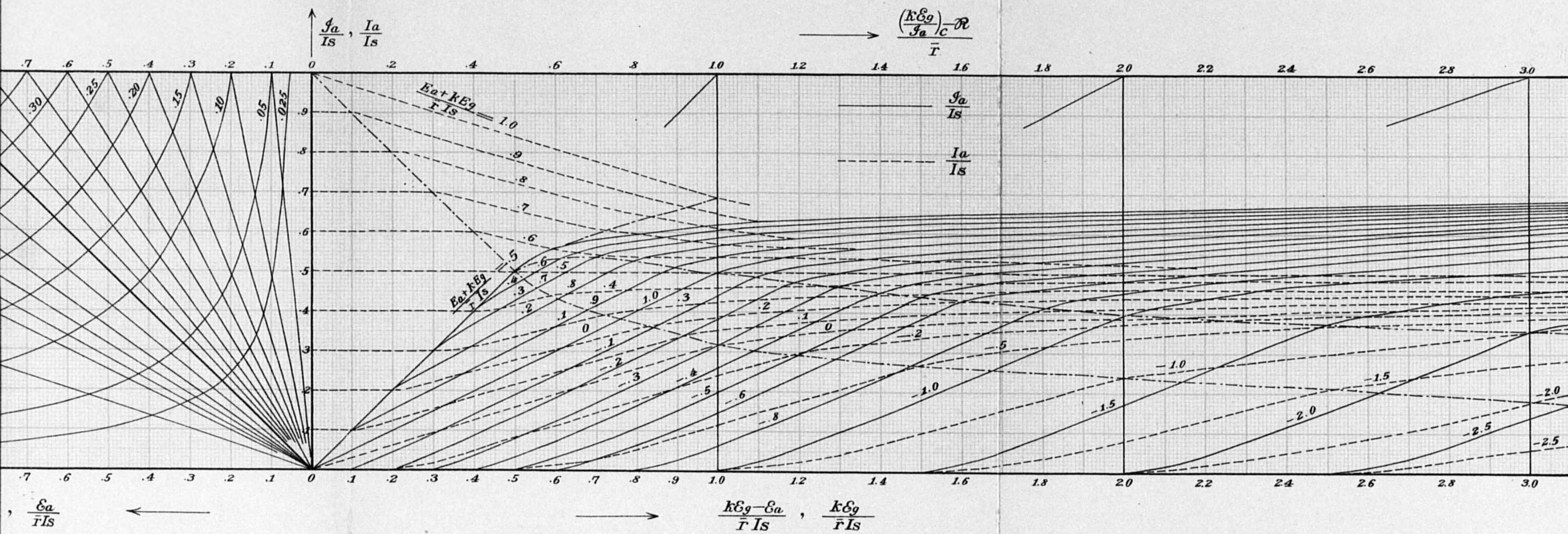
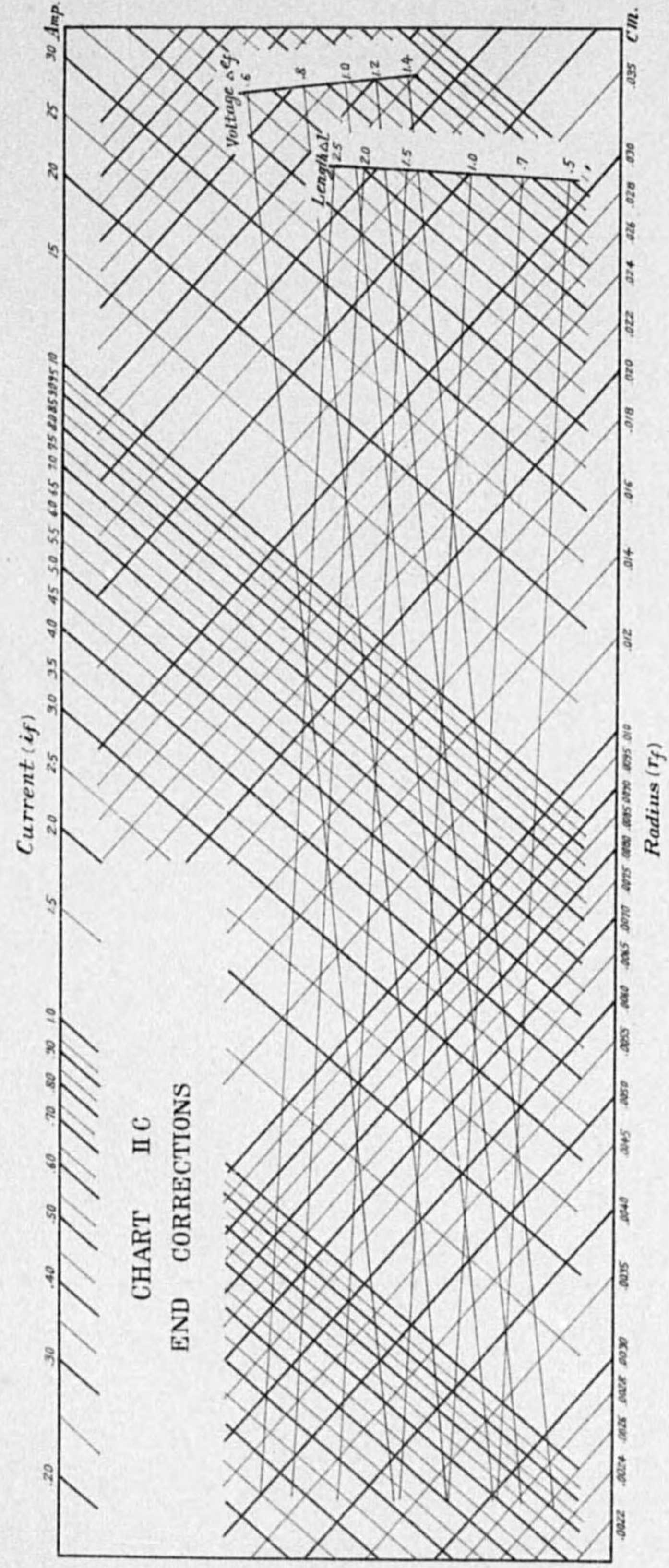
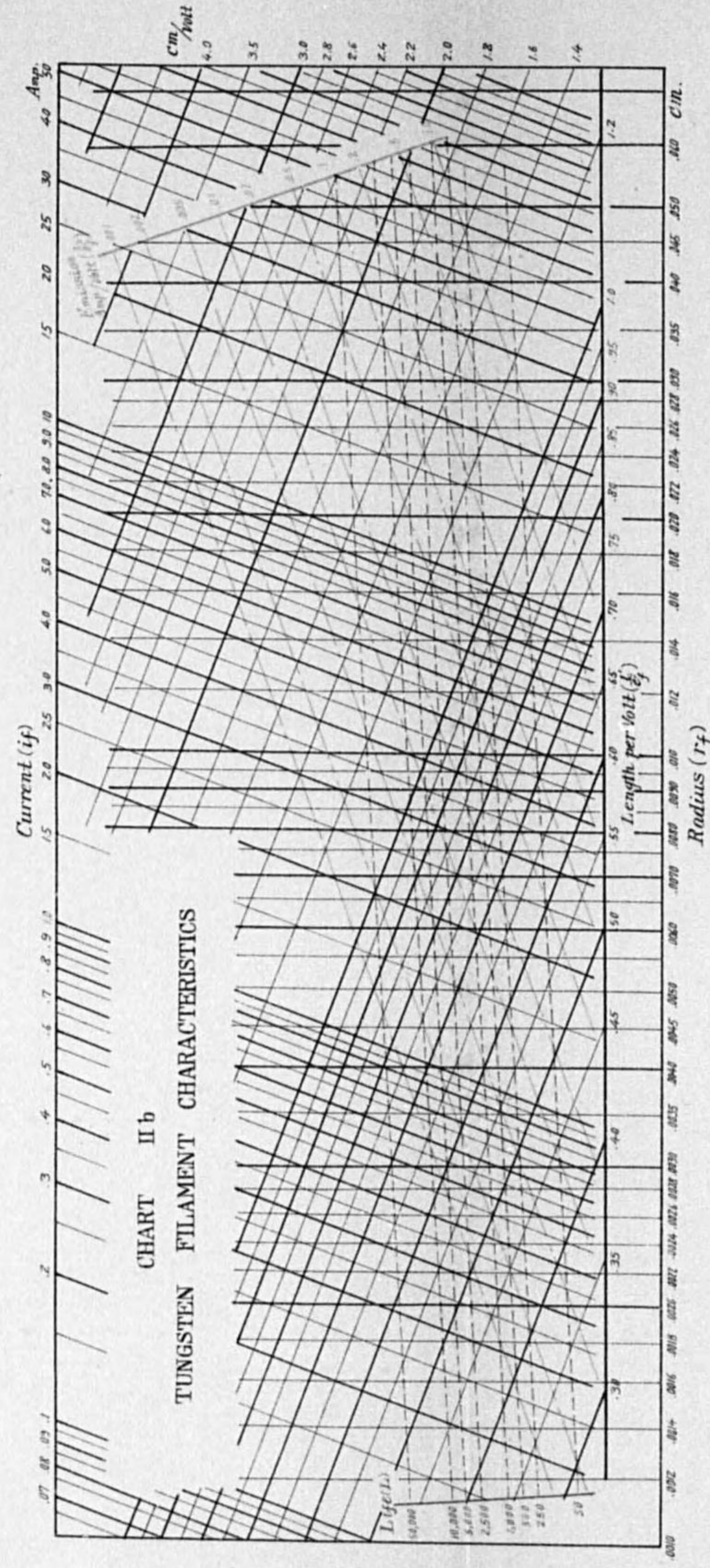
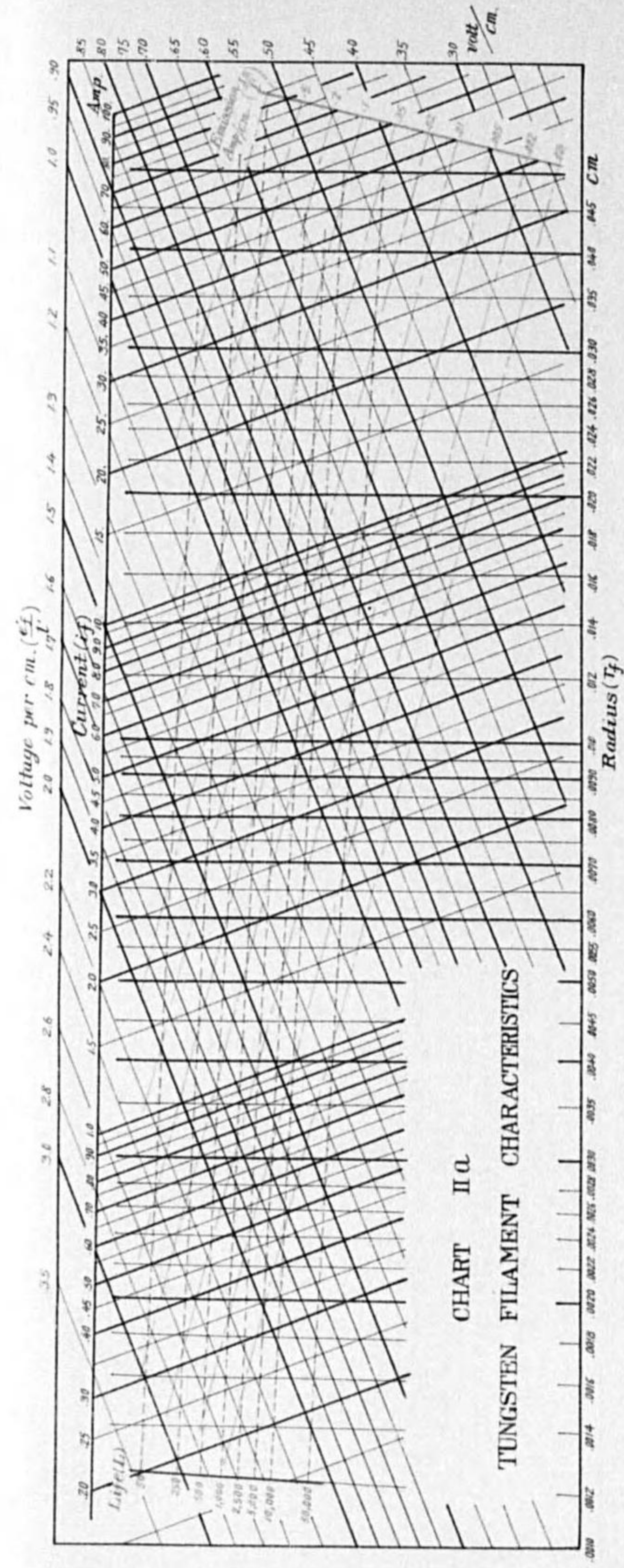


CHART I. DYNAMIC CHARACTERISTIC DIAGRAM

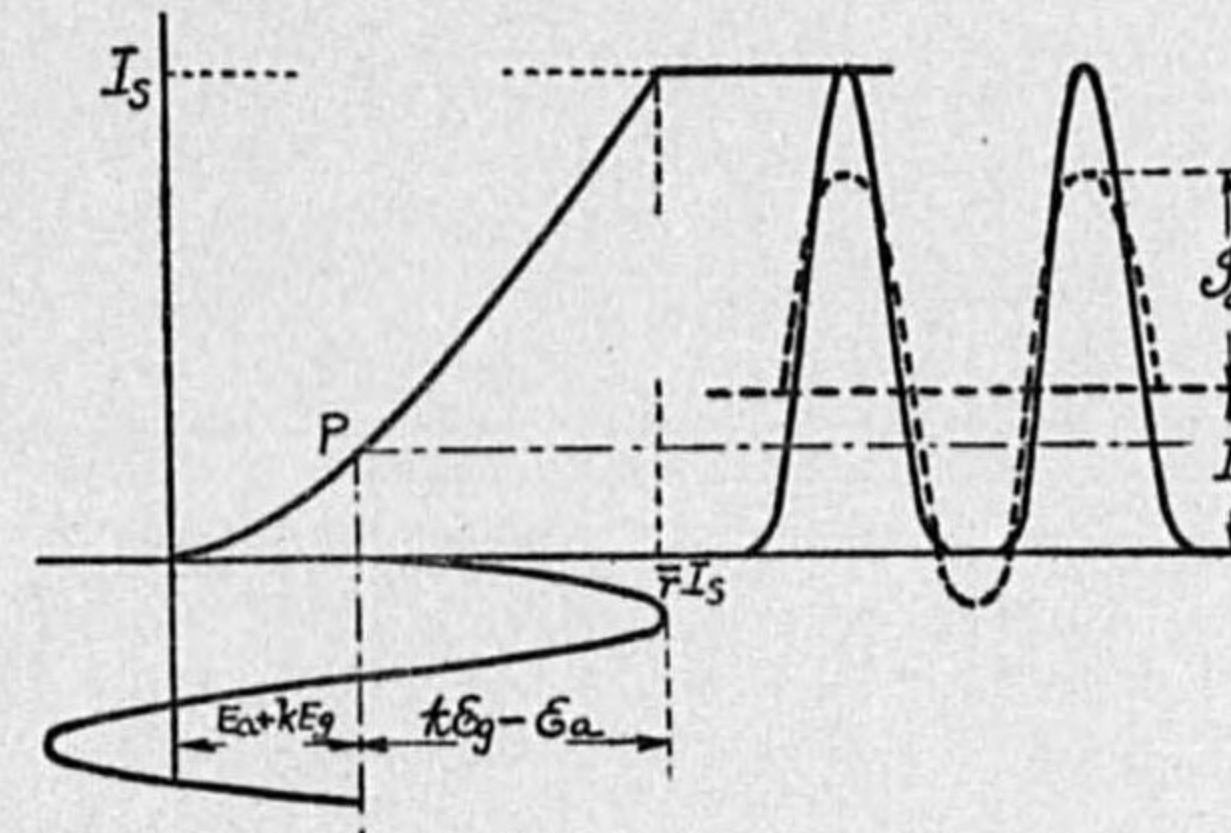


APPENDIX

After this paper had been put to press, the writer worked out the dynamic characteristic diagram in a more rigorous way than described in the text.

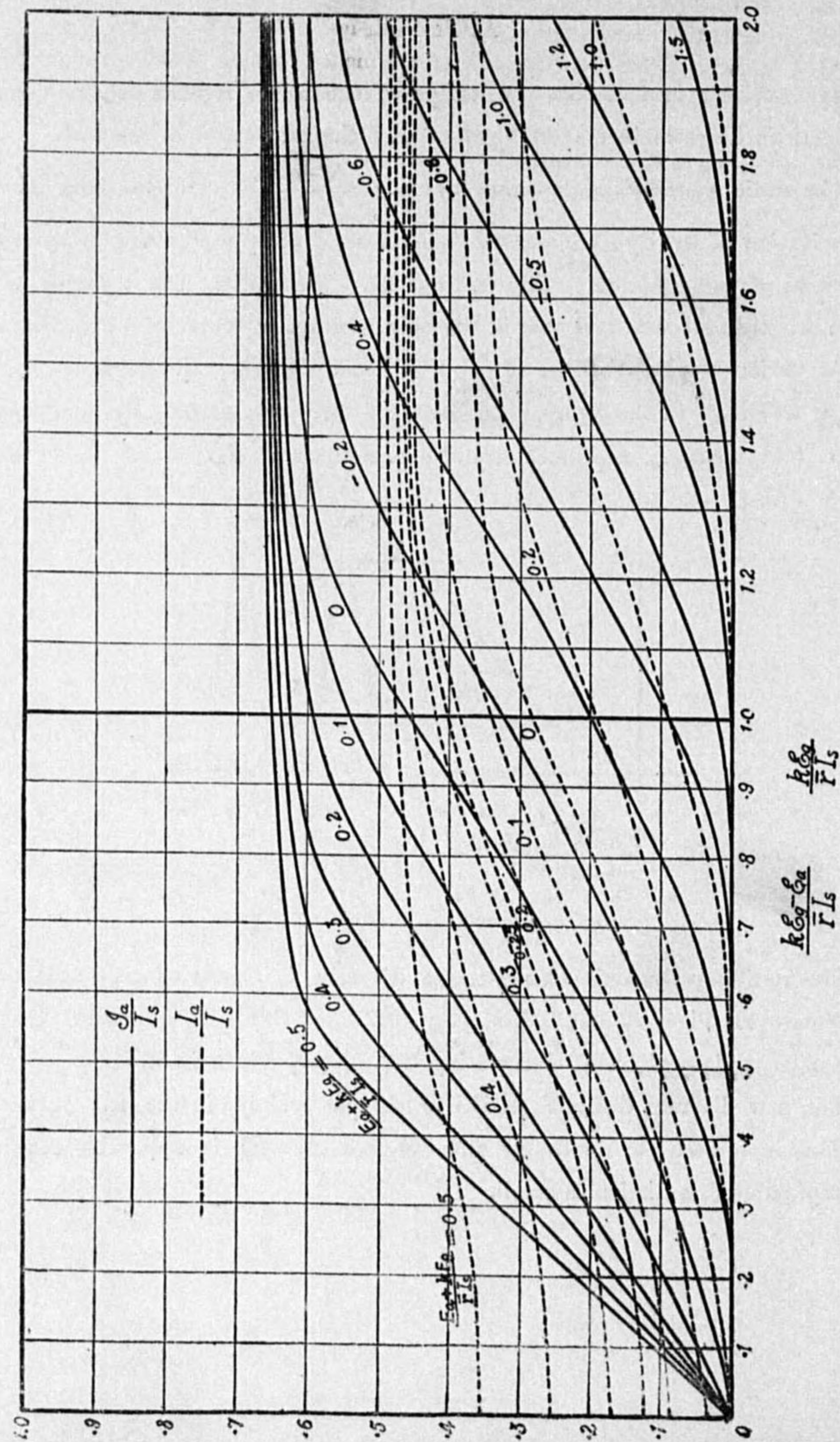
The static characteristic expressed by $\frac{i_a}{I_s} = \left(\frac{e_a + kE_g}{\bar{r}I_s} \right)^{\frac{3}{2}}$ has been taken for the derivation of the dynamic characteristics, instead of approximating it by a linear relation as given in equation (18) on page 91. Saturation was assumed to take place abruptly as before and this is the only assumption which still remains.

At various applied voltages of $E_a + kE_g$ and $kE_g - E_a$ the anode current was depicted as shown in the figure, and its wave form was graphically analyzed into its d. c. component I_a and fundamental a. c. component \mathcal{I}_a .



The resulting dynamic characteristic diagram is shown on next page, which corresponds to Figs. 42 and 43 on page 102, and it is recommended that this diagram be used in CHART I replacing that already given in it.

The new diagram differs from the former one mainly in the left part of it, and gives more accurate results for d. c. component, and is applicable even when the amplitude of oscillation is small.



CIRCULARS

No. 2.	Radiotelegraphic Installations for Fishery.	1921.
No. 13.	Antenna Constants.	1925.
No. 14.	Wavemeters.	1925.
No. 16.	General Characteristics of American-made Vacuum Tubes.	1925.
No. 20.	General Characteristics of German-made Vacuum Tubes.	1925.
No. 21.	Recent Developments in High Frequency Telephony over Power Transmission Lines.	1926.
No. 22.	Regenerative Reception.	1926.
No. 25.	On the Radio dry Batteries (Part 1), "A" Batteries.	1926.
No. 26.	On the Radio dry Batteries (Part 2), preliminary Report on "B" Batteries.	1926.
No. 27.	Ionization Manometers.	1926.
No. 29.	General Characteristics of British-made Vacuum Tubes.	1926.
No. 30.	The Characteristics of transmitting Vacuum Tubes.	1926.
No. 32.	Oscillating and amplifying Properties of Crystals.	1926.
No. 34.	Properties of a thoriated Tungsten Filament and simple graphical Diagrams relating to its Diameters, Heating Currents, and Temperatures.	1927.
No. 42.	On Battery eliminated receiving Sets.	1927.
No. 43.	A Résumé of Methods in measuring the Field-Intensity of Radio Waves.	1927.
No. 44.	Modern Methods of Radio Field-Intensity Measurement.	1927.
No. 47.	On manufacturing Processes of small Radio Vacuum Valves.	1927.
No. 49.	On the Standardization of high Frequencies.	1928.
No. 50.	Graphs for the Design of bright-emitting Tungsten Filament.	1928.

昭和3年12月27日印刷
昭和3年12月30日發行
(不許複製)

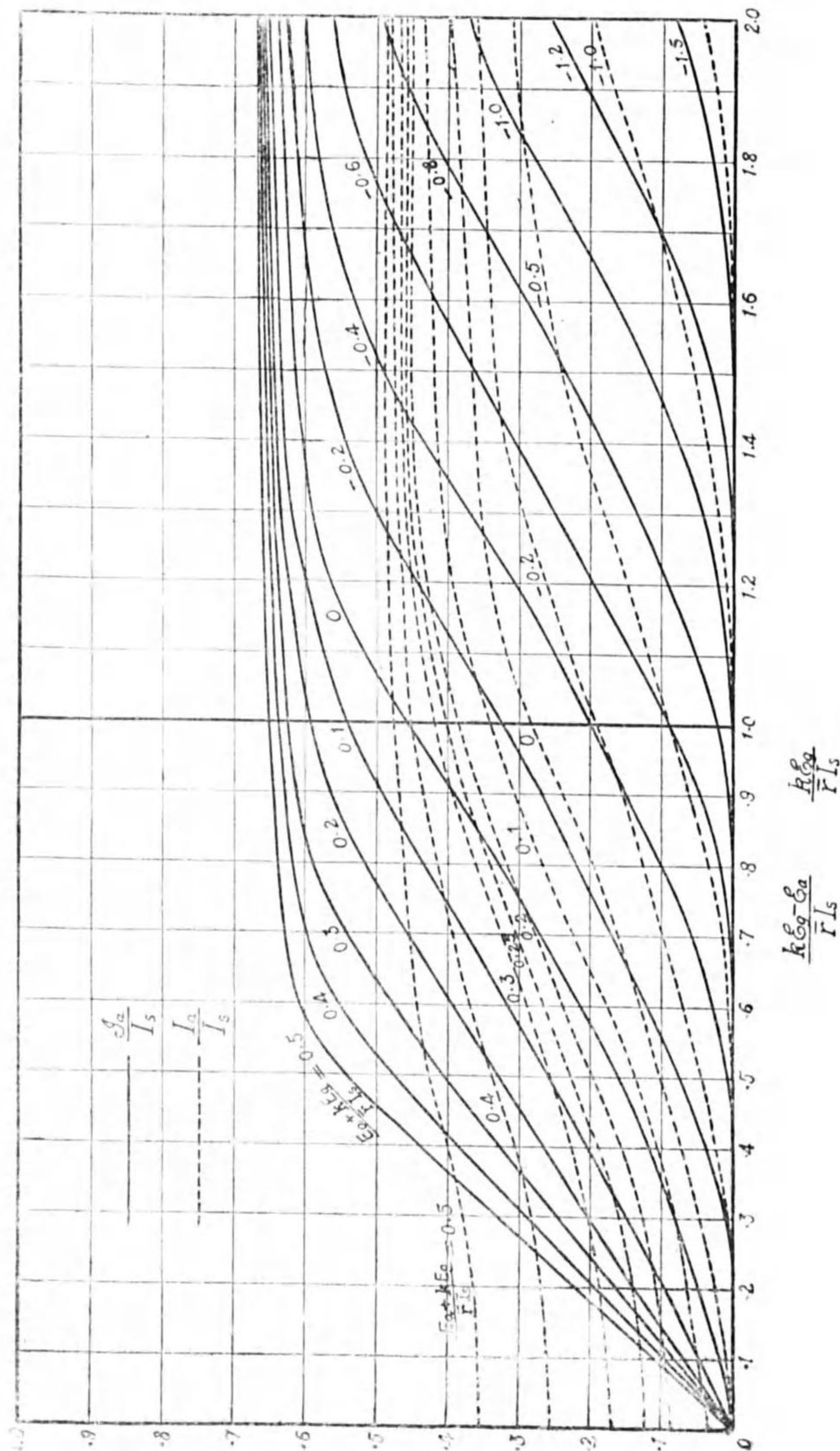
電氣試験所編

發行兼印刷人
倉橋藤治郎
東京市麹町區有樂町1工政會

發行所
工政會出版部

東京市麹町區有樂町1—1
電話丸の内(23) 3980番
振替東京 27724番

¥3.55



CIRCULARS

No. 2.	Radiotelegraphic Installations for Fishery.	1921.
No. 13.	Antenna Constants.	1925.
No. 14.	Wavemeters.	1925.
No. 16.	General Characteristics of American-made Vacuum Tubes.	1925.
No. 20.	General Characteristics of German-made Vacuum Tubes.	1925.
No. 21.	Recent Developments in High Frequency Telephony over Power Transmission Lines.	1926.
No. 22.	Regenerative Reception.	1926.
No. 25.	On the Radio dry Batteries (Part 1), "A" Batteries.	1926.
No. 26.	On the Radio dry Batteries (Part 2), preliminary Report on "B" Batteries.	1926.
No. 27.	Ionization Manometers.	1926.
No. 29.	General Characteristics of British-made Vacuum Tubes.	1926.
No. 30.	The Characteristics of transmitting Vacuum Tubes.	1926.
No. 32.	Oscillating and amplifying Properties of Crystals. ...	1926.
No. 34.	Properties of a thoriated Tungsten Filament and simple graphical Diagrams relating to its Diameters, Heating Currents, and Temperatures.	1927.
No. 42.	On Battery eliminated receiving Sets.	1927.
No. 43.	A Résumé of Methods in measuring the Field-Intensity of Radio Waves.	1927.
No. 44.	Modern Methods of Radio Field-Intensity Measurement.	1927.
No. 47.	On manufacturing Processes of small Radio Vacuum Valves.	1927.
No. 49.	On the Standardization of high Frequencies.	1928.
No. 50.	Graphs for the Design of bright-emitting Tungsten Filament.	1928.

昭和3年12月27日印刷
 昭和3年12月30日發行
 (不許複製)

電氣試驗所編

發行兼印刷人
 倉橋藤治郎
 東京市麴町區有樂町1工政會

發行所
 工政會出版部

東京市麴町區有樂町1-1
 電話丸の内(23) 3980番
 振替東京 27724番

¥3.55

**BULLETINS PUBLISHED IN CONNECTION
WITH RADIO TECHNICS.**

The papers with asterisks () are written in English while the others in Japanese.*

RESEARCHES

No. 9.	Effect of earthed Conductors near Radio Stations.	1910.
No. 13.	Minerals available as Wireless Detectors and their Sensitivity.	1911.
No. 16.	Enamelled Condensers for Radio Telegraphy.	1911.
No. 17.	Utilization of both Waves emitted from closely coupled Systems of Radio Telegraphy.	1911.
No. 18.	On the Degree of Coupling of Oscillation Transformers in Radio Telegraphy.	1912.
No. 19.	On diurnal Variation of the Intensity of Radio Signals.	1912.
No. 22.	"T-Y-K" Oscillation Gaps for Radio Telegraphy and Telephony.*	1912.
No. 33.	The "Teishinsho" Type commercial Radio Telephone Set.	1913.
No. 34.	Discharge Frequency of the "T-Y-K" Oscillation Gaps.*	1913.
No. 35.	"T-Y-K" System of Radio Telegraphy and Telephony.*	1913.
No. 55.	Radio Transmission and Reception through intermediate overhead Lines between Antenna and Instrument.	1916.
No. 56.	Oscillation Gaps in rarefied Gases.	1916.
No. 63.	Radio Apparatus for Ship Use.	1917.
No. 83.	Generation of undamped oscillating Current from a Three-Electrode Vacuum Bulb.	1920.
No. 106.	High Frequency Wave Telephony applied on a Power Transmission Line.	1922.
No. 115.	Standardization of Wavemeters.*	1922.
No. 134.	Experimental Determination of fundamental dynamic Characteristics of a Triode.*	1924.
No. 136.	High Frequency Telegraphy and Telephony.	1924.
No. 160.	On the Performance of Rectifiers.	1925.
No. 161.	On the Life of Vacuum Tubes.	1925.
No. 167.	Vibrating Rectifiers.	1926.
No. 168.	On the Uniformity of foreign-made receiving Tubes.	1926.
No. 173.	On the Synthesis of Galena Crystal.	1926.
No. 177.	A simplified Method of Calibration of Wavemeter by standing Waves on parallel Wires.*	1926.
No. 180.	On the Voltage Wave Form of Direct Current Machines.	1926.
No. 187.	Experiments on electromagnetic Shielding for long electric Waves.	1926.
No. 192.	Puncture Damage on the Glass Wall of a Vacuum Tube.	1927.
No. 196.	A further Investigation of synthetic Galena Detector and a new Theory of Crystal Rectifiers.*	1927.
No. 206.	Plate Current-Plate Voltage Relation of a Vacuum Tube.	1927.
No. 207.	Crystal Reception and its Distance to be covered.	1927.
No. 217.	Long Distance Radio receiving Measurements.*	1927.
No. 218.	Study on the Operation of the Multivibrator.*	1927.
No. 229.	The Measurements of the Field Intensities of Some High-Power Long-Distance Radio Stations. Part I—Bolinas and Bordeaux.*	1928.
No. 230.	The Effect of chemical Composition on the Sensitivity of Galena as a Radio Detector and the cold Emission from Crystal.*	1928.
No. 233.	The Measurement of the Field Intensities of Some High-Power Long- Distance Radio Stations. Part II. Malabar, Palao and Rugby.*	1928.
No. 236.	Standardization of Frequency.*	1928.

(Over)

終